Structural evolution of the Jebel Akhdar culmination and its implications for exhumation processes in the northern Oman Mountains

Mohammed AL-Wardi

Submitted in accordance with the requirements for the degree of

Doctor of Philosophy

The University of Leeds
School of Earth and Environment

March 2006

The candidate confirms that the work submitted is his own and that appropriate credit has been given where reference has been made to the work of others.

CONTAINS PULLOUTS

Acknowledgments

Indeed, first and foremost, all praises and thanks should go to Allah, the most compassionate and the most merciful, for providing me with the health and giving me the opportunity to do a PhD. I would also like to thank my supervisors Rob Butler for his help and critical advice particularly during the field work and the writing up stage. His critical comments have greatly aided in transforming this thesis into a finished product. The PhD scholarship was funded by Sultan Qaboos University. The field work was funded by Petroleum development Oman. I owe my sincere gratitude to Dr Samir Hanna and Dr Jack Filbrandt for initiating and supporting the project throughout my PhD study.

Valuable assistance was provided by S. freeman, who thankfully helped me in dealing with various sophisticated software programs. I would also like to thank all the rest of the academic and support staff of the Earth and environment department.

Next there are all the friends I've made in Leeds, the list is too long to mention, however my first thank goes to M. AL-Kindi and P. Kellman for their valuable review of the manuscript, which helped me to improve this thesis. Lots of thanks go to my friends in Leeds including A. AL-Anbori, B. AL-Busafi, J. Vinules, D. Tatham, J. Maddock. Many thanks also to my field assistants over the years, especially S. AL-Abri for searching for fault striations with me.

I want to give my warmest thanks to my parents for their unselfish efforts to help their son in all field of life. Finally, I express my loving thanks to my wife for her support and patience. I also wish to thank my wonderful children, Ward and Jihad. They mean everything to me.

Abstract

Many orogenic belts show evidence for coeval extension and compressional tectonics. Here I present new evidence for such activity during the tectonic evolution of the Oman Mountains, a Late Cretaceous orogenic system on the NE margin of the Arabian continent. The tectonic significance and implications of this discovery are discussed within the context of convergent plate boundary processes. During the Late Cretaceous the NE margin of the Arabian continent was overthrust by "exotic" sheets of oceanic and continental margin units (the Semail ophiolite allochthon). Some parts of this margin (Saih Hatat Massif) were deeply buried through subduction, to depths suitable for eclogite facies metamorphism, while other parts are unmetamorphosed (Jebel Akhdar Massif). Consequently an almost continuous metamorphic gradient is preserved, that creates an ideal setting with which to relate both shallow and deep-seated tectonic processes to orogenic development

Current mapping and structural studies reveal that the extensional deformation that followed the obduction of the allochthons and concomitant partial subduction of the continental margin is very much more extensive than previously recognized and was synchronous with the folding of the culminations of the Oman orogen. The extensional deformation appears to be partitioned into two orthogonal structural styles: NNE-directed shearing and vertical thinning, together with a local NW-SE contraction manifested by lineation-parallel folds. In the Jebel Akhdar massif the NNE-shear deformation is extensively developed, forming steep faults and bedding-parallel detachments that extend stratigraphy with a top-to-the-NNE sense of shearing. No evidence of ongoing NW-SE contraction is seen, and hence deformation is apparently plane strain. In contrast, Jebel Nakhal is marked with widespread deformation of both NNE-shearing and the concomitant NW-SE contraction, indicating non-plane strain. In Saih Hatat NNE-shearing is penetrative, with a component of orthogonal contraction.

Coeval orthogonal layer contraction, layer-thinning and elongation describe the bulk constrictional 3D strain. While this might be indicative of regional transtension, large-scale strike-slip faults active during the extension, as predicted by general transtensional models, are not evident. Consequently it is inferred that the constriction was the result of laterally-varying crustal extension, where the top NNE extension was locally combined with left-lateral shearing. For the Nakhal anticline, where the direction of the finite elongation axis is N030E, the orientation of sinistral transtension deformation is NNE-SSW. Exhumation of the metamorphic series occurred beneath a carapace of extending allochthons which defined

an elongate pip of material that returned to shallow crustal levels. There is an imbalance however, between the net extension and the possible contraction within the Arabian continent which requires deformation within a volume of net-divergent tectonics. Thus crustal extension continued after the end of convergent tectonics in the region.

Table of contents

Chapter 1: Introduction 1
1.1 Introduction 1
1.2 Location of the study area 2
1.3 Thesis aims 3
1.4 Thesis format 4
1.5 Methodology 5
Methodology of data collection 5
Methodology of data presentation and analysis 5

Chapter 2: Literatures 8
2.1 Introduction 8
2.2 HP rocks in Oman 8
2.3 Tectonic and geological Setting 9
2.4 Exhumation processes 11
Erosion 11
Ductile flow 12
Normal faulting 12
Thrusting 13
2.5 Methodology for testing various exhumation processes 13
2.6 Role of extension in the mountain built 14
Extension-related exhumation 14
Folding associated with an extensional shear zone 15
2.7 The distribution of the extensional tectonics in the Oman Mountains 15
2.8 The structures and exhumation of HP rocks in Saih Hatat 16
2.9 Geology of Jebel Akhdar 18
2.10 Previous interpretations for the folding of the northern Oman Mountains 21

Chapter 3: Structural deformation along the Akhdar anticline 24
3.1 Introduction 24
3.2 AL-Hamra transect 26
Introduction 26
Large scale structures 26
Deformation fabrics 27
Interpretation and summary 27
3.3 Wadi Ghul transect 28
3.3 Wadi Ghul transect 29
3.3 Wadi Ghul transect 30
Introduction 30
Large scale structures 30
Deformation fabrics 30
Interpretation and summary 31
3.4 Summary of the structural deformations along the Southern flank 34
3.7 Wadi Mistal transect 35
3.7 Wadi Mistal transect 36
Introduction 36
Large scale structures 36
Deformation fabrics 37
Interpretation and summary 38
3.6 Wadi beni Harras transect 42

Introduction 42
Large scale structures 42
Deformation fabrics 42
Interpretation and summary 43
3.7 Wadi beni Kharus transect: 45
Introduction 45
Large scale structures 45
Deformation fabrics 46
Interpretation and summary 46
3.7 Wadi beni Awf transect 50
Introduction 50
Large scale structures 50
Deformation fabrics 51
Interpretation and summary 51
3.8 Wadi Fara transect 56
Introduction 56
Large scale structures 56
Small scale structures 57
Deformation fabrics 57
Interpretation and summary 58
3.9 Wadi Sahtan transect 60
Introduction 60
Large scale structures 60
Deformation fabrics 61
Interpretation and summary 61
3.10 Wadi Ghariz transect: 65
Introduction 65
Large scale structures 65
Small scale structures 65
Deformation fabrics 66
Interpretation and summary 66
3.11 Wadi Yiqa transect 69
Introduction 69
Large scale structures 69
Deformation fabrics 70
Interpretation and summary 70
3.12 Summary of the structural deformations along the Northern flank 75
3.13 Structural correlation between the southern and northern flank of the Akhdar anticline 78

Chapter 4: Structural deformation along the Nakhal anticline 81
4.1 Introduction 81
4.2 Wadi Hedk transect 82
4.2 Wadi Hedk transect 83
Large scale structures 83
Small scale structures 84
Deformation fabrics 85
Interpretation and summary 86
4.3 Wadi Alsarir transect: 91
Large scale structures 91
Deformation fabrics 92
Interpretation and summary 93
4.4 Wadi Hasnat Transect: 96

Large scale structures 96
Small scale structures 96
Deformation fabrics 96
Interpretation and summary 97
4.5 Wadi Qarah transect 99
4.5 Wadi Qarah transect 100
Large scale structures 100
Small scale structures 101
Deformation fabrics 101
Interpretation and summary 101
4.6 N-S transect across the Fanja anticline 104
Large scale structures 104
Deformation fabrics 105
Interpretation and summary 106
4.7 E-W transect along the Fanja anticline 110
Large scale structures 110
Deformation fabrics 111
Interpretation and summary of the structural deformation of the Fanja anticline 111
4.8 Al-Meeh transect 115
Large scale structures 115
Deformation fabric 117
Interpretation and summary 118
4.9 AL-Tayah transect 125
Large scale structures 125
Deformation fabrics 127
Interpretation and summary 127
4.10 AL-bir transect 131
4.10 AL-bir transect 132
Large sale structures 132
Deformation fabrics 133
Interpretation and summary 134
4.11 Dhabiah Transect 138
Large scale structures 138
Deformation fabrics 141
Penetrative deformation type locality 142
Interpretation and summary 144
4.12 AL-Qet Transect 151
Large scale structures 151
Small scale deformations 155
Interpretation and summary 156
4.13 Toyan transect 163
Large scale structures 163
Deformation fabrics 164
Interpretation and summary 164
4.14 Afiah transect 169
Large scale structures 169
Deformation fabrics 170
Interpretation and summary 171
4.15 Discussion and Summary 174
The NE-extensional system 174
The NW-SE contractional deformation 176
Linking between the extensional and contractional deformational systems 177

Chapter 5: Saih Hatat 181
5.1 Introduction 181
5.2 Structural setting of Saih Hatat 181
5.3 The structural geology of HP rocks in Saih Hatat (according to the literature) 183
Structural style of the upper plate 183
Structural style of the lower plate 184
N-S trending folds 184
Timing of the eclogite metamorphism 184
5.4 Results of the current work 184
Structural style of the upper plate 184
Structural style of the lower plate 187
N-S trending folds 187
5.5 Interpretation and Summary 189

Chapter 6: Data synthesis 190
6.1 Introduction 190
6.2 Top-to-the-NNE layer-extensional shearing 190
6.3 NW-SE compressional deformation 193
6.3 NW-SE compressional deformation 194
6.4 Steeply dipping faults 194
6.5 Interpretation and assessment of the relative chronology of various structural deformations 198
The Jurassic faulting 199
The NNE-extensional deformation 200
The NW-SE compression 204
The NNE-oriented faults along the eastern flank of the Nakhal anticline 205
The massif-bounding faults 206

Chapter 7: Discussion of a transtensional model for the structural evolution of the Akhdar Massif 208
7.1 Introduction 208
7.2 Geometry and kinematics of Late Cretaceous extensional deformation in the Oman orogen 208
7.3 Evaluating the plane strain extension model (Breton's model) 209
7.4 Synchronicity of folding and extension deformations 210
7.5 Geometry of synchronous folding and extension deformations 211
Jebel Akhdar 211
Jebel Nakhal 211
Saih Hatat 212
Partitioning of NNE-extension deformation 213
Summary 213
7.6 Why a transtension model ? 213
Folding models of the Oman orogen 213
Extension and exhumation of the NE margin of the Arabian plate 214
Models of synchronous folding and extension 215
Transtension model 216
7.7 Geometry and kinematics of transtensional deformation 217
Geometry and kinematics of transtensional deformation applied to Oman 217
Kinematics 218
7.8- Mechanisms of transtension deformation 219
Strike slip faulting 220

Lateral differential extension 220
7.9 Discussing implications of transtension model 222
Synorogenic crustal deformations 222
Synorogenic exhumation 229
The cross-folding in the Oman orogen 230
Tertiary uplift and deformation 232
7.10 Summary 234

Chapter 8: Conclusions and Implications 236
8.1 Introduction 236
8.2 Conclusions 236
8.3 Implications 238

References 240

List of Figures

Chapter 1
Fig. 1- 1 Geological map of the northern Oman Mountains 3

Chapter 2
Fig.2- 1 The Jolivet et al. (1998) model of NNE-directed extensional detachments throughout the Saih Hatat culmination 9
Fig.2- 2 Schematic illustration of three exhumation processes: normal faulting, ductile flow and erosion 11
Fig.2- 3 Gravity collapse model for the Akhdar culmination 16
Fig.2- 4 The Miller et al. (2002) model of NNE-extension and thrusting along a SSW-dipping intracontinental subduction zone 17
Fig.2- 5 The Searle et al. model for Saih Hatat of thin-skinned, SSW-directed thrusting above NNE-dipping subduction zone 18
Fig.2- 6 Stratigraphic log of the northern Oman Mountains 19
Fig.2- 7 Structural models of Jebel Akhdar 22

Chapter 3
Fig. 3- 1 Geological map of Jebel Akhdar shows the locations of the constructed transects 25
Fig. 3- 2 The Al-hamra transect with stereograms of the different structural elements 28
Fig. 3- 3 Faults and deformation fabrics along the Al-hamra transect 29
Fig. 3- 4 The Ghul transect and the stereograms of the various structural elements. The photograph shows steeply dipping NW-trending faults within Salil 32
Fig. 3- 5 Deformation fabrics along the Wadi Ghul transect 33
Fig. 3- 6 Summary of structural elements mapped along each transect of the southern flank 35
Fig. 3- 7 The Mistal transect with stereograms of the various structural elements collected along the transect 40
Fig. 3- 8 Fault structures along the Mistal transect 41
Fig. 3- 9 The Wadi beni Harras transect with stereograms of the different structural elements 44
Fig. 3- 10 The Kharus transect as constructed across the Mehsaneh structure, with stereograms for the various structural elements 47
Fig. 3- 11 Sedimentation and erosional features along the Kharous transect 48
Fig. 3- 12 The Mahsanah half graben structure 49
Fig. 3- 13 The Awf transect with stereograms of the various structural elements 53
Fig. 3- 14 Imbricate structures within the Jurassic-Cretaceous units 54
Fig. 3- 15 Deformation fabrics along the Awf transect 55
Fig. 3- 16 The Fara transect with stereograms of the various structural elements 59
Fig. 3- 17 The Sahtan transect with stereograms of the various structural elements 63
Fig. 3- 18 The different styles of faulting along the Sahtan Transect 64
Fig. 3- 19 The wadi Ghariz transect with stereograms of the various structural elements 67
Fig. 3- 20 Deformation fabrics along Ghariz transect 68
Fig. 3- 21 The Yiqa transect with stereograms of the various structural elements 72
Fig. 3- 22 Deformation fabrics along the Yiqa transect 73
Fig. 3- 23 Extensive NW-trending normal faults forming a series of horst and graben structures within the Shams Fm 74
Fig. 3-24 Summary of the structural elements mapped along each transect of the Northern flank 77
Fig. 3-25 Structural correlation across the Akhdar anticline 80

Chapter 4

Fig. 4- 1 Geological map of Jebel Nakhal showing the locations of the constructed transects 82
Fig. 4- 2 The Hedk transect with stereograms of the various structural elements collected along the transect 88
Fig. 4- 3 Fracturing along the Hedk transect 89
Fig. 4- 4 Fold and cleavage structures along the Hedk transect 90
Fig. 4- 5 The Sarir transect with stereograms of the different structural elements collected along the transect 94
Fig. 4- 6 Deformation fabrics along the Sarir transect 95
Fig. 4- 7 The Hassnat transect with stereograms of the different structural elements collected along the transect 98
Fig. 4- 8 Deformation fabrics along the Hasnat transect 99
Fig. 4- 9 The Qarah transect with stereograms of the different structural elements collected along the transect. 102
Fig. 4- 10 Monoclinal folding along the Qarah transect 103
Fig. 4- 11 N-S transect across the eastern plunge of the Nakhal anticline with stereograms of the different structural elements collected along the transect 107
Fig. 4- 12 Steep E-W and NW-striking faults along the Fanja anticline 108
Fig. 4- 13 Highly stretched and partitioned sandstone lenses floating within a matrix of clayey limestone 109
Fig. 4- 14 The E-W transect along the eastern plunge of the Nakhal anticline, with stereograms of the various structural elements collected along the transect 113
Fig. 4- 15 Faults along the southern flank of the Fanja anticline 114
Fig. 4- 16 The Almeeh transect with stereograms of the different structural elements collected along the transect 120
Fig. 4- 17 NW-SE and E-W steep faults along the Almeeh transect 121
Fig. 4- 18 Isoclinal folds within the Jurassic-Cretaceous succession along the Almeeh transect 122
Fig. 4- 19 Isoclinal folds in a highly stretched and boudinaged limestone bed in the upper part of the Kh2 Fm 123
Fig. 4- 20 Deformation fabrics along the Almeeh transect 124
Fig. 4- 21 Tayah transect with stereograms of the different structural elements collected along the transect 129
Fig. 4- 22 Faulting and folding deformation along Almeeh transect 130
Fig. 4- 23 Deformation fabrics along the Tayah transect 131
Fig. 4- 24 The Albir transect with stereograms of the different structural elements collected along the transect 135
Fig. 4-25 Faulting deformation along the Albir transect 136
Fig. 4- 26 A half graben structure occupied with the Jurassic-Cretaceous succession and its association with the major NE-fault 137
Fig. 4- 27 The Dhabiah transect with stereograms of the different structural elements collected along the transect 146
Fig. 4- 28 Different phases of faulting along the Dhabiah transect 147
Fig. 4- 29 Structural elements of the extensional duplex structures mapped within the Kh2 Fm 148
Fig. 4- 30 Line drawing for the various penetrative structures, with their stereographic projections, as mapped in the type locality [5] 149
Fig. 4- 31 Close up view of the penetrative structures type locality 150
Fig. 4- 32 (a) Qet transect with stereograms of the different structural elements collected along the transect 159
Fig. 4- 33 Lower Jurassic faulting marked by thickening of the lower Sa succession across the fault 160
Fig. 4- 34 Deformation fabrics along the Qet transect 161

Fig. 4-35 Structural analysis of NW-trending graben structures mapped along the Qet transect 162
Fig. 4- 36 The Toyan transect with stereograms of the different structural elements collected along the transect 166
Fig. 4- 37 The major NE-fault across the Toyan transect 167
Fig. 4- 38 Structural deformations in the fold crest 168
Fig. 4- 39 The Afiah transect with stereograms of the various structural elements collected along the transect 172
Fig. 4- 40 Fault and deformation fabrics along the Afiah transect 173
Fig. 4- 41Summary of the NE-directed extensional deformation along each transect of the Nakhal anticline 179
Fig. 4- 42 Summary of the NW-SE directed shortening deformation along each transect of the Nakhal anticline 180

Chapter 5

Fig. 5-1 Geological map of northeastern Saih Hatat 181
Fig. 5-2 Structural transect across the Saih Hatat culmination 186
Fig. 5-3 Different folding styles within the Saih Hatat culmination. 188

Chapter 6

Fig. 6- 1 Schematic cross section across the Akhdar-Nakhal-Hatat culminations 191
Fig. 6- 2 Lineations and fold hinge data throughout the Oman orogen 193
Fig. 6- 3 Attitude and kinematics of the NW-striking 196
Fig. 6- 4 Collation of structural relationships at the base of tectonic allochthon 199
Fig. 6- 5 Schematic representation of geometry and kinematics of NNE-directed extension within the NE margin of the Arabian plate. 202
Fig. 6- 6 Schematic cross section across the Akhdar culmination 201
Fig. 6- 7 Schematic block diagram of the Saih Hatat 203
Fig. 6- 8 Schematic block diagram across the Nakhal culmination 205
Fig. 6- 9 Structural models for the development of lineation-parallel folds. 206
Fig. 6- 10 The distribution of the massif-bounding faults throughout the Oman orogen. 207

Chapter 7

Fig. 7- 1 The Breton et al. (2004) model of the Late Cretaceous structural deformation of the NE margin of the Arabian plate 210
Fig. 7- 2 NW-striking faults with massif-pitching lineations across the Nakhal anticline 212
Fig. 7- 3 Models for constriction. 216
Fig. 7- 4 The coexistence of extension and stretching lineation-parallel folds 217
Fig. 7- 5 Partition of the NNE-directed extensional deformation 218
Fig. 7- 6 Hypothetical sinistral transtensional deformation along the Masirah fault 220
Fig. 7- 7 3-D conceptual model for the Late Cretaceous structural deformation 221
Fig. 7- 8 Schematic illustration for the crustal deformation during the exhumation 223
Fig. 7- 9 Qualitative structural model for the Late Cretaceous exhumation 226
Fig. 7- 10 Qualitative structural model for the Akhdar anticline 227
Fig. 7- 11 Channel flow model proposed for the High Himalaya 229
Fig. 7- 12 kinematic models for linking synchronous extension and contraction. 229
Fig. 7- 13 Tertiary uplifting of the northern Oman orogen due to rifting along the Gulf of Oman 233

Abbreviations

Hp	High pressure rocks
Mi	Mistal Formation
Sq	Saiq Formation
Ma	Mahil Formation
Sa	Sahtan Formation
Kh1	Rayda Formation
Kh2	Salil Formation
Kh3	Shams Formation
Nu	Nahr umr Formation
Na	Natih Formation
Ar	Aruma Formation
Op	Ophiolite
Hw	Hwasina sediments
Fm	Formation

Chapter 1: Introduction

1.1 Introduction

Deformation of the NE margin of the Arabian continental crust followed the Late Cretaceous obduction of the Semail Ophiolite and deepwater Hawasina sediments (Glennie et al. 1974). Meanwhile, the Arabian plate was partially subducted and metamorphosed under high pressure conditions. Subsequently the Arabian continent, below the allochthons, was bulged up to form a series of culminations, the largest of which is Jebel Akhdar. The culminations are classically attributed to thrust-related folding-structures that emerge in the foreland to the south. Late fault structures along the flanks of the culmination have been attributed to shallow-level gravitational collapse (Hanna et al. 1990). These structures locally omit tectonic sections, for example placing ophiolite directly against self sediments of the Arabian continent

Large scale deformations of the Oman orogen have been attributed solely to contractional origin (e.g.: Hanna et al., 1990; Miller et al., 2002 and Searle et al. 2004), based on interpretation of shear deformation mapped in Saih Hatat. The Saih Hatat culmination, where the deeply buried rocks of eclogite and blueschists facies are exposed, is characterized by extensive NNE-directed shear deformation associated with pressure gaps. However, Jolivet et al. (1998) argued for crustal extension in Saih Hatat, because the detachments omit metamorphic sections by placing rocks that have not experienced ecolgitic conditions on top of those that have. Furthermore they attribute the exhumation of the deeply subducted tract of the Arabian plate to synconvergence crustal extension. For this reason the tectonic significance of top-NNE-directed shear within the metamorphic rocks of Saih Hatat is controversial.

Recently Breton et al. (2004) found evidence of NNE-directed extension within the shallowly buried rocks of Jebel Akhdar. This extensional deformation is manifested by top-NNE low angle detachments along with NNE-verging ductile shear deformation. The deformation increases northeastwardly toward the deeply buried rocks of the Hatat culmination. Breton et al. (2004) linked the extensional deformation to the exhumation of the autochthon during the Campanian, based on top-NNE kinematic data and retrograde metamorphic parageneses associated with the deformation fabrics. However, their work was conducted at only a few localities distributed throughout the Akhdar-Nakhal massifs including just one single site over the whole of the Nakhal anticline. That led to provide a slight qualitative description of the extensional deformation and the associated deformation

fabrics, but neither accounts for the folding of the different culminations nor the relationships between folding and the NNE-directed extension. Consequently, the current study explores thoroughly the NNE-directed extension over the whole Akhdar-Nakhal culminations and presents evidence of synorogenic extension associated with the exhumation of the HP rocks.

1.2 Location of the study area

The Sultanate of Oman is situated on the southeastern margin of the Arabian plate (Fig. 1.1). Geographically, the most prominent feature is the northern Oman Mountains, also known as the Hajar Mountains, with a length of about 700 km, a width varying between 40 and 130 km, and elevations of up to 3,000 m above sea level (Rabu et al, 1986). Plate boundaries of several different types delineate the Arabian Plate. In the west, a divergent boundary extends through the Red Sea and into the Gulf of Aden. In the northwest, the sinistral Dead Sea transform fault system separates the Arabian Plate from the Sinai and Levantine sub-plates of the African Plate. The northern and the northeastern boundaries are continent-continent collision zones between the Arabian and the Eurasian plates along the Bitlis and Zagros sutures. The Zagros suture continues south and transforms into the continent-oceanic Makran subduction zone. The Owen and Murray transform faults mark the southeastern boundary of the Arabian Plate with the Indian Plate (AL-Lazio et al. 2002).

Two prominent domal structures in the Oman Mountains are the 3,000-m-high Jebel Akhdar and Saih Hatat. They provide a window onto the stratigraphy of the pre-Permian and Hajar Supergroup sequences and have been intensively investigated with regards to the timing and mechanism of the deformation. In the Saih Hatat culmination, the Permian Saiq and Triassic Mahil formations of the Hajar Supergroup dip away from the pre-Permian rocks exposed in their cores. The fold axis of Saih Hatat plunges gently to the SE and steeply to the west. The two domal structures are offset from each other across an important divide known as the Semail Gap and by contrast, the Jebel Akhdar structure plunges gently to the WNW and very steeply to the east. There is however another structural complication in having a narrower anticlinal arch (known as Jebel Nakhal), which extends northwards parallel to the Semail Gap, but has a short, east pointing "nose" at its northern end.

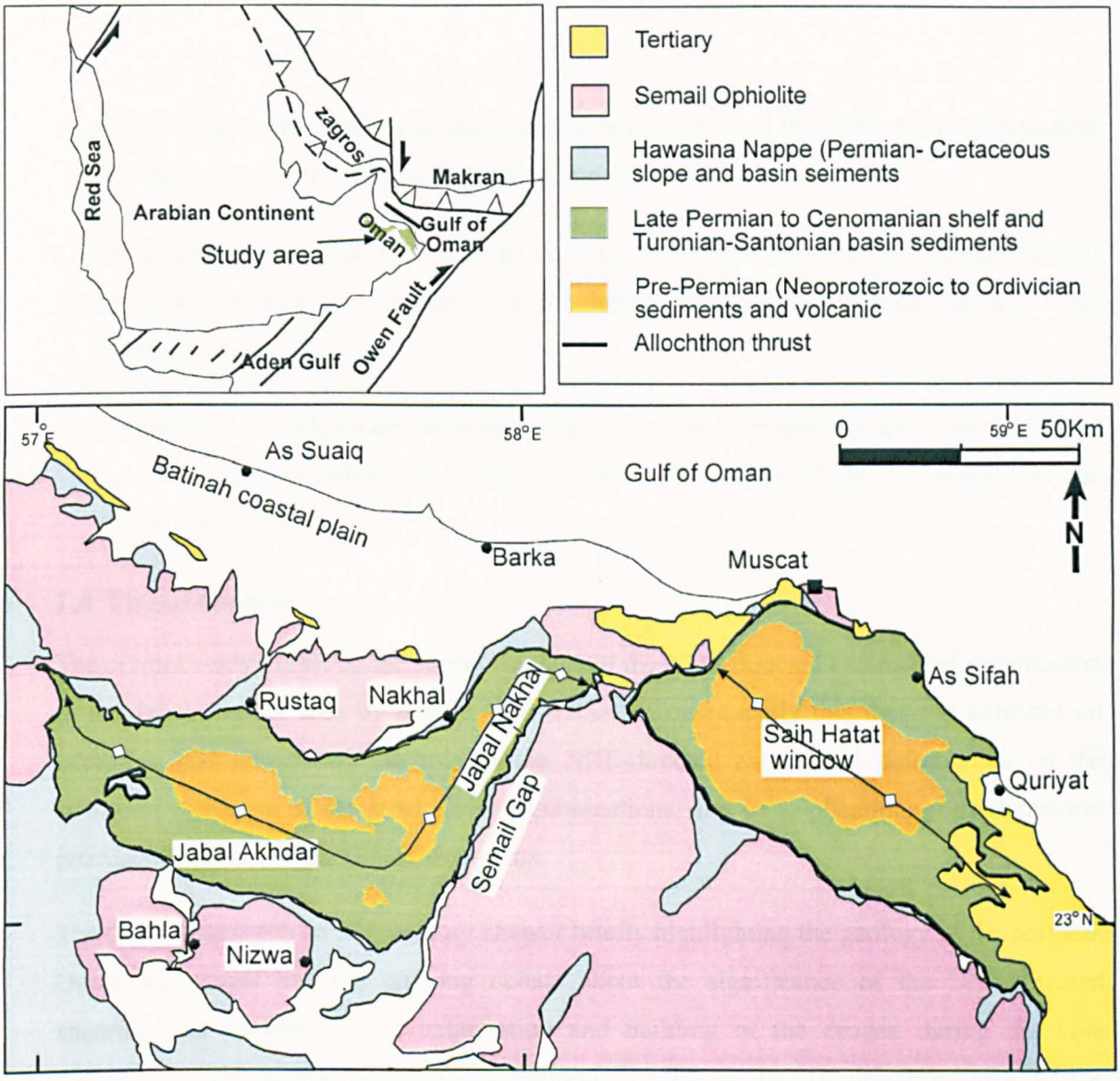

Fig. 1- 1 Geological map of the northern Oman Mountains shows the location of the study area. The inset illustrates the plate tectonic setting of the Arabian plate

1.3 Thesis aims

This thesis concentrates on the structural deformations of the Akhdar-Nakhal culminations, particularly the NNE-directed extension which took place during the Late Cretaceous following the Ophiolite emplacement. A model developed by Breton et al. (2004) model pointed out the existence of a NNE-directed extension over Jebel Akhdar, and this study will use that work as a starting point. The aims of the research which will be accomplished and documented in this thesis are:

- To explore thoroughly the extent of the NNE-directed extension over the entire Akhdar-Nakhal culminations, and to present advanced and complete qualitative analysis of this deformation.

- To investigate the relationship and relative timing between the NNE-directed extension and the folding of the Akhdar-Nakhal culminations.

- To correlate and link between the structural deformations of the Akhdar-Nakhal culminations with the structures of the highly metamorphosed rocks of the Hatat culminations.

- To present a reliable model accounting for the crustal extension and the cross-folding of the Oman orogen, while addressing the rapid exhumation of the NE margin of the Arabian plate.

1.4 Thesis format

The current study builds on the recent findings of the NNE-directed extensional deformation in the Jebel Akhdar area by Breton et al. (2004). Consequently this thesis is centered on exploring and reassessing the role of the NNE-directed extensional deformation on the structural evolution of the Jebel Akhdar culminations, and its implications for exhumation processes in the northern Oman Mountains.

The thesis starts with an introductory chapter briefly highlighting the geology of the northern Oman Mountains and the ongoing debate about the significance of the NNE-directed shearing and its role on the exhumation and building of the orogen during the Late Cretaceous. The second chapter is a literature review of the structural geology of the northern Oman Mountains, particularly the Akhdar culminations and the HP rocks of Saih Hatat. The various models of exhumation processes and cross-folding are reviewed in detail. The transtension deformation, which will be the base of the newly proposed model, is also thoroughly reviewed.

The collected field data is presented in three main chapters, Jebel Akhdar, Jebel Nakhal and Saih Hatat according to their topographic locations. Each chapter is divided into several structural transects, which were constructed in the field. In each transect, data is presented and analysed relative to its size, starting with the regional large-scale structures like km-long faults and folds, and finishing up with small scale deformation fabrics like cleavage and intrafolial small folds. A local interpretation and summary are presented at the end of each transect, while regional interpretations and conclusions are embedded at the end of each chapter.

Data from the various culminations is then collectively synthesised and interpreted in a regional term at chapter six. Findings are discussed and a new model of the transtensional deformation is proposed, along with its implications for the exhumation process in the

northern Oman Mountains, in chapter seven. Finally, chapter eight concludes the field findings and the results achieved.

1.5 Methodology

Several methods were used for field data collection and the subsequent data presentation and analysis. These methods are explained individually as follows.

Methodology of data collection

The current study was based on field work conducted over three consecutive field seasons (2003, 2004, and 2005), which lasted a total of 9 months. The field work was designed to construct numerous structural transects across and along the Akhdar and Nakhal anticlines. A total of 23 structural transects were constructed along almost every accessible wadi. Vast amounts of planar and linear structural data was collected from every stratigraphic unit crossed by each transect, especially data related to the NNE-directed extensional deformation. Structural elements were measured by using a Silva Ranger 15TD-CL compass-clinometer. Unless otherwise stated, all readings are strike/dip and dip direction for planar fabrics and plunge/plunge direction for linear fabrics. All measurements of fold orientations are based on measuring the hinge lines unless otherwise stated

The most striking structural features are bedding-parallel shear zones. These zones are manifested by intensive ductile deformation, localised within the fine-grained units. The shear zones separate variously deformed strata and are marked by pervasive lineations, commonly of calcite fibres. Steep normal faults merge and branch onto the shear zones. Consequently, these shear zones behave as detachments and are hence referred to as detachments throughout the entire thesis.

Methodology of data presentation and analysis

The collected field data was presented and analysed alongside its corresponding transect. For each transect, data is presented and analysed relative to its size, beginning with the regional large-scale structures such as km-long faults and finishing up with small-scale deformation fabrics like cleavage and intrafolial small folds. A structural analysis and summary are presented at the end of each transect. The mapped structures are documented by photographic images, which involve an easily recognized scale such as hat or field note, otherwise scale is written in the image captions.

Structural data is stereographically represented on a lower-hemisphere stereonet by the use of TectonicsFP (version: 1.62.1.11159-DEM) by Franz Reiter and Peter Acs. Transect data of similar structures (folds for example) is grouped together and presented on one

stereogram, despite different stratigraphic locations providing it was collected along the same transect. Since stratigraphic beds are tilted throughout the study area, it was frequently necessary to restore the tilting deformation in order to obtain the initial geometry of the associated structures, such as faults and cleavage. Restoring the tilting or folding deformation was achieved by rotation of beds back to horizontal around a horizontal axis presumed to be parallel to the culmination axis. The fold axis is calculated based on the average dip of the deformed strata, usually Jurassic-Cretaceous strata. When it comes to restoring the faults and lineation data, it has been assumed that, if unfolding of clustered faults and lineations produces scattered patterns then this is used to infer that faulting must post-date the folding deformation. The location of each transects and the most important photos are documented in UTM configuration.

One of the thesis objectives is to assess the interrelation between the culmination folding and the dominant NW-trending faults. This assessment relies mainly on the fault attitudes and kinematics. Such an assessment can not be addressed on the Akhdar anticline due to sub-parallelism between the fault trends and the fold axis, unlike on the Nakhal anticline, where faults and folds are highly oblique to each other. If faults were initiated prior to the folding deformation they would be subsequently deformed by the folding deformation. The consequences of the folding deformation over the pre-folding normal faults is manifested by rotation of the faulted beds and associated dip slip fault lineations (see, (Tavarnelli and Peacock 1999)). The pre-folding, NW-trending faults exhibit lineation pitching towards the massifs on both flanks of the Nakhal anticline. However, the post folding NW-trending faults are marked by dip slip lineations which are not affected by the folding deformation.

Faults are classified relative to their length into large faults running for several km's and small faults of metric length. Furthermore, faults are also classified according to their inclination angle. Faults dipping less than 30° are described as gently dipping faults, faults dipping between 30°-60° are called moderately dipping faults, and steep faults are those dipping at more than 60°.

The interpretation of the NNE-directed shear deformation in Saih Hatat is controversial as to whether it is crustal extension or contraction. The same question can be asked for the mapped apparent extension on Saih Hatat whether it represents stratal or crustal extension. These controversies are relevant in the internal zones of orogens where intense deformation may have created non-horizontal layering prior to the formation of possible extension structures (Wheeler et al., 1994). However, a better understanding of such matters may be achieved by linking the complicated structures of the deeply buried rocks of Saih Hatat with the structures of the shallowly buried rocks of the Akhdar-Nakhal culminations. This

approach was followed during this study. Other criteria such as discriminating between stratal and crustal extension are discussed thoroughly in the literature chapter.

Chapter 2: Literatures

2.1 Introduction

In this chapter, the main areas related to the current study are reviewed thoroughly, starting with the geological setting of the northern Oman Mountains, and in particular the structure of the HP rocks in Saih Hatat. Examining the various models of exhumation of the HP rocks is essential in understanding the Late Cretaceous structural evolution of the Oman orogen. Such an exhumation is controversial between different research groups (Jolivet et al. 1998; Miller et al. 2002; Searle et al. 2004), therefore reassessment of the various exhumation mechanisms and identification of the diagnostic features of each mechanism is crucial in pinpointing the model relevant to the northern Oman Mountains. This study focus on extension-related exhumation as the results becomes clear about the role of extension in the Oman orogen. The applications of the extensional tectonics of the Oman orogen are also explored with respect to the cross folding observed in the Akhdar-Nakhal culminations. Eventually, the geology and the various folding models of Jebel Akhdar are reviewed in detail.

2.2 HP rocks in Oman

The presence of high-pressure eclogites in the northeast Saih Hatat window of the Oman Mountains has major implications for the tectonic evolution of the Arabian margin. The position of the HP rocks in Saih Hatat and the lack of agreement upon their structural association have produced varying geometrical interpretations of the window. Kinematic interpretations for the rocks beneath the ophiolite range from south-directed thrusting (e.g. Hanna et al. (1990), northeast-vergent nappes overprinted by south-vergent imbricate faults (Le Metour et al. 1990) and a series of folded units separated by large-scale low-angle extensional detachments (Michard et al. 1994). The controversy on the structural association of the rocks has led to various tectonic/exhumation models (e.g. Jolivet et al. 1998 and Miller et al. 2002). For this reason the structure of the Saih Hatat window, in particular the northeastern segment is of major importance for understanding the tectonic evolution of the Oman Mountains and for comprehending the mechanisms that eventually lead to the exhumation of high-pressure rocks.

Major detachments associated with metamorphic gaps have been identified by several researchers (e.g. Jolivet et al. 1998 and Miller et al. 2002), cutting down through the metamorphic section. One of these detachments separates the higher pressure blueschists and eclogites of As Sifah from the less metamorphosed upper plate rocks, involving fold-nappes

developed in the pre-Permian basement and the Hajar Supergroup (Fig.2- 1). Interpreting the nature of these detachments and the associated structures is essential in understanding the formation and exhumation of the high-pressure rocks in Oman. As previously mentioned, the interpretation of these detachments with top-NNE shearing is of great controversy among different research groups.

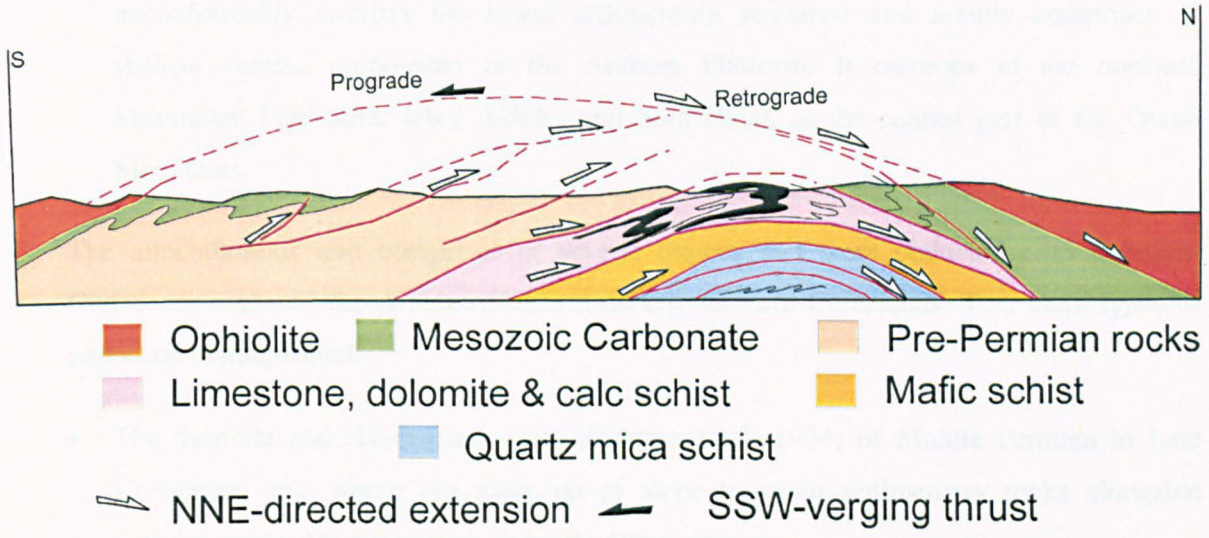

Fig.2- 1 The Jolivet et al. (1998) model of NNE-directed extensional detachments throughout the Saih Hatat culmination

Structurally, Saih Hatat is made up of a series of early-formed, regional, isoclinal recumbent folds, which are refolded by later upright N-S and NW-SE more open folds. The map pattern of Saih Hatat is dominated by dome and basin interference within the flat-lying layering and schistosity of the early recumbent folds (Miller et al., 2002).

2.3 Tectonic and geological Setting

The northern Oman Mountains comprises three major structural units that from the base up, are called Autochthon, Allochthon and NeoAutochthon respectively (Le Métour et al. 1995).

The autochthonous unit consists of:

- a crystalline basement of Late Proterozoic age (Roger et al. 1991), which outcrops mainly in the Jebal Ja'alan area in the southeastern part of the northern Oman Mountains. This crystalline basement is composed of igneous and metamorphic rocks above a sedimentary succession.
- a lower sedimentary sequence (Autochthon A) of Late Proterozoic to Devonian age. This unit mainly outcrops in Jebel Akhdar and Saih Hatat (Mann et al. 1990) in the central

part of the Oman Mountains, and locally in the southeastern and northern parts of the mountains.

- the Hajar Unit (Autochthon B) of Middle Permian to mid-Late Cretaceous age, which unconformably overlies the lower sedimentary sequence and mainly comprises of shallow marine carbonates of the Arabian Platform. It outcrops at the northern Musandam Peninsula, Jebel Akhdar and Saih Hatat, in the central part of the Oman Mountains.

The allochthonous unit comprises of several nappes that were obducted onto Permian-Cretaceous rocks of the Arabian Platform during the Late Cretaceous. Two main types of nappe are distinguished:

- The Sumeini and Hawasina nappes (Glennie et al. 1974) of Middle Permian to Late Cretaceous age, which are made up of slope to basin sedimentary rocks alongside volcanic rocks that outcrop all along the Oman orogen.

- The overlying Semail Nappe (10- to 12-km-thick), which represents relics of the Cretaceous Neotethyan oceanic lithosphere (Nicolas et al. 1988).

The neoautochthonous unit unconformably overlies all the other units and represents a postnappe sedimentary cover of Late Cretaceous to Late Tertiary age (Glennie et al. 1974; Nolan et al. 1990; Roger et al. 1991).

Rifting events that began in the Precambrian/Cambrian and early Permian led to the development of the pre-Permian units (Autochthon A) and the Hajar Supergroup (Autochthon B). The emplacement of the Late Cretaceous ophiolite was one of the most important tectonic events to have affected the eastern margin of the Arabian Plate (Glennie et al., 1974) and led to the emplacement of the Allochthonous sequence, composed of the Semail ophiolite and the Sumeini and Hawasina nappes (Shelton et al. 1990). The emplacement event spanned the Cenomanian to Coniacian stages (Béchennec et al. 1995), with the Late-Cretaceous deformation recorded by the various units of the Aruma Group. Units of the Muti Formation deposited during the Turonian-Coniacia/Santonian mark the transition from a passive continental margin to a foreland basin (Robertson 1987). The syntectonic Fiqa Formation was deposited during the Campanian to Maastrichtian, while the Simsima Fm, the upper part of the Aruma, was deposited in the Maastrichtian as post orogenic deposits after the ophiolite emplacement. The post-emplacement period was followed by the deposition of the Tertiary and Quaternary cover rocks (Glennie et al. 1974).

2.4 Exhumation processes

HP rocks are commonly exposed in the interior of many divergent and convergent orogens (Nie et al. 1994; Ring et al. 1999). Plate tectonics can account for high-pressure metamorphism by subduction and crustal thickening, but the exhumation of these metamorphosed crustal rocks is a more complicated problem. There are various processes such as normal faulting, ductile thinning and erosion which contribute to the exhumation of metamorphic rocks. Therefore, what are the criteria which can be used to distinguish between these different exhumation processes? Some of the exhumation processes that are relevant to the study area are described thoroughly below, along with their diagnostic features (Fig.2- 2).

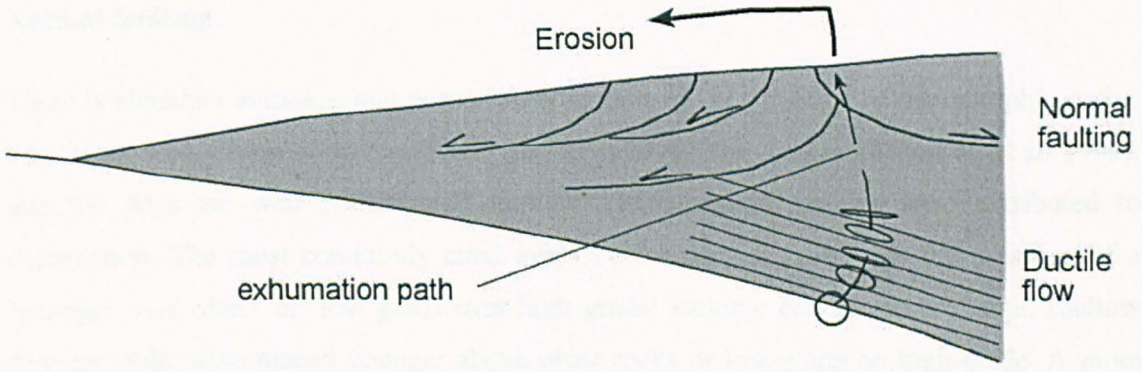

Fig.2- 2 Schematic illustration of three exhumation processes: normal faulting, ductile flow and erosion. The circles show undeformed particle accreted at the base of the wedge, which become deformed along the exhumation path, modified after Ring et al. (1998).

Erosion

Erosion has been recognized as an important process of unroofing the internal metamorphic zones of convergent mountain belts. The large volume of detrital deposits found adjacent to convergent continental orogens provides solid evidence that erosion is a significant exhumation process. Erosion is commonly assumed to be a slow exhumation process, but recorded erosion rates reach local values of 5-13 km^{-1} (e.g. Southern Alps of New Zealand and the Taiwan Alps). However, the exhumation rate alone can not distinguish different exhumation processes. Erosion acting as the main exhumation mechanism should expose HP rocks as part of a semi-complete crustal section. If this is not the case then at least one other mechanism must have been active, with or without erosion. Erosion will also produce a large volume of eroded sediment, which should match the volume of exhumed rocks if the erosion

was the sole exhumation mechanism (Nie et al. 1994). However, the preservation of such sediments will be low, particularly if delivered to trench-slope basins.

Ductile flow

HP rocks and their overburden may be initially thinned or thickened by ductile flow at a depth below the ductile-transition (Ring et al. 1999). This process can either support or obstruct exhumation, depending on whether the flow induces vertical thinning or thickening. The presence of sub-horizontal foliation is generally diagnostic of ductile thinning. Penetrative fabric is required for the ductile flow to contribute to a exhumation, rather than being limited to the margins of normal and strike slip faults. Ductile flow alone however, cannot fully exhume rocks to the surface and an additional exhumation process is required (Ring and Brandon 1999).

Normal faulting

There is abundant evidence that normal faulting aids the exhumation of metamorphic rocks. The Basin- and- Range province (Foster and John 1999), the Aegean (Thomson et al. 1999), and the Alps are well documented settings where normal faulting has contributed to exhumation. The most commonly cited evidence for normal faulting is the presence of a 'younger over older' or 'low grade over high grade' tectonic contact, where large, shallow dipping faults have placed younger above older rocks or low-grade on high-grade. A more diagnostic feature of a large-slip normal fault is the juxtaposition of a ductily deformed footwall with a brittlely deformed hanging-wall (Lister and Davis 1989).

The pattern of cooling ages can also provide evidence about the exhumation processes. Exhumation due to normal faulting commonly results in abrupt breaks in the cooling-age pattern, with younger ages in the footwall of the normal fault (Wheeler & Butler 1994). In contrast, erosional exhumation should be characterized by a relatively smooth variation in cooling age across the eroded region. Attenuation of stratigraphic or metamorphic units by itself is not diagnostic of tectonic thinning by normal faulting (Wheeler and Butler 1994), as thrusts faults can thin a stratigraphic or metamorphic section, provided that the section is tilted rearward before thrusting. In this case, the thrust may cut down section in the direction of transport, whilst cutting upwards towards the earth's surface. Occasionally, thrusts may be rooted by folding, block tilting or differential exhumation until their geometry resembles normal faults at the front of a thrust culmination. Conversely, normal faults are sometimes domed by isostatic rebound due to unloading of the footwall, until the fault has a local thrust sense of offset (Buck 1988; Lister & Davis 1989). For these reasons the kinematic development of a fault must be connected to the P-T evolution in its footwall and hanging-

wall at the time of tectonic transport. Alternatively, the displacement of a fault relative to the palaeosurface at the time of fault activity has to be expressed, in order to discriminate between normal faults and thrusts (Wheeler and Butler 1994).

Thrusting

(Platt 1993) pointed out that thrusting alone cannot tectonically exhume rocks. This is true if thrusting is restricted to a thin zone at the base of a sequence of nappes. However, in the internal zones of convergence orogens, nappes display a pervasive degree of internal deformation and flat-lying foliations. Such foliations indicate that the nappe stacking was associated with vertical thinning, which would eventually contribute to the exhumation of the nappes. In this regard it is interesting to note that high-pressure belts, as a rule, occur above lower grade units, indicating that the overburden of the high-pressure nappes must have been reduced prior to their emplacement above the lower pressure units. Pervasive ductile flow in the hanging wall associated with thrusting of high-pressure nappes may have supported the exhumation of the latter. Note that vertical ductile thinning can be associated with erosion and/or normal faulting in the upper parts of the nappe pile (Ring et al. 1999)

2.5 Methodology for testing various exhumation processes

The key to testing various tectonic models of the exhumation of specific metamorphic terrains is to trace structures from deep to shallow crustal levels and to be able to quantify the magnitude and timing of other displacements within an orogen. In many systems the exhumation of metamorphic rocks occurs before the end of the tectonic life of a mountain belt, e.g. the Alps (Freeman et al. 1998). One of the most confusing matters is differentiating exhumation induced by thrusting and that caused by normal faulting, since faults and shear zones in orogens may be related to crustal shortening or extension or both. There is a key distinction between the extension or shortening of layering (which is relatively straightforward to determine in the field), and the extension or shortening of the crust itself. The present dip of a fault in an orogen and its relation to local layering is an unreliable guide, while the observation of low-pressure metamorphic rocks structurally above high-pressure metamorphic rocks is not sufficient to identify crustal extension (Jolivet, et al., 1998). This is common in the internal zones of orogens where intense deformation may have created tilted layering prior to the formation of extensional structures (Wheeler and Butler 1994). Several criteria can be used to solve such problems. In the first criterion, true extensional structures should eventually intersect the Earth's surface when traced out in a direction opposite to that of the hanging-wall transport, and vice versa for the thrust structures (Wheeler and Butler 1994). The second criterion is based on the difference in pressure-time histories between the footwall and the hanging-wall. If the shear zone was related to crustal extension then the

pressure recorded by rocks in the footwall should, during shear zone movement decrease more rapidly than pressure recorded in the hanging-wall. The pressure-time history can be constrained via the temperature-time and pressure-temperature histories. Ideally, crustal extension inferred from structural data should be confirmed using diagnostic PT information (Wheeler &Butler 1994).

2.6 Role of extension in the mountain built

Extension-related exhumation

Extension within orogenic belts is now widely invoked, especially as a mechanism by which once deeply-buried metamorphic rocks are returned to the Earth's surface. Many mountain belts contain high strain zones separating metamorphic rocks that preserve large peak metamorphic pressures, from rocks above that show no evidence of having reached these conditions. Such an apparent loss of "barometric section" is generally interpreted as resulting from low-angle extensional shear (e.g. Jolivet et al., 1998). There are various kinematic models of the exhumation of once-deeply buried slabs of continental crust within mountain orogenies. (Wheeler et al. 2001) suggested two options; where once-subducted continental crust exhumed as either an "sliver" of crust open to the synorogenic surface, or as a completely fault-bounded "pip". In common with many models of synorogenic exhumation of HP metamorphic rocks, both options involved faults and shear zones with extensional kinematics on the upper side and contractional ones on the lower side of the exhuming rocks. These paired kinematic systems can be embedded within generally net convergent systems, such as the western Alps (Wheeler et al. 2001) or in areas where there is no net convergence on the plate scale as suggested for the Neogene Tyrrhenian-Apennine system (Lavecchia 1988). The driving force for these systems is the buoyancy of the subducted continental crust, relative to the mantle. Where the magnitude of extensional tectonics is not matched by displacements on the underside of exhumed, once-deeply buried crust, the plate kinematics must have been divergent (e.g. Krabbendam & Dewey 1998). The exhumation is accomplished isostatically, therefore the density of subducted crust is important but the driving factor is divergent tectonics.

The most dramatic example of exhumation related to truly divergent plate tectonics comes from the Caledonian chain in Norway (Krabbendam and Dewey 1998). The ultra high-pressure western Gneisses lie in the footwalls of major low-angle normal faults, some of which carry successions of Devonian syn-rift sediments (e.g. Hornelen Basin). Devonian rifting is inferred to have been oblique, governed in part by major basement lineaments. Consequently the kinematics were transtensional, as evidenced by concurrent thinning and constriction (Krabbendam & Dewey 1998). These transtensional models are interesting, not

least because they require concurrent orthogonal layer-parallel extension and contraction (Dewey et al. 1998).

Folding associated with an extensional shear zone

The synchronous development of low-angle normal faults (extensional detachments) and large-scale upright folds has been well documented in extended terranes throughout the world (Malavieille 1987; Mancktelow and Pavils 1994; Martinez and Soto 2002). Moreover, doubly plunging antiformal (domal) and synformal (basinal) geometries affecting both the detachment faults and their respective footwalls have fold axes both parallel and perpendicular to the direction of extension. It is a matter of debate as to whether these folds are formed by a single process or are related to the superposition of two mechanically independent processes. The single-process models that have been proposed are (1) the emplacement of synextensional plutons (Davis and Henderson 1999) (2) uncompensated undulatory Moho geometry during extension (Yin 1991) and (3) horizontal compression perpendicular to the direction of extension, generating finite constrictional deformations (Mancktelow and Pavils 1994; Krabbendam and Dewey 1998).

2.7 The distribution of the extensional tectonics in the Oman Mountains

The first workers who described the extensional deformation of the Oman orogen were Le Metour et al. (1990) and Breton et al. (2004). Their most striking conclusions can be summarized as follows:

- Regional foliations and cleavage, formed by the NE extension affect the entire autochthonous series A and series B up to the Muti Fm. They are therefore post-Coniacian in age.

- The intensity of metamorphism and deformation decreases from the northeast to the southwest, and dies out at the southern border of Jebel Akhdar. This is interpreted as the result of a northeastwards subduction of the autochthon.

- The Campanian obduction led to imbrications verging SSW within the autochthons

- The doming of Jebel Akhdar was post-cleavage and a multiphase event.

Coffield (1990) interpreted the decollement surfaces and associated cleavage and folds, observed in the autochthon at the northeastern end of Jebel Akhdar and at the western end of Saih Hatat, as a synobduction deformation that had been reactivated by a gravity collapse on the flanks of a Campanian-formed culmination. Breton et al. (2004) showed that the faults within the Arabian carbonate platform have a NE vergence and are associated with the

regional cleavage, resulting from a ductile shear deformation of the same vergence. Finally, a SSW-NNE seismically constrained crustal transect by Al-Lazki et al. (2002), crossing the Jebel Akhdar range from Fahud to the coastal plain provided a more precise view of the various crustal units. This demonstrated that there was no major repetition within the autochthon, but did suggest the presence of a crustal root beneath Jebel Akhdar. Hanna (1990) interpreted the massif-bounding faults in terms of a "culmination collapse", a process of gravity sliding from positive topography, represented here by the major antiform (Fig.2-3).

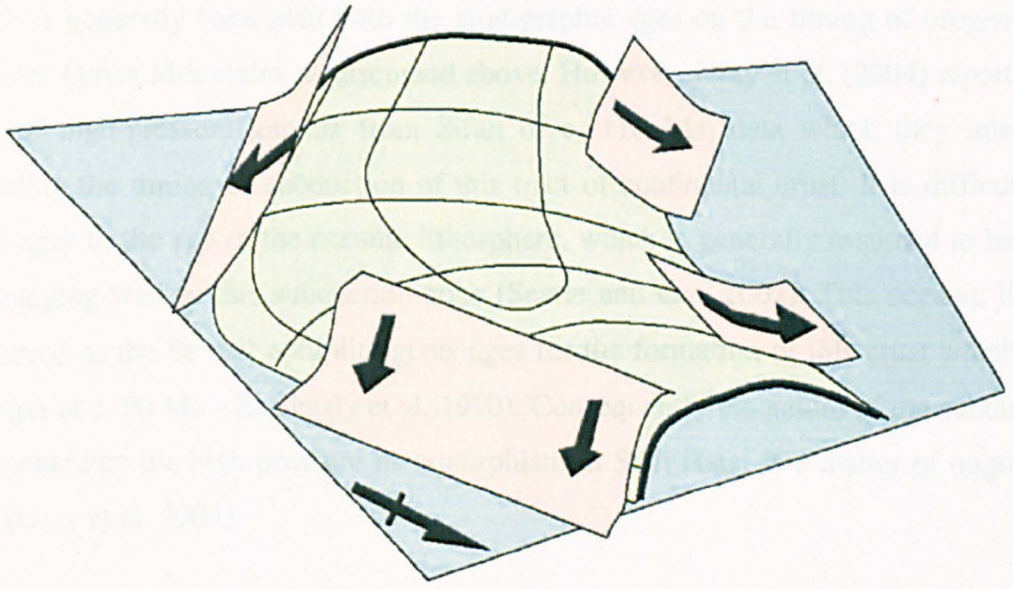

Fig.2- 3 Gravity collapse model for the Akhdar culmination, modified after Hanna et al. (1990)

2.8 The structures and exhumation of HP rocks in Saih Hatat

Metamorphic rocks recording the highest burial pressures are found on the NE part of the Saih Hatat Massif, near the village of As Sifah (El-Shazly et al. 1990). These eclogites are likely to have experienced peak pressure conditions of c. 20 kbar, although some workers suggest a burial to 25 kbar (Searle et al. 1994). The structural geology of these high-pressure rocks and their relationship to other parts of the Saih Hatat Massif has been studied recently by two different groups (Searle et al. 2004 and Miller et al. 2002). In these studies the relationship between the Sifah eclogites and the lower pressure rocks remains controversial. Nevertheless both groups show the importance of regional, NNE-trending mineral lineations and parallel sheath folds together with important detachment shears. The eclogites lie in a structural window overlain by rocks that have not experienced such extreme pressures. The two domains are separated by a folded detachment surface. Moving towards the western and

southern flanks of the Saih Hatat Massif the metamorphic grade decreases markedly, through glaucophane-carpholite bearing units (10-12 kbar) to the Fe-Mg carpholite isograd (7-8 kbar; see Jolivet et al, 1998 for discussion). The deformation state of these rocks is markedly less than that of the higher pressure sections of the massif. Jolivet et al. (1998) argued for a largely undeformed, but exhumed, subduction channel of continental rocks, from weakly buried to blueschist-facies conditions.

The timing of peak HP metamorphism within the eclogites of Saih Hatat is controversial. Rb-Sr (El-Shazly et al. 2001) and $^{40}Ar/^{39}Ar$ cooling ages (Miller et al. 1999) are 82-78 Ma, which is generally consistent with the stratigraphic ages on the timing of orogenesis in the northern Oman Mountains as discussed above. However, Gray et al. (2004) reported Sm-Nd ages of high-pressure garnets from Sifah of c. 110 Ma, data which they interpreted as recording the timing of subduction of this tract of continental crust. It is difficult to relate these ages to the age of the oceanic lithosphere, which is generally assumed to have formed the hanging-wall to this subduction zone (Searle and Cox 2002). This oceanic lithosphere, preserved as the Semail ophiolite gives ages for the formation of this crust which are much younger at c. 80 Ma, (El-Shazly et al. 1990). Consequently the nature of the subduction zone that generated the high-pressure metamorphism in Saih Hatat is a matter of ongoing debate (see (Gray et al. 2004).

The structural state and history of the higher grade parts of the Saih Hatat Massif have been variously explained in terms of simple NNE-directed extension of previously subducted crust (Jolivet et al. 1998) (Fig.2- 1), NNE-extension and thrusting above a SSW-dipping intracontinental subduction zone (Miller et al. 2002) (Fig.2- 4) and thin-skinned back-thrusting and extension associated with a single, evolving NNE-dipping subduction zone (Searle et al. 2004) (Fig.2- 5).

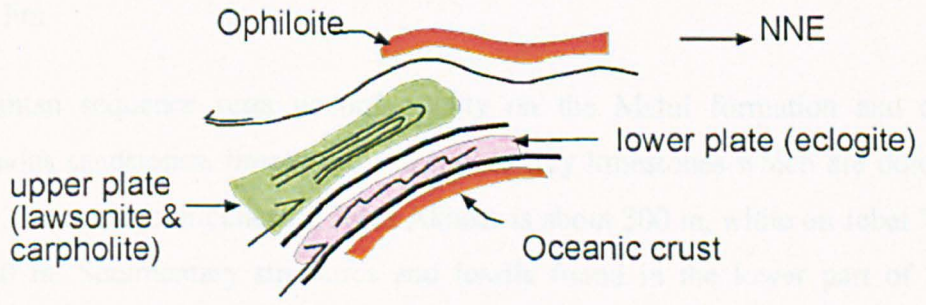

Fig.2- 4 The Miller et al. (2002) model of NNE-extension and thrusting along a SSW-dipping intracontinental subduction zone

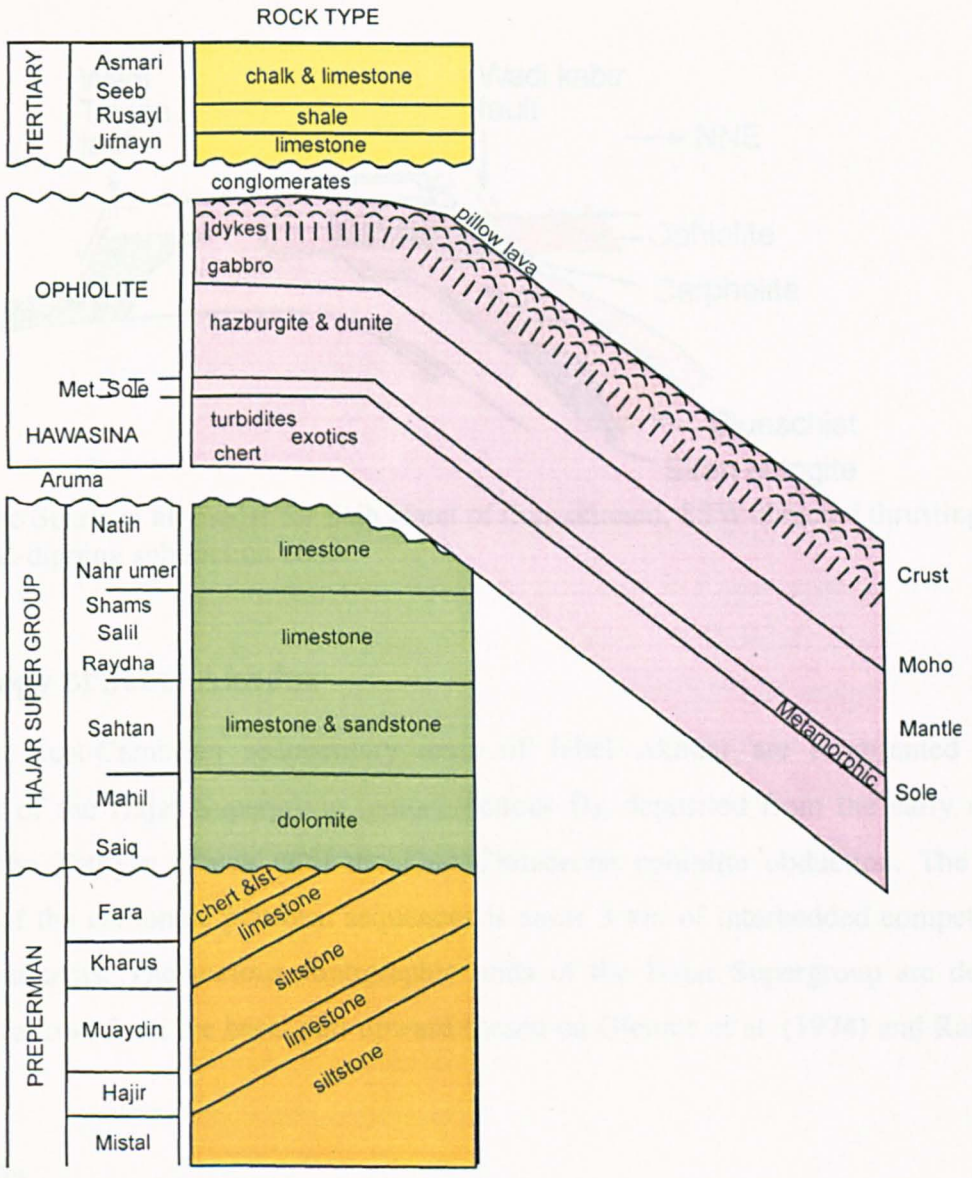

Fig.2- 6 Stratigraphic log of the study area

- Sahtan Fm

  The Sahtan sequence rests unconformably on the Mahil formation and consists of ferruginous sandstones, limestones and bluish-grey limestones which are dolomitized in places. The average thickness at Jebel Akhdar is about 300 m, while on Jebel Nakhal it is just 150 m. Sedimentary structures and fossils found in the lower part of the Sahtan Group point at a subtidal to intertidal depositional environment. The formation is rich in benthonic foraminifera, which indicates a Jurassic age of deposition.

- Rayda Formation

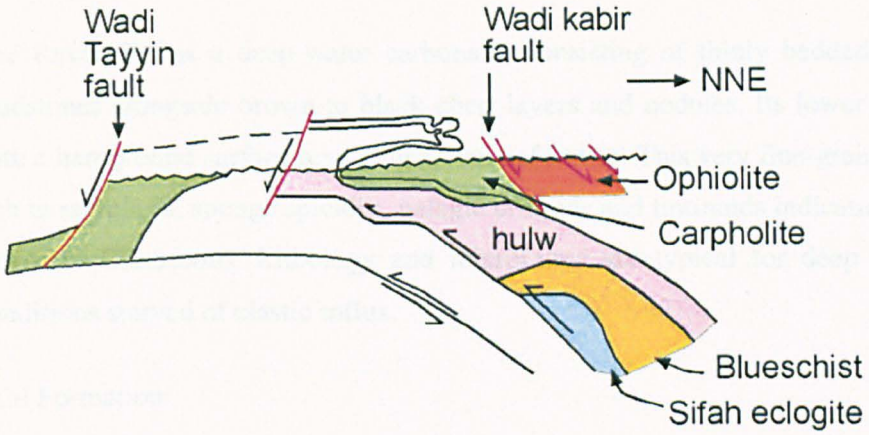

Fig.2- 5 The Searle et al. model for Saih Hatat of thin-skinned, SSW-directed thrusting above NNE-dipping subduction zone

2.9 Geology of Jebel Akhdar

The oldest post-Cambrian sedimentary units of Jebel Akhdar are represented by the carbonates of the Hajar Supergroup (autochthonous B), deposited from the early opening phase of the Tethyan Ocean until the Late Cretaceous ophiolite obduction. The typical thickness of the carbonate platform sequences is some 3 km of interbedded competent and incompetent units. The various stratigraphic units of the Hajar Supergroup are described briefly as follows from the basal part upward (based on Glennie et al. (1974) and Rabu et al. (1986).

- Saiq Fm

  The Permian Saiq Fm consists of dark, well bedded carbonates which unconformably rest on Pre-Permian sequences, with a type locality thickness of around 500 m. The formation comprises of limestones at the base and dolomites at the top. The depositional environment of the Saiq carbonates ranges from very shallow marine, lagoonal and supratidal in the lower part, to proximal subtidal in the upper section.

- Mahil Fm

  The Mahil Fm conformably rests over the Saiq Fm and is composed mainly of yellowish dolomite some 600 m thick. The lower and upper parts are composed of thin-bedded dolomites with detritus and intraformational breccias, while the remainder is constituted of massively bedded dolomite. The Mahil dolomites have been deposited in a highly restricted shallow marine to supratidal environment.

The Rayda Fm is a deep-water carbonate, consisting of thinly bedded, porcellaneous mudstones alongside brown to black chert layers and nodules. Its lower base is marked with a hardground surface revealing an unconformity. This very fine-grained limestone is rich in radiolaria, sponge spicules, pelagic crinoids and tintinnids indicating deposition in the early Cretaceous. Lithology and microfauna are typical for deep marine bathyal conditions starved of clastic influx.

- Salil Formation

The Salil Fm conformably overlays the Rayda Fm. The lower part consists of grey yellow argillaceous lime mudstones. The middle section is composed of massive dark coloured lime-mud and wackestone that forms steep cliffs. While in the upper beds interbedded lime-wackestones and argillaceous mudstones form numerous small cliffs. In contrast to the underlying Rayda Fm, this formation is characterized by the appearance of fine clastics suggesting turbiditic events and deposition in the proximal basin and on the slope. This Lower Cretaceous deposits represents the thickest incompetent succession of the platform succession.

- Shams Formation

The Shams Fm is composed of massive, competent fossiliferous limestone forming steep cliffs seen at the mouth of almost every wadi. It is approximately 400 m thick and rests conformably over the Salil Fm. The massive succession of this formation is interbedded with thin horizons of incompetent shaly limestone. Large pelecypods, rudists, gastropods and bryozoans indicate a very shallow and probably protected environment. On the extreme north of the Nakhal anticline this formation is eroded at the Wasia-Aruma break.

- Nahr Umr Formation

The Nahr Umr Formation forms a retreating slope and consists of Orbitolina marls and argillaceous limestone, suggestingdeposition in the middle to inner shallow shelf. The thicknesses of these incompetent deposits vary from 100 to 200 m.

- Natih Formation

The Natih Formation comprises of a number of sedimentary cycles consisting of shale and argillaceous limestone. The Natih limestone contains rudists and larger foraminifera (Orbitolinidae, Miliolidae, Alveolinidae) and is interpreted to have been deposited in a proximal shallow shelf area. The top of the Na Fm is marked by a hardground with an iron-rich crust, and is overlain by iron oolites of the basal Muti Formation.

The Hajar Supergroup is capped with the Late Cretaceous sediments of the Aruma Group. The lower part of this group called the Muti Fm was deposited in a foreland basin during the ophiolite obduction. The Muti Fm unconformably rests on the Natih Fm and consists of reworked ferruginous oolites, yellow-grey silty marls and conglomerate intercalations. The abundant biogenic content includes planktonic foraminifera, indicating deposition in deeper open marine waters, and bioclasts reworked from shallow environments. The Muti Formation is overlain and tectonically truncated by the Hawasina Nappe.

The flanks of the culminations are marked with slivers of the allochthonous units known as the Hawasina complex, comprising of deep clastic sediments deposited during extension and rifting in the Permian to Cretaceous. The development of the Hawasina basin was terminated in the Santonian, when compression that initiated the first stage of obduction closed the basin. Orogenic obduction during the Campanian led to thrusting of the Hawasina sequences and the Semail ophiolite nappes onto the Arabian platform (Glennie et al. 1974).

The ophiolite is the largest, best exposed and most studied ophiolite complex in the world. The crustal sequence of the ophiolite from the top is basaltic pillow lavas, sheeted dykes and then gabbros, while the mantle would be made of a rock known as peridotite. The Late Cretaceous ophiolite was obducted over the Arabian carbonate platform together with the deep turbiditic sediments of the Hawasina complex. The obduction took place somewhere between the Coniacian-Early Santonian (Jolivet et al. 1988).

2.10 Previous interpretations for the folding of the northern Oman Mountains

Much investigation of the origin and structural history of the Oman Mountains has been undertaken in recent years, and several different mechanisms have been proposed. The formation of the Jebel Akhdar anticline was attributed to Cretaceous-Tertiary uplift, while a major orogenic deformation in the core of the range was considered to be of Late Proterozoic age (Mann et al. 1990). The pre-Permian rocks exposed in the core of the Akhdar and Hatat culminations are deformed into a series of NE-SW trending folds and thrust imbrications, with deformation increasing in intensity towards the NE (Glennie et al. 1974). The authors considered this deformation to be syn-metamorphic and Hercynian in age.

Glennie et al. (1974) suggested that the present form of Jebel Akhdar and Saih Hatat resulted from Oligocene-Miocene uplift accompanied by gravity tectonism, rather than ophiolite obduction related deformation.

Cawood et al. (1990) and Hanna et al. (1990) attributed the pre-Permian folds and imbrications in Jebel Akhdar to a Late Paleozoic ductile deformation event associated with the cleavage. Hanna et al. (1990) argued that general south-westerly thrusting of the autochthon was responsible for the doming of the range into a flat-topped ramp anticline, synchronously with the emplacement of the Semail-Hawasina nappes above (Fig.2- 7a). It must be noted that according to this model, the whole autochthon of the Northern Oman Mountains would therefore be considered para-autochthonous.

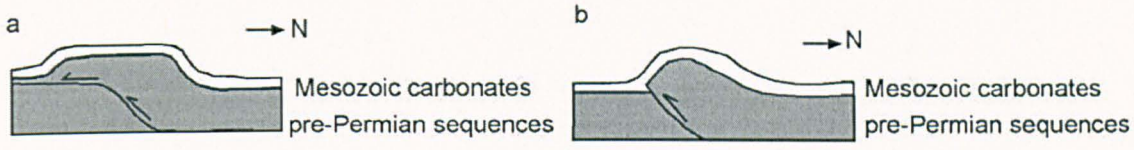

Fig.2- 7 Structural models of Jebel Akhdar. (a) Fault-bend fold proposed by Hanna et al. (1990), (b) Fault-propogation fold proposed by Mount et al. (1998)

Le Metour et al. (1995) concluded that the structures of Jebel Akhdar and Saih Hatat were probably inherited from Late Permian horst and graben features at the edge of the continental shelf.

Mount et al. (1998) suggested that the doming of Jebal Akhdar and Saih Hatat represented frontal tip folds related to blind reverse basement faults (Fig.2- 7b). They argued that these dip steeply towards the north-northeast along the southern dome flanks, rooting into a deep decollement to the north. Using apatite fission track data, they dated the compression and the resulting rapid uplift as Oligocene.

Jolivet et al (1998) attributed the late antiformal folding of the nappe stack in Saih Hatat to the Paleocene, as suggested from the unconformable calcarenites on ophiolite and blueschists, subsequently enhanced during the Mio-Pliocene.

Al-Lazki et al. (2002) interpreted the present-day structures of Jebel Akhdar as the results of deformation concentrated along lines of weakness. These lines were interpreted as possible shear zones associated with the Permian rifting event that formed the eastern margin of the Arabian Plate. Gravity modeling was seen to show a sudden decrease in the pre-Permian sequence thickness on the northern limb of the structures.

The present structure of the Oman Mountains is mostly the outcome of a major uplift during the Late Miocene to the present, with some 2000 m of uplift of early Tertiary marine

carbonates and all underlying rocks, with only minimal compression (Searle et al. 2004). This uplift seems to have followed the opening of the Red Sea, which began to open in the Eocene –Oligocene when oceanic crust was emplaced. Effective SW-NE compression, leading to the uplift of the Oman Mountains and folding of the Zagros Range was probably most effective from Late Miocene onwards (Glennie, 2005). However, the causal mechanism behind the continued Late Tertiary vertical uplift of the Oman Mountains is still unclear (Mann et al. 1990).

Chapter 3: Structural deformation along the Akhdar anticline

3.1 Introduction

The Jebal Akhdar anticline (ESE-WNW) encompasses the highest peak in the country and comprises of the heart of the Northern Oman Mountains extending from the Semail gap until the Hawasina window in the west. The massif is composed of autochthonous rocks ranging in age from Late Proterozoic to Late Cretaceous, with a large hiatus corresponding to practically the entire the Paleozoic. The Akhdar anticline is cored with highly deformed pre-Permian clastics and carbonates rocks, and flanked with Permian to Late Cretaceous carbonate platform sequences.

The focus of this chapter is to investigate and explore structural deformation across the Akhdar anticline, particularly the extensional deformation. The extensional deformation was previously studied, but briefly by Le Metour et al. (1990) and Breton et al. (2004). However, here is the first time in which a detailed investigation has been conducted to study such deformation in the Akhdar culmination. This deformation is manifested by a linked system of shear and detachments, with a sense of shearing directed top-NNE. Different ductile structures are developed by the extensional deformation, particularly within the Jurassic-Cretaceous succession.

Ten structural transects have been constructed across both the southern and the northern flank of the Akhdar anticline. The southern flank is less deformed and dips more gently than the steeply dipping northern flank. Various structural data have been collected along each transect, comprising of both brittle and ductile structures. In this chapter, data from each transect is presented and analyzed in great depth, depicted by field photos and sketches. The chapter is started with the southern flank then proceeds to the northern flank. Transects of each flank are analyzed separately and completed with a short summary illustrating the processes occurring. The chapter concludes with correlations of the structural data of each flank, and a summary of the structural deformation across the entire culmination.

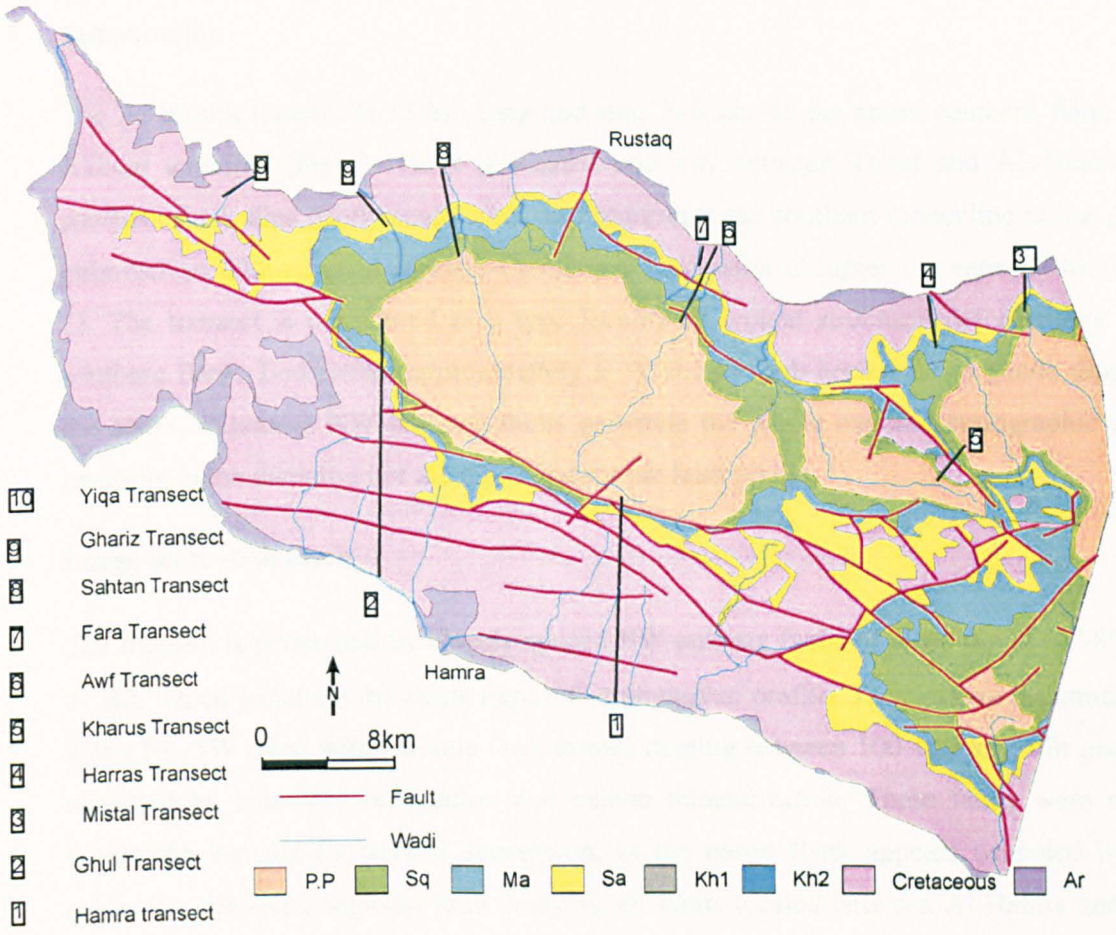

Fig. 3- 1 Geological map of Jebel Akhdar shows the locations of the constructed transects. (The used abbreviations are explained in the list of abbreviations)

3.2 AL-Hamra transect

Introduction

The Al-Hamra transect is 13 km long and runs N-S across the entire southern flank of the Akhdar anticline (Fig. 3- 1). It is located mid-way between Tanuf and AL-Hamra. The southern flank dips gently southwards and represents the southern monocline of the Akhdar culmination. The exposed Jurassic-Cretaceous succession occupies the entire flank (Fig. 3- 2). The transect is considered as a type locality of typical structural deformations on the southern flank. Beds strike approximately E-W and are sub-horizontal to gentle dipping to the south. Extensive NW-oriented faults penetrate the whole exposed stratigraphic profile, resulting in the disruption of the dips adjacent the fault planes.

Large scale structures

The transect is penetrated by closely spaced NW-striking faults of steep dip at 60°-80° (Fig. 3- 3a), which penetrate the entire exposed stratigraphic profile. They extend the stratigraphy along NE-SW trend with variable fault throws ranging between 100-400 m. Fault planes are occupied by extensive brecciation and calcite mineralization. These faults were mapped within the Jurassic-Cretaceous succession, as the entire flank appears occupied by these rocks. To conduct a regional fault analysis, all faults located between Al-Hamra and Tanuf are grouped and analyzed collectively. Kinematicaly, two slip components were identified: dip slip and strike slip (Fig. 3- 2). Both sinistral and dextral senses of movements were identified for the strike slip displacements (Fig. 3- 2). The dominant trend of the dextral displacement is WNW-ESE, while for the sinistral displacement is E-W. Both sinistral and dextral components enclose the WNW-ESE compression direction. Assessment of the relative timing of the various fault components relative to the folding event is difficult as both faults and fold axis are subparallel.

Extensive fracturing and veining are common along the transect, particularly within the competent rocks of the Natih and Shams Fm's. The most prominent vein orientation is NW-SE, which appears within each stratigraphic unit as tensile fractures. Such vein trend is parallel to the extensively developed NW-oriented faults, which may suggest that both are part of the same system. Tension gashes are robust along each fault, expressing both dextral and sinistral shear sense with a measured compression direction trending roughly WNW-ESE.

Deformation fabrics

Deformation fabrics are manifested by pervasive N-verging cleavage and layer-parallel shearing within some incompetent units of the Salil and Nahr Umr Fm's. The layer-parallel shearing zones involve intensive deformation surrounded by dissimilarly deformed strata, and hence can be described as detachments. Layer-parallel detachments dip gently SSW and are marked with calcite fibre lineations pitching SW (Fig. 3- 2). These detachments concentrate within the fine-grained units of the Jurassic-Cretaceous succession. Minor detachment lineations trend E-W and NNW-SSE. In places, layer-parallel detachments within Salil are folded by open folds of NW-SE-trending fold axes (Fig. 3- 2) and (Fig. 3- 3b). Spaced pressure-solution cleavage of NW-SE orientation and NE vergence is pervasively developed particularly within the Nahr Umr and the Salil Fm's (Fig. 3- 2) (Fig. 3- 3b). The cleavage exhibits small intersection angles with the corresponding beds.

Interpretation and summary

The transect is mainly dominated by extensive brittle faulting forming NW-trending normal faults of dip and strike slip displacements. Deformation fabrics are weakly developed and mainly represented by bedding-parallel detachments and NE-verging cleavage, constrained within the fine-grained units. Top-to-the-NNE shearing was inferred from these deformation fabrics. The NW-striking faults and the deformation fabrics of the Jurassic-Cretaceous succession collectively indicate a top-to-the-NNE extensional deformation. Thus, it is likely that both are part of the same deformation system, top-to-the-NNE extension, but are detached within different stratigraphic levels. The NW-striking faults penetrate the entire exposed section, therefore could be detached along a deeper detachment, probably within the pre-Permian sequences. Furthermore, there is a component of WNW-ESE compression, as indicated by conjugate sets of strike slip faults and the resultant tension gashes, together with WNW-ESE stretching lineations along some detachments. This structural feature will be explored thoroughly at the end of the chapter.

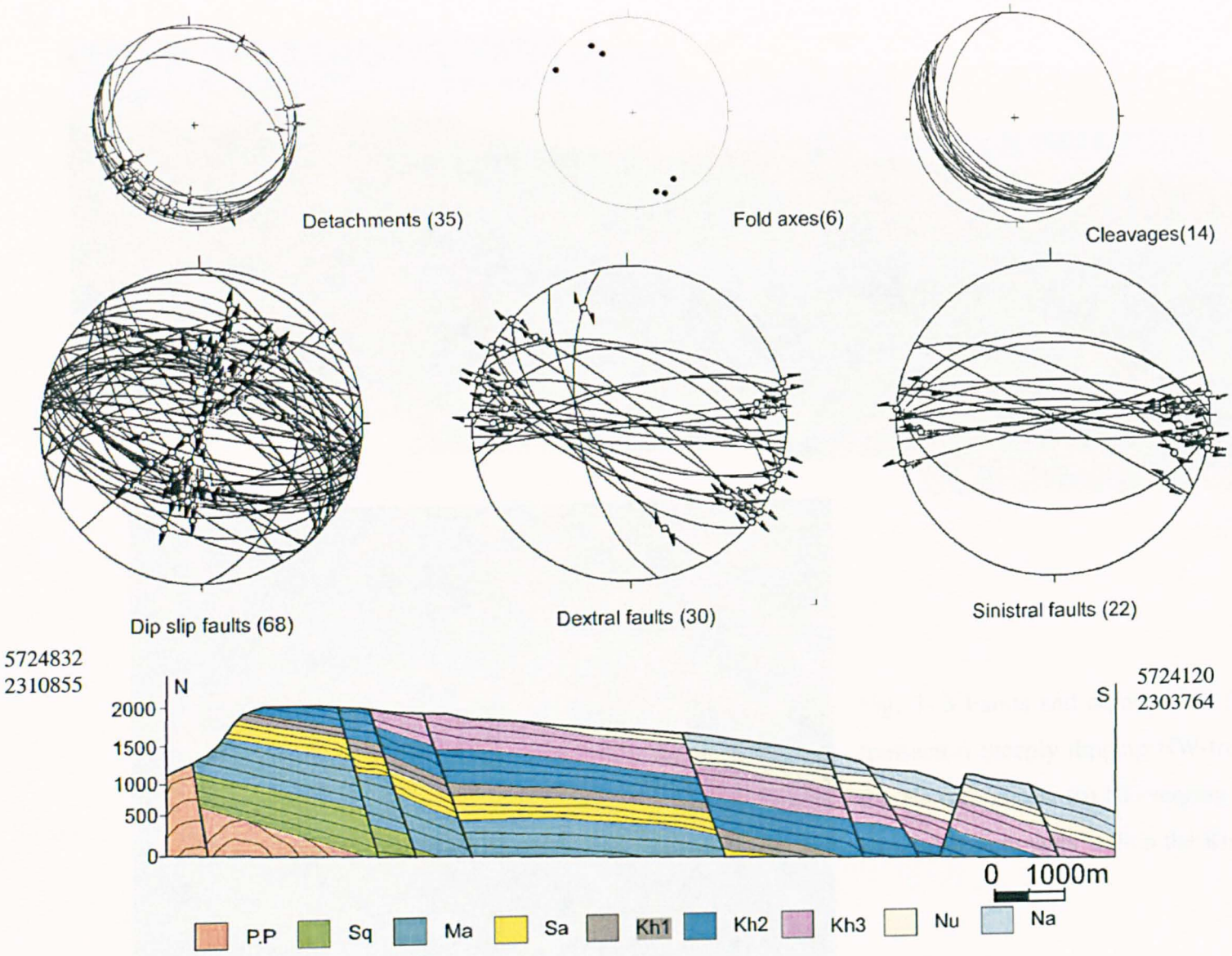

Fig. 3- 2 The Al-hamra transect with stereograms of the different structural elements

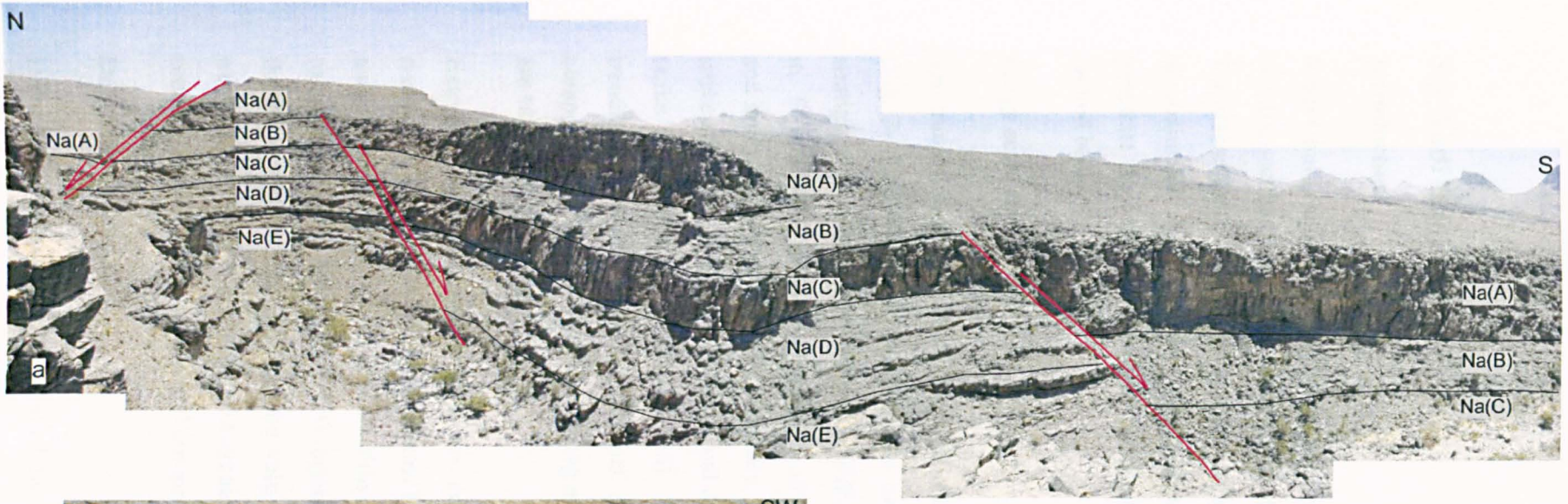

Fig. 3- 3 Faults and deformation fabrics along the Al-hamra transect(a) Steeply dipping NW-trending normal faults along the Na carbonates. (b) NE-verging cleavage with folded layer parallel detachments within the Kh2.

3.3 Wadi Ghul transect

Introduction

Wadi Ghul is situated 10 km to the west of the town of Al-hamra (Fig. 3- 1). A 17-km-long, N-S transect has been constructed across the entire preserved Mesozoic carbonate sequences. The transect runs across the southern monocline of the Akhdar anticline, where beds strike approximately E-W and dip at approximately 20° S. Extensive NW-SE and E-W faults penetrate the complete exposed stratigraphic profile, resulting in steepening of the adjacent faulted beds.

Large scale structures

The transect is marked by WNW-ESE and E-W faults dipping steeply southward at 60°-80° (Fig. 3- 4). These faults penetrate the entire exposed stratigraphic profile and extend the stratigraphy along an approximately NNE-SSW trend, with variable fault throws of 100-200 m. To conduct regional fault analysis, all faults located to the west of Al-hamra are grouped and analyzed collectively. Kinematicaly, two slip components were identified: dip slip and strike slip (Fig. 3- 4). Both sinistral and dextral senses of movements were identified for the strike slip displacements (Fig. 3- 5d). The available data does not show any dominant trending of the strike slip components. Evaluating the relative timing of the various fault components, with respect to the folding event cannot be done since both faults and fold axis are subparallel.

Extensive fracturing and veining are common along the transect, especially within the competent rocks of the Natih and Shams Fm's. The most common vein orientation is NW-SE and of tensile origin, which arises within each stratigraphic unit. Such trending is subparallel to the extensively developed WNW-oriented faults, which may suggest that both are part of the same system. The NE-trending vein set is less developed compared with the NW-SE trending set. Tension gashes are robust along each fault, expressing both dextral and sinistral sense of shearing, with a measured compression direction between E-W to WNW-ESE.

Deformation fabrics

Deformation fabrics are represented by NE-verging cleavage and layer-parallel shearing within the incompetent units of the Jurassic-Cretaceous succession. The layer-parallel shearing zones comprise of intensive deformation separating variably deformed strata, and therefore can be called detachments. Layer-parallel detachments are aligned E-W and WNW-ESE and dip of 20° SSW (Fig. 3- 4). Mineral lineations within the detachments exhibit two

different plunging directions: SSW and W, with the sense of shearing top-to-the-NNE and top-E respectively (Fig. 3- 5 a). Spaced pressure-solution cleavage of NW-SE orientation and NE vergence is pervasively developed, particularly within the Nahr Umr, Salil and Sahtan Fm's (Fig. 3- 4) and (Fig. 3- 5b). The cleavage dips at approximately 20°-40° SW and intersects the corresponding bedding at small angles. Layer parallel stylolites with a teeth-like geometry, arise within the competent units of the Natih and Shams Fm (Fig. 3- 5c). These stylolites are truncated by the E-W and NW-SE trending faults and fractures.

Interpretation and summary

Extensive E-W and NW-SE trending normal faults were mapped along the transect, and the NE-directed ductile deformation was seen to be weakly developed. For this reasons, most of the NE-directed ductile deformation such as folds and boudinage structures are not common, whereas layer parallel slipping can frequently be seen within the Salil. The SSW pitching-lineations can be related to the NE-directed simple shear.

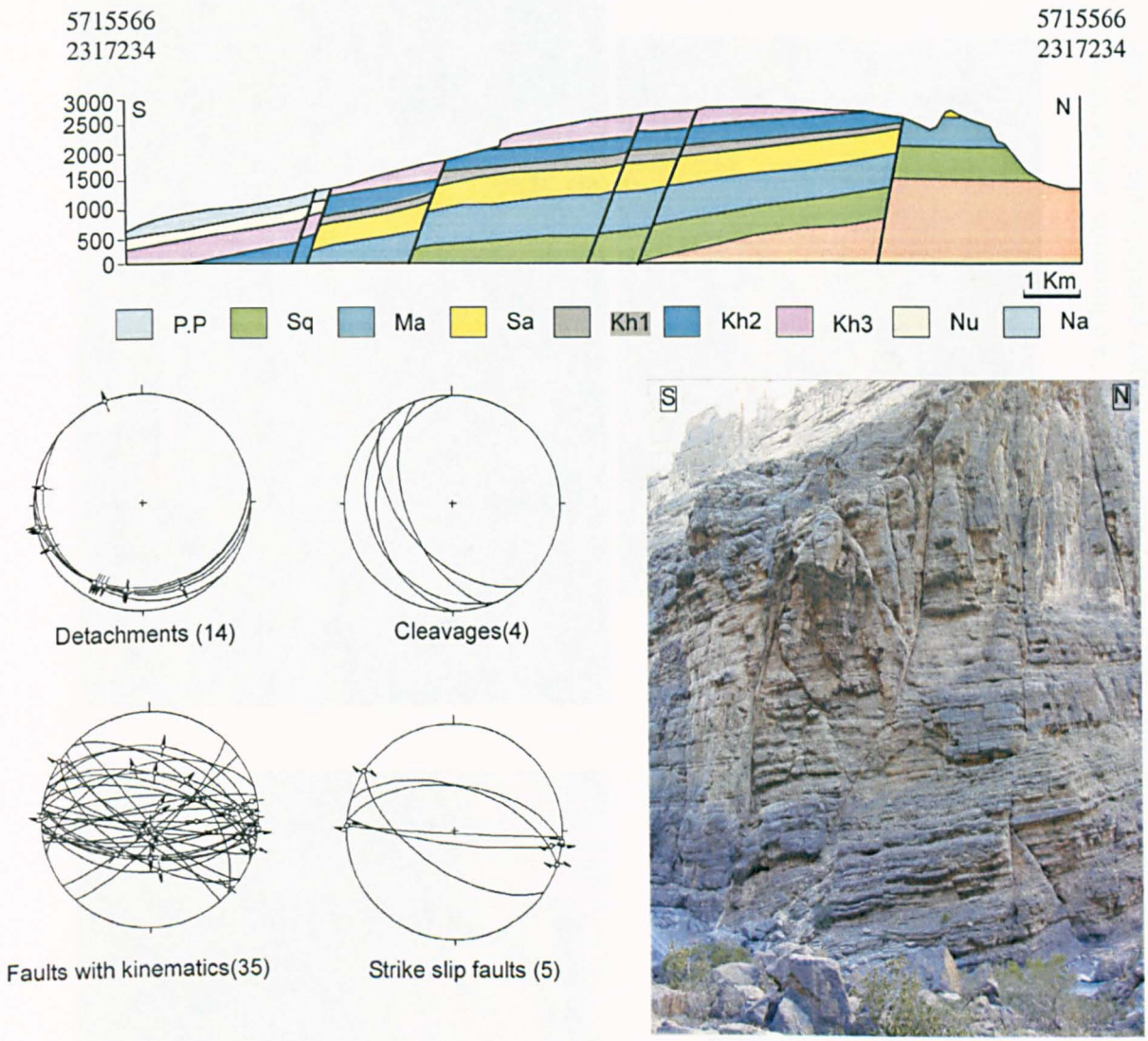

Fig. 3- 4 The Ghul transect and the stereograms of the various structural elements. The photograph shows steeply dipping NW-trending faults within Salil.

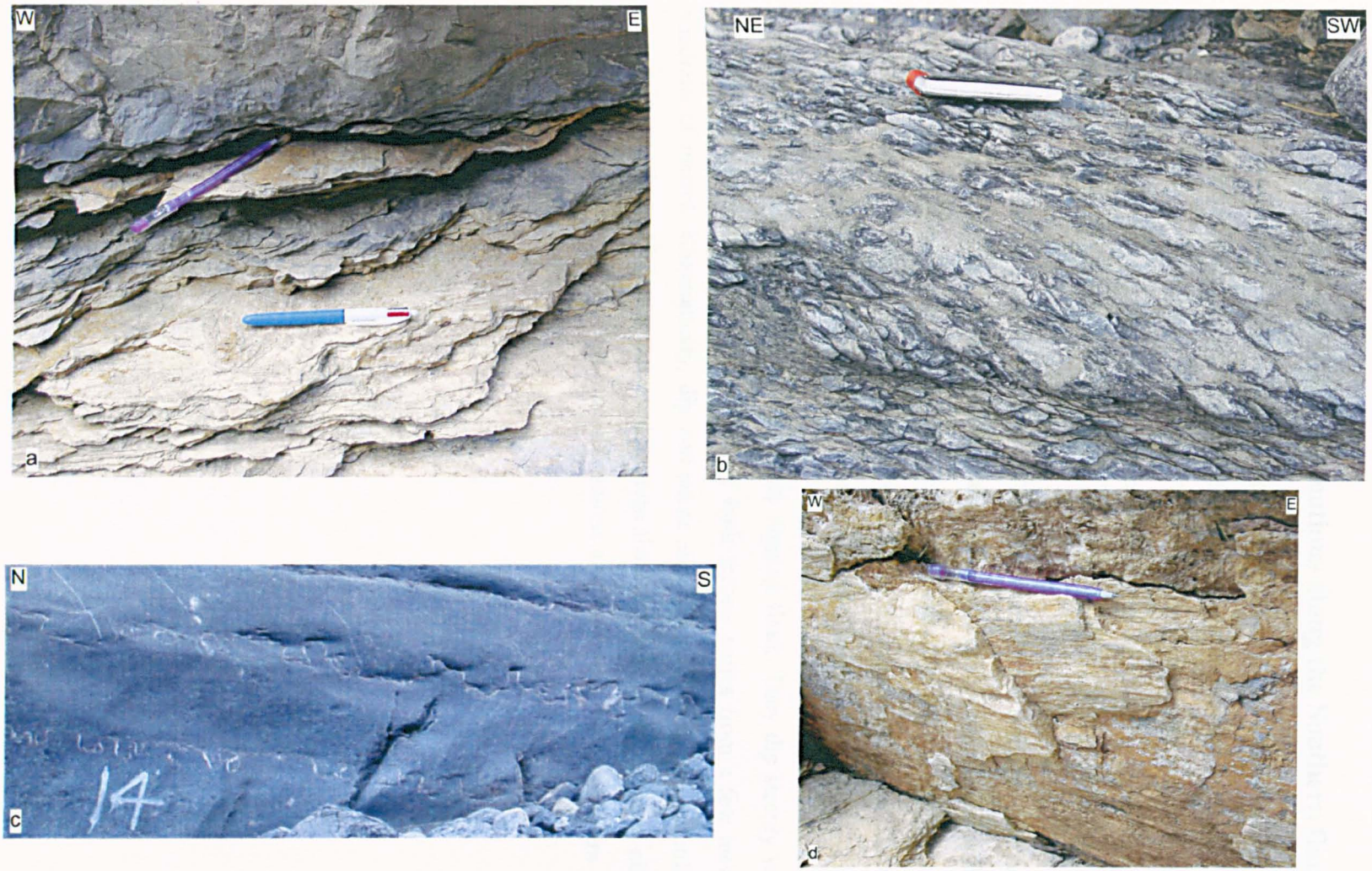

Fig. 3- 5 Deformation fabrics along wadi Ghul transect. (a) Layer-parallel detachments with two lineation sets trending NE-SW & E-W respectively. (b) NE-verging cleavage within the Kh2 Fm. (c) Teeth-like, layer-parallel stylolites within the massive limestone beds of Kh3. (d) Horizontal slickensides trending E-W.

3.4 Summary of the structural deformations along the Southern flank

The southern flank of the Akhdar anticline dips gently to the south, with extensive EW- and NW-trending normal faults. NE-directed ductile deformation is weakly developed along the incompetent units of Cretaceous sequence, while brittle normal faulting is well established throughout the whole flank despite the gentler bed tilting. A summary of all the structural elements along the various structural transects of the Northern flank is shown in Fig. 3- 6.

Ductile deformation is weakly developed, forming layer parallel slipping surfaces, NE-verging cleavage and a few minor fold structures. Slipping surfaces are marked with NE-SW trending fibre lineations with a top to the NE sense of shearing. The rarely developed fold structures, trend NW-SE, with upright geometries and open interlimb angles. Cleavage with NE-vergence is well established especially along the Nahr Umr Fm.

Intensive normal faulting dominates this gently dipping flank. They dip steeply with EW and NW-SE orientation, while the amount of fault throws varies from a few metres up to hundreds of metres. Kinematicaly, dip and strike slip components can be identified along these faults. Little fault rotation occurred because since the fault orientations are observed to be parallel to the fold strike. Fault-related fractures and background fracturing are very well established along this flank.

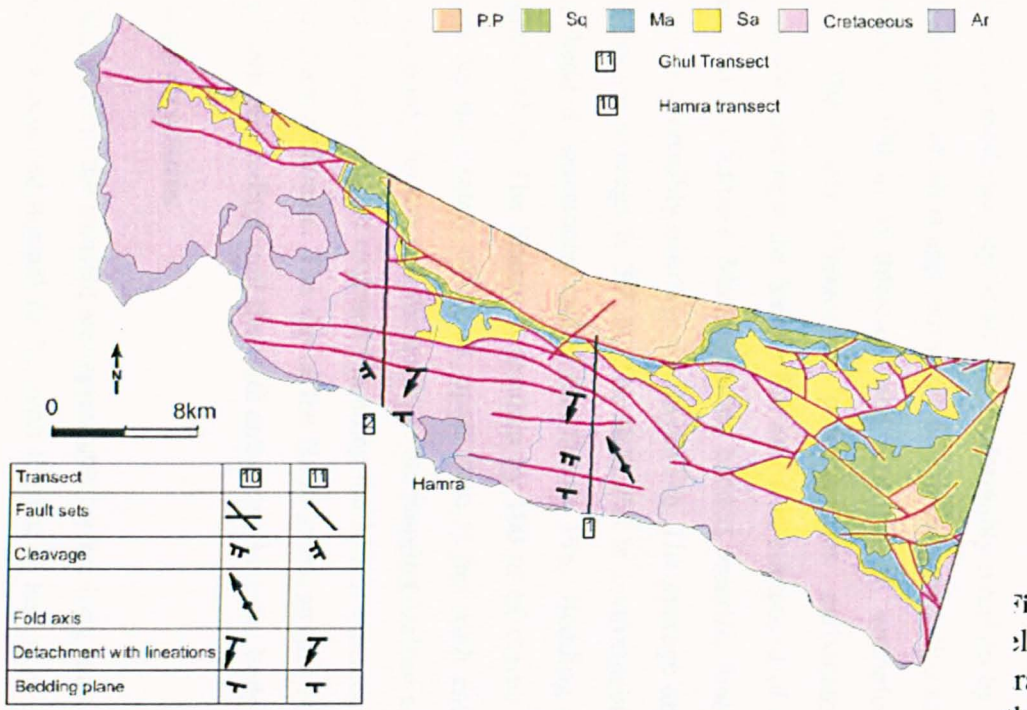

Fig. 3- 6 Summary of the structural elements mapped along each transect of the southern flank. Note that each structure is drawn as seen in the field.

3.7 Wadi Mistal transect

Introduction

Wadi Mistal is located mid-way between Nakhal and the town of Awabi, approximately 20 km west of the town of Nakhal (Fig. 3- 1). A 3.3-km-long, N-S transect has been constructed along the wadi crossing the whole preserved Mesozoic succession (Fig. 3- 7). The transect crosses the northern monocline of the Akhdar anticline, where beds strike ENE-WSW and dip of 40° NNW. It starts with the Permian Saiq carbonate in the south and finishes with the Late Cretaceous Natih carbonate in the north. The thickly bedded Saiq carbonate is some 500 m thick with a moderate dip of 40° N, conformably overlain by the massive bedded Triassic Mahil dolomite, which is approximately 600 in thick and dips at 40° N. The Jurassic Sahtan Fm, which is 100 m in thickness and dips 30° N, unconformably overlays the Mahil dolomite. The Early Cretaceous porcellaneous carbonate known as Rayda Fm, unconformably overlays the Sahtan Fm and it is composed of thinly bedded limestones of less than 100 in thickness. Massive thinly bedded, micritic limestones of some 400 m thick called Salil conformably overlays the Rayda Fm. The average dip of the Salil strata is locally variable but on average is 30° N. The Salil Fm is conformably overlain by 400 m thick, massive bedded limestones called the Shams Fm. Bedding planes within this Fm dip consistently 30° N. The Shams is overlain by 100 m of clastic sediments of the Nahr Umr Fm. Beds dip moderately of 30° N, apart from at the wadi entrance where Nahr Umr and Natih beds gently dip towards the north, in the hanging-wall of a km-long, NW-striking fault. Natih Fm is the youngest exposed Fm along the Mistal transect. It is Late Cretaceous in age of 200 m thick carbonate. The dip of the Natih strata within the hanging-wall flattens away from the fault proceeding until the wadi entrance where the beds are sub-horizontal.

Large scale structures

Major structures in the transect are represented by km long fault structures. Faults are steeply dipping, NW-oriented normal faults, with throws of less than 100 m affecting the exposed stratigraphic section (Fig. 3- 7). Faults are observed throughout the transect, and are described in turn.

A series of NW-striking normal faults were mapped at the middle of the transect (Fig. 3- 8a). These faults affect the lower Mesozoic succession until the Salil Fm where they are less common. Only the largest fault [1] is illustrated on the transect. The faults dip steeply at 60° to 80° NE and SW. The hanging-wall strata are tilted adjacent the fault planes, forming drag folds and reflecting a sense of normal movement. In places the steep NW-striking faults,

which dip towards the massif are characterized with up-thrown blocks overlaying the fault plane, and so appear as reverse faults (Fig. 3- 7). When the structures were restored, by rotating them 30° around horizontal axis trending 060 (chosen parallel to the fold axis), these reverse-like faults transposed into normal faults with down-throw towards NE. This may reveal that these faults took place before or during the early stage of the folding onset. Kinematic data of the NW-striking faults varies from oblique lineations pitching SW and NE to sub-horizontal slickensides. When the oblique lineations unfolded around 060/30, the NW-faults became dip slip (Fig. 3- 7). On the other hand were unfolding disperses the sub-horizontal lineations, which means they took place after or during the latest stage of the folding onset.

At the northern end of the wadi there is a sub-vertical, NW-oriented fault displacing the Nahr Umr and Natih Fm's down towards NE for 40 m [2] (Fig. 3- 8b). The incompetent units of the Nahr Umr Fm are highly deformed adjacent to the fault plane and form NW-plunging folds. In a down profile the fault plane is segmented in an en echelon manner. Dip and strike slip lineations were recorded on the fault plane (Fig. 3- 8b) but Cross-cutting relations between these lineation sets are not constrained.

A NE-verging thrust appears at the mouth of the wadi thrusting the Nahr Umr Fm above the Natih Fm (Fig. 3- 8b) for 100 m. A hanging-wall anticline, with a horizontal fold axis and NW-SE orientation, has developed within the hanging-wall strata. The fold axial plane is tilted NE and hence the northern limb is overturned.

Deformation fabrics

Deformation fabrics manifested by bedding parallel cleavage, fracture cleavage, mineral elongations and small scale folds are well developed along the incompetent Jurassic and Cretaceous rocks. The fine-grained units of the Jurassic and Cretaceous succession contain zones of locally intensive deformation, which separate differently deformed units and therefore behave as detachments. These bedding-parallel detachments strike NE-SW and dip of 40° NW. The detachments are marked by calcite fibre lineations pitching NE (Fig. 3-7). Normal faults of metric-offset and NW-SE orientation branch and merge onto the detachments. Along the Rayda-Salil contact, a 10 m thick zone of intensive bedding parallel detachments is marked by calcite mineralization. Stretching lineations are very common within the Rayda and Salil Fm's, plunge NE (Fig. 3- 7).

Intraformational folds are oriented perpendicular to highly oblique (N280° to N340°) to the NE stretching direction, while fold axes pitch NW. The folds verge towards NE and exhibit

open-close interlimb angles. Spaced pressure-solution cleavage varies in vergence direction, depending on the attitude of the hosting beds (Fig. 3- 7). For example within sub-horizontal beds, cleavage verges NE, while within tilted beds, cleavage is gentler than bedding and verges SW. By restoration of the tilting deformation the SW-verging cleavage became NE verging. In this manner cleavage of both sub-horizontal and tilted beds constitute NE-verging cleavage, formed before or during the early stage of the folding deformation. Bedding-parallel cleavage appears along the highly sheared zones. Boudinage structures arise within the Salil Fm. In this structure, competent units are stretched along bedding planes, giving rise to pull-apart structures or necks, which become filled with incompetent material from either side. The boudinage axes are oriented NW-SE, orthogonal to the NE stretching direction. Layer-parallel, wavy stylolites are extensively developed within the incompetent shale units of the Shams and Natih Fm's, while the more competent units display anastomosing stylolites.

Interpretation and summary

The transect is characterized by steep NW-oriented faults of variable kinematics reflecting various structural evolutions. Faults with oblique lineations pitching SE and NE [1], mapped at the middle of the transect, indicate pre-folding dip slip movements. On the other hand the horizontal lineations along the same fault suggest that the faults were reactivated after the folding event as strike slip faults. Such an interpretation of pre-folding fault activities can also be suggested from the rotation of these faults, to an extent that some faults appear like steep reverse faults. However, faults with dip and strike slip lineations [2] such as those mapped at the wadi entrance reveal post-folding fault movements, because the associated lineations are not rotated by the folding deformation. It is worth noting that the timing of the NW-striking faults can be assessed with respect to the folding deformation, unlike elsewhere along the same flank, since here both faults and fold axes are oblique to each other. In short, dip slip faulting took place before or during the early stage of the folding onset, then extensional faulting and strike slip faulting was resumed after or during the latest stage of the folding deformation.

Deformation fabrics are common within the Jurassic-Cretaceous succession, particularly in the fine-grained units. Deformations show evidence of layer-parallel extension manifested by extensional detachments and boudinage structures. The shear sense indicators, where evident express top to NE shearing. The deformation fabrics are transected by the steeply dipping, NW-striking faults and are tilted due to the folding of the massif. As a result these fabrics must have occurred before or during the early stage of the folding deformation.

Brittle faulting and deformation fabrics seem to be interrelated, as both indicate top-to-the-NNE extensional shearing and coexisted before or during the early stage of the folding deformation. The NNE extensional shearing manifests a linked system of faults and layer-parallel extensions.

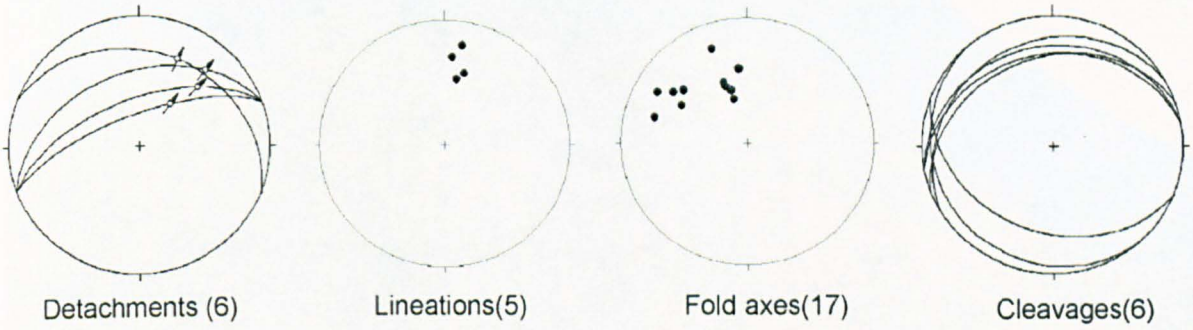

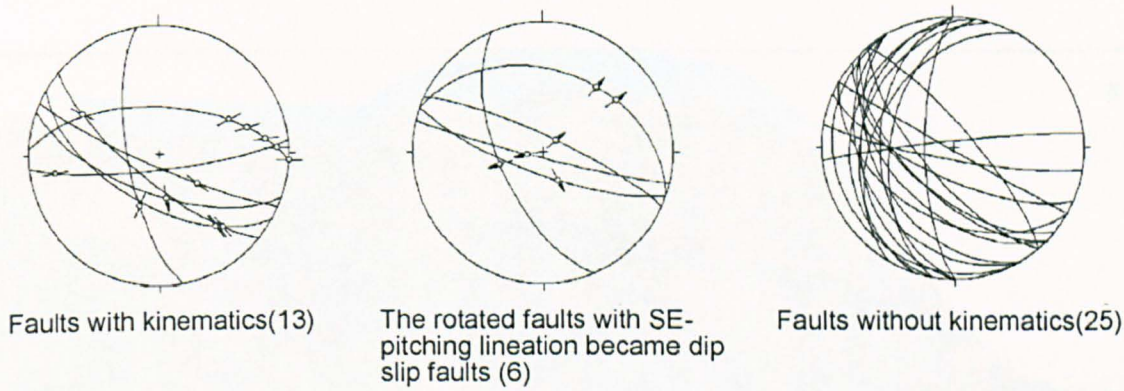

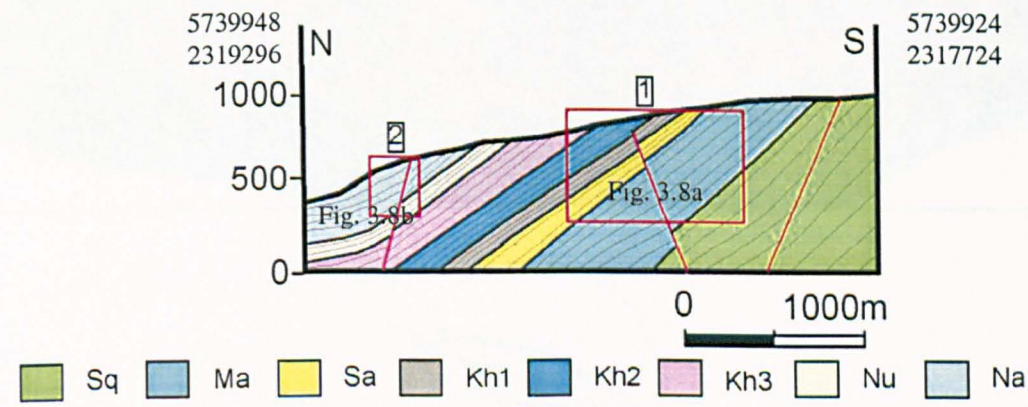

Fig. 3- 7 The Mistal transect with stereograms of the various structural elements collected along the transect. Note that faults with SE pitching lineations are transformed into dip slip faults when they are unfolded by rotating them 30° around a horizontal axis trending 060.

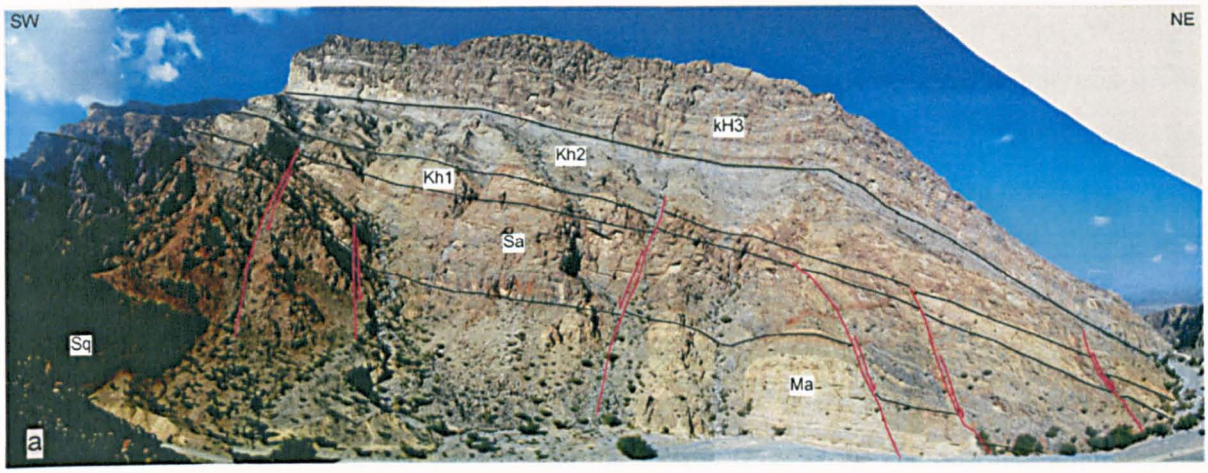

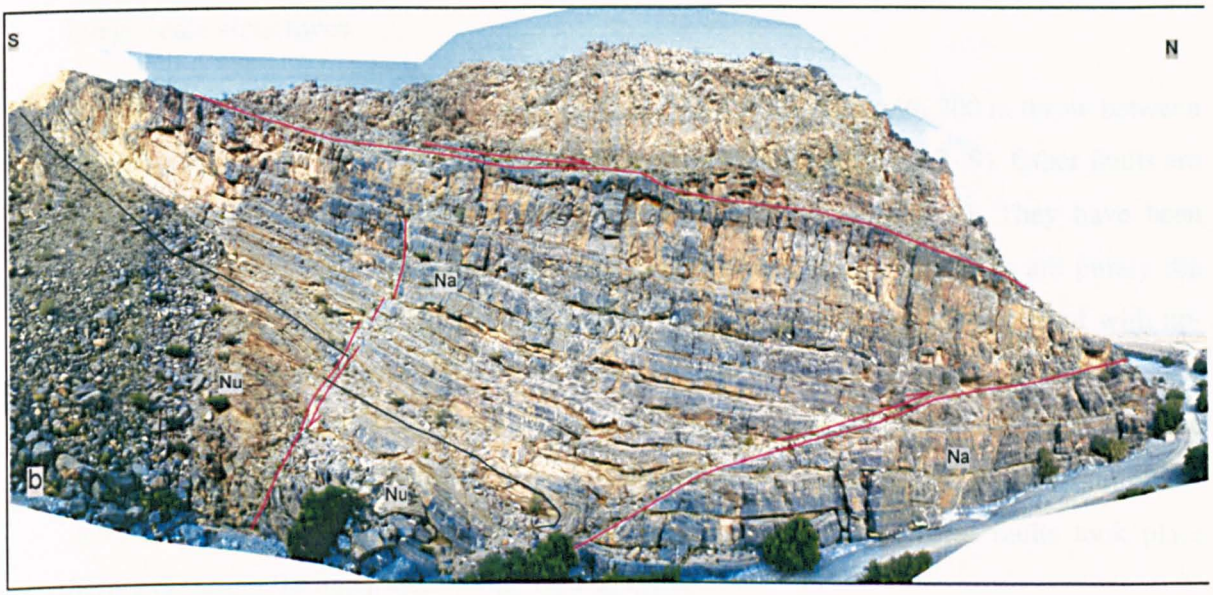

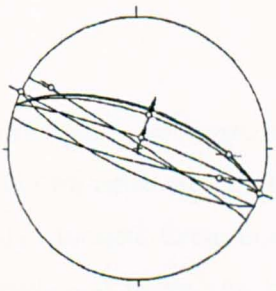

The steeply dipping normal fault (9)

Fig. 3- 8 Fault structures along the Mistal transect. (a) Panoramic view of the NW-trending faults which cuts the whole stratigraphic section apart from Kh3 at the uppermost part of the cliff (Field of view approximately 2km). (b) Structures at the mouth of wadi Mistal, with a NE-verging thrust and a steeply dipping normal fault showing both dip- and strike-slip lineations as seen from the stereogram (Field of view approximately 1km).

3.6 Wadi beni Harras transect

Introduction

Wadi beni Harras is situated 10 km to the East of Awabi (Fig. 3- 1). A 3.4 km long, NS-oriented transect was constructed along this wadi, starting from the Triassic Mahil dolomite up to the Mid-Cretaceous Natih carbonate, which is overlain by the Late-Cretaceous obducted ophiolite at the Northern end of the section (Fig. 3- 9). The different stratigraphic units, on average, strike ENE-WSW with a moderate dip of 35° NNW.

Large scale structures

The transect is marked with a km-long, NW-trending normal fault with 200 m throw between the Shams and Nahr Umr Fm's mapped at the mouth of the wadi (Fig. 3- 9). Other faults are of metric offsets and are oriented NW-SE and ENE-WSW (Fig. 3- 9). They have been mapped throughout the various stratigraphic units. Kinematically, the faults are purely dip slip. Some steep NW-striking faults dipping towards the massif are characterized with up-thrown blocks overlaying the fault plane, and so appear as reverse faults. When structures were restored by rotation 30° around horizontal axis trending 070, presumed parallel to the Akhdar fold axis in that area, these reverse-like faults transposed into normal faults with down-throws along the regional dip direction. This suggests that these faults took place before or during the early stage of the folding onset.

Deformation fabric

Deformation fabrics are common within incompetent units of the Cretaceous successions. Thin zones of intensive shear deformation are manifested by folds and cleavage, situated along fine-grained units of the Jurassic-Cretaceous succession. These zones separate variously deformed structural units and hence can be described as detachments. Bedding-parallel detachments are marked with NE-plunging calcite fibre lineations (Fig. 3- 9) and similarly, stretching lineations defined by elongate carbonate aggregates within the Salil&KH3 Fm's show the same NE-SW trend. Folds are aligned NW-SE, perpendicular to the NE stretching direction, with NE vergence. They have gentle-open interlimb angles and plunge parallel to the regional dip direction. Kink bands of NW-SE orientation appear within the Nahr Umr Fm (Fig. 3- 9a), while massive units of the Shams and Natih Fm's exhibit wavy layer-parallel stylolites.

Very well developed flanking structure appears within Nahr Umr Fm (Fig. 3- 9b) and along this structure; layers are deflected alongside a cross-cutting tensile vein. The processes of formation of this type of flanking fold develop as follows: a tensile fracture develops at a high angle to the bedding in rocks where ductile non-coaxial progressive deformation is in progress. Such a fracture will tend to rotate with progressive deformation and a result of this type of rotation, the flanking fold is developed (Swanson 1999). Deformation fabrics manifested by detachments and NE-verging folds reflect top-NE shearing.

Interpretation and summary

The transect is dominated by NW-oriented, bedding-confined faults of metric offsets. These faults therefore must be detached within the same stratigraphic unit. Consequently, it is likely that these faults merge onto the bedding-parallel detachments mapped within the key horizons in the Jurassic-Cretaceous sequences. Thus the NW-oriented normal faults of NE-down throw, the deformational fabrics defined by the detachment, and NE-verging folds are interrelated and probably express the same deformational system of top-NE shearing. The top-NE shear deformation is assumed extensional in kinematic, as detected from the associated normal faults.

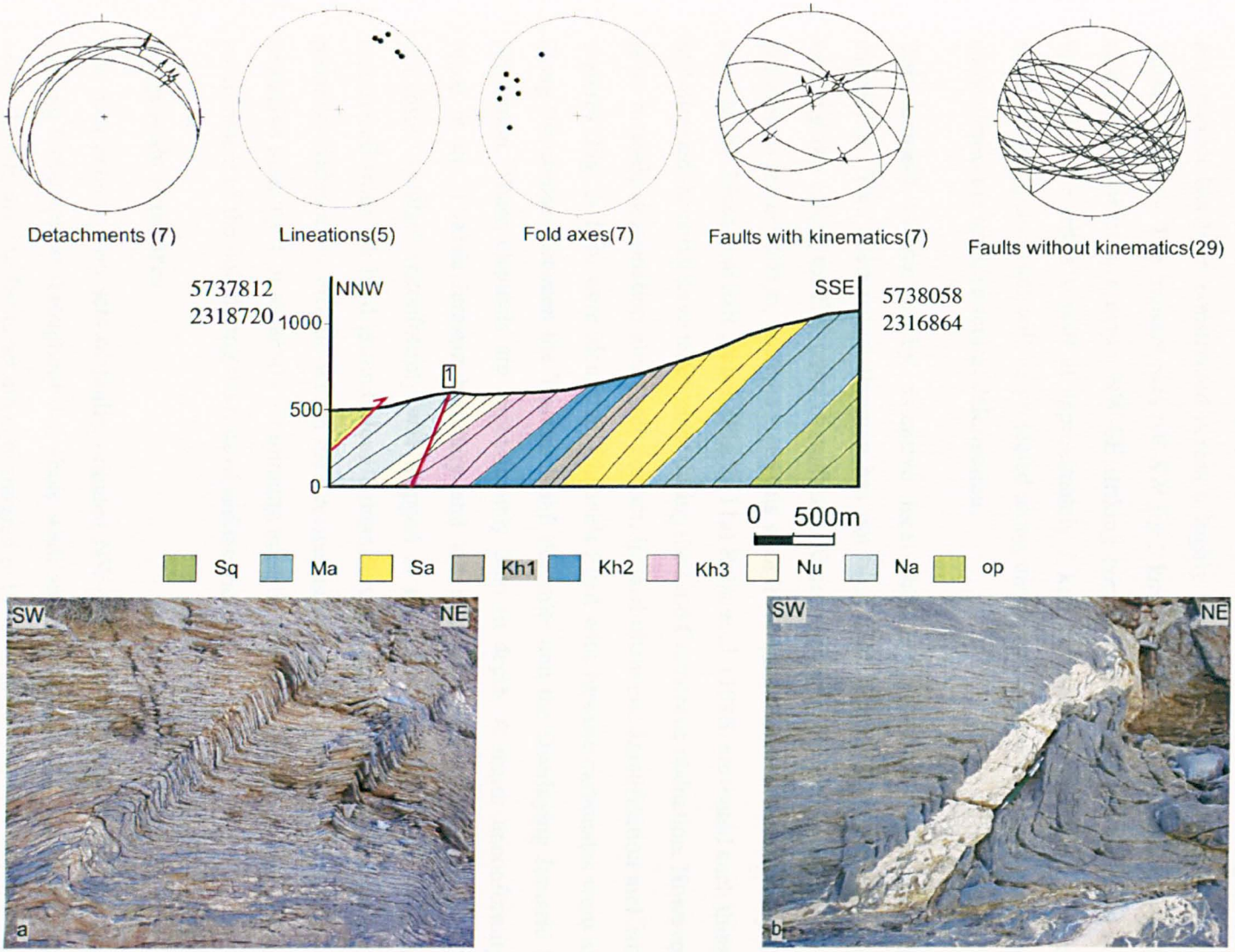

Fig. 3- 9 The Wadi beni Harras transect with the stereograms of the different structural elements. (a) NE-verging kink bands. (b) Well developed flanking structure within Nu Fm.

3.7 Wadi beni Kharus transect

Introduction

Wadi beni Kharus can be reached directly from Wilaiat AL-Awabi, which is positioned along both banks of this historic wadi (Fig. 3- 1). Despite that the whole wadi being investigated, the transect has been constructed across a highly faulted part separating the Kharus and Mistal windows. The transect runs NE-SW for 3 km. The most important structural element along this transect is a major NW-SE striking normal fault, which has the highest throw throughout the entire massif at approximately 1 km. For simplicity all the structural data acquired along the wadi will be projected along the transect, since all the investigated sites show almost the same structural deformation.

This transect is marked by extensive local thinning within the Triassic-Cretaceous succession. This phenomenal thinning has not been seen elsewhere apart from this EW-trending axis (along the EW-trend of wadi beni Kharous). The typical thickness for the Mahil dolomite is around 600 m, whereas along this wadi it is highly variable reaching only 10 m as seen at the Mahsanah half graben (Fig. 3- 11a) Rabu et al. (1986) attributed such thinning to SW-directed thrusting have taken place during the Late Cretaceous obduction. However there is no tectonic deformation along this contact, instead channels, karstification and erosional features (Fig. 3- 11b) were identified. Channels filled with Jurassic carbonates were mapped along the contact between the Triassic Mahil dolomite and the Overlaying Jurassic Sahtan Formation. These channels are approximately 20m in depth. A major unconformity took place at the Triassic-Jurassic boundary and led into incredible erosion of the Triassic dolomite. Another unconformity was mapped at the Jurassic- Cretaceous boundary, as manifested from the hard ground along Sahtan-Rayda contact. However, there is not one piece of evidence for erosion within the Cretaceous carbonates which could account for its extensive thinning. Consequently the thinning must be original and related to the depositional environment of the unit during the time of sedimentation.

Large scale structures

The area exhibits two sets of faults, oriented NW-SE and NE-SW (Fig. 3- 10). The NW-striking faults appear throughout the whole wadi and involve both the fold flank and crest, while the NE-striking faults set are concentrated in the fold crest. The NW-striking faults are variable in length from km-to-m's. The km-long faults are strongly developed in the fold crest between Sunaybah and Mahsanah, where the transect has been constructed and form a series of half graben structures (Fig. 3- 12). The fault throw of the main fault [2] is some 1 km (Fig. 3- 10) juxtaposing the Cretaceous Shams Fm against the Permian Saiq Fm in the

footwall. Thus Jebel Mahsanah is a major half graben structure bounded on all sides by km-long SW-dipping normal faults. Kinematically, the large NW-striking faults are mainly dip slip, while the smaller faults display fault striations of highly variable trends, to the extent that they cannot be constrained or interpreted (Fig. 3- 10).

The NE-striking faults are localized in the fold crest, are small in length with metric throws. The associated fault striations reflect dip slip movement for both large and small faults (Fig. 3- 10). There is no obvious cross-cutting relationship between the NE-and-NW-striking faults, so their relative chronology cannot be revealed.

Deformation fabrics

Deformation fabrics are manifested along the transect through layer-parallel detachments, mineral lineations, folds and cleavage. Extensive layer-parallel deformation zones are well developed along the shaley units, marked with intensive localized deformation including cleavage and layer-parallel veins. These zones decouple the variously deformed stratigraphic units and consequently have been interpreted as detachments. Bedding-parallel detachments strike NW-SE and marked with NNE-SSW trending mineral lineations (Fig. 3- 10). Folds, mostly within the thinly incompetent units of the Jurassic and Cretaceous successions, are oriented perpendicular to highly oblique to the NE-directed lineations and verge towards NE. They show gentle to open interlimb angles. Spaced pressure-solution cleavage appears verge to two directions: NNE and SSE (Fig. 3- 10). The NNE-verging cleavage is common across sub-horizontal strata, while the SSE-verging cleavage appears across bedding that is tilted northwards. When the tilting deformation was restored by rotating bedding 30° back along a horizontal axis trending 090 the vergence of the SSE-verging cleavage transposed into NNE. Consequently the NNE-verging cleaving formed whilst beds were still horizontal and therefore before the folding deformation.

Interpretation and summary

It has been found that the stratigraphic omission along this wadi is associated with the Triassic- Jurassic unconformity rather than tectonic thrusting as indicated by Rabu et al., (1986). Evidenced for this is seen by channels and karstification features at the boundary of the Triassic Mahil dolomite and the overlaying Jurassic carbonates. The fold crest along this transect is highly faulted forming two sets of faults, NW-SE and NE-SW and both are generally dip slip normal faults. The mechanism for such intensive faulting will be investigated at the end of the chapter. The deformation fabrics, which are localized along the fine-grained units of the Jurassic-Cretaceous succession, indicate consistent top-to-the-NNE shear deformation.

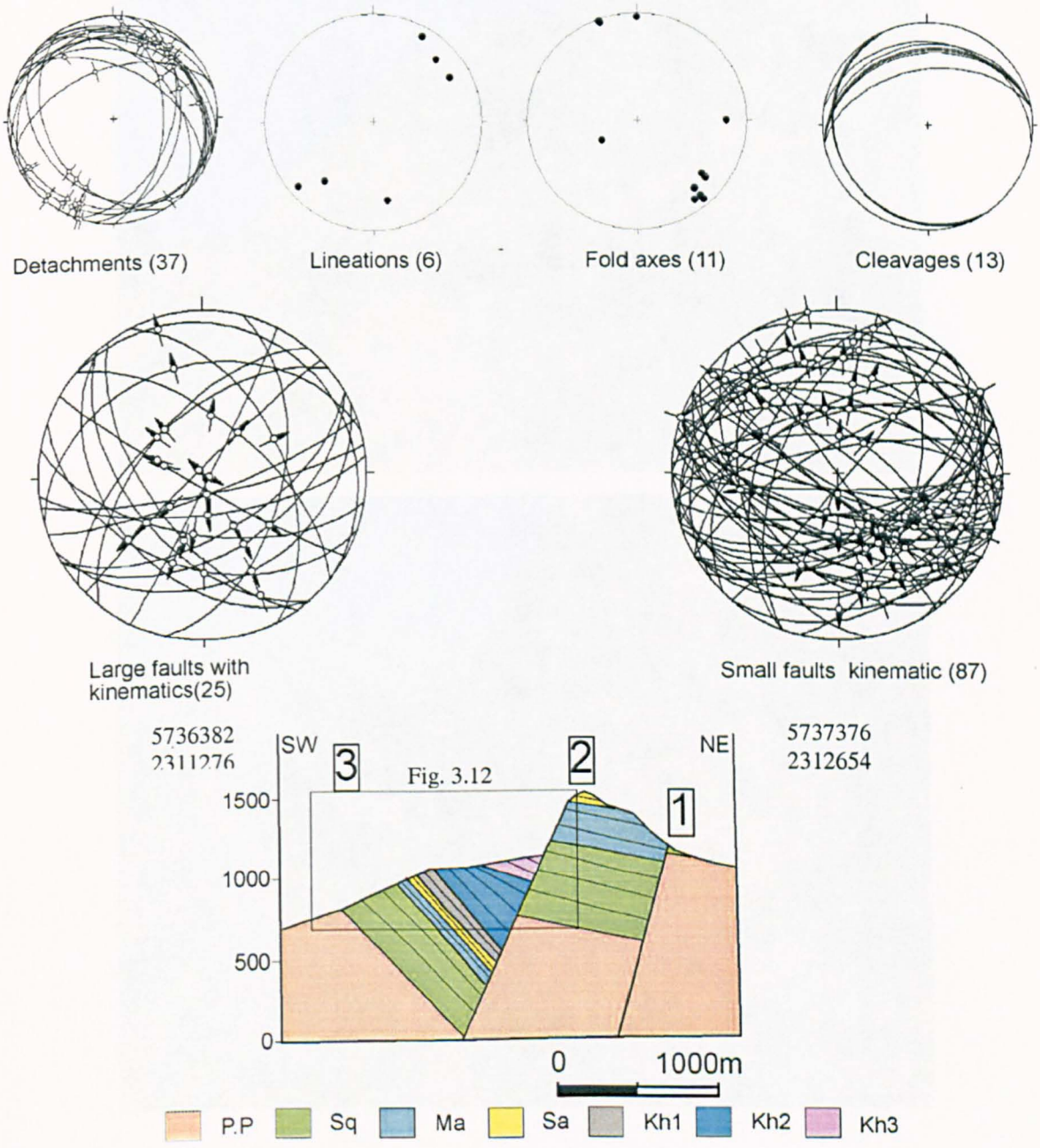

Fig. 3- 10 The Kharus transect as constructed across the Mehsaneh structure, with stereograms for the various structural elements

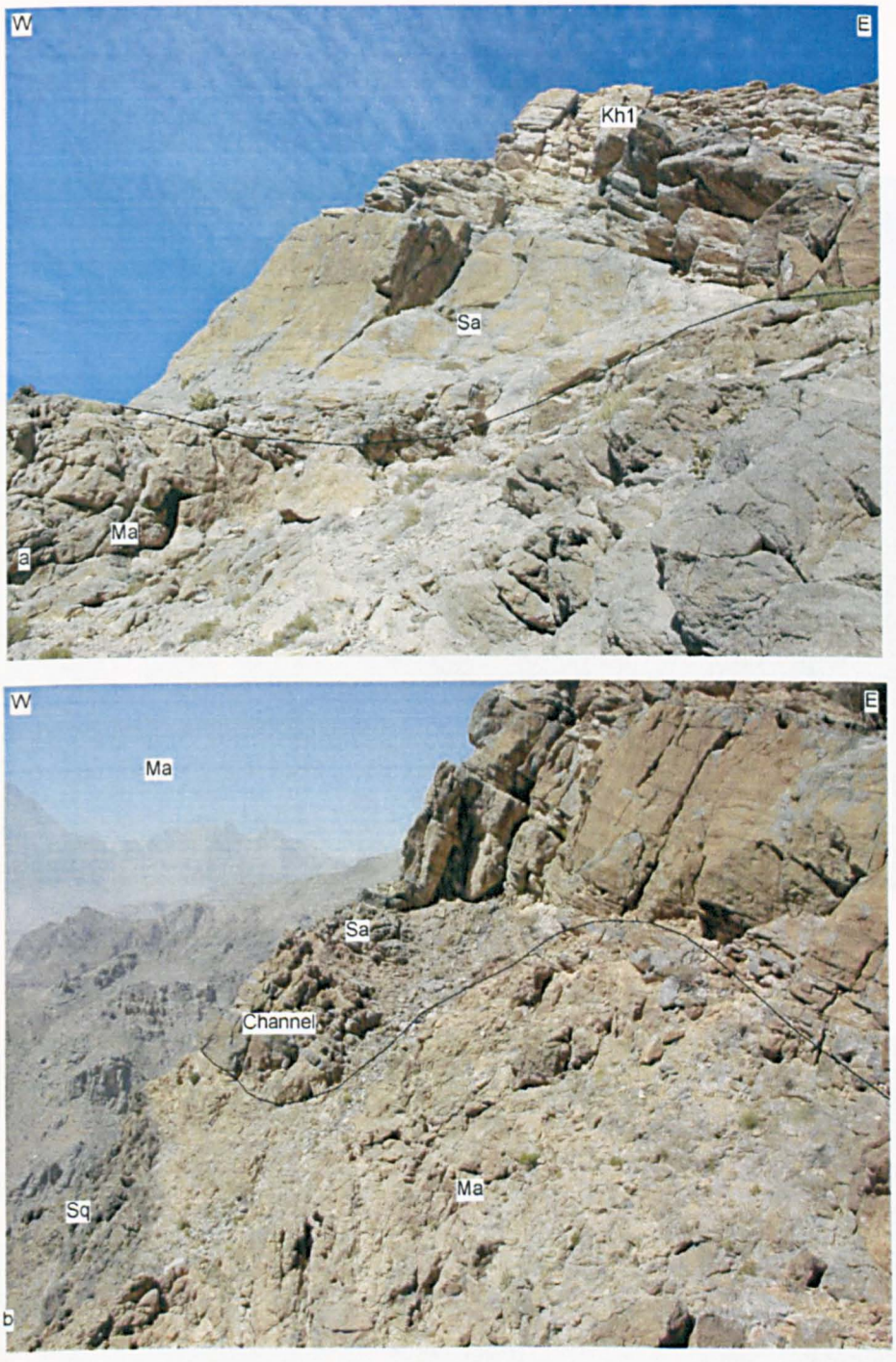

Fig. 3- 11 Sedimentation and erosional features along the Kharous transect. (a) Intensive stratigraphic thinning across the Mesozoic successions, Note the incredible thinning of the Sa Fm (Field of view approximately 10 m). (b) Channel seen at the contact between the Triassic Ma dolomite and the overlying Jurassic carbonates (Field of view approximately 40 m). (5736562,2311642)

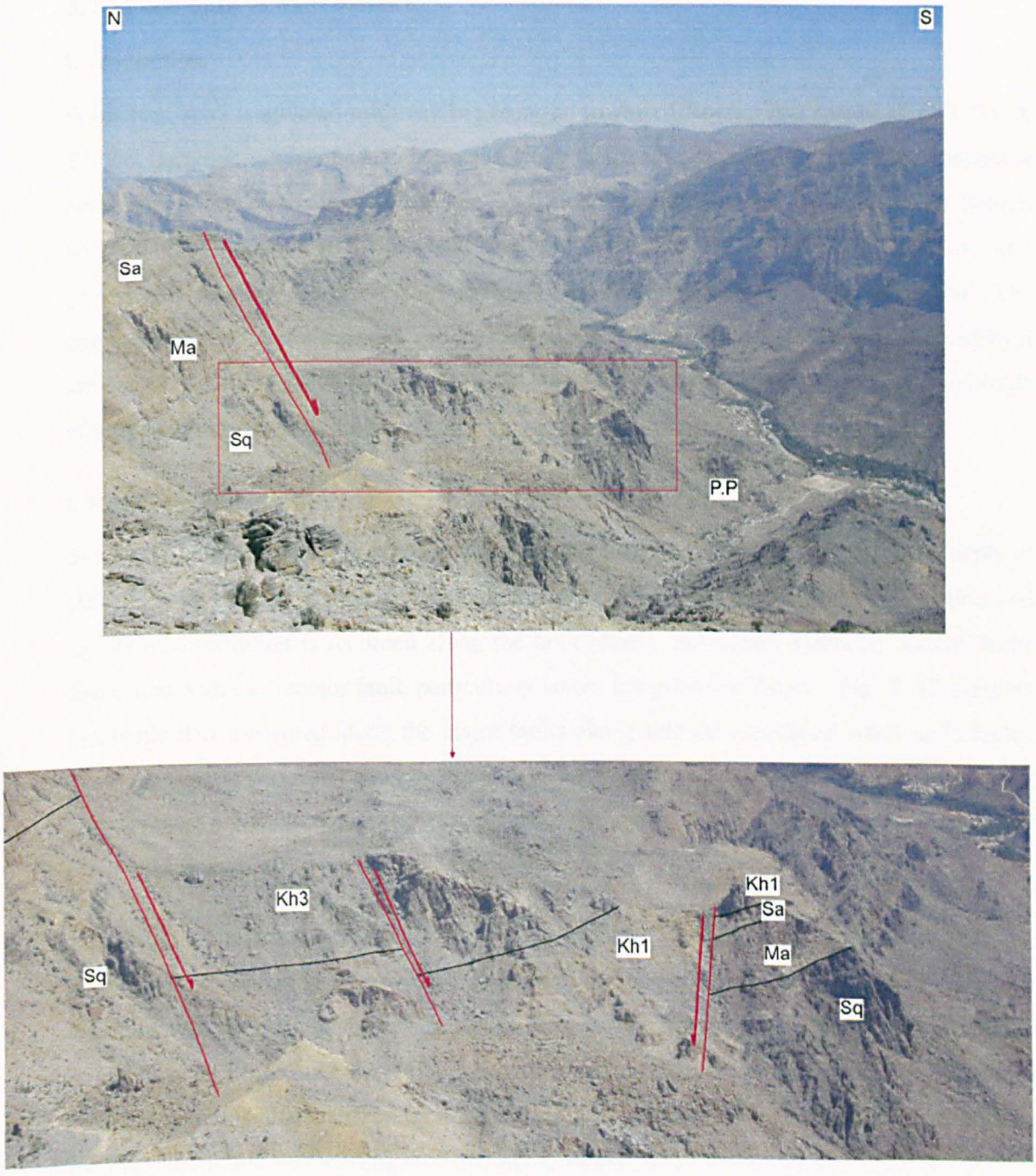

Fig. 3- 12 The Mahsanah half graben structure showing the juxtaposition of the Kh3 with the Sq Fm. The lower interpreted image is a close up of the structure (Field of view approximately 3 km).

3.7 Wadi beni Awf transect

Introduction

Wadi beni Awf is situated mid-way between the towns of Rustaq and Awabi (Fig. 3- 1). A 5.5 Km long transect has been constructed along this wadi passing, from the Mid-Cretaceous Natih Fm at the northern mouth of the wadi until the pre-Permian Fara Fm at the Sahtan window. The transect transverse the northern monocline of the Akhdar anticline and generally beds along the transect are oriented NW-SE, with an average dip of 35° NE. The contact between the pre-Permian sediments and the Permian Saiq carbonates is marked by a km-long NW-striking fault. The Jurassic-Cretaceous sequences exhibit intraformational folds of tens of metres in amplitude.

Large scale structures

Three km-long NW-striking normal faults penetrate the transect[1, 2, 3], dipping steeply at 60° NE with estimated fault throws ranging from 100 to 600 m. Intensive brecciation and calcite mineralization is recorded along the fault planes. Subsidiary synthetic normal faults associated with each major fault, particularly across hanging-wall blocks. Fig. 3- 13 presents kinematic data measured along the major faults along side the associated small scale faults. The data reveals two main slip components: dip slip and strike slip. The dip slip component demonstrates a NE-directed extension, whereas the sense of the strike slip component could not be discriminated.

The Jurassic-Cretaceous succession is marked with two separate bedding-parallel structures, however it is confusing as to whether they are contraction or extension related. The first structure was mapped west of Fara village (Fig. 3-14), showing Jurassic Sahtan carbonates overlaying the Cretaceous Rayda Fm along a bedding-subparallel fault. The fault plane dips gently NE and is characterized by mineral lineations pitching NE. Structural features along the fault and in the surrounding area including normal faults branching and merging onto the fault reflect extensional deformation. Consequently the bedding-subparallel fault is not contractional in kinematics but in fact extensional. The deformation mechanism will be explained shortly after describing the second structure.

The second structure is seen at the entrance to the wadi, where a sliver of Natih carbonate is intercalated within the Nahr Umr shale (Fig. 3-14b). The upper boundary of the sliver is marked by a NE-dipping fault surface, while the lower boundary is seemingly a normal contact between the Nahr Umr and Natih Fm's. The fault appears to duplicate the

stratigraphy. However, similar to the previous example, there is no single piece of evidence of any compressional deformation. The structure has been interpreted as a result of ramping along a shallowly dipping extensional detachment, directed top-to-the-NNE and this interpretation is schematically illustrated in Fig. 3-14c. Ramping across a gentle extensional detachment imbricates the stratigraphy in a similar way to thrust tectonics. Wheeler and Butler, (1994) pointed out that for detachment ramping to happen, beds must be slightly tilted.

Deformation fabrics

Intensive localized shear deformations including folds, stretching lineations and cleavage are common in shaley limestone units separating variously deformed structural units. Therefore, such structures can be considered as detachments. Bedding-parallel detachments dip gently NE with fibre lineations pitching NE (Fig. 3- 13). Steep NW-striking, normal faults branch and merge onto the detachments, expressing NE-extension shearing (Fig. 3- 13). Stretching lineations especially within the Rayda Fm pitch NE. Commonly there is an intensive top-NE shearing along each bed of the Rayda. *Belemnite* fossils within the Rayda Fm are deformed inconsistently: some are undeformed (Fig. 3- 15a) while other are highly stretched along a NE-SW trend (Fig. 3- 15b). The amount of NE-directed stretching is 10.3%, as measured by correlation of the actual length of the fossils with the width of the crossing veins.

Intraformational folds with NE-vergence are aligned perpendicular to highly oblique to the NE-trending stretching direction (Fig. 3- 13). They have gentle-close interlimb angles and fold axes pitch NW. Boudinage structures arise along layer parallel veins marked with NE stretching lineations, while boudin axes are oriented NW-SE, orthogonal to the NE stretching direction (Fig. 3- 15c). Thus, it seems that under the progressive NE-shear deformation, some layer parallel detachments were boudinaged and folded. This may have occurred when a detachment was locked allowing the initiation of a new detachment and subsequent deformation of the earlier locked one. Cleavage within sub-horizontal beds verges NE with gentle dip (Fig. 3- 13), while along tilted beds cleavage is gentler than bedding and verges SW. However, when tilting structures were restored by rotating them 35° around a horizontal axis trending 120 chosen to be parallel to the fold axis, the apparent SW-verging cleavage became NE-verging cleavage. In addition cleavage is folded by the NE verging folds (Fig. 3- 15d).

Interpretation and summary

The transect is marked with km-long, NW-striking faults representing NE-SW extension. The fault chronology with respect to the Akhdar folding deformation cannot be revealed,

since both faults and the fold are parallel. The NE-directed extension is also manifested by low-angle detachments and NE-verging deformation fabrics. Ramping of the extensional detachments led to duplication of the stratigraphy, making the resultant structures resemble contractional deformation. The occurrence of such ramping suggests that the extensional deformation took place while the bedding was gently tilted, and that is likely to have been the case during the early stage of the folding deformation. The heterogeneously distributed deformation fabrics reflect a non-penetrative strain, concentrated within the fine-grained units. Although, the km-long, NW-striking faults transect the NE-verging deformation fabrics situated within the Jurassic-Cretaceous Fm's, both deformations still reflect NE-extensional shearing. The major faults are detached along a deeper detachment probably situated within the pre-Permian sequences.

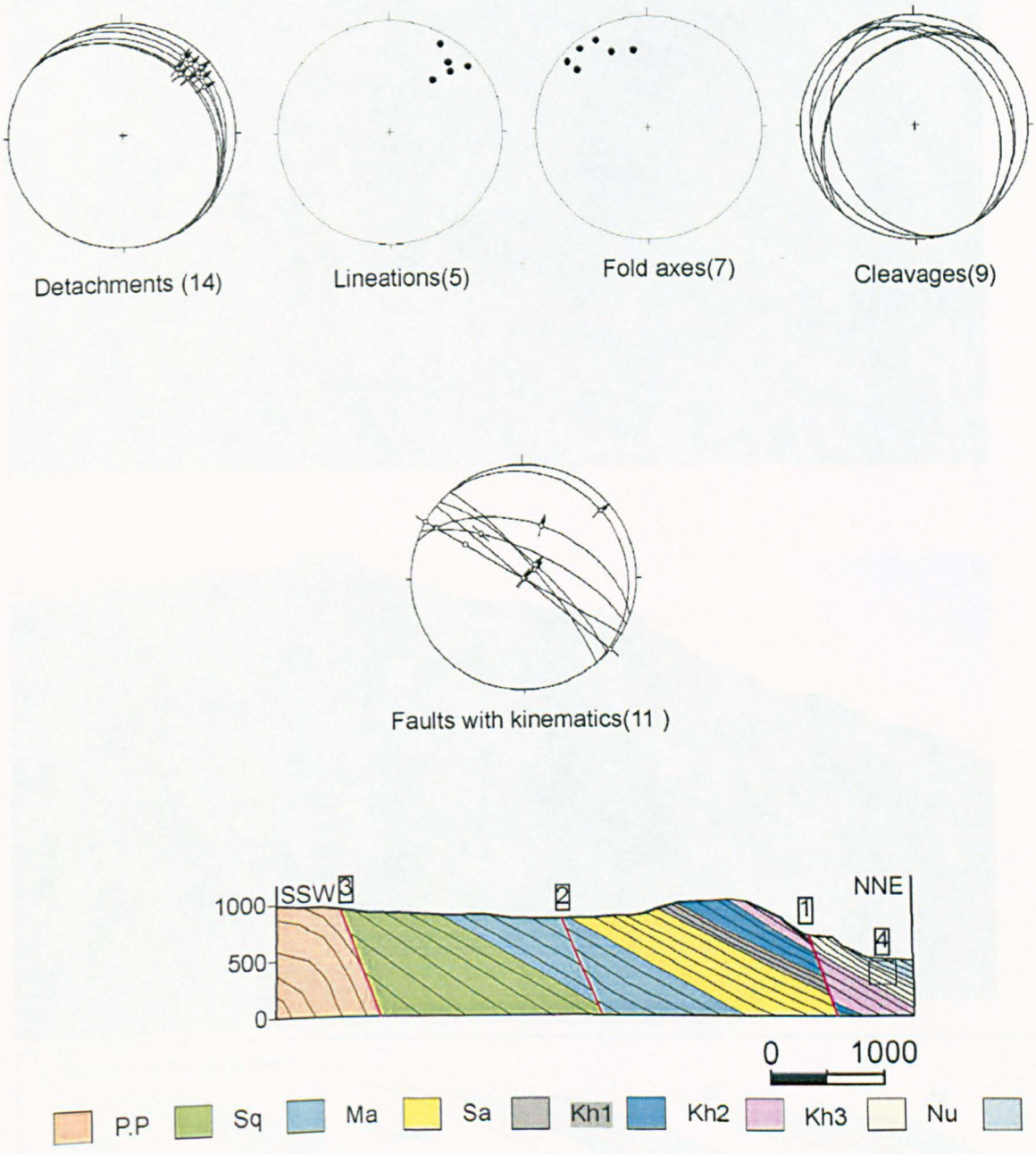

Fig. 3- 13 The Awf transect with stereograms of the various structural elements

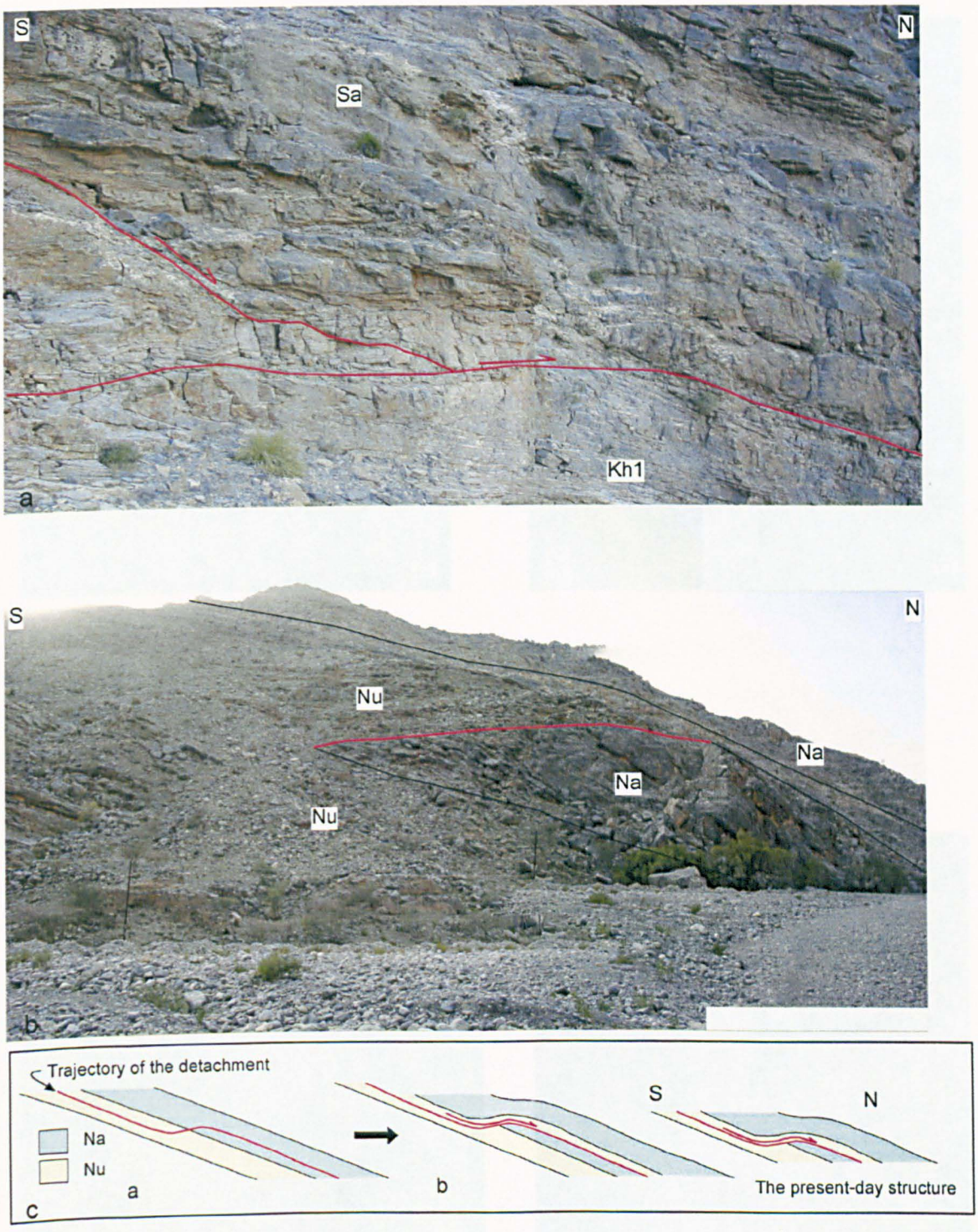

Fig. 3- 14 Imbricate structures within the Jurassic-Cretaceous units (a) and the mouth of the wadi (b) (Field of view approximately 50 m and 300 m respectively). (C) Schematic interpretation for this structure as a result of a ramping across a low-angle extensional detachment.

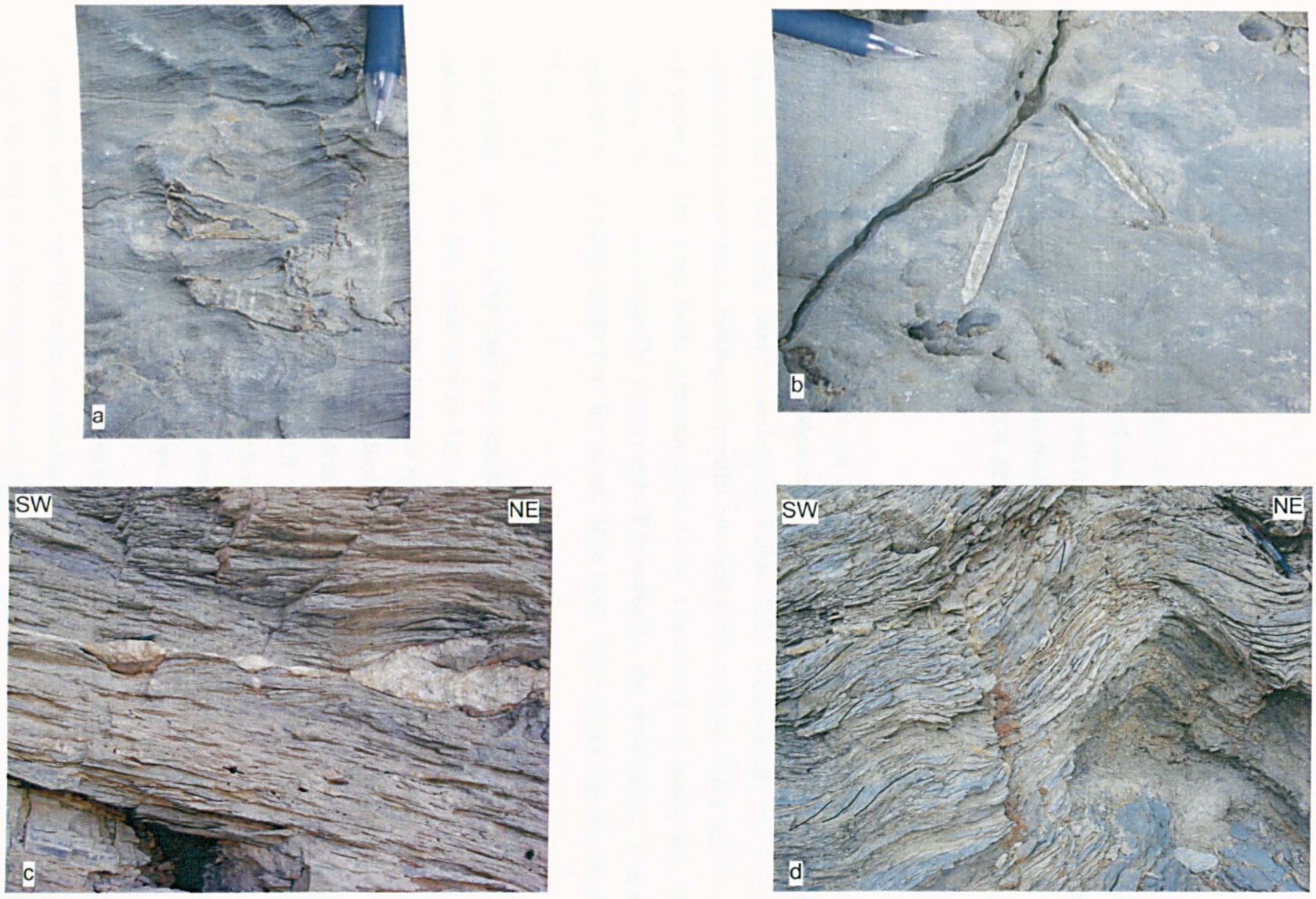

Fig. 3- 15 Deformation fabrics along the Awf transect (a) Stretched belemnite fossil showing 10% extension. (b) Undamaged Belemnite fossil. (c) Boudinaged layer-parallel detachment. (d) Folded cleavage within the a NE-verging fold.

3.8 Wadi Fara transect

Introduction

Wadi Fara is situated 12 km to the east of the town of Rustaq (Fig. 3- 1). A detailed N-S transect 1 km long has been constructed across the wadi (Fig. 3- 16). This detailed transect is considered as a type locality of structural deformation in the northern flank of the Akhdar anticline. The transect passes across the Natih carbonates and the upper part of the Nahr Umr Fm. Beds are aligned approximately NW-SE, but dip variably as the transect is disrupted by numerous low-angle faults.

Large scale structures

The Natih carbonates in the transect are dominated by low-angle faults situated within micritic limestone units (Fig. 3- 16). More competent units are faulted by steep NW-striking normal faults that merge onto the underlying shallow faults. Consequently, the low-angle faults can be described as bedding-subparallel extensional detachments, with a top-NE sense of shearing. The steep faults represent horse faults, constituting an extensional duplex bounded by bedding-subparallel detachments. Kinematically, the detachments are marked with NE-SW trending calcite fibre lineations, while steep faults exhibit dip slip lineations (Fig. 3- 16).

The linked system of steep faults and detachments is further explored at several localities as follows (Fig. 3- 16). Area number [1], exhibits an extensional duplex structure. The subsidiary normal faults are dip slip, have metric throws (1-3 m), and are bounded by major detachments, while they themselves displace small bedding-parallel detachments. This suggests that there are several orders of detachments overprinting one another. At the middle of the transect, a hanging wall ramp [2] was identified. It forms a gentle hanging-wall anticline with a fold axis aligned perpendicular to the detachment stretching lineations. The corresponding footwall ramp cannot be detected within the entire section, which suggests a minimum of 500 m displacement along this detachment.

The northern end of the transect is marked by a steep NW-striking fault [3], within the Natih carbonate, with a top-NE sense of shearing. The fault transects the low-angle detachments alongside their associated structures and therefore this fault can be regarded as the latest faulting event along the transect. Thick calcite mineralization and brecciation was recorded along the fault planes.

Small scale structures

Small normal faults of metric throw are common in the transect particularly across competent limestone units as already discussed. On the contrary, small reverse faults with sub-metric throws were also mapped within the Nahr Umr and Natih Fm's. Reverse faults [4] strike E-W to NW-SE with gentle to moderate dip (Fig. 3- 16), and are mainly localized along shear zones within incompetent units. The question arises, how these reverse faults coexist within an extensional context? All reverse faults within the gently dipping Natih Fm at area [4] verge NE in agreement with the top-NE extensional shearing (Fig. 3- 16), hence it is more likely that these faults were once pre-existing normal faults subsequently inverted by the progressive NE-directed simple shear deformation. However, a few thrusts exist on the same stereogram of thrust structures (Fig. 3- 16) expressing SW vergence. This data was taken from the northward dipping Nahr Umr strata. When the tilting deformation was restored by rotating it 35° around a horizontal axis trending 120, presumed to be parallel to the fold axis in that area, the SW-verging thrusts became NE-verging reverse faults. Thus the previous justification of inversion deformation by NE-directed simple shear extension can also be applied

Faults without kinematic data are mainly oriented NW-SE with minor faults trending NE-SW (Fig. 3- 16). Extensive micro-fracturing filled with calcite mineralization is very common within the competent units of the Natih carbonates, with both tensile and shear fractures recognized. The majority of the veins trend NW-SE with a minor set trending NE-SW.

Deformation fabrics

Bedding-parallel detachments are characterized by intensive deformation fabrics manifested by cleavage and fold structures. Detachment structures are greatly variable in size. In this section only the outcrop-scale detachments are analyzed since the major detachments are already described in the large scale structures section. The detachments strike approximately NW-SE with gentle to moderate dips. The majority of the detachment stretching lineations trend NNE-SSW, although minor lineations trend NW-SE (Fig. 3- 16). Intraformational folds are sub-metric in amplitude, with fold axes trending SE-NW and plunging gently SE and NW (Fig. 3- 16). Where folds are asymmetrical, they verge NE. In places, axial planes have been rotated by the progressive shear rotation to lean towards the detachment surfaces.

Cleavage is common within the incompetent units of the Shams, Nahr Umr and Natih Fm's. In the hanging-wall anticline [2], where Natih units are approximately sub-horizontal, cleavage is steeper than bedding and verges NE. In contrast, cleavage verges SW across the northward dipping strata of the Shams and Nahr Umr Fm. Such southward verging cleavage

cannot be related to the folding deformation of the Akhdar anticline, because beds are steeper than cleavage. However, when tilting was restored, cleavage verged towards NE. This reveals that cleavage generation took place before or during the early stage of the folding deformation. Stretching lineations recorded on the cleavage surfaces trend NE-SW. Cleavage leans over the layer-parallel detachments due to the progressive shear deformation, until ending up parallel to the detachments. Weak anastomosing cleavage with NE-vergence arises within competent beds of massive limestone. Commonly, cleavage is folded by NE-verging folds.

Deformations within Shams and Nahr Umr indicate the existence of the NE-directed simple shear, but are weakly developed compared with what is seen within the Natih Fm. Layer-parallel detachments with NE-verging folds and cleavage are also seen.

Interpretation and summary

There are two main systems of deformation along the transect. The first system is dominant and represented by a linked systems of extension faults and detachments. Extensional faults, which are bedding-confined and NW-oriented, are detached along low-angle detachments. The detachment zones comprise of deformation fabrics reflecting consistently top-to-the-NNEshearing. Kinematically, this system as a whole shows extensional shearing directed top-NNE. However, deformation fabrics indicate an opposite sense of shearing where beds are moderately tilted. When tilting structures were restored, deformation fabrics appear to have originally verge NNE. As the result, the NNE-extension shear deformation is suggested to have occurred before or during the early stage of the folding process, before the moderate tilting of strata.

The second deformational system is expressed by a steep NW-striking normal fault [3], developed at the edge of the Akhdar culmination and transecting the low-angle faulting system. Although both deformation systems infer a top-to-the-NNE extension, cross-cutting relationships reveal that the system of the steep NW-striking faults is younger. The relationships and mechanisms of each deformation system will be investigated at the end of the chapter. Furthermore, the mapped detachments involve minor lineations trending NW-SE, and this local observation will be explored at the end of the chapter.

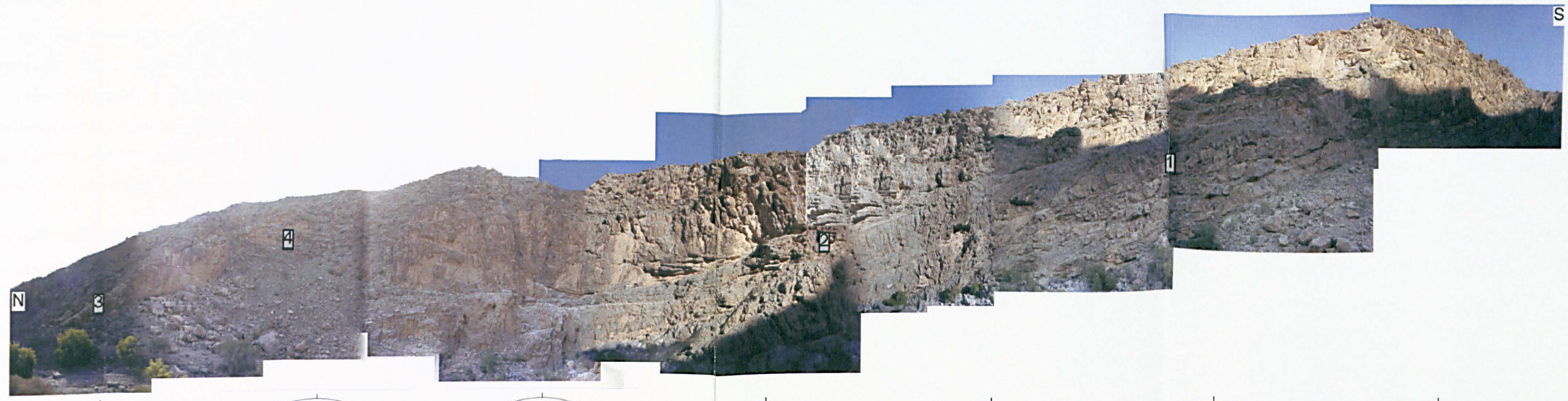

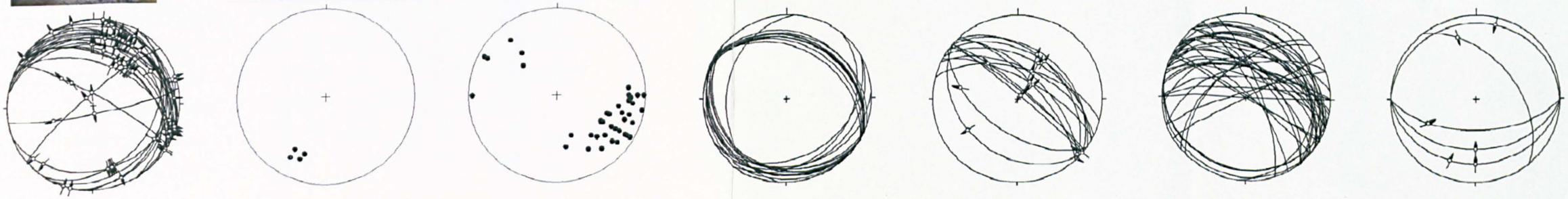

Detachments (70) lineations (4) Fold axes (46) Cleavage (25) Faults with kinematic(15) Faults without kinematic(43) Thrusts (9)

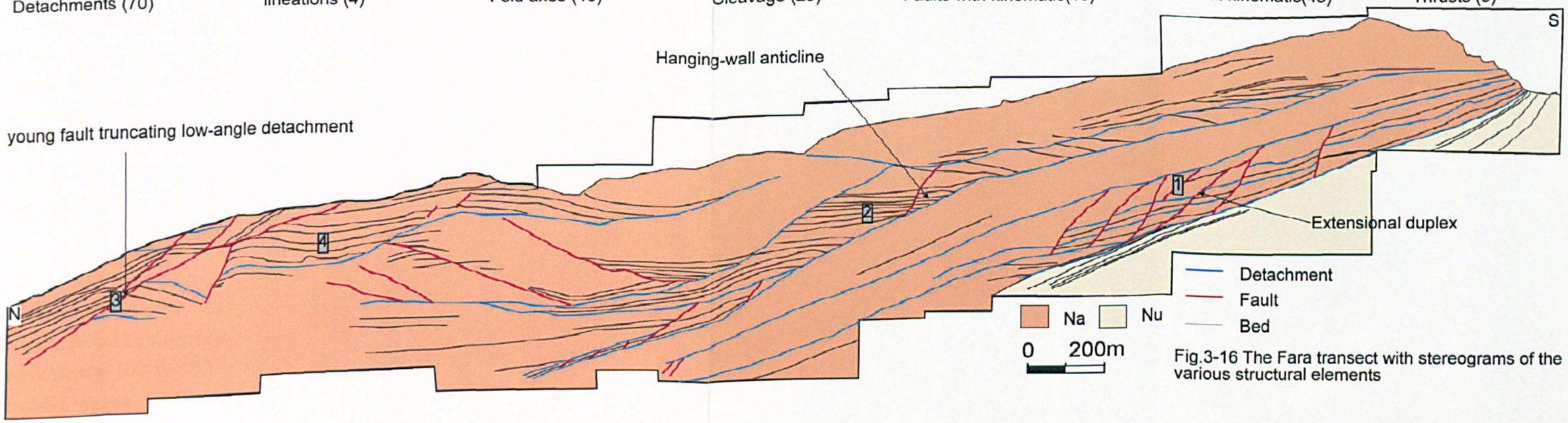

Fig.3-16 The Fara transect with stereograms of the various structural elements

3.9 Wadi Sahtan transect

Introduction

A 6 km long transect has been constructed along wadi Sahtan, which is located approximately 10 km to the west of the town of Rustaq (Fig. 3- 1). The transect covers the entire preserved Mesozoic carbonate sequences, starting at the Permian Saiq carbonate, to the Mid-Cretaceous Natih carbonate at the northern wadi entrance (Fig. 3- 17). Beds are oriented E-W to NE-SW, with moderate dips of 30° NW. The transect is marked by low-angle normal faults transected by a steep E-W fault at the mouth of the wadi.

Large scale structures

Large scale structures of km-length are manifested along the transect by two fault types: bedding-subparallel and steeply dipping faults. The bedding-subparallel faults are oriented NE-SW with a moderate dip of 30° NW (Fig. 3- 17). They exhibit NE-plunging fibre lineations (Fig. 3- 17).

The most prominent bedding-subparallel fault was mapped along the contact between the Shams and Nahr Umr Fm's before down cutting into the massive competent units of the Shams Fm, forming an extensional duplex structure (Fig. 3- 17). Where this gentle fault cuts down across the Shams Fm and forms ramp structures, the hanging wall strata of the overlaying Nahr Umr Fm are folded into NW-oriented folds. The minimum amount of net displacement along the fault is around 300 m, as measured by correlation of the hanging-wall ramps.

A another major bedding-subparallel fault is present along the contact between the Salil and Shams Fm's, forming layer-extension structures in the lower part of the Shams Fm. Fig. 3- 18a shows low-angle, northward directed extensional faults developed through the Cretaceous limestones of Shams. These gentle faults carry thin panels of the limestone along the top of the weakly deformed basal Shams. The slices of Cretaceous limestones show extensional ramp geometries, off cutting both against the footwalls and hanging-walls of the detachments faults. The detachments show top-to-the-NNE shear senses.

The transect is also marked by a major, steep E-W fault, which lies at the mouth of the wadi between the Nahr Umr and Natih Fm's (Fig. 3- 18b). This fault cannot be traced further up into the Natih Fm, however the hanging-wall strata of the Nahr Umr Fm are folded adjacent to the fault plane and form drag folds, indicative of normal sense fault shearing. Kinematic elements of the main fault vary from dip slip to oblique NW-pitching lineations (Fig. 3- 18b). Such variably suggests a poly-displacement fault. The dip slip lineations indicate post-

folding fault of dip slip displacements, since they are not rotated by the folding deformation. When the oblique lineation structures were restored by rotating the tilted beds back, they transformed into horizontal, revealing a pre-or-syn-folding strike slip displacement. In short, the steep fault experienced a strike slip movement before or during the early stage of the folding deformation and then reactivated as a dip slip fault after the folding event. The strata of the hanging-wall display low-angle extensional faults truncated by the main steep fault. However, these gentle faults cut beds at a steep angle of 60°. The majority of the faults trend approximately N-S and are marked with shallow pitching lineations aligned NNW-SSE. The amount of fault dip decreases downward (Fig. 3- 18b). When tilting was restored by rotating it 50° around a horizontal axis trending 070, the low-angle extensional faults turned into steep WNW-oriented dip slip faults (Fig. 3- 18b). This means that these faults were once steeply dipping WNW-striking faults, created by an earlier NE-directed extensional regime before the tilting event. They were subsequently tilted and most probably reactivated by the main E-W fault.

Deformation fabrics

Deformation fabrics are expressed by shear zones, cleavage and folds. The shear zone of intensive localized shear deformation bounded by less deformed rocks is called a detachment. The detachments are bedding-parallel and characterized with intraformational folds and cleavage. Although the detachment orientations are variable according to the attitude of the bearing strata, the associated mineral lineations trend consistently NNE-SSW.

Intraformational folds less than a metre in amplitude, plunge moderately NW (Fig. 3- 17), and where folds are asymmetrical, they verge NE. Cleavage is aligned NE-SW with a gentle NW dip and a SE vergence (Fig. 3- 17). Cleavage dips gentler than the corresponding beds and therefore cannot be related to the Akhdar folding, where the respective cleavage dip would be steeper than that of the bedding. By untilting the beds, cleavage verges towards NE expected cleavage from NE-shearing. The apparent SE-verging cleavage is therefore generated by NE-shearing before the folding onset. The massive competent beds of the Shams carbonates express extensive wavy-like stylolites with intensive kink bands oriented normal to the NE-stretching direction.

Interpretation and summary

There are two geometrically contrasting styles of faulting, although both imply NNE-extension. Firstly, the low-angle bedding-subparallel faults are confined within the Jurassic-Cretaceous succession. Bedding-confined, NW-oriented normal faults merge onto these gentle faults. Gentle and steep faults collectively extend stratigraphy with a top-to-the-

NNEshear. Secondly, steep E-W normal faulting truncates and deforms the structures of the low-angle faulting. Both styles of faulting are likely to have been part of the same ongoing extensional deformation, yet both took place at different stages. The timing and mechanisms of each style will be explored thoroughly at the end of the chapter.

The observed deformation fabrics indicate top-to-the-NNE shearing. Thus, deformation fabrics and the shallow and steep brittle extensional faulting reflect a similar sense of shearing, top-NNE. Consequently all the features are the products of a broad NE- extensional deformation, with the distribution of the ductile and the brittle deformation constrained by the competency of the deformed units.

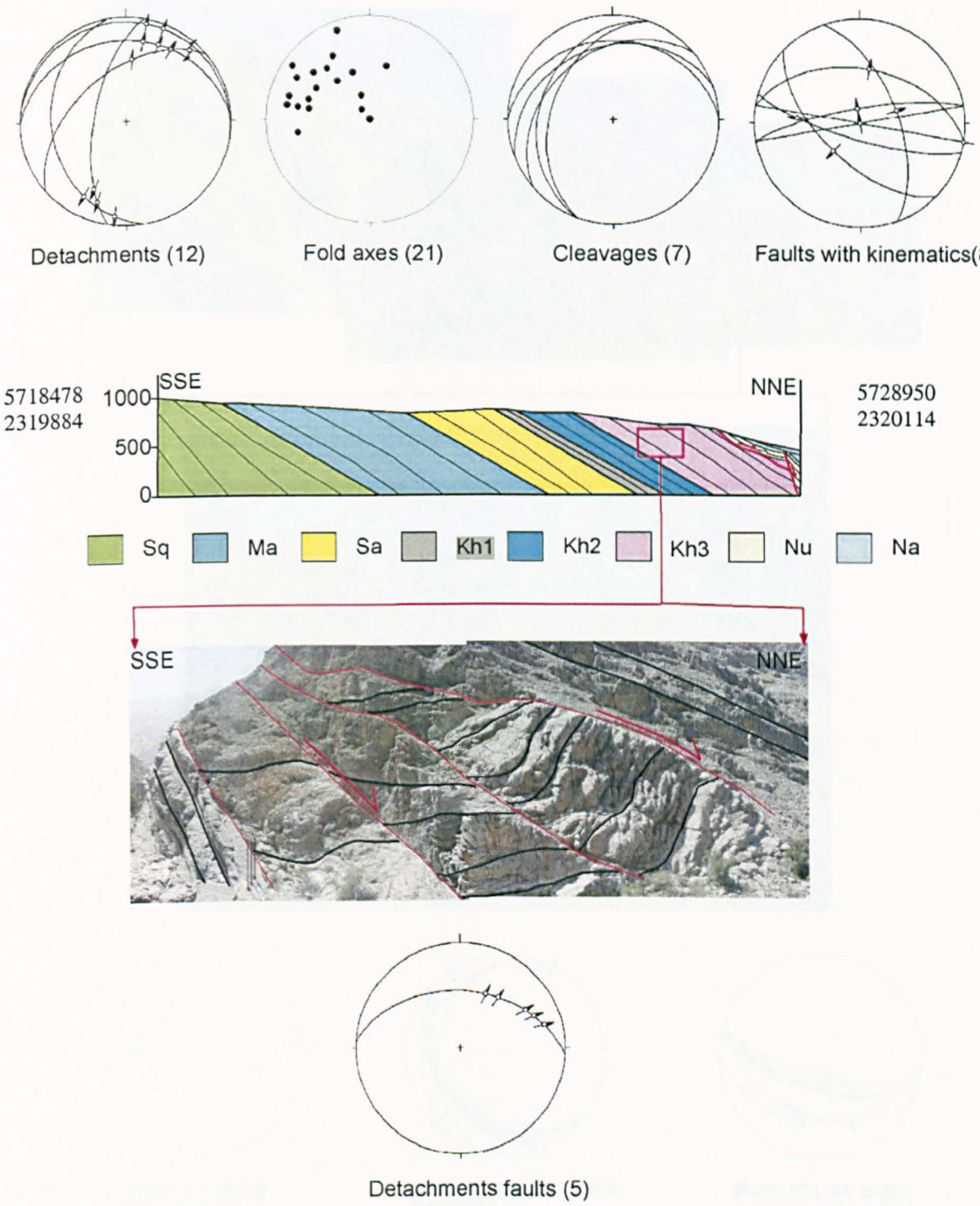

Fig. 3- 17 The Sahtan transect with stereograms of the various structural elements. The lower image is of the steeply dipping, E-W trending normal faults, along the base of Shams with their kinematics are shown by the lower stereogram.

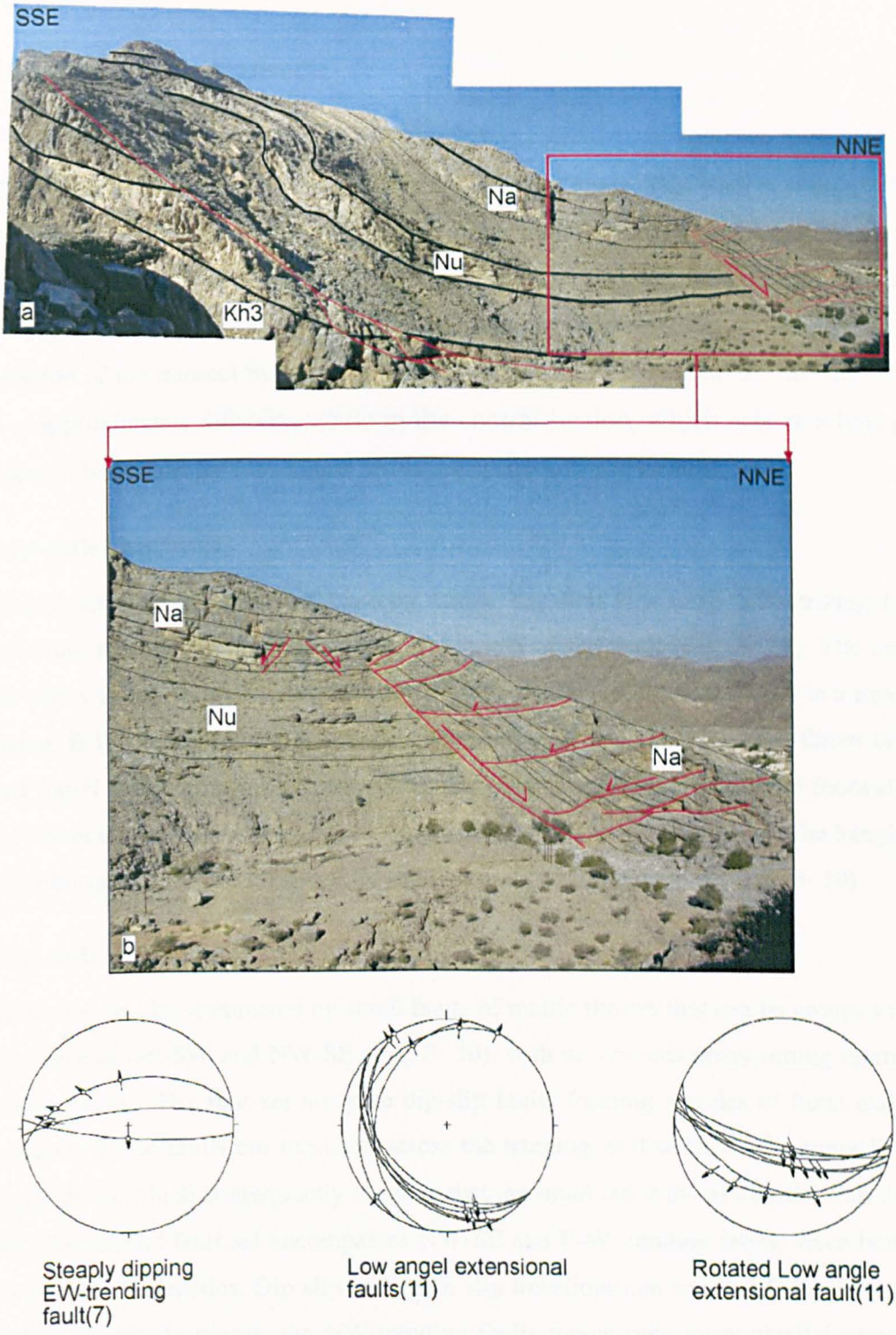

Fig. 3- 18 The different styles of faulting along the Sahtan Transect (a) The major NE-directed detachment along the Kh3\Nu contact, notice folding within Nu along the hanging-wall (Field of view approximately 1km). (b) The steeply dipping E-W trending fault at the mouth of the wadi, the apparaant low-angle extensional faults used to be steeply dipping normal faults before the faulting event (rotated 50° around a horizontal axis trending 070).as seen from the last two stereograms (Field of view approximately 300 m).

3.10 Wadi Ghariz transect:

Introduction

A 3 km-long transect has been constructed along wadi Ghariz. This wadi is situated 15 km to the west of the town of Rustaq (Fig. 3.1). The transect runs NW-SE mainly across the Jurassic-Cretaceous succession. In this part of the Akhdar culmination, strata trend consistently NE-SW and dip some 40° NW. However, bedding dip is variable due to the disruption of the transect by km-long faults (Fig. 3- 19). At either end of the transect, beds dip at approximately 40° NW, while in the central section, which acts as a half graben structure bounded by two major faults, beds are sub-horizontal.

Large scale structures

The transect is marked by two km-long faults. The first is a steep NW-striking fault [1] separating, the Natih and Aruma Gp at the mouth of the wadi (Fig. 3- 19). The estimated fault throw is some 100 m with down-throw towards NW. The second fault is a moderately dipping, E-W fault [2] lying across the Cretaceous succession with a fault throw of 400 m and a top-N shear. The Natih Fm is juxtaposed against the Shams Fm of the footwall, while the Nahr umr strata in the hanging-wall are tilted parallel to the fault plane. The hanging-wall strata dips gently and are truncated by small-offset, NE-trending faults (Fig. 3- 19).

Small scale structures

The transect is also dominated by small faults of metric throws that can be grouped into two sets, trending NE-SW and NW-SE (Fig. 3- 20), with no obvious cross-cutting relationships between them. The first set are pure dip-slip faults forming a series of horst and graben structures. These faults are localized across the hanging-wall strata of the major E-W fault (Fig. 3- 20 b), which consequently suggests that the small faults are associated with the major fault. The second fault set encompasses NW-SE and E-W trending faults, since both trends share similar kinematics. Dip slip and strike slip lineations can be identified along this fault set (Fig. 3- 19). In places, the NW-trending faults merge onto layer parallel detachments, typified with NE-pitching lineations (Fig. 3- 20c).

Various phases of veining were identified particularly within the competent carbonate units. In general, veins mainly trend NE-SW and NW-SE. The NE-SW set is minor and considered to be related to the NE-striking faults. The NW-SE set is dominant and well established, with two different origins: tensile and shear (Fig. 3- 20d). The tensile fractures developed normal to bedding under layer-parallel extension and thick calcite mineralization subsequently precipitated within the tensile fractures. Shear fractures are oblique to bedding and bounded

from both tips by layer-parallel detachments, along which shear fractures dip. The thickness of the shear calcite veins is variable depending on the fracture attitude, with respect to the bounding layer-parallel detachments. Both types of the NW-SE vein set are related to the NE-extension shear deformation.

Deformation fabrics

Deformation fabrics such as cleavage and folds are well established within the Jurassic-Cretaceous succession, especially within fine-grained units. These fabrics are intensively developed in highly strained narrow zones surrounded by less deformed wall rocks, and therefore behave as detachments zones. Low-angle detachments strike NE-SW with NNE-pitching fibre lineations (Fig. 3- 19). The sense of shearing along the detachments is top to the NNE, and the most intensified detachments were mapped within the Salil Fm, where several closely spaced detachments are present (Fig. 3- 20a). Mineral lineations of NE-SW trend were documented along the layer parallel cleavage surfaces (Fig. 3- 19). Intraformational folds, mainly within the Salil Fm, are orthogonal to oblique to the NE stretching direction, and verge NE (Fig. 3- 19). They exhibit open-close interlimb angles and plunge NW. Cleavage along most sheared zones is layer parallel. Bedding-parallel stylolites are common within the competent carbonate units.

Interpretation and summary

The transect is characterized with two different extensional systems: top-NE and top-NW extension. The NE-extension is dominant over the whole area and manifested by a linked system of faults of variable length and detachments. Small NW-striking faults of metric throw merge onto bedding-parallel detachments, situated along key horizons within the Jurassic-Cretaceous succession. However, the km-long NW-striking fault penetrates the entire stratigraphic profile and presumably merges onto a detachment situated within the pre-Permian sequence. Kinematically, faults under this system experienced dip and strike slip displacements. Bedding-parallel detachments within the Jurassic-Cretaceous succession display deformation fabrics such as cleavage and NE-verging folds. The top-NW extension is simply expressed by major NE-striking faults situated at the edge of the culmination, alongside small NE-oriented faults. Kinematically, faults of this system are mainly dip slip. The timing and mechanism of such local extension will be explored at the end of the chapter.

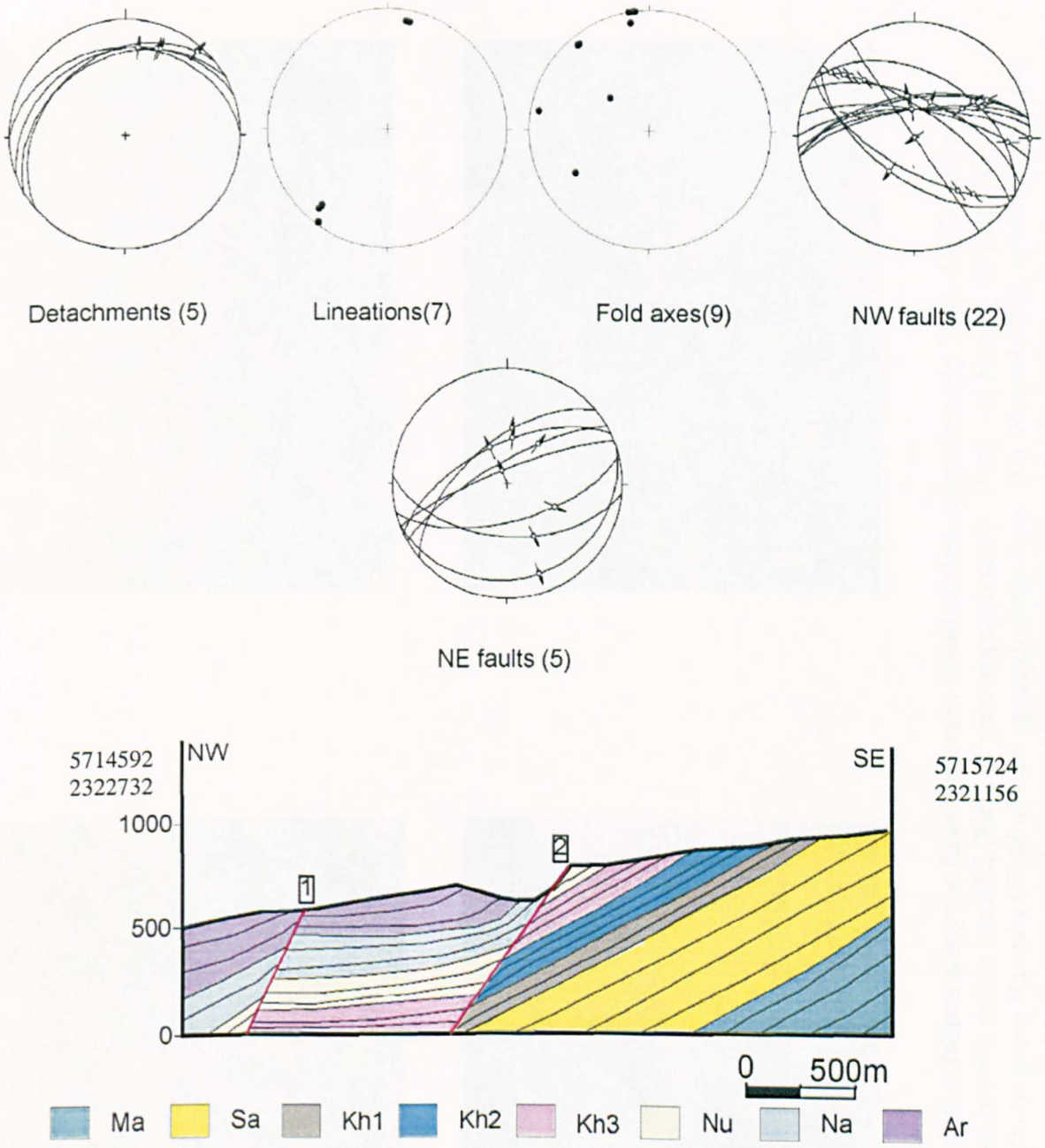

Fig. 3- 19 The wadi Ghariz transect with stereograms of the various structural elements

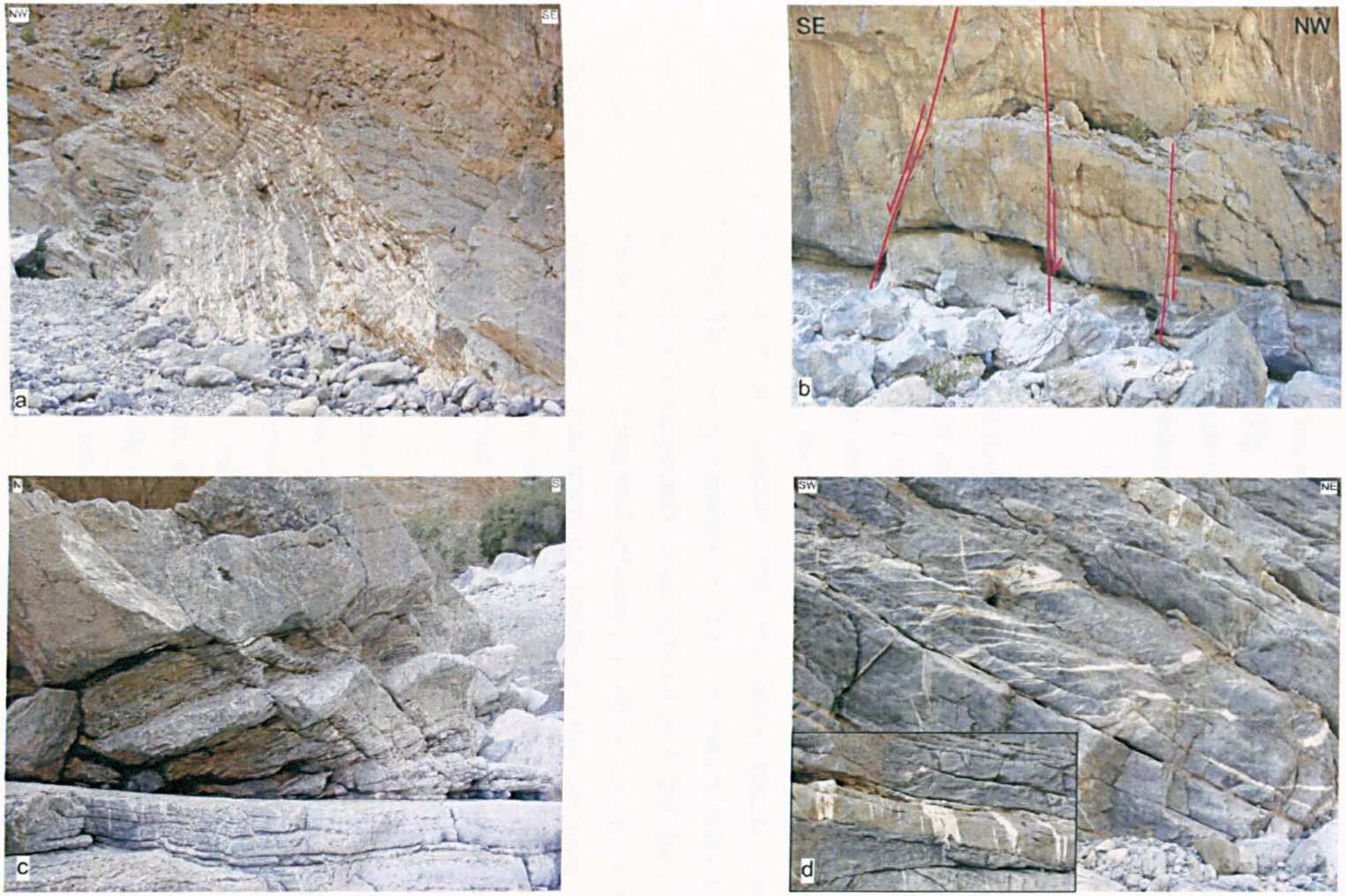

Fig. 3- 20 Deformation fabrics along the Ghariz transect (Field of view approximately 20 m) (a) Extensive layer-parallel detachments within the Kh2 (Field of view approximately 50 m). (b) Steeply dipping, NE-trending normal faults along Na units (Field of view approximately 5 m). (C) Normal faults branching onto the NE-directed extensional detachment. (d) Bedding-oblique shear veins bounded by layer parallel detachments (Field of view approximately 3 m)

3.11 Wadi Yiqa transect

Introduction

A 2.5-km-long, NE-SW transect has been constructed along wadi Yiqa, which is 20 km to the west of the town of Rustaq (Fig. 3- 1). The transect passes across the massive bedded Cretaceous carbonates. Beds in general vary between sub-horizontal and gently dipping at 20° NE (Fig. 3-21) However, bedding attitude is disrupted by extensional faults forming a rollover anticline.

Large scale structures

The transect is extensively faulted through a series of steep and shallow dipping extensional faults. Faulting deformation can be classified into two separate systems based on the fault geometry and the fault extent. The first system is represented by a linked system of steep and low-angle faults. The steep faults are NW-oriented, bedding-confined, have metric-offsets and form a series of horst and graben structures. They merge downwards onto low-angle faults. Conjugate tension gashes associated with these faults indicate a vertical thinning direction (Fig. 3- 22d). The low-angle extensional faults are oriented NW-SE [1] and flatten gradually down section into bedding-parallel detachments (Fig. 3- 20). Such listric geometry has led to the formation of a hanging-wall anticline [2] lying orthogonal to the extensional direction. Any change in the detachment dip results in extensive steep faulting of the overlying hanging-wall strata, as can be seen in (Fig. 3- 23). The bedding-parallel detachments are concentrated within the fine-grained units and marked by NE-trending mineral lineations.

The second faulting system is manifested by a km-long, NW-striking fault [3], which cross-cut the entire exposed stratigraphic profile, presumably merge onto a deeper detachment (Fig. 3-21). This steep fault transects the low-angle faulting and hence can be dated as a younger fault. Steep faults of both faulting systems exhibit dip and strike slip movements as evidenced from the fault striations, but the relative timing of each component cannot be resolved. The sense of the strike slip displacement is not well constrained, although dextral movements can be identified along some NW-striking faults.

Tensile and shear fractures are common along the wadi. Shear veins are gently dipping, highly boudinaged and truncate the NE-verging cleavage (Fig. 3- 22b). How were such shear fractures developed? Initially shear fractures were initiated by NE-directed simple shear deformation as steeply dipping shear fractures dipping SW. As the deformation proceeded the shear fractures were rotated and subsequently stretched and boudinaged. Eventually, during the final stage of the same deformation, brittle deformation took place inducing

normal faults to cross-cut the pre-existing shear veins and other ductile structures (Fig. 3-22c). Tensile fractures were later filled with calcite mineralization a few cm in thickness. The intensive heterogeneous tension gashes are associated with this phase of brittle deformation.

Deformation fabrics

Deformation fabrics comprise bedding-parallel detachments, fold cleavage and boudinage structures. The transect displays highly deformed bedding-parallel zones with intensive ductile shear deformation bounded by less deformed rocks. Such structures can be called detachments. Bedding-parallel detachments strike NW-SE and dip of 20°. Mineral lineations on the detachments, trend NE-SW (Fig. 3-21). The hinge lines of the NE-verging fold structures trend perpendicular to slightly oblique to the NE stretching direction (Fig. 3-21). Folds exhibit gentle-open interlimb angles and plunge down dip towards NW. Layer parallel stylolites arise within the competent massive units of the Shams Fm. Cleavage is common within the shaly units of the Shams & Nahr Umr Fm's. Cleavage verges NE within sub-horizontal beds, while within tilted strata the apparent cleavage vergence is SW (Fig. 3-21). However, when tilting structures were restored by rotating them around the 100/20 axis, calculated to be parallel to the fold axis, the SW-verging structures transposed into NE-verging cleavage. This indicates that cleaving occurred before or during the early stage of the folding deformation. Cleavage along some bedding-parallel detachments is horizontal. Boudinage structures appear within the interbedded limestone and shale succession with the boudin axes aligned orthogonal to the NE stretching direction (Fig. 3- 22a). S-C structures, where present indicate top-NE shearing.

Interpretation and summary

There are two main systems of deformation along the transect. The first system is dominant and represented by a linked steep faults and low-angle faults. The steep faults are bedding-confined, NW-oriented and merge onto low-angle faults, which shallow down-section to become bedding-parallel detachments with top-to-the-NNE extension. The detachments are also characterized by ductile structures reflecting top-to-the-NNE shearing. Kinematically, this whole system indicates extensional shearing directed top-NNE. However, within tilted beds, deformation fabrics such as cleavage indicate an opposite sense of shearing. However when tilting structures were restored, deformation fabrics appeared to verge to NNE. As a result, the NNE-extensional shear deformation is suggested to have occurred before or during the early stage of the folding process. Furthermore, it seems to be that the ductile deformations are transected by the brittle faulting. Consequently, brittle deformations may have taken place at a later stage of the evolving NE extension deformations.

The km-long, NW-striking normal fault [3] represents the second deformation system. This steep fault penetrates the entire exposed stratigraphic profile and transects the low-angle faulting system. Although both deformation systems infer top-to-the-NNE extension, cross-cutting relationships reveal that the system of steep NW-striking faults is younger. The relationships and mechanism of each deformation system will be explored at the end of the chapter.

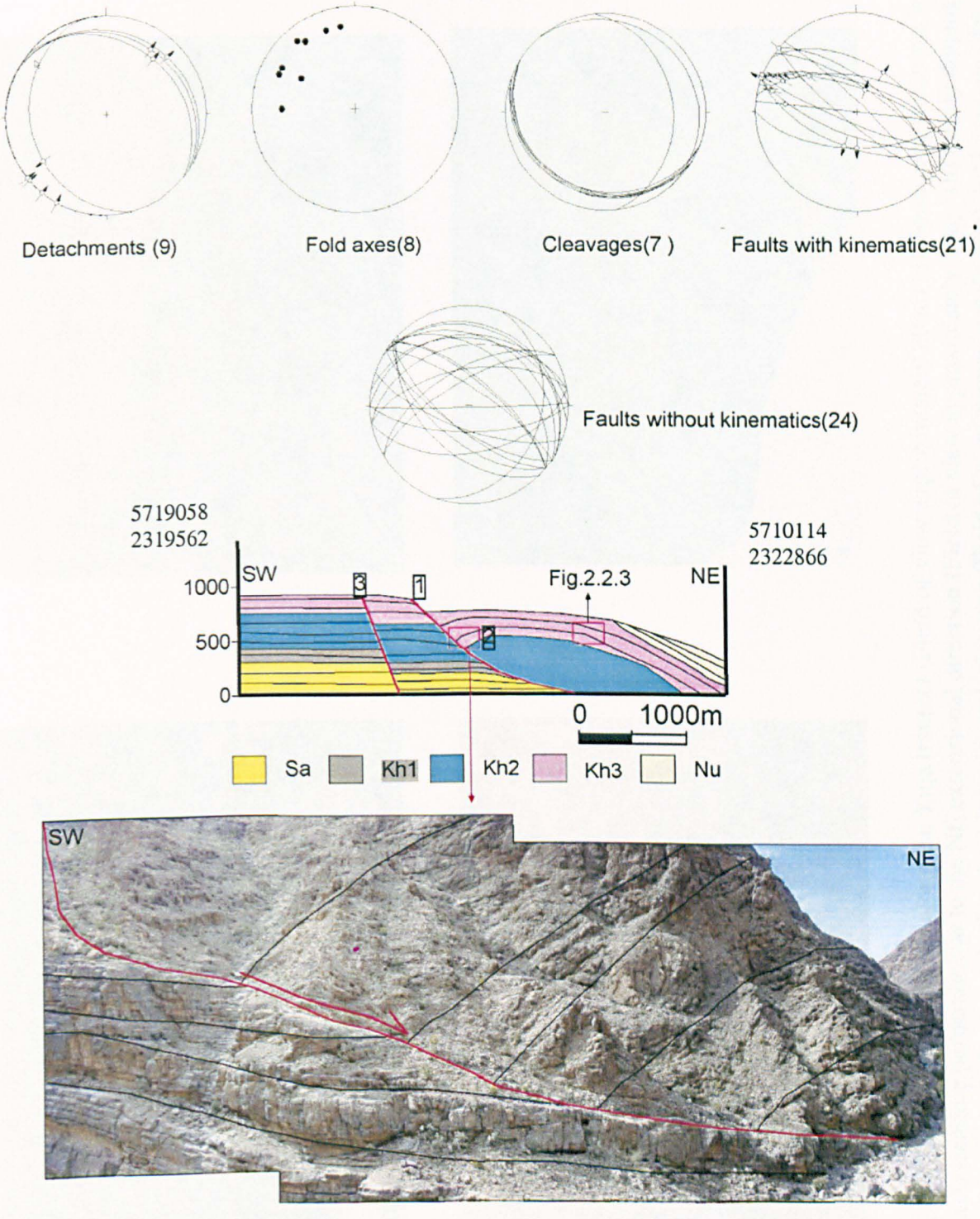

Fig. 3- 21 The Yiqa transect with stereograms of the various structural elements, the lower image is for rollover anticline above NE-directed extensional detachment along Salil (Field of view approximately 500 m)

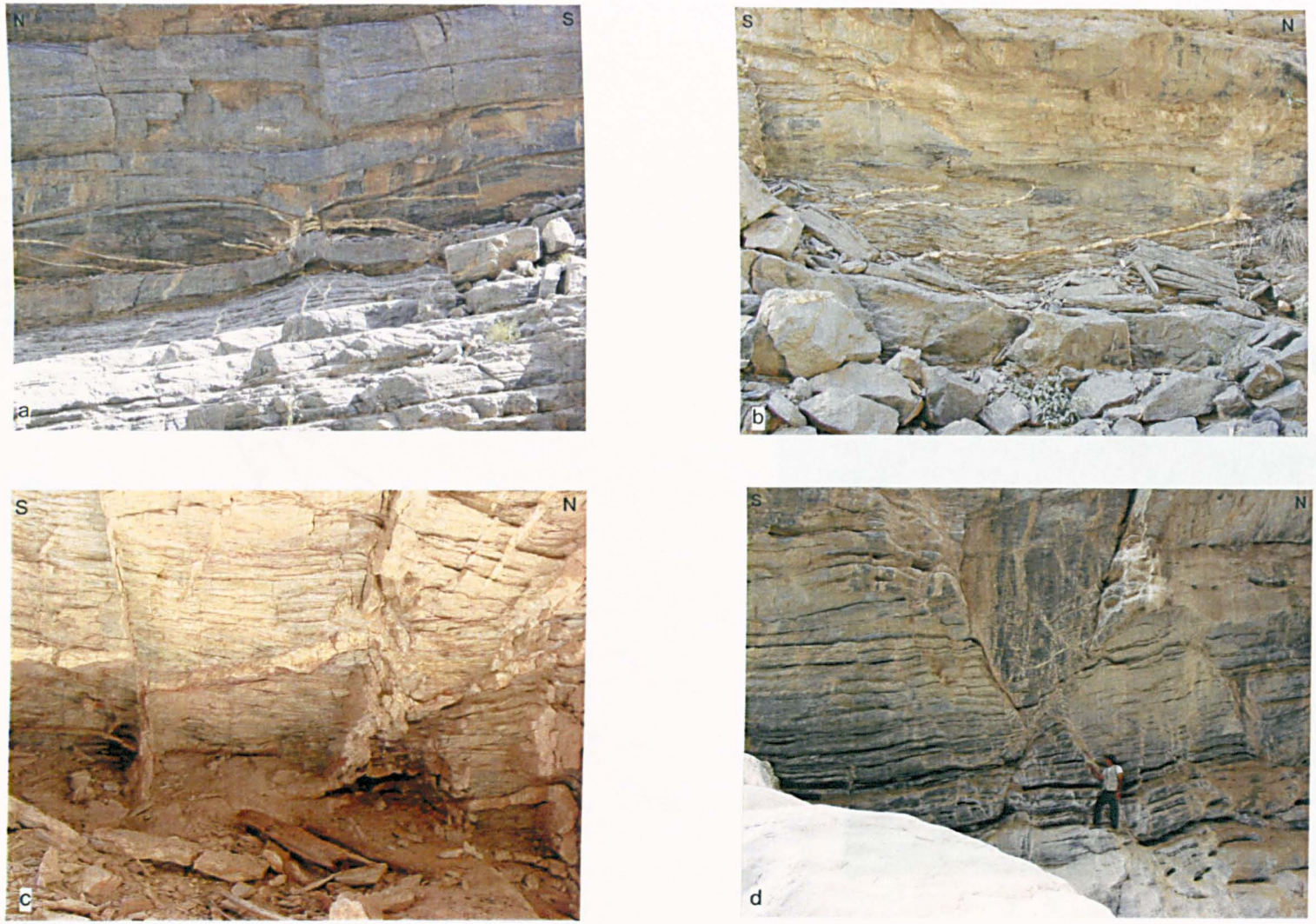

Fig. 3- 22 Deformation fabrics along the Yiqa transect (Field of view approximately 20 m) (a) Boudinage structures with the axis trending perpendicular to the NE extensional direction (Field of view approximately 5 m). (b) Gently dipping boudinaged shear fractures cutting the sub-horizontal cleavage (Field of view approximately 3 m). (c) Layer-parallel detachments crossed by NW-trending tensile veins. (d) Classic NW-trending conjugate normal faults in the Kh2 Fm (Field of view approximately 50 m).

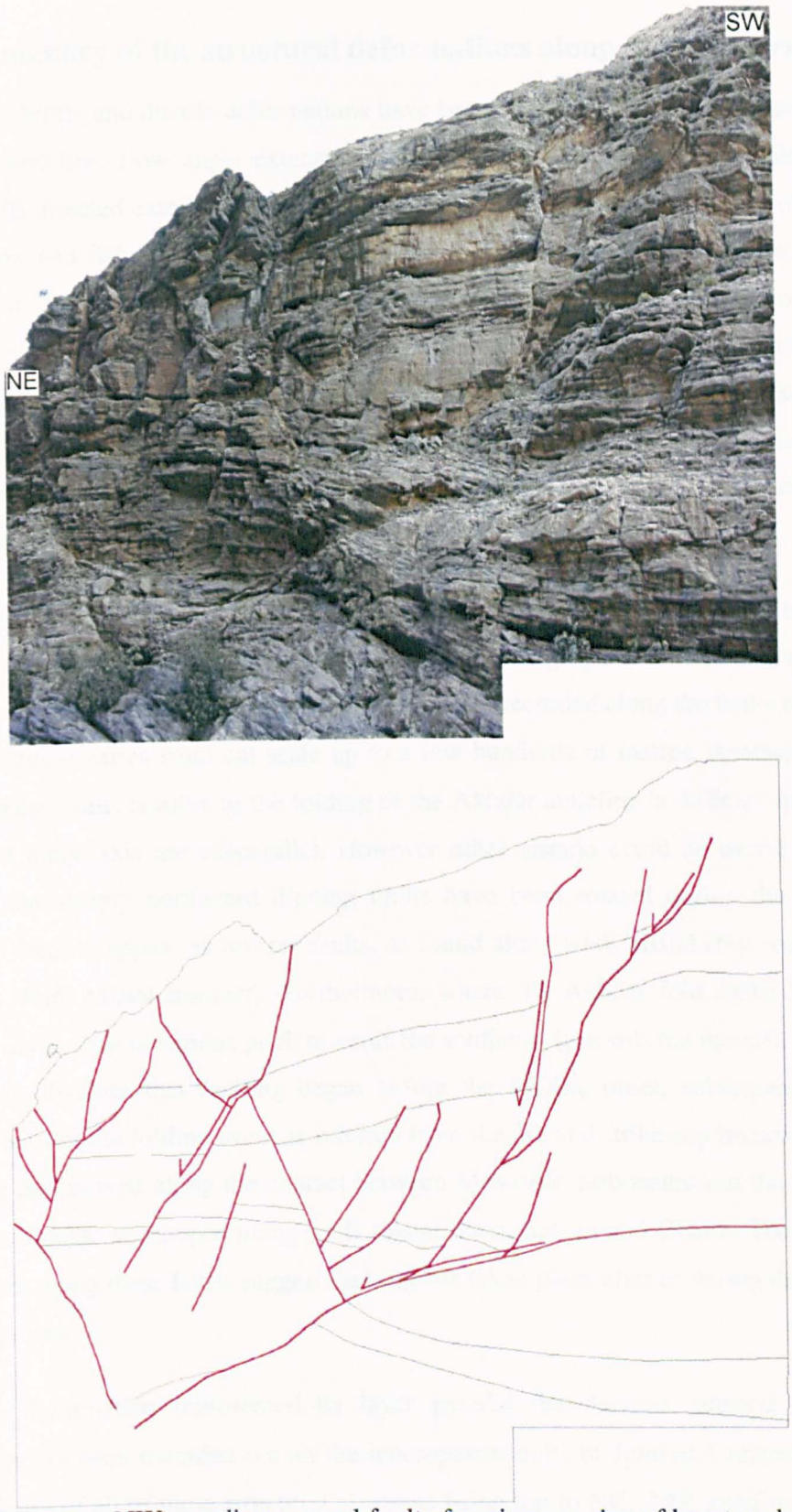

Fig. 3- 23 Extensive NW-trending normal faults forming a series of horst and graben structures within the Shams Fm

3.12 Summary of the structural deformations along the Northern flank

Intensive brittle and ductile deformations have been mapped along the Northern flank of the Akhdar anticline. Low angle extensional detachments with NE-pitching calcite lineations reflect NE-directed extension (Fig. 3-24). A remarkable example of that was observed along wadi Fara and Sahtan, where horizontal displacement along some detachments can reach more than 500 m. Extensive NW-oriented normal faults forming duplex and half graben structures branch onto the detachments. Where a detachment cuts down section, hanging-wall ramps and folds are developed within the hanging-wall strata. Intensive calcite mineralization a few cm's in thickness precipitated along all the detachments. Mineral lineations developed on layer parallel cleavage within incompetent units pitches to the NE direction.

The flank is marked by steep NW-striking faults cross-cutting the preexisting NE-verging ductile structures. These faults affect the entire stratigraphic column including the Pre-Permian rocks. Dip and strike slip components were recorded along the faults and the amount of fault throw varies from cm scale up to a few hundreds of metres. Assessing the relative age of these faults relative to the folding of the Akhdar anticline is difficult since both faults and fold hinge axis are subparallel. However other criteria could be useful as follows. In places, the steeply northward dipping faults have been rotated during the folding onset, altering them to appear as reverse faults, as found along wadi Mistal (For more information see the Wadi Mistal transect). Furthermore, where the Akhdar fold strike NE as in wadi Mistal, some fault lineations pitch towards the southeast (towards the massif). Together these structures disclose that faulting began before the folding onset, subsequently reactivated during or after the folding event as inferred from the dip and strike slip lineations. Significant faulting is observed along the contact between Mesozoic carbonates and the Lat-Cretaceous obducted rocks, as mapped along wadi Mistal, Fara, Sahtan and Ghariz. The purely dip slip lineations along these faults suggest faulting has taken place after or during the latest stage of folding event

Ductile deformation represented by layer parallel detachments, mineral elongation and cleavage has been recorded within the incompetent units of Jurassic-Cretaceous age, with a shear sense of all of these structural elements being top to NE. NW-trending faults with dip and strike slip components dominate this flank, particularly along the contact between the Mesozoic carbonates and the Lat Cretaceous obducted rocks. A Summary of all the structural elements along the various transects of the Northern flank is shown in Fig. 3-24.

Small scale folds structures plunging NW and verging NE were recorded within the incompetent units across the entire northern flank (Fig. 3-24). They have open-close interlimb angles. Along thinly-bedded limestone units such as those within the Salil and Nahr umr Fm's, kink band are well established.

Widespread NE-verging cleavage was mapped across the entire flank (Fig. 3-24). Where beds are sub horizontal, cleavage verges NE, while in contrast it verges SW within beds dipping steeply northwards. Through fold restoration however, the SW-verging cleavage regains it's original NE directed vergence, which clearly reveals a pre-folding cleaving deformation. During the progressive shear deformation, cleavage is rotated northwards to align parallel to the shear zone boundary. Extensive layer parallel, wavy- and teeth- like stylolites are developed along the massively-bedded Shams and Na limestone units as found along wadi Harras and Sahtan. Boudinage structures trending NW are documented along wadi Mistal, Awf and Yiqa. Boudin axes are oriented perpendicular to the NE-stretching direction.

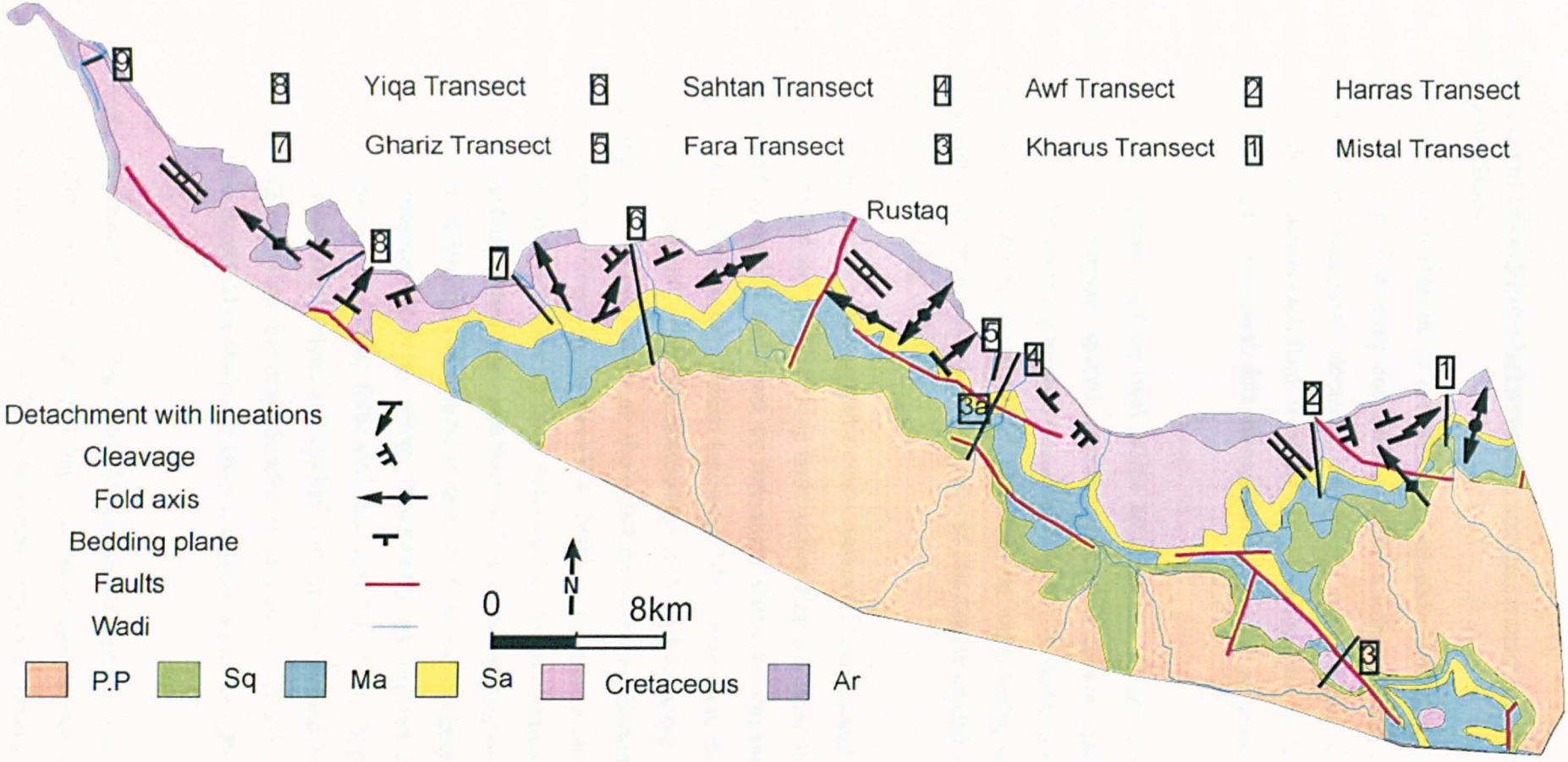

Fig. 3-24 Summary of the structural elements mapped along each transect of the northern flank

3.13 Structural correlation between the southern and northern flank of the Akhdar anticline.

The Akhdar anticline is marked by extensively developed extensional deformation, with a top-to-the-NNE sense of shearing and manifested by a linked system of steep faults and layer-parallel shear. Structural elements, comprising steep faults and the associated deformation fabrics, across each flank were previously summarized in detail in this chapter. Therefore in this part, structural data throughout the massif is presented and analyzed collectively.

Across the gently dipping southern flank of the Jebel Akhdar, layer-extensional shearing is manifested by NNE-verging spaced pressure-solution cleavage and bedding-parallel detachments with NNE-trending mineral lineations (Fig. 3-25). Bedding-confined faults and intraformational folds are rarely developed. However, the steep faults, which penetrate the entire stratigraphic profile, are extensively developed and closely spaced, with an average of WNW-ESE orientation (Fig. 3-25).

The steep northern flank is characterized by two systems of extensional faulting. The first system is represented by steep NW-striking faults penetrating the entire stratigraphic profile, while the second system is expressed by low-angle faults accompanied with bedding-confined steep faults. Both systems reflect top-to-the-NNE extensional shear. The low angle faulting is chiefly expressed within the interbedded shale and limestone of Cretaceous age and is manifested by linked system of shear and detachments. Bedding-confined, NW-oriented steep faults developed at high angle to bedding and merge onto bedding-parallel detachments. Listric low angle dipping faults inducing hanging-wall anticlines are prominent before becoming bedding-subparallel detachments. The estimated displacement along these low angle faults are of hundreds of meters, as detected from the hanging-wall and footwall ramps. However, incompetent units, where detachments are situated are deformed in a ductile manner forming NE-verging folds and cleavage (Fig. 3-25). Intraformational folds exhibit open to close interlimb angles and marked with hinges oriented orthogonal to highly oblique to the NNE stretching direction. Boudinage structures of NW-oriented boudin axes are common, within interbedding shale and limestone succession, but reflect small amount of stretching.

Kinematically, the steep NW-striking faults throughout the massif show dip and strike slip striations. It is difficult to assess the chronological relationships between these faults and the folding of the Akhdar massif, since both are subparallel. However, other criteria such as fault dip (for more information see section 3.12) suggest that some faults were initiated before or during the folding onset since they have been rotated by the folding deformation.

Subsequently faulting was resumed during or after the folding event, as reflected from dip and strike slip lineations recorded along the Mistal transect, where both faults and the Akhdar fold are oblique. The NW-striking faults are also marked by sinistral and dextral strike slip components, indicating NW-SE maximum compression direction.

The contact between the Mesozoic carbonates and the allochthon rocks along the northern boundary of the Akhdar culmination, is disrupted by steep dip slip faults, which are oriented parallel to the massif boundary with down-throw away from the massif. These faults are only localized along the culmination boundary. On the other hand, such disruptions can not be seen along the southern flank of the Akhdar anticline, where the same contact is concordance. These massif-bounding faults will be analyzed in the Data syntheses chapter.

In summary, the Akhdar anticline is marked by pervasive extensional deformation of top-to-the-NNE shearing. The intensity of extensional deformation increases of NE trend. For this reason extensional deformation is more pronounced in the northern flank compared with the southern flank.

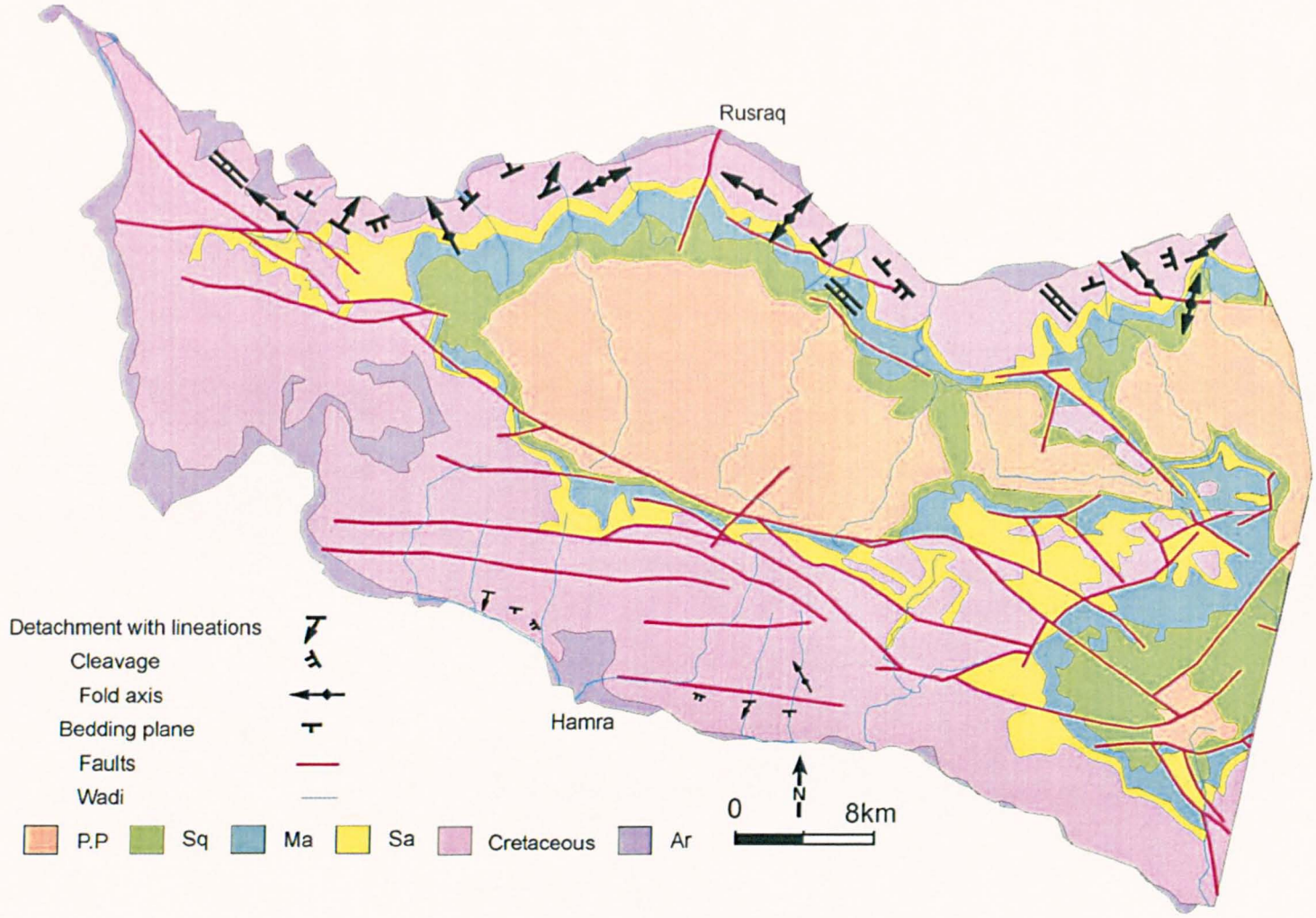

Fig. 3-25 Structural correlation across the Akhdar anticline.

Chapter 4: Structural deformation along the Nakhal anticline

4.1 Introduction

The Nakhal anticline (NNE-SSW) is an intervening anticline between the Akhdar and Hatat massifs. The anticline trends NNE-SSW for approximately 30 km. The northern continuation of the Nakhal anticline is a 10-km-long, E-W trending anticline called the Fanja anticline. The Nakhal Massif is composed of sedimentary basement and carbonate platform deposits ranging in age from Late Proterozoic to Late Cretaceous with a large hiatus corresponding to practically the whole of the Paleozoic. The core of the anticline is occupied with the pre-Permian clastics and carbonate rocks, and overlain with the Mesozoic carbonate platform sequences (Hanna et al. 1990).

The focus of this chapter is to present and interpret data collected during a study investigating the structural deformation along the Nakhal anticline, which is marked by two contrasting styles of deformations NE-directed extensional deformation and NW-SE compressional deformation. The extensional deformation was initially recognized by Le Metour et al. (1990) and Breton et al. (2004). However, this is the first time in which a detailed investigation has been conducted to study such deformations across the northern Oman Mountains.

Thirteen transects have been constructed across and along both flank of the massif, including the Fanja anticline (Fig. 4- 1). On each flank a detailed transect has been selected and thoroughly studied to represent a type locality of the structural deformation along that particular flank. These detailed transects are Hedk, Dhabiah and AL-Qet. Structural data is presented in a systematic way starting from regional structures to small scale deformation fabrics through the outcrops structures. Data is presented and synthesized in parallel as appropriate, to provide greatest clarity. Mappable structures have been labeled in the drafted transects to cross-reference to the corresponding text description. Each transect is concluded with interpretation and synthesis of all the presented structural data.

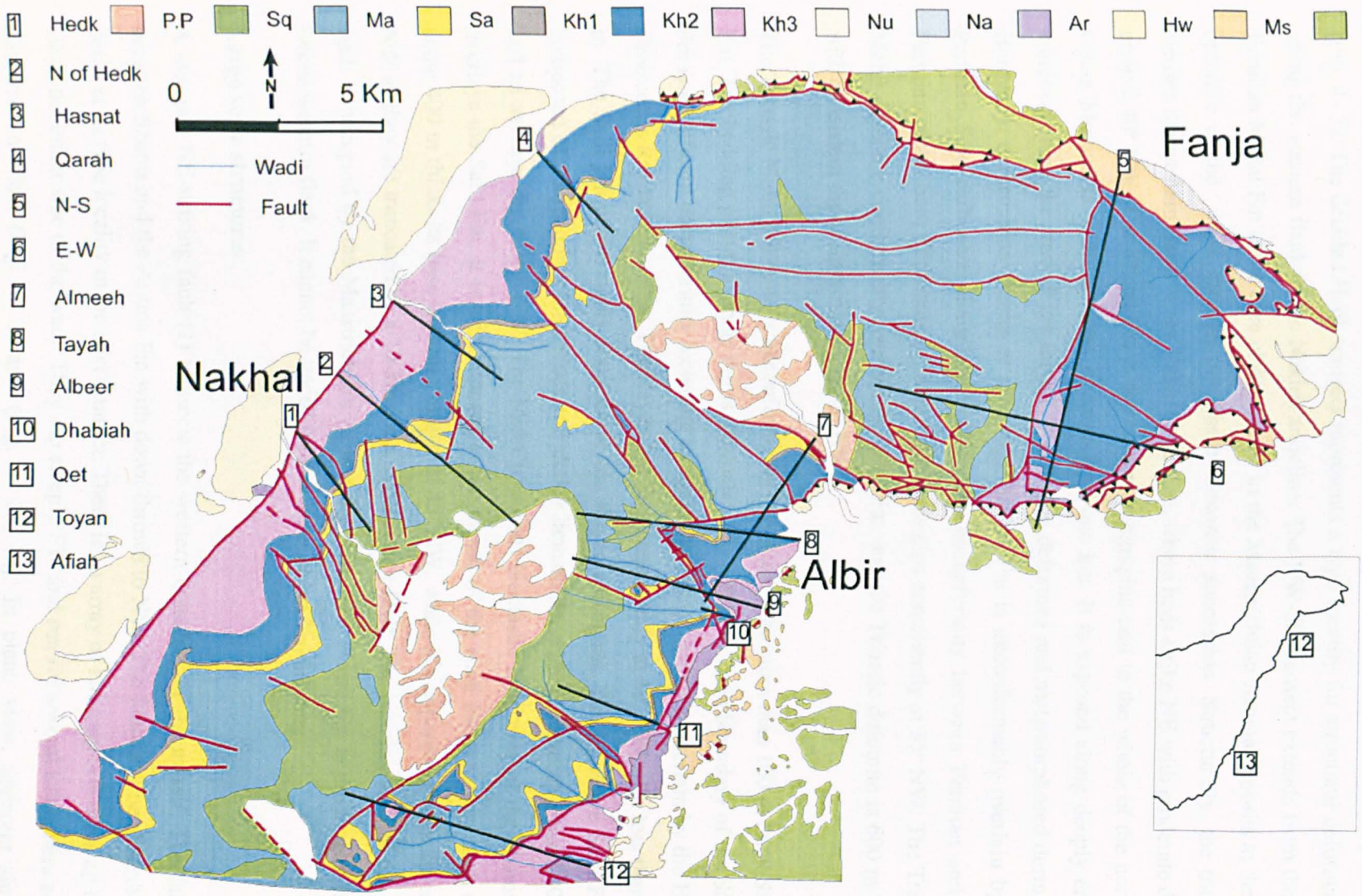

Fig. 4- 1 Geological map of Jebel Nakhal showing the locations of the constructed transects

4.2 Wadi Hedk transect

Wadi Hedk is situated behind the town of Nakhal at the mouth into the pre-Permian hedk window (Fig. 4- 1). A detailed transect 4.5 km in length has been constructed along the wadi (Fig. 4- 2). The detailed Hedk transect represents a type locality for structural deformations along the western flank of the Nakhal anticline. The NW-SE transect extends from the pre-Permian Mistal Fm at the core of the massif to the Maastrichtian Aruma deposits at the NW entrance of the wadi, through the whole Mesozoic succession. Structurally, the transect crosses the western flank of the Nakhal anticline, where beds strike NE with moderate dip of around 40° NW. The Mistal Fm is the oldest stratigraphic unit in the whole of the northern Oman Mountains with thickness of more than one km. It is exposed along deeply eroded windows along the crest of the massif. It is highly deformed and metamorphosed during the Hercynian deformation (Mann et al. 1990). Mistal Fm is unconformably overlain by the Permian Saiq carbonate along a major angular unconformity between Permian and pre-Permian rocks. Saiq Carbonate of 500 m thickness dips consistently at 35° NW. The Triassic Mahil dolomite conformably overlies the Saiq Fm, and the Triassic dolomite is 600 m thick with consistent dip of approximately 45° NW.

The Triassic Mahil dolomite is unconformably overlain by the more than 100 m thick Sahtan Fm. The bedding planes average dip is approximately 40° NW. Each boundary of the Sahtan Fm is significant unconformity including its upper boundary, which is overlain by the Early-Cretaceous Rayda limestones. The Rayda Fm dips consistently at 40° NW with less than 100 m. The Salil Fm conformably rests above the Rayda sediments. The recessive Salil Fm is composed of interbedding limestones and shaley limestones, with a thickness around 400 m, and an average dip of 40° NW. The Mid-Cretaceous bioclastic limestone of the Shams Fm overlays the Salil Fm. It is well exposed at the mouth of the wadi forming very high cliffs some 400 m thick. Its base dips an average of 45° NW, while it's uppermost beds dip at 50° NW as they are truncated by a 10-km-long, NE-striking fault. The hanging-wall of this long fault is occupied by the Maastrichtian Aruma deposits. The Wasia Gp is missing from the whole western flank. It cannot be traced further north of the Nakhal area.

Large scale structures

A km-long NE-striking fault [1] transects the western boundary of the massif. The fault is between Shams and the Aruma Fm with down-thrown to NW. The fault will be described in detail at its type locality in the next transect. There is an array of km-long NW-striking faults along the either side of the wadi. They dip steeply SW and run for several kilometers across the western flank (Fig. 4- 2) and (Fig. 4- 3a) [2]. In plane view, apparent sinistral displacements of hundreds of metres are recognized along these faults. Subsidiary faults of

variable length associated with the km-long faults can also be seen, particularly across the hanging-walls.

Two sets of subsidiary faults were identified trending NE-SW and NW-SE. The NE- set is minor with less than a metre of throw. Kinematicaly, these faults are oblique with slickensides pitching moderately to the NE. When the structures were restored by rotating them around the 040/30 axis (chosen to be parallel to the fold axis) these faults turned into dip slip faults. The NW-striking fault set is dominant with variable displacement ranging from sub-metre to ten's of metres. Kinematicaly, these faults show differently plunging lineations. The dominant lineations are oblique slickensides pitching both to NW and SE (Fig. 4- 2), while the minor lineations are dip- and strike-slip slickensides. When the structures were restored by rotating them 30° around a horizontal axis trending 040 (Fig. 4-2) the oblique faults with SE-pitching lineations turned into dip slip faults, while the oblique faults with NW-pitching lineations turned into strike slip. Fault sets of oblique lineations most likely occurred before or during the early stage of the folding onset. The purely dip- and strike- slip striations became distorted and scattered in an inconsistent manner when the unfolding was applied. This may suggest that the purely dip- and strike- slip displacement occurred after the folding deformation. In short the NW-striking faults underwent two phases of movement. The first movement took place before or during the early stage of the folding deformation as sort of dip-and- strike-slip displacements, while the second movement took place after the folding deformation with similar displacement.

Small scale structures

Extensive well developed tensile and shear veins have been developed throughout the stratigraphic section. They are variable in attitude from bedding parallel to bedding orthogonal. Bedding-parallel veins concentrate within the incompetent micritic limestone units along detachments and slipping surfaces, involving a shear strain as suggested from the associated calcite fibre lineations. On the contrary, bedding-orthogonal veins are more developed along the competent limestone beds. They are filled with spar calcite without fibrous stretching lineations, indicative of tensile origin. In relation to the NE-directed deformation, two distinctive phases of tensile veins have been distinguished. The first predates the NE extension as veins were stretched and boudinaged along a NE-SW axis and eventually rotated into parallelism with the NE-verging cleavage (Fig. 4- 3b). The second phase is associated with the NW-striking faults and crosscuts the ductile fabrics. The cross-cutting relationship indicates that these veins are younger than the deformation fabrics, which is explored shortly.

Deformation fabrics

Deformation fabrics are manifested along the transect through layer-parallel detachments, mineral lineations, folds and cleavage. Extensive layer-parallel deformation zones developed along the shaley units, marked with intensive localized deformation involving layer parallel cleavage and layer-parallel veins. These zones decouple the differently deformed stratigraphic units; in this way they have been interpreted as detachments. Bedding-parallel detachments strike NE- with a moderate dip of 40° NW (Fig. 4- 2). They are more frequent along the finer-grained units of Sahtan, Rayda and Salil Fm. NW-oriented normal faults, which branch and merge onto the detachments, extend strata along a NE-SW axis. Mineral lineations along the detachments, trend NE-SW (Fig. 4- 2). Stretching lineations such as elongate carbonate aggregates, recognized at shaley horizons, pitch gently towards the NE and the SE quadrant (Fig. 4- 2).

Intraformational folds are widely developed especially along the bedding-parallel detachments. Fold axes are scattered in trend, ranging from normal to parallel to the NE extensional direction, with variable plunging directions towards NW and NE (Fig. 4- 2). Geometrically, folds can be subdivided into two distinct groups. In the first group, folds plunge moderately NW with close to tight interlimb angles (Fig. 4- 4b). Steeply dipping axial planes bisected by massif-verging cleavage, verge towards NE and SW (Fig. 4- 4e). Folds are associated with detachments showing top-NE directed shearing. In the second group, folds are oriented sub-parallel to the massif (NE-SW), with gentle to moderate pitching to the NE and SW directions. Folds are tilted towards the massif with close interlimb angles (Fig. 4- 4a) and possess axial plane cleavage also verging to the massif. In places they fold the NE-directed detachments. This group of folds is accompanied with massif-verging cleavage and thrusts.

Cleavage, mainly spaced pressure solution cleavage and foliations, are common throughout the Jurassic-Cretaceous sequences. Foliations concentrate within the highly deformed detachments. Spaced pressure solution cleavage strikes NE-SW and shows apparent SE vergence (Fig. 4- 4f). When the folding deformation was unfolded by rotating them 30° around a horizontal axis trending 040, two distinct vergence directions can be identified. The dominant one is towards the E direction while the minority is towards NE (Fig. 4- 4f). The dip of the NE-verging cleavage is more gentle than bedding, unlike the E-verging cleavage which dips steeper than bedding. The NE-verging cleavage is associated with the NE-directed extensional detachments, while the massif-verging cleavage accompanied with the massif-verging folds and thrusts. NE-oriented subvertical extensional crenulation cleavage

has been found locally within the Sahtan Fm which deflects and displaces the massif-verging cleavage (Fig. 4- 4c). Additionally, the Jurassic and Cretaceous sequences have been subjected to extensively develop Layer-parallel stylolitic cleavage.

Interpretation and summary

The area is dominated with two kinematic systems, as deduced from the NE- and the massif-verging structures. These are the NE-directed deformation and the massif-verging deformation. The NE-directed deformation is manifested by the NE-directed detachments, NE-SW stretching lineations, and NE-verging folds and cleavage. The sense of shearing along these detachments is top to NE as suggested from the NE-verging cleavage and folds seen along the detachment zones. Tilting of the fold axial planes and tightening of the corresponding interlimb angles may have a proportional relationship with the progressive shear deformation. Differing orientations of cleavage arose from this deformation. Foliations developed along the intensively deformed detachment zones, while the NE-verging spaced pressure solution cleavage developed along the zones of less deformation. The pre-existing fabrics like the earliest tensile veins were stretched, boudinaged and rotated into parallelism with the NE-verging cleavage. This may indicate that the NE-directed simple shear extension was preceded by pure shear extensional deformation.

The massif-verging deformation is expressed by massif-verging folds and cleavage and the bedding-parallel detachments with NW-pitching lineations. These structures collectively mark NW-SE shortening deformation. As a result the interpreted bedding-parallel detachments with NW-pitching lineations are actually layer-parallel slipping surfaces resulting from flexural folding of the Nakhal anticline. The sense of displacement along these slipping surfaces would be up-dip towards the fold hinge. Folds are accompanied with axial planar cleavage verging towards the massif. The massif-verging cleavage accommodated the applied NW-SE shortening through intensive pressure solution along the micritic limestone units. Under the progressive deformation, shortening was supplementary accommodated through the development of extensional crenulation cleavage, which dissolved and truncated the pre-existing massif-verging cleavage.

The relative timing of the different deformational system are now discussed. The bedding-perpendicular tensile veins formed firstly, together with the layer-parallel stylolites. This is concluded due to the distortion of the tensile veins by the NE-simple shear deformation. Therefore the tensile veins occurred under pure shear deformation preceding the NE-directed simple shear extension, which is manifested by layer-extension shear and steep faults. The major NW-striking faults cross-cut the deformation fabrics of both the NE- and the massif-

verging deformation, indicating that the faults were formed late in the local structural history. The massif-directed deformation clearly postdates the NE-simple shear deformation mapped along the Jurassic-Cretaceous succession, as indicated by several observations: Top-NE detachments are folded by massif-verging structures; NE-verging folds are overprinted by the massif-verging cleavage; NE-verging cleavage is overprinted by the massif-verging cleavage and the detachments are folded over the massif.

The structural deformation along the transect is summarized as follows. The transect is dominated by two distinct styles of deformations. The first is the NE-directed simple shear, extensional deformation manifested by bedding-parallel detachments alongside NW-striking faults, NE-verging folds and cleavage. The second is related to NW-SE shortening forming the massif-verging folds and cleavage.

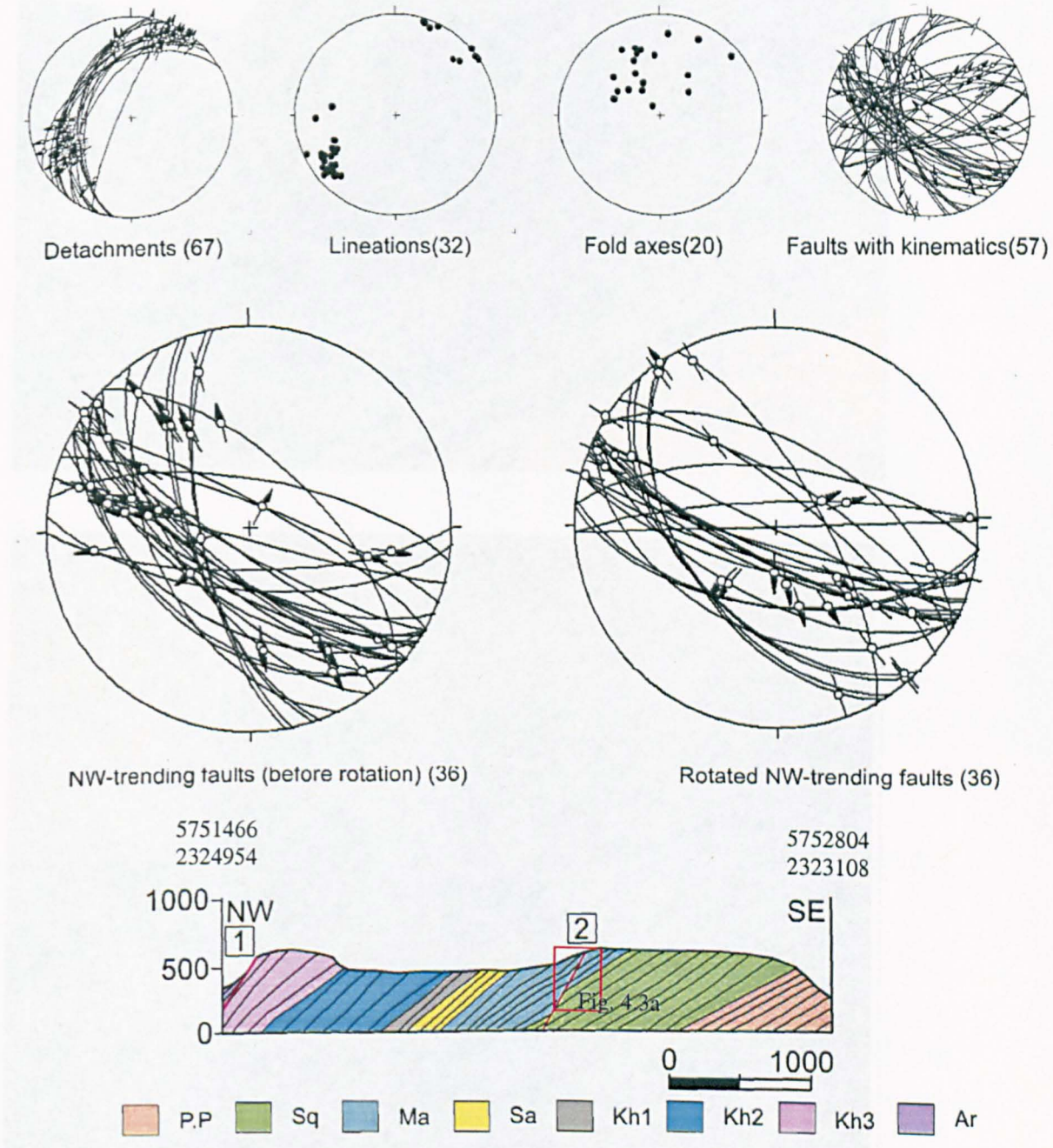

Fig. 4- 2 The Hedk transect with stereograms of the various structural elements collected along the transect (faults were rotated 30° around a horizontal axis trending 040).

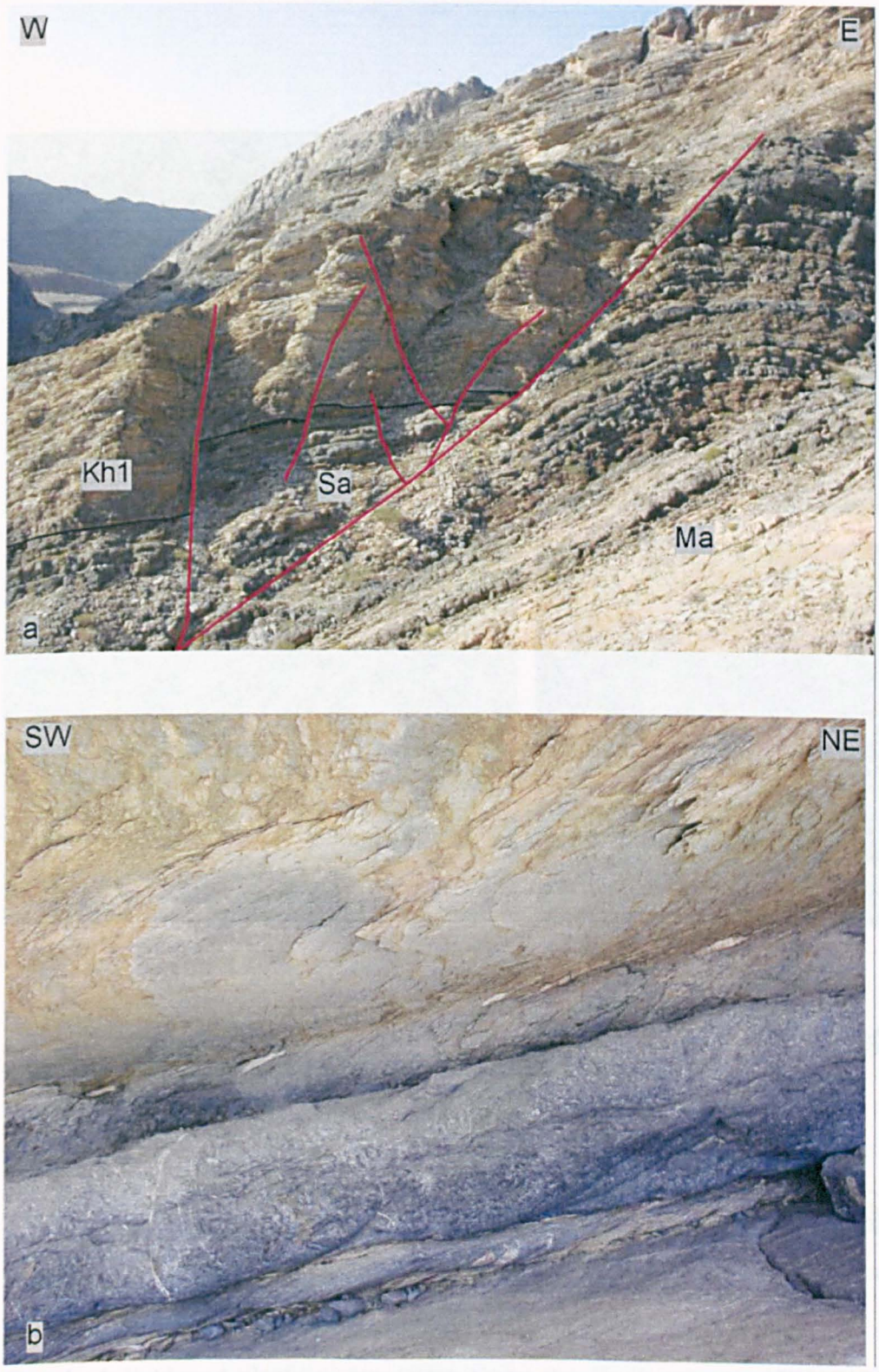

Fig. 4- 3 Fracturing along the Hedk transect (a) the major NW-fault between the Triassic dolomite and the Jurassic-Cretaceous succession, extensive subsidiary faults took place within the hanging-wall (field of view approximately 100 m). (b) Stretched and boudinaged tensile veins under the NE-directed extensional deformation (field of view approximately 1m).

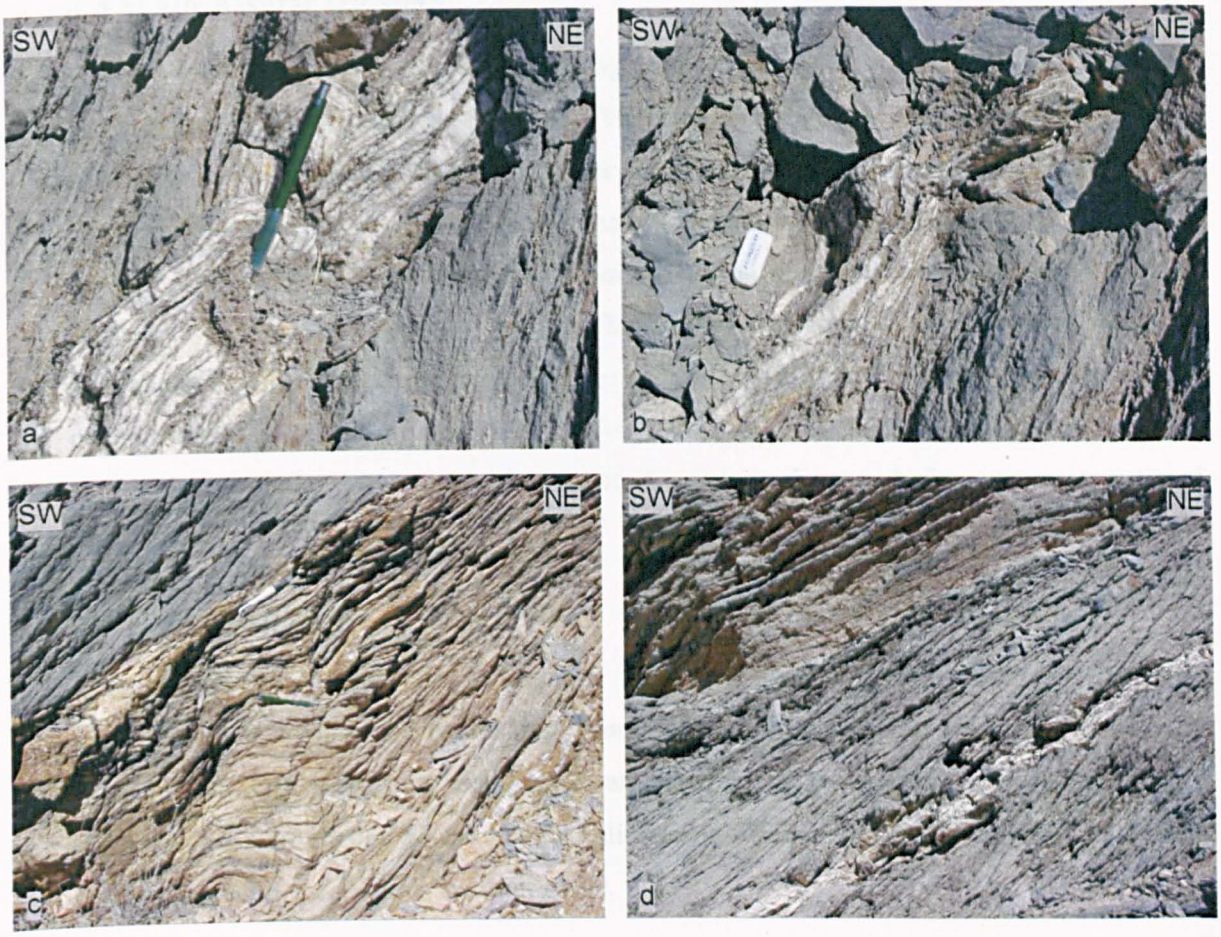

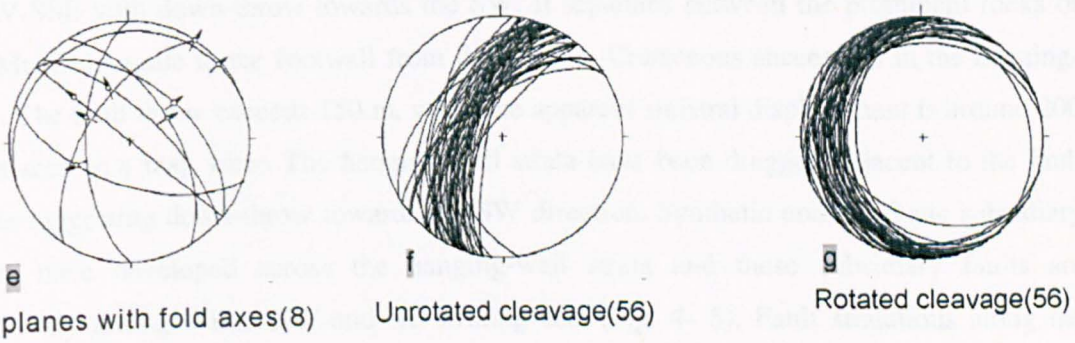

Fig. 4- 4 Fold and cleavage structures along the Hedk transect (5751710, 2324360). (a) Folding of bedding-parallel detachments along a massif-parallel fold. (b) Folding of bedding-parallel detachments at a NW-plunging fold. (c) Extensional crenulation cleavage affecting the bedding-parallel detachment and massif-verging cleavage. (d) Massif-verging cleavage (field of view approximately 1m). (e) Stereogram of fold axial planes with their corresponding fold axes for different small-scale folds recognized along the transect. (f) and (g) Stereograms for cleavage before and after unfolding, notice the different directions of cleavage vergence obtained after rotation. (Cleavage were rotated 30° around a horizontal axis trending 040)

4.3 Wadi Alsarir transect

A 6 km long transect was constructed along wadi Alsarir. The wadi is about 1 km to the north of the AL-Hedk window (Fig. 4- 1). The transect runs across the western flank of the Nakhal anticline transecting the entire preserved Mesozoic succession, starting from the Pre-Permian Mistal sediments to the Mid- Cretaceous carbonates of the Shams Fm at the NW (Fig. 4- 5). The Wasia Gp is missing from the whole area, probably because it was not deposited. The average dip of the western flank where the transect was located is about 40° NW and generally, the stratigraphic units dip consistently at around 35°-45° NW. The middle of the transect is crossed by a km-long NW-striking fault. The Jurassic-Cretaceous hanging-wall strata are deflected along the fault plane for a short distance before resuming a dip of 40° NW.

Large scale structures

The western flank of the Nakhal anticline is terminated along a kilometric NNE-striking fault. The fault separate the Shams and Aruma Fm with down-throw away from the massif (Fig. 4- 5 and Fig. 4- 6a). It extends northward from the city of Nakhal for more than 12 km. Fault striations are mainly gently pitching slickensides plunging to NNE and SSW and there is no evidence of shear along the fault plane.

Another large fault is situated at the middle of the transect (Fig. 4- 5). The fault strikes NNW-SSE with down-throw towards the SW. It separates between the prominent rocks of the Mahil dolomite in the footwall from the Jurassic-Cretaceous succession in the hanging-wall. The fault throw exceeds 150 m, while the apparent sinistral displacement is around 200 m as seen in a map view. The hanging-wall strata have been dragged adjacent to the fault plane suggesting down-throw towards the SW direction. Synthetic and antithetic subsidiary faults have developed across the hanging-wall strata and these subsidiary faults are apparently arranged into NW-and-NE-striking sets (Fig. 4- 5). Fault straiations along the master fault gently pitch away from the massif (Fig. 4- 5) and when untilted by the local flank dip of the culmination, the oblique lineations turn into approximately dip slip. Furthermore, the subsidiary faults become NW-oriented dip slip faults with some oblique. On this basis the fault is a pre-folding dip slip fault.

Metric-scale symmetric fold structures have developed at the uppermost part of the Salil Fm (Fig. 4- 6b). They have gentle interlimb angles and fold axes pitching to the NW quadrant, with axial planes at right angles to bedding. Folds gradually die-out upwards, until they

cannot be seen at the contact between Salil and Shams Fm. Such folding must be related to intra-formational shearing directed NE-SW as inferred from the fold orientations.

Deformation fabrics

Deformation fabrics are chiefly localized along the incompetent fine-grained units of Jurassic-Cretaceous age. It is expressed in term of layer-parallel detachments, cleavage and fold structures (Fig. 4- 5). Layer-parallel detachments are zones of intensive localized deformation separating variously deformed rock packages. Layer-parallel detachments strike NNE-SSW with a moderate dip towards the NW (Fig. 4- 5). The detachment fibre lineations cluster into two domains trending NE-SW and ENE-WSW. Small-scale fold structures pitch moderately towards the NW with open interlimb angles, and verge towards the NE (Fig. 4- 5). Cleavage is well developed especially within the Sahtan and Salil Fm. It dips 60° NW and strikes NNE-SSW (Fig. 4- 5 and Fig. 4- 6c). When untitled back 40° around a horizontal axis trending 030, cleavage appears to verge in two directions NE- and ESE (Fig. 4- 5)

A limestone bed surrounded by shaly limestone strata of the Sahtan Fm demonstrates NW-oriented veins which are tilted, stretched and boudinaged along a NE-SW axis (Fig. 4- 6d). The surrounding less competent shaly limestone responded to the same deformation by forming intensive NE-verging cleavage. The boudinaged veins are interpreted as being bedding orthogonal before being rotated, stretched and boudinaged under the NE-directed deformation later on.

Interpretation and summary

The NNW-striking fault took place before or during the early stage of the folding onset. However the major NNE fault, which bounds the western limb, must be a post folding strike slip fault as revealed from the sub-horizontal lineations. Nevertheless the fault dip and the significant vertical displacement may suggest a dip slip component as well.

The structural elements along the transect exhibit two distinctive systems of deformation. The bedding-parallel detachments with NE-SW trending lineations, along with the NE-verging folds and cleavage, express NE-directed deformation. The early formed bed-orthogonal veins were rotated, stretched and boudinaged during this deformation. Small NW-trending normal faults branch and merge onto the detachments revealing extensional deformation. The major NNW-striking fault is part of the same deformational system as suggested from its NNE-directed displacement.

The massif-verging cleavage illustrates NW-SE shortening with a top-to-SE sense of shearing. The west-pitching detachment lineations suggest that some of the bedding-parallel

detachments were utilized as slipping surfaces under the shortening deformation, accommodating the folding deformation.

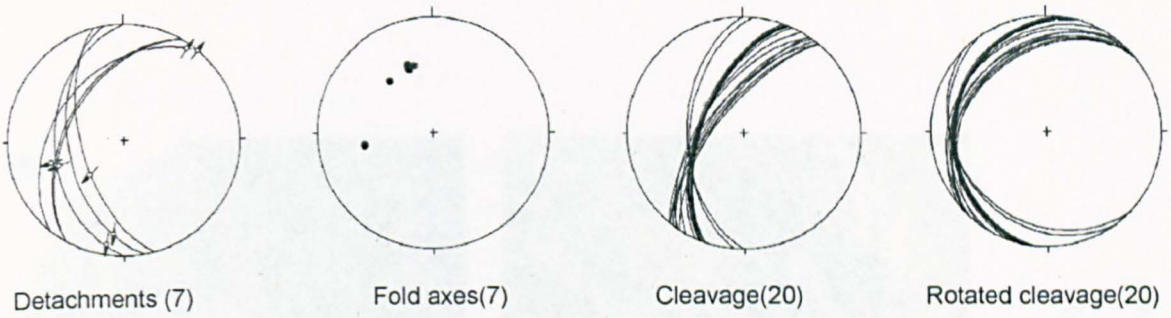

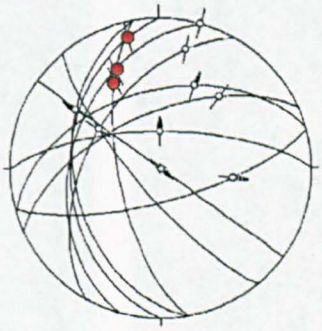

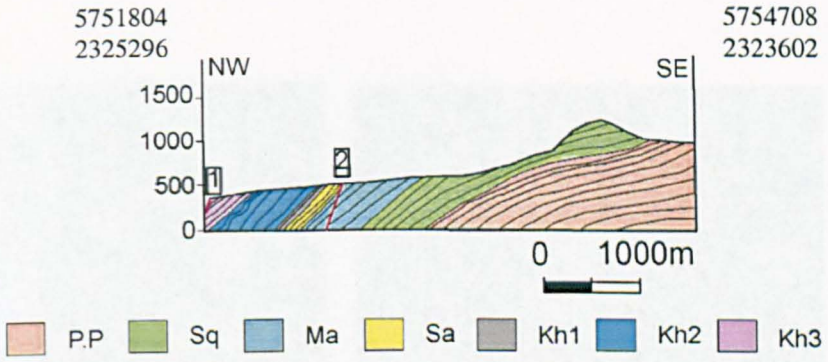

Fig. 4- 5The Sarir transect with stereograms of the different structural elements collected along the transect. The red circles on the fault stereogram are for the away from the massif-pitching lineations along the major NNW- fault (Cleavage is rotated 30° around a horizontal axis trending 040).

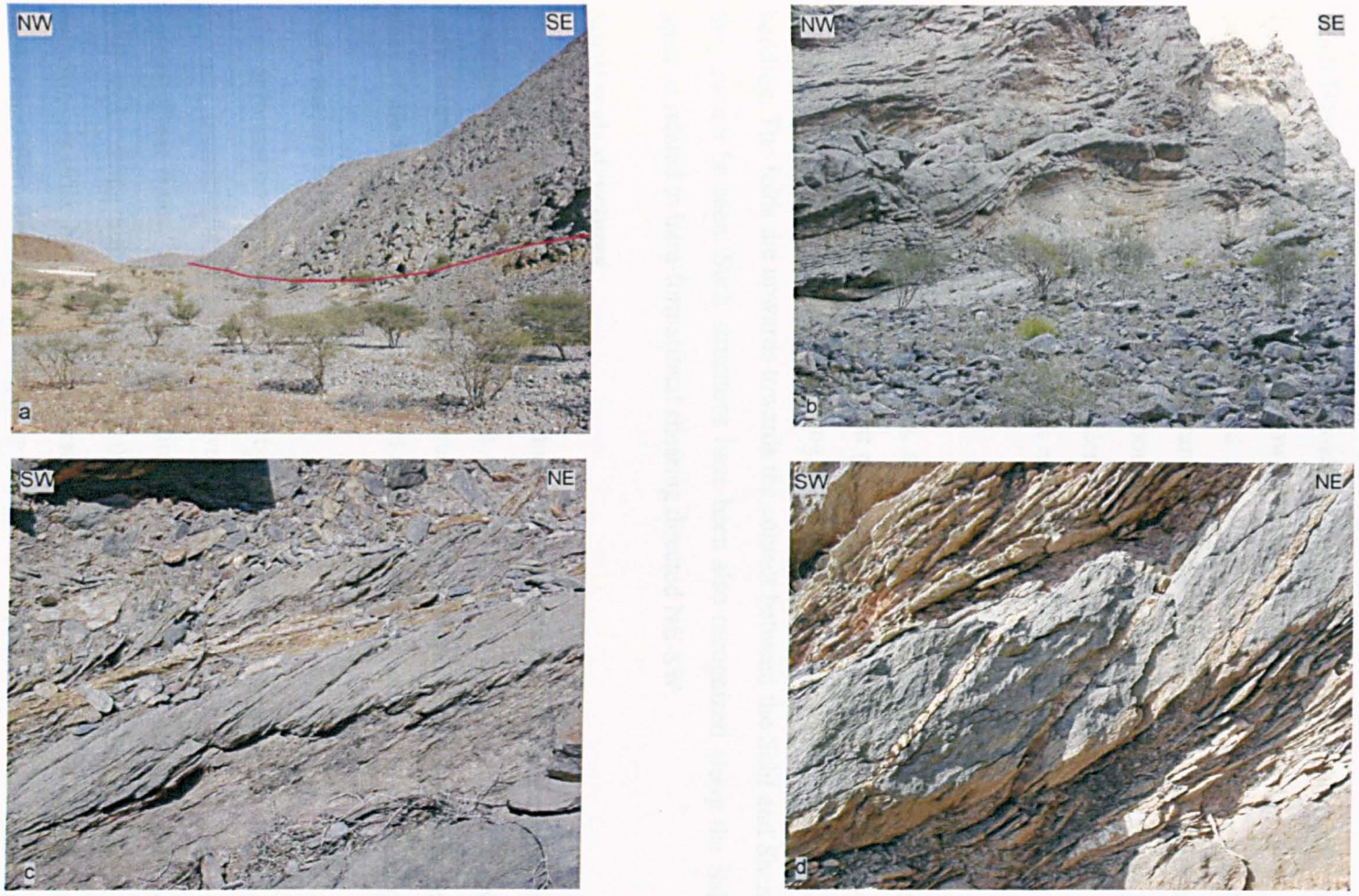

Fig. 4- 6 Deformation fabrics along the Sarir transect (a) The major NE-fault bounding the western flank of the Nakhal anticline (field of view approximately 100 m). (b) A gentle NW-plunging folds in Kh2 carbonates (field of view approximately 50 m). (c) Massif-verging cleavage (field of view approximately 1m). (d) Stretched and boudinaged tensile veins from the NE-directed extensional deformation (field of view approximately 1m)

4.4 Wadi Hasnat Transect

Wadi Hasnat is situated across the middle of the western flank of the Jebel Nakhal (Fig. 4-1). It is 5 km to the east of the town of wadi Al-Mawel. A 3 km long transect was constructed across the whole exposed Mesozoic succession, apart from the Permian Saiq carbonate (Fig. 4- 7). The transect started with the Triassic Mahil dolomite at the SE and ended with the Mid- Cretaceous carbonate of the Shams Fm in the NW. In general, beds along this wadi strike NE with a moderate dip of approximately 35°-40° NW. The transect lacks any km-long structures like folds or faults of km-scale.

Large scale structures

The transect lacks km-scale structures, apart from metric scale symmetric folds, which have been recognized within the uppermost part of the Salil Fm (Fig. 4- 8a). They show gentle interlimb angles with fold axes pitching to the NW quadrant. Axial planes are orthogonal to bedding. The folds die upwards towards the contact between the Salil and Shams Fm, where they cannot be seen. Such structures have been also recognized along the Sahtan Fm, and must be related to intra-formational shearing directed NE-SW.

Small scale structures

Small scale faults of NW orientation have been recorded, merging along detachment zones localized within fine-grained units (Fig. 4- 7). Fault throw is in the order of a few centimeters only. Intensive corridor vertical fractures are well developed across the massively competent beds of the Shams Fm, as demonstrated along the western entrance of the wadi (Fig. 4- 8b).

Deformation fabrics

The deformation fabrics is reflected by different structural elements described in turn as follows. Intensive layer parallel cleavage with layer parallel veins is concentrated along narrow shear zones. These highly strained, narrow zones are surrounded by less deformed wall rocks along either side. They therefore behave as detachment zones. Bed-parallel detachments strike NE- and dip moderately at about 40° NW (Fig. 4- 7). The majority of the detachment fibre lineations pitch gently NE and SW apart from a minor component pitching moderately to the west. Stretching lineations defined by elongate carbonate aggregates plunge gently to the NE (Fig. 4- 7). Folds are concentrated within the fine-grained units of the Sahtan and Salil Fm. Two sets of folds were identified (Fig. 4- 7). Folds of the first set verge to the NE with gentle-close interlimb angles, while in the second set folds verge towards the massif with open-tight interlimb angles (Fig. 4- 8c). Massif-verging thrusts show

small displacements in the order of a few centimeters. The developed hanging-wall anticlines are oriented parallel to the massif. Both the massif-verging folds and thrusts imply a NW-SE shortening. Cleavage is pervasive, particularly within the fine-grained units of the Jurassic-Cretaceous succession. Spaced pressure solution cleavage is oriented NE-SW and dips with a steeper angle than bedding at 45° NW (Fig. 4- 7). Cleavage within the detachment zones tend to be bedding-parallel. When the folding structure was unfolded by rotating it 30 °around a horizontal axis trending 040, two direction s of cleavage vergence were identified (Fig. 4- 7). The dominant direction verges towards the massif (E), while the minor one verges NE. In some places, extensional crenellation cleavage arises transecting the bedding parallel detachments with a normal sense of shearing (Fig. 4- 8d). They have been interpreted as a result of the continuing shortening deformation.

Interpretation and summary

The structural elements along the transect exhibit two distinctive systems of deformations. The bedding-parallel detachments with the NE-plunging stretching lineations, together with the NE-verging folds and cleavage, express NE-directed extensional deformation. The massif-verging folds, thrusts and cleavage reflect NW-SE shortening. The west-pitching detachment lineations suggest that some of the bedding-parallel detachments were utilized by the shortening deformation as slipping surfaces with a top-to-the-massif sense of shearing. The shortening strain was accommodated through the development of different structures throughout the folding process. Initially, massif-verging folds, thrusts and cleavage were developed during the early stage of the folding deformation. The extensional crenulation cleavage was eventually formed and hence cross-cut the earlier massif-verging cleavage.

The question arises, what is the relative timing between the two deformational systems? Several different structural features indicate that the NW-SE shortening has affected the NE-directed extensional deformation, mapped within the Jurassic-Cretaceous succession. Firstly, the detachments marked with NE-plunging lineations are folded by the massif-verging minor folds and by the Nakhal anticline itself. Secondly, the NE-directed extensional structures are folded across the Nakhal culmination, the product of the NW-SE shortening.

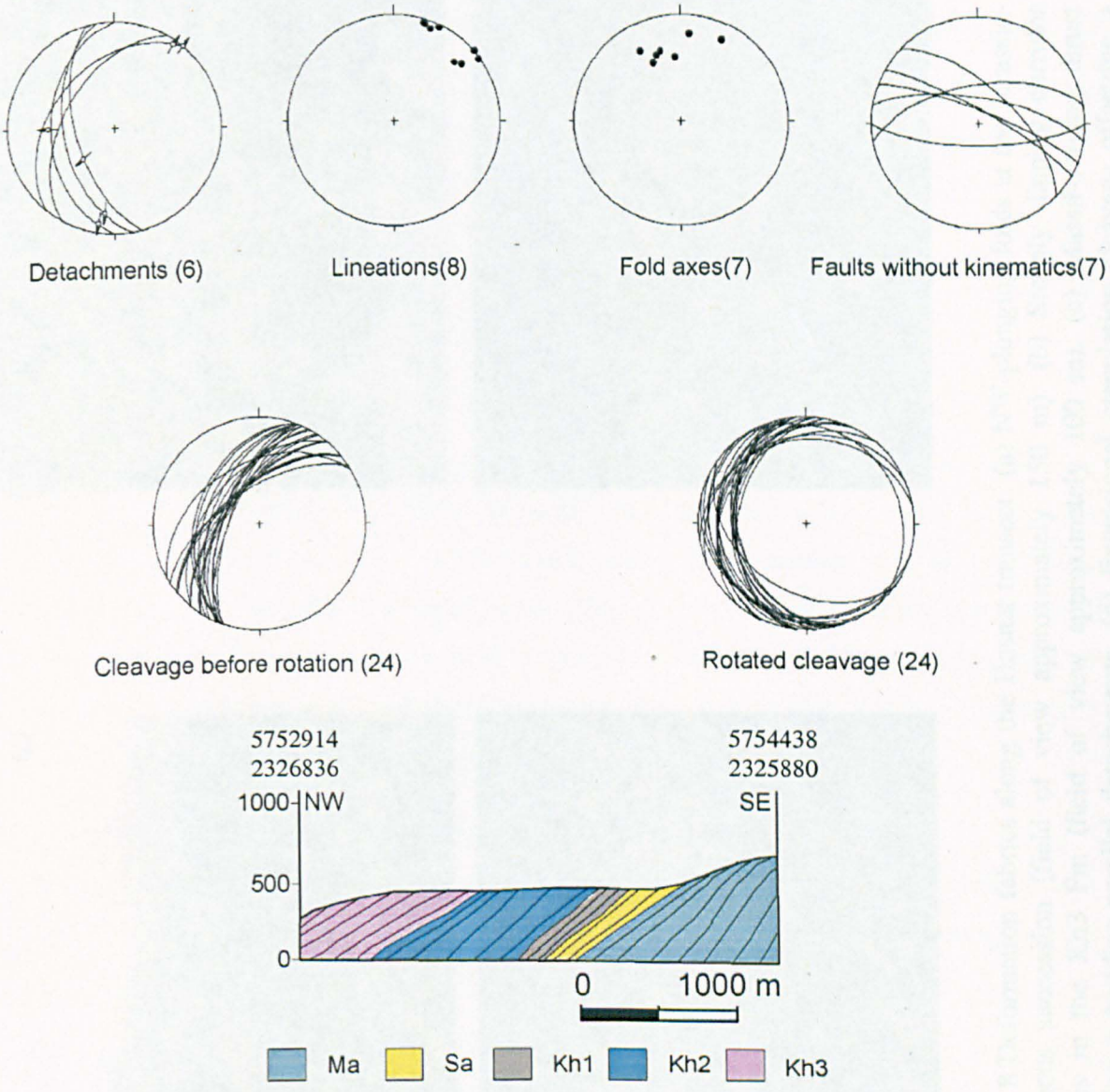

Fig. 4- 7 The Hassnat transect with stereograms of the different structural elements collected along the transect (Cleavage is rotated 30° around a horizontal axis trending 040).

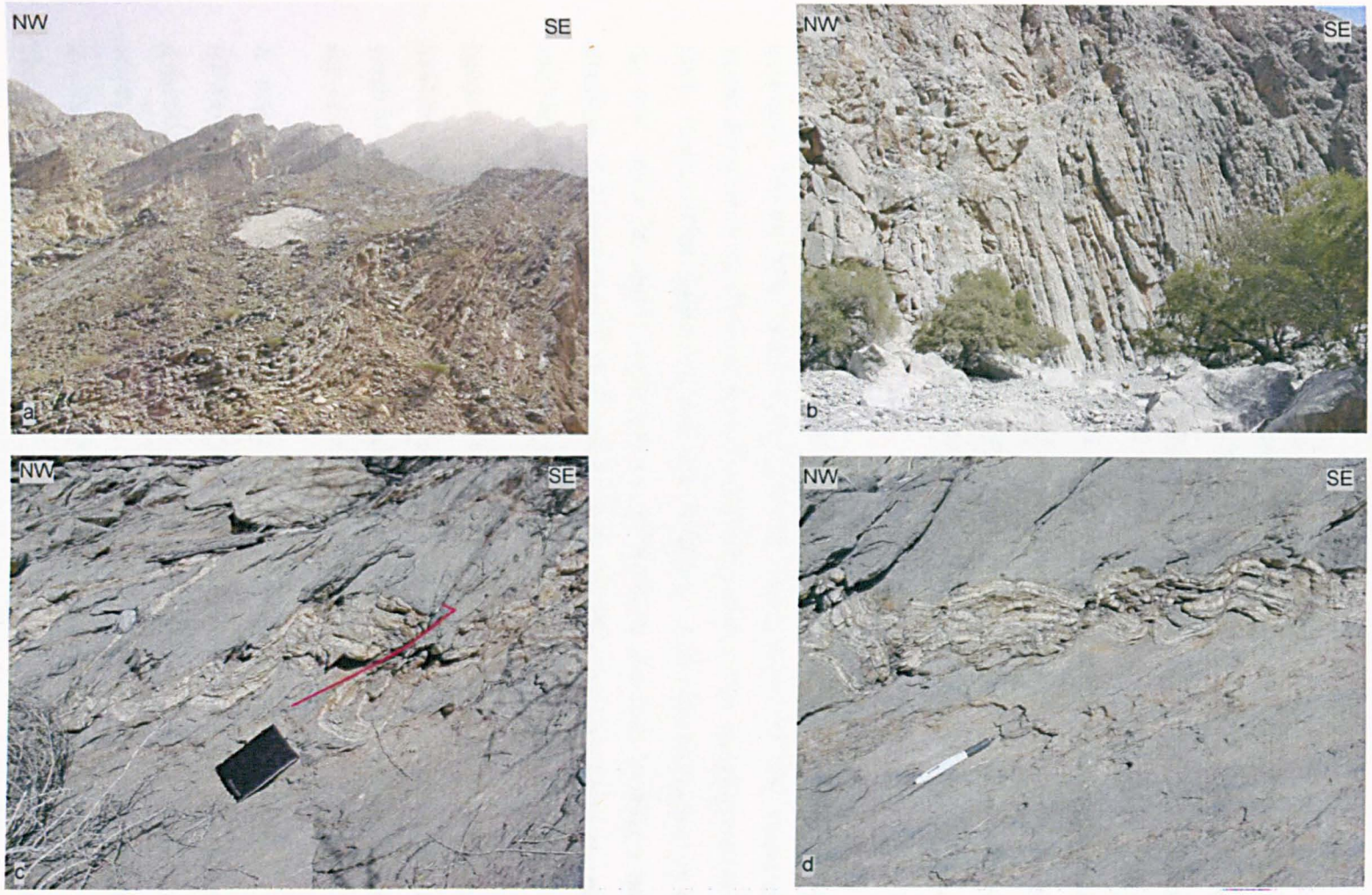

Fig. 4- 8 Deformation fabrics along the Hasnat transect (a) NW-plunging folds at the Jurassic-Cretaceous succession (field of view approximately 150 m). (b) Steeply dipping corridor fractures in the Kh3 Fm (field of view approximately 100 m). (c) Massif-verging thrust truncating a bedding-parallel detachments. (d) Extensional crenulation cleavage offsetting a bedding-parallel detachment in a normal sense

4.5 Wadi Qarah transect

The Wadi Qarah lies on the NW corner of the Nakhal culmination (Fig. 4- 1). It is about 50 km away from the town of Seeb. A 5 km transect was constructed along the wadi, oriented NW-SE starting from the Permian Saiq carbonates in the SE up to the Maastrichtian Aruma deposits at the wadi entrance (Fig. 4- 9). The transect extends from the western flank, where beds dip at approximately 30° NW, to the fold crest, where Permian-Triassic carbonates are sub-horizontal to gently dipping NW. The transect lies on the NW corner of the Nakhal culmination. km-long NE-striking faults penetrate the Jurassic-Triassic succession resulting in the formation of a monoclinal fold within the Sahtan Fm of the hanging-wall.

Large scale structures

Large structures along the transect are reflected by NE-striking fault and NW-plunging fold structures. The km-long, NE-striking fault with a steep dip of 60° NW separates between the Mahil dolomite of the footwall from the Sahtan clastics of the hanging-wall (Fig. 4- 9). The lower clastics of the Sahtan Fm have been displaced across the fault plane by 60 m towards the NW, while the upper carbonates are deflected by the fault forming a monocline fold structure. The hanging-wall strata are truncated by NE-subsidiary faults showing strike slip and oblique slip lineations pitching gently towards the NE quadrant (Fig. 4- 9).

Large NW-plunging, intraformational folds developed within the Sahtan (Fig. 4- 10a) and Salil Fm (Fig. 4- 10c). The fold axis pitch 25° towards the NW quadrant, while axial planes verge towards NE. The fold amplitude is approximately 30 m and folds are monocline with a sub-vertical to steeply dipping NE limb, reflecting top-NE shearing.

A fold within the Sahtan Fm has been examined in detail as follows. The fold is intraformational monocline within the Sahtan Fm and bounded by bedding-subparallel detachments. The fold axial surface is concave upward and hence the fold looses its amplitude away from the underlying detachment. This results in the development of a tight isocline immediately above the detachment and an open monocline further up (Fig. 4- 10b). The isoclinal fold is decoupled from units below by a bedding-parallel detachment. The lower isocline limb is truncated and sheared along the detachment surface, with calcite fibre lineations along the detachment pitching gently to the NE. NE-verging axial planar cleavage dominates the entire monocline fold structure, especially at the core of the isoclinal fold. The monocline structures within the Sahtan and Salil Fm are interpreted as follows. These folds are intraformational and underlain by bedding-parallel detachments with top-to-NE shearing. The progressive movement of the detachment resulted in folding of the hanging-wall strata and the formation of monoclinal structures.

Small scale structures

Small scale NW-trending faults of sub-metric displacements have been mapped within the Jurassic and Cretaceous rocks (Fig. 4- 9). This fault set encompasses a wide array of fault orientations, striking from WNW to NNW with a steep dip towards NE and SW. In places, they merge onto bedding-parallel detachments marked with NE-pitching lineations, while elsewhere they cross-cut the bedding-parallel detachments. Fault striations are dip slip and moderately pitch towards the massif. When tilting was restored relative to the local dip, the moderately pitching lineations turned into approximately dip slip, which may imply that the NW-oriented faults took place before or during the early stages of the folding onset.

Deformation fabrics

Deformation fabrics are manifested by bedding-parallel detachments, cleavage and fold structures. The bedding-parallel detachments are intensively deformed zones, decoupling the differently deformed stratigraphic units. Bedding-parallel detachments strike NE- with moderate dip away from the massif (Fig. 4- 9). The detachment mineral lineations pitch NE and NW. The NW-oriented normal faults branch and merge onto the detachments extending the stratigraphic unit along the NE-SW axis. Small folds are centimetric in scale and pitch NW (Fig. 4- 9), and where asymmetric, folds verge NE. Cleavage is oriented NE- and dips NW, with vergence directed towards the massif (Fig. 4- 9).

Interpretation and summary

The transect exhibits two sets of faults trending NE-SW and NW-SE, existing at all scales. Restoring the folding deformation has indicated that the NW-SE fault set formed before or during the early stages of the folding deformation. while on the other hand there is no adequate evidence about the relative timing of dip-and strike- slip displacements of the NE-striking fault set. The bedding-parallel detachments with NE-pitching lineations and the associated NW-oriented normal faults are all indicative of layer extension along NE-SW axis. Shear criteria such as asymmetrical folds imply top to NE shearing. In contrast, the bedding-parallel detachments with NW-pitching lineations and the massif-verging cleavage, the SE-verging cleavage, reflect NW-SE shortening. In short the transect was deformed under two kinematically contrasting systems; the NE-directed simple shear deformation and the NW-SE shortening deformation.

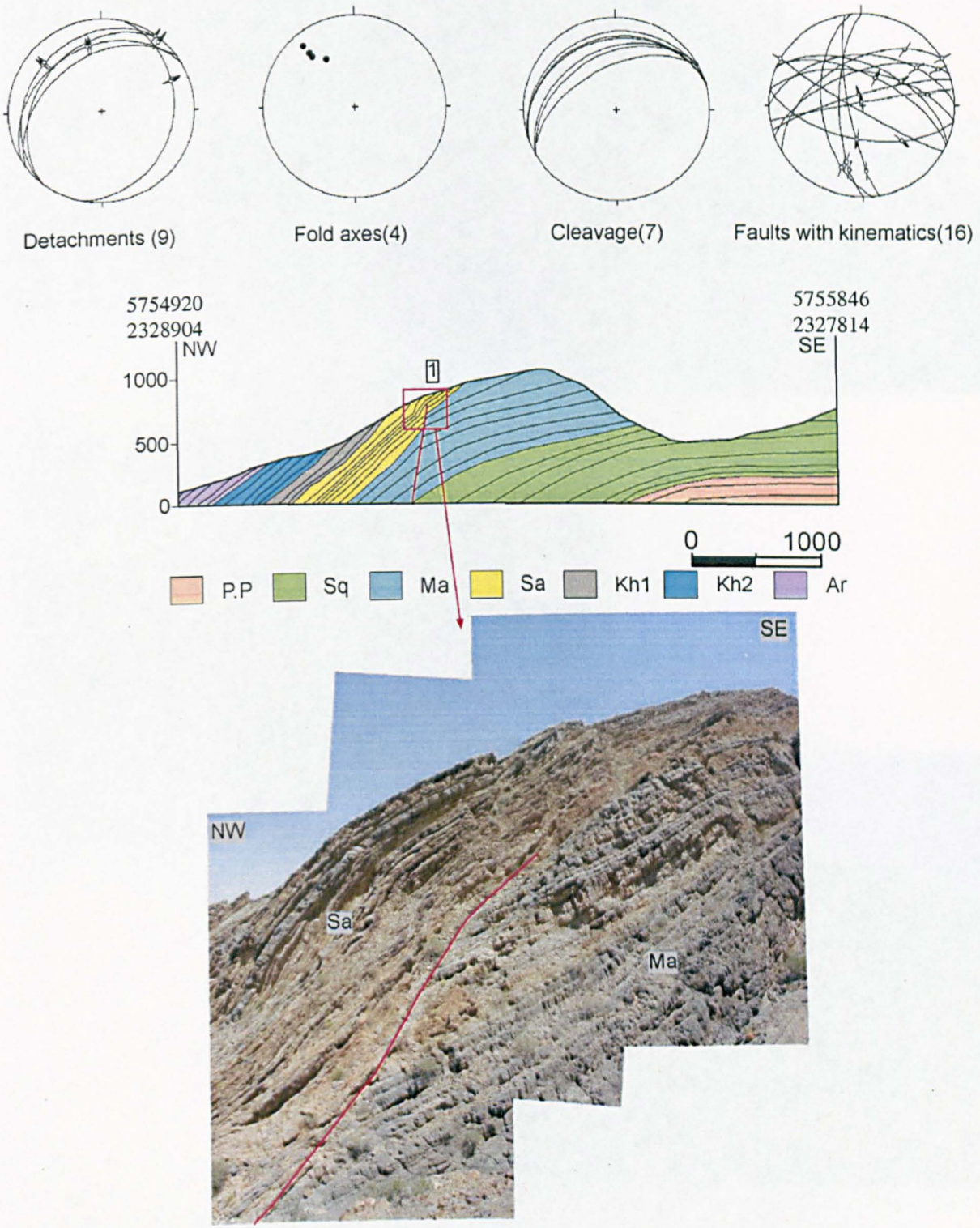

Fig. 4- 9 The Qarah transect with stereograms of the different structural elements collected along the transect. The lower image is of the major NE-fault between the Triassic Ma Fm and the Jurassic Sa Fm (Field of view approximately 200m).

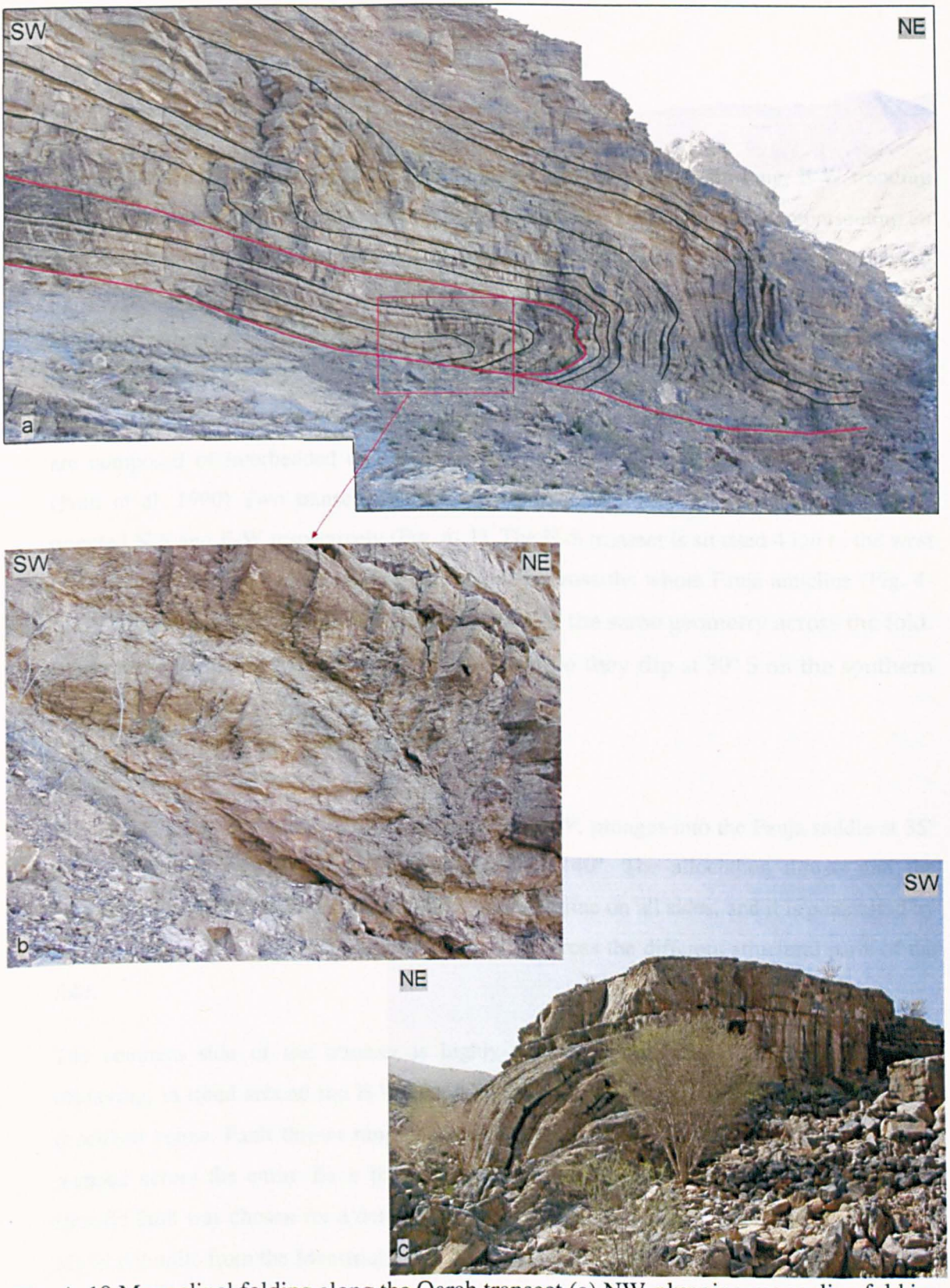

Fig. 4- 10 Monoclinal folding along the Qarah transect (a) NW-plunging monocline fold in the lower part of the Sa Fm (field of view approximately 100 m). (b) A close up view of the core of the monocline fold showing a recumbent fold with an axial planner cleavage (5755560, 2328350). (c) A classic NW-plunging monocline fold in the lower part of the Kh2 Fm(field of view approximately 50 m)

4.6 N-S transect across the Fanja anticline

The northern continuation of the Nakhal anticline constitutes a 10-km-long, E-W trending anticline plunging to E. This plunging structure is named the Fanja anticline, representing an intervening area between the Nakhal and Hatat Massif. This plunging anticline is occupied by the Permian-Cretaceous carbonate platform sequences, however the stratigraphy of the Jurassic-Cretaceous succession is slightly different here than those seen in Jebal Akhdar and Nakhal. Such stratigraphic differences arise abruptly across 10-km-long N-S fault, ascribed to be active during the Jurassic and Cretaceous (Pratt et al. 1990). The Cretaceous sequences are composed of interbedded micritic limestone, along with limestone and conglomerate (Pratt et al. 1990) Two transects have been constructed along and across this anticline, oriented N-S and E-W respectively (Fig. 4- 1). The N-S transect is situated 4 km to the west of the village of Fanja and is 10 km long running across the whole Fanja anticline (Fig. 4- 11). All of the exposed stratigraphic units exhibit the same geometry across the fold. Beds on the northern flank dip gently at 25° N, while they dip at 30° S on the southern flank.

Large scale structures

The Fanja anticline of the Nakhal anticline trends E-W, plunges into the Fanja saddle at 35° E. It is marked with a broad interlimb angle of 140°. The allochthon thrusts and the Maastrichtian Aruma sediments bound the Fanja anticline on all sides, and it is penetrated by steeply dipping E-W and WNW faults, distributed across the different structural parts of the fold.

The southern side of the transect is highly penetrated by steep to sub-vertical faults clustering, in trend around the E-W axis (Fig. 4- 11). These will be named E-W faults as described below. Fault throws range from one metre to more than 200 m. They have been mapped across the entire flank throughout the whole Permo-Jurassic succession, but one specific fault was chosen for a detailed analysis. The studied fault [1] separates the Jurassic Mahil dolomite from the Maastrichtian Aruma sediments along the southern flank. This fault dips steeply of 80° N and strikes WNW. The fault damage zone is marked with a series of steeply dipping faults branching upward (Fig. 4- 12a) and merging downward along a sub-vertical master fault. The fault throw is some 200 m. In some places, the fault appears as a steeply dipping reverse fault with hanging-wall anticline plunging of 38° SE. Different fault lineations have been recorded along the fault zone defining two populations: moderately plunging NW-pitching lineations and shallowly to horizontally plunging lineations pitching to either side of the fault (Fig. 4- 11). The shallow to horizontal lineations associated with a

strike slip displacement, probably took place after or during the latest stage of the folding deformation, since lineations are not significantly rotated. In order to reveal the relative timing between this faulting and the folding of the massif, the latter must be restored. When the folding structure was unfolded by rotating it around E-W axis, the moderately NW-pitching lineations became approximately dip slip, and the locally appearing reverse fault was converted into a normal fault. On this basis, the fault is interpreted as a dip slip normal fault that took place before or during the early stage of the folding deformation. The upward branching of the steeply dipping faults can be related to a post-folding strike slip event. Such a configuration indicates a negative flower structure formed under transtensional deformation (Davis, 1996). In short, the E-W faults were initiated as a dip slip before the folding onset, and then were rejuvenated as strike slip faults after or during the latest stage of the folding deformation

The northern flank of the Fanja anticline is dominated by moderately dipping NW-oriented faults. They are mostly dipping down slope towards the NE. The largest fault occurs between the Salil limestone and the Aruma sediments [2], which was displaced downwards for more than 100 m at least. Listwaenite thermal deposits developed along this fault. Kinematically all these faults show dip slip and occasionally strike slip lineations (Fig. 4-11and Fig. 4- 12b). Both lineation components are associated with post-folding faults as they are not affected by the folding deformation. Unlike what has been recorded at the southern flank there is no reliable evidence for pre-folding faults.

Deformation fabrics

Deformation fabrics on the southern flank are manifested by shear zones, stretching lineations, folds and cleavage and are common in the fine-grained units, particularly the Salil sediments. Intensively deformed narrow shear zones with bedding-parallel fabrics have been mapped, separating differently deformed rock sequences and therefore can be called detachments. These detachments strike NW-SE with variable dipping directions depending on the host rocks (Fig. 4- 11). Regardless of the dipping direction, fibrous lineations within the detachments trend NE-SW, while elongate carbonate aggregates are oriented N-S (Fig. 4-11). Mylonitic textures reflecting intense strain deformation have been recognized along some detachments, and a variety of ductile structures have also been recognized including bed-parallel cleavage, NE-verging spaced pressure solution cleavage and folds. Bedding-parallel pressure-solution cleavage is extensively developed, particularly within the shaly limestone. Spaced pressure solution cleavage dips gently SW implying a top to NE sense of shearing (Fig. 4- 11), and centimeter-scale folds plunge W and NW nearly orthogonal to the NE-SW stretching lineations. Most folds are upright, but where they are asymmetrical they

reflect a top to N sense of shearing (Fig. 4- 11). Lenses of sandstones interbedded within a shaly limestone matrix are highly stretched and separated along a NE-SW axis (Fig. 4- 13), and the measured amount of stretching is highly variable ranging from 16% to 68% based on boudinage spacing, indicative of a heterogeneous deformation.

Deformation fabrics on the northern flank are expressed by bedding-parallel detachments, folds and cleavage structures. Detachments strike NW-SE and dip moderately towards the NE (Fig. 4- 11). The associated fibre lineations plunge NE (Fig. 4- 11). Folds plunge in a wide trend ranging from NW to NE (Fig. 4- 11) and are of centimetric in scale and associated with axial planar cleavage.

Interpretation and summary

The general structural interpretation of this transect will be postponed until analyzing the E-W transect along the Fanja anticline.

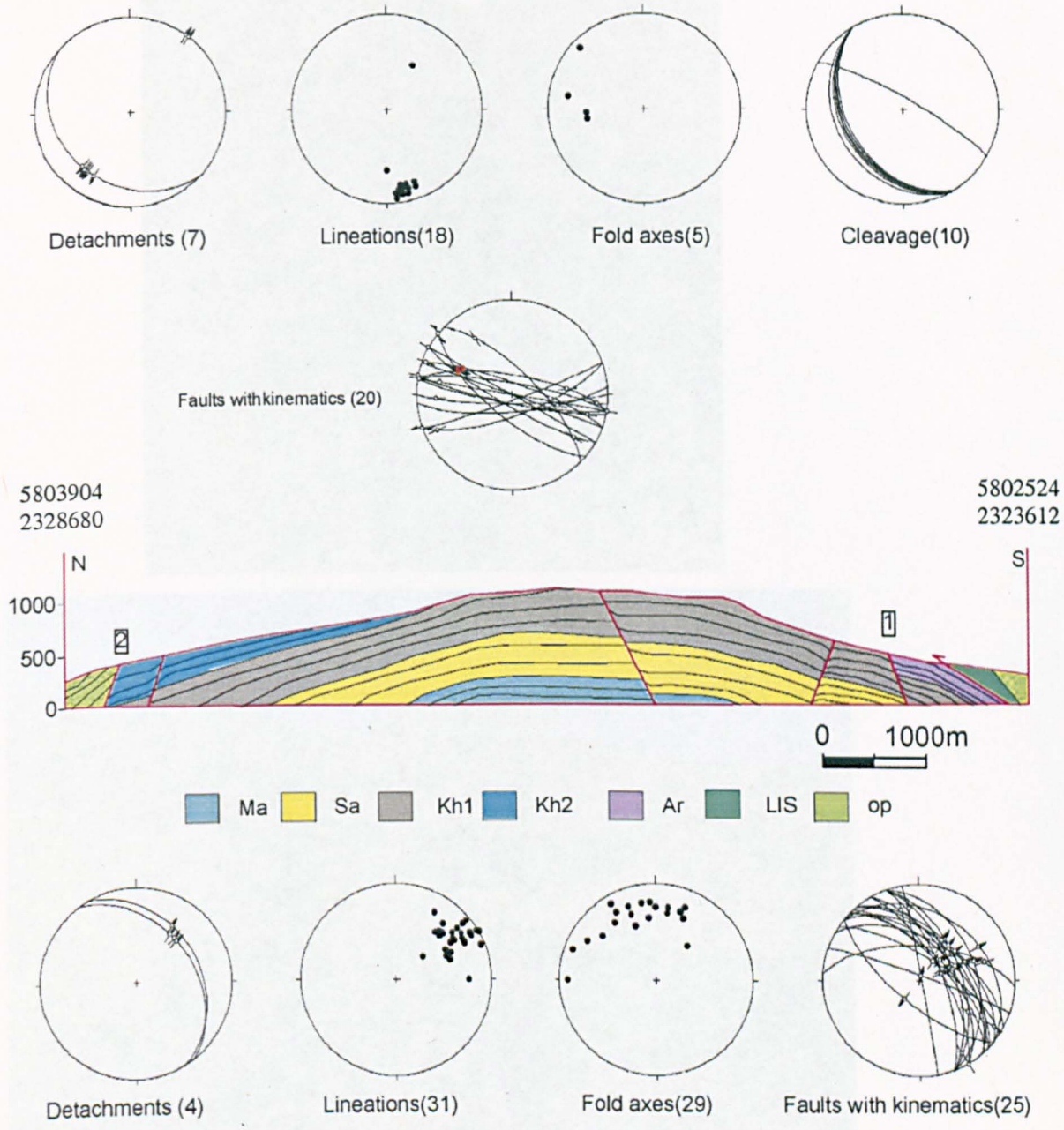

Fig. 4- 11 N-S transect across the eastern plunge of the Nakhal anticline with stereograms of the different structural elements collected along the transect. The upper stereograms are for the southern flank. The red circles on the fault stereogram represent steep, NW-pitching lineations along the WNW-faults. The lower stereograms are for the northern flank.

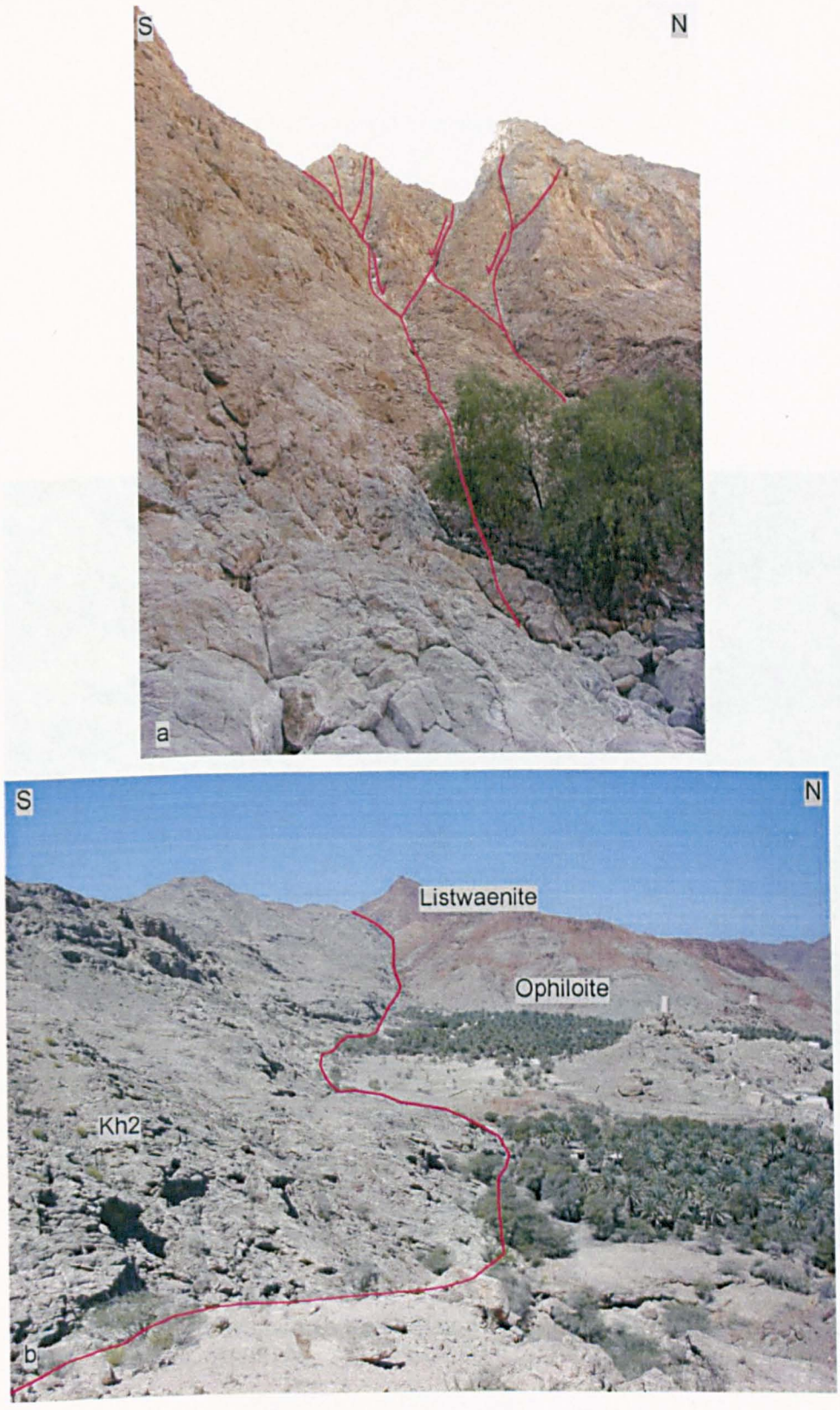

Fig. 4- 12 Steep E-W and NW-striking faults along the Fanja anticline (a) The steeply dipping E-W faults [1] with palm tree configuration in the Triassic Mahil dolomite (field of view approximately 20 m). (b) NW- trending fault [2] between the carbonate platform and the allochthon units mapped along the northern flank, Listwaenite appears along the fault (field of view approximately 200 m)

Fig. 4- 13 highly stretched and partitioned sandstone lenses floating within a matrix of clayey limestone (5804100, 2324760).

4.7 E-W transect along the Fanja anticline

A general insight into the lithology and the stratigraphy of the Fanja anticline has already been given in the previous N-S transect. The E-W transect was constructed along the Fanja anticline, parallel to the anticline axis (Fig. 4- 1) and it starts nearby the village of Alfarfarah situated at the eastern plunge of the anticline and extends westward for 8 km. The eastern end of the transect is marked by moderately dipping allochthonous units, unlike the western end where Permian and Triassic beds gently dip of 10° E (Fig. 4- 14). Generally, the dip of stratigraphic units increases eastwards from 10° to 30°, before they submerge beneath the Fanja saddle. Nevertheless, the hanging-wall strata dip 20° W towards a km-long, N-S fault exposed at the middle of the transect.

Large scale structures

The prominent structural feature across the Fanja anticline is a km-long N-S trending normal fault [1]. The fault dips 80° E and runs across the entire anticline for about 8 km, separating the massive Triassic Mahil dolomites in the footwall and the Jurassic-Cretaceous sequences in the hanging-wall. The fault throw is more than 400 m, and the hanging-wall beds are tilted towards the fault plane, forming a major roll over anticline (Fig. 4- 14). The fault has a prolonged history, since it was active during Jurassic and Cretaceous time as revealed from lithological and stratigraphical changes across fault.(Coffield et al. 1990; Pratt et al. 1990). The transaction of the Aruma sediments against this fault reveals that the must have been active after the deposition of Aruma Gp.

The area is also affected by a series of faults trending E-W and WNW- ESE parallel to the fold hinge (Fig. 4- 14). An example of such a fault is a sub-vertical WNW-trending fault [2] and further west its orientation changes to become E-W (Fig. 4- 14). This fault offsets the allochthon units, Aruma sediments and the Cretaceous carbonates for 200 m in a left lateral sense of shearing (Fig. 4- 15a). The hanging-wall units are disrupted by synthetic faults of metric displacement while kinematically, fault striations plunge gently westward (Fig. 4- 14).

Another example of an E-W fault has been mapped, separating the Aruma sediments from the Cretaceous carbonates with down-throw towards the south (Fig. 4- 15b). The fault displacement is more than 50 m and conjugate tension gashes reflecting a vertical $\sigma 1$ have been recorded across the hanging-wall. Three different fault lineations have been identified (Fig. 4- 14). These dip- and strike- slip, together with oblique lineations pitch westward. The purely dip- and strike- slip lineations took place after or during the latest stage of the folding deformation as they are not rotated by the folding deformations. However, in order to justify the oblique lineations, the folding deformation has to be restored. When unfolding was

applied by rotation around an E-W axis, the oblique lineations turned into dip slip, reflecting a pre-folding fault movement.

The main N-S fault [1] is displaced in a sinistral and dextral sense of shearing by a series of faults clustering around the E-W axis (Fig. 4- 14). The sinistral offset is associated with faults oriented 250°-320°, while the dextral offset corresponds to faults oriented at 320° (Fig. 4- 14). In this setting, the conjugate strike slip sets enclose σ1 oriented at 280°.

Deformation fabrics

Zones of intensive localized deformation have been identified, particularly along the fine-grained units of the Jurassic and Cretaceous successions. These narrow shear zones with bedding-parallel fabrics have been mapped separating rocks of contrasting deformation. Therefore these zones can be called detachments. Detachments are sub-parallel to bedding and strike NW-SE (Fig. 4- 14). They are characterized by fibrous calcite lineations trending NE-SW and are favorable site for extensive penetrative deformations such as cleavage. Elongated fragments lie along a NE-SW trend (Fig. 4- 14) while cleavage structures comprise a bedding-parallel fabrics and a spaced pressure solution cleavage. The latter strikes NW-SE with a gentle inclination towards SW (Fig. 4- 14). Shear criteria along the detachments mark a top-NE sense of shear as deduced from the spaced pressure solution cleavage. All of these deformation fabrics are cross-cut by the already described km-long faults.

Interpretation and summary of the structural deformation of the Fanja anticline

The Fanja anticline represents an intervening structure between the Nakhal and Hatat culminations and has been ascribed to a flat-ramp-flat thrust geometry in the sedimentary basement (Coffield et al. 1990). Structurally the Fanja anticline is transected by steeply dipping faults striking approximately N-S and E-W with the most prominent fault being a major N-S-striking fault crossing the entire anticline and developing a roll over anticline. According to literature the fault has a prolonged history involving Jurassic and Cretaceous movements (Coffield et al. 1990; Pratt et al. 1990). This fault is displaced in a strike slip manner by E-W-trending faults. The E-W faults are steeply dipping to sub-vertical, and run parallel to the fold hinges throughout the entire fold. They were initiated as dip slip faults before the folding deformation, and then reactivated as strike slip and dip slip faults. The majority of these strike slip faults are sinistral with a few dextral movement and collectively they enclose a 280° oriented maximum compression. The whole Fanja anticline is bounded from al sides by extensional faults displacing the allochthons and the Aruma sediments away from the massif. Consequently, the extensional faults are variable in trend,

striking in all directions depending upon the culmination geometry. Tertiary Listwaenite thermal deposits occur along some extensional faults. Wilde, (2002), dated the Oman Listwaenite as Tertiary, and hence the mapped listwaenite along this fault is considered as Tertiary in age, suggesting a Tertiary fault movement. Kinematically, all these faults display a dip slip component away from the massif, however along the southern flank both dip-and-strike- slip components coexist together.

The relative chronology of the faulting and folding events is assessed below, based on the following criteria. Firstly, the various fault sets experience poly-movements started before the folding onset and reactivated after or during the last stage of the folding process. Secondary, some of the culmination-bounding normal faults were active in the Mid Tertiary as dated by the Tertiary Listwaenite thermal deposits (Wilde et al. 2002). Thirdly, the major N-S fault was displaced by E-W-striking strike slip faults. Consequently, the N-S fault took place, subsequently truncated by E-W strike slip faults, with the massif-bounding extensional faults occurring latest. The massif-bounding faults must be induced after or during the last stage of the folding deformation, as they are localized and controlled by the geometry of the fold structures.

Ductile deformations appear everywhere along the Fanja anticline. They show a top-NE layer extensional shear. Correlating the deformation fabrics between the Fanja and Nakhal anticlines, gave rise into two contrasting points. Firstly, the frequency of the NE-directed deformations is less in the Fanja anticline than the Nakhal anticline. This variation could be attributed to the lithological differences between these anticlines, ascribed to the major N-S fault, which was active during Jurassic-Cretaceous time. However, the deformation intensity increases northwards as reflected by the mylonitic textures and the amount of stretching percent. Secondly, the NW-SE-shortening deformations, which are significantly developed in the Nakhal anticline, are missing from the Fanja anticline. This point in particular will be addressed at the end of the chapter.

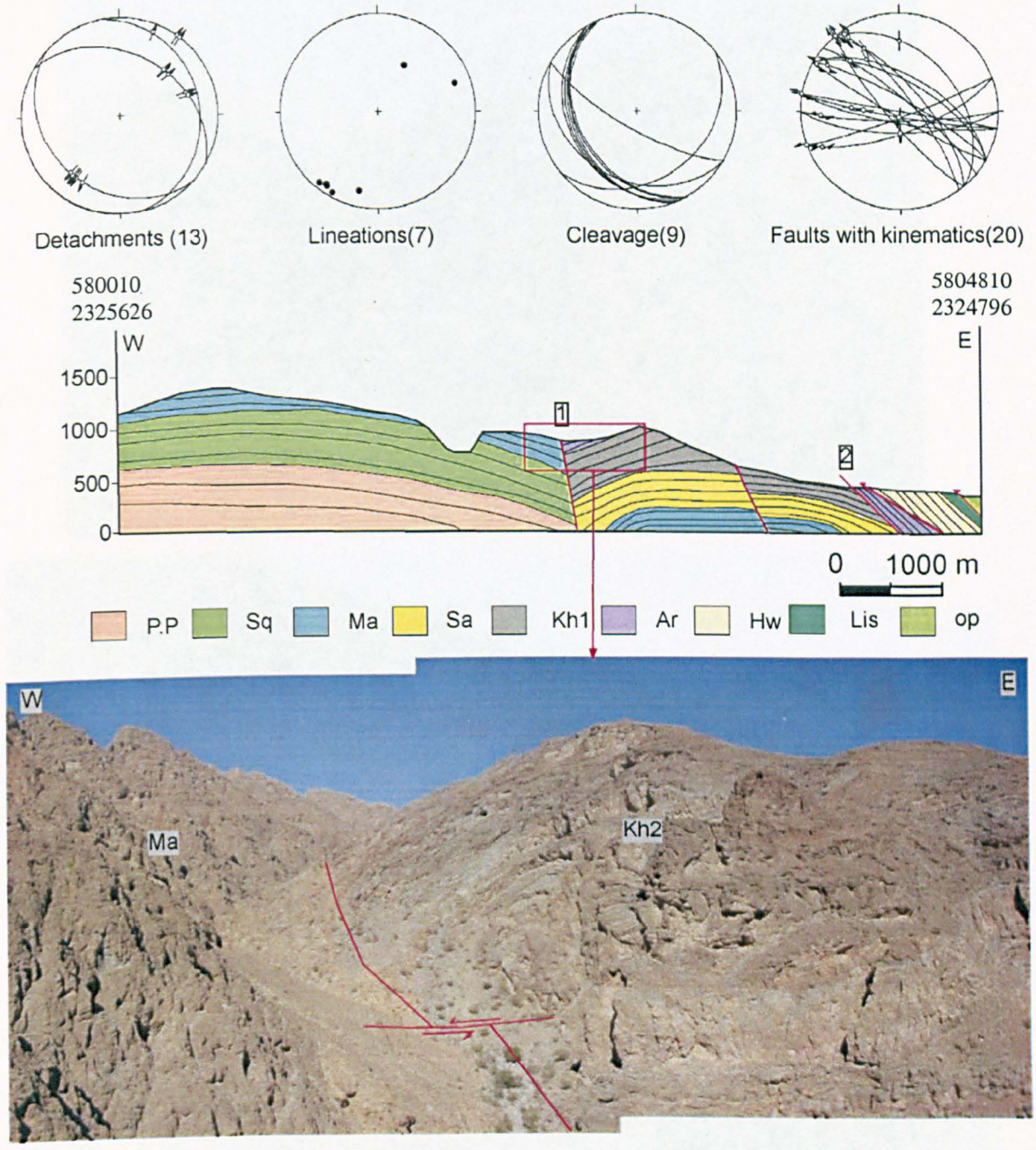

Fig. 4- 14 The E-W transect along the eastern plunge of the Nakhal anticline, with stereograms of the various structural elements collected along the transect. The lower image is of the rollover anticline developed along the major N-S fault [1], which is displaced in a sinistral manner across E-W fault (field of view approximately 300 m).

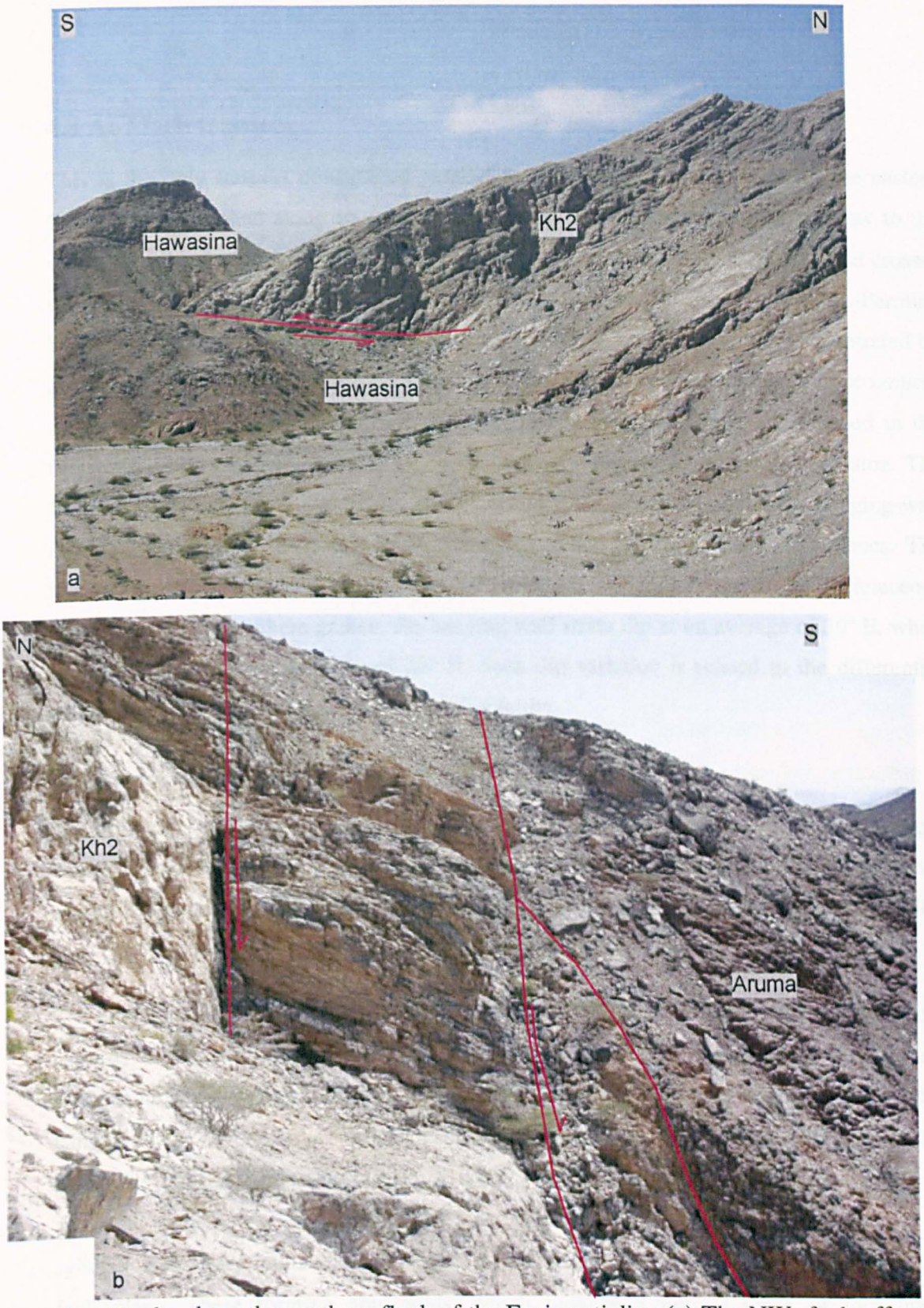

Fig. 4- 15Faults along the southern flank of the Fanja anticline (a) The NW- fault offsetting the allochthons units in a sinistral manner for more than 200 m (field of view approximately 300 m). (b) The E-W fault [2] between the Kh2 and Aruma sediments (field of view approximately 50 m).

4.8 Al-Meeh transect

This is the only transect constructed parallel to the Nakhal Massif and along the eastern flank. It is established along an area extending from the pre-Permian Albir window to the village of Albir further south (Fig. 4- 1). The transect is approximately 5 km long and crosses the entire preserved Mesozoic carbonate platform sequence along with the pre-Permian Mistal sediments outcropping at the Albir window (Fig. 4- 16). The transect is penetrated by a series of steeply dipping NW-striking faults which form graben structures. The prominent rocks of the Permian Saiq carbonate and the Triassic Mahil dolomite are exposed in the footwalls, while the hanging-walls are occupied by the Jurassic-Cretaceous succession. The footwall strata dips at approximately 40° SE, while the bedding attitude in the hanging-wall is highly variable, as the beds are deflected and folded adjacent to the fault planes. The transect is marked with two, km-long graben structures occupied by the Jurassic-Cretaceous succession. In the northern graben, the hanging wall strata dip at on average of 30° E, while in the northern graben, they dip of 20° N. Such dip variation is related to the differential displacements along the km-long NW-striking faults.

Large scale structures

The transect is crossed by several km-long faults penetrating the whole stratigraphic section. Faults dip steeply and range in orientation from E-W to NW-SE forming a series of horsts and graben structures (Fig. 4- 16a and Fig. 4- 17a), with large fault throws ranging from 500 m to 1500 m. Below the faults are described individually, from N to S.

The first fault [1] varies in strike from E-W to WNW-ESE with steep to moderate dip towards the south. It separates the pre-Permian Mistal Fm and the Permo-Triassic succession in the footwall from the Cretaceous carbonate and Hawasina sediments in the hanging-wall. A very large vertical displacement of 1.5 km has been recorded along the fault. The fault penetrates the whole of the Nakhal anticline, and together runs further E along the western flank of the Fanja anticline. The hanging-wall strata are highly faulted by synthetic subsidiary faults oriented parallel to the master fault and are deflected adjacent the fault plane. These forming drag folds, which indicate a normal sense of movement. Horizontal slickensides have been recorded along the fault plane, indicating post-folding strike slip faulting (Fig. 4- 16b).

The second km-long fault [2] strikes NW-SE and dips steeply of 80° NE. The footwall block is occupied by the prominent rocks of the Mahil dolomite, while the Jurassic-Cretaceous succession occupies the hanging-wall. The vertical fault displacement is more than 300 m. Hanging wall strata are folded adjacent to the fault plane forming a rollover anticline running parallel to the fault and plunging parallel to the regional dip (Fig. 4- 17b). The rollover anticline dies down section along the more competent unit of the Mahil dolomite. When folding deformation was restored, the plunging rollover anticline turned into non plunging anticline. This readjustment within the anticline geometry reveals that such a structure must be associated with a pre-folding dip slip fault

The third main fault [3] trends E-W and dips 60° S. It separates the massive resistant units of the Mahil dolomite of the footwall from the Jurassic-Cretaceous units of the hanging-wall (Fig. 4- 17c). The fault throw is approximately half a km. The hanging-wall strata are folded and form a hanging-wall syncline. Beds close to the fault are tilted parallel to the fault plane, while distant beds dip in the opposite direction of 20° N.

The fourth fault [4] strikes NW- and dips steeply of 60° NE. The footwall block is occupied by the prominent rocks of the Mahil dolomite, while the Jurassic-Cretaceous succession is exposed along the hanging-wall. The fault will be explained in detail within the Albir transect , where it is well exposed.

Metric scale intraformational fold structures are common in the inter-bedded shale limestone succession. The fold amplitude is highly variable ranging from centimetric to metric scale. The metric scale folds are described in this section based on the hosting stratigraphic formation; however the small-scale folds will be addressed in the section of deformation fabric section. The frequency and intensity of folding deformation increases northwards along the transect.

Sahtan beds are deformed by isoclinal folds that plunge gently S (Fig. 4- 18a). Folds possess axial planner cleavage, which converges around the axial plane (Fig. 4- 18b). Bedding-parallel stylolites are folded, which reveals that the stylolites predate the folding deformation. These asymmetric folds indicate top-NE shearing, while the axial planes verge northward. This apparent disagreement was resolved by restoring the tilting deformation, which turned the axial plane vergence towards the NE (Fig. 4- 18c).

Metric scale folding within the Salil Fm is developed in a 4 m thick stiff limestone bed surrounded by incompetent micritic limestone units (Fig. 4- 19a). The limestone bed is highly stretched and thinned, forming pinch and swell structures and lenticular boudins. In places the attenuated bed is isoclinaly folded with overturned short limbs. Fold axes plunge

gently towards the south; while bedding-subparallel axial planes strike NW-SE, with moderate dip of 35° SW. The fold asymmetry indicates a vergence towards the massif, while the axial planes verge towards NNE. This contradiction can be resolved by restoring the tilting deformation as the area was subjected to severe tilting related to the folding and NW-oriented faulting deformation. When the fault-related tilting was restored by tilting beds 40 ° around a horizontal axis trending 340, the axial plane vergence turns into NW (Fig. 4- 19b).

Deformation fabric

Intensive localized shear deformations with foliations are common in shaley limestone units separating between variously deformed structural units. For this reason, such structures can be considered as detachments. Owing to the intensive faulting and tilting along the transect, the orientations of bedding-parallel detachments are highly variable as seen in Fig (Fig. 4-16a). However, regardless of the variability in the strike of the detachments, the associated mineral lineations cluster into two main trends; NE-SW and E-W. Normal faults clustering around a N-S axis have been recorded merging and branching onto the detachments. Such faults are bedding confined, small in length and have sub-metric displacements. Kinematically, normal faults dipping away from the massif are oblique with fibre lineations plunging towards NE. When the folding structure was unfolded by rotating it 30 ° around a horizontal axis trending 040, these oblique N-S faults became NNW-striking faults with dip slip lineations. Similar readjustments took place over the massif-dipping N-S faults. Such faulting indicates NE-SW directed extension, and as a result, the bedding-parallel detachments reflects top-NE layer extension shear. Stretching lineations, such as elongate sediment clasts trend NE-SW with a minor component trending approximately E-W (Fig. 4-16a).

Small scale intraformational folds in the micritic limestone units of the Salil Fm have axes that form SE and SW plunging populations (Fig. 4- 16a). The SE-plunging folds are oriented perpendicular to the NE-stretching direction, marked with tight interlimb angles and are associated with NE-plunging cleavage. However, the SW-plunging folds are oriented parallel to the stretching lineations, marked with open interlimb angles and are associated with massif-verging cleavage. How each group was formed will be addressed later.

There are different phases of cleavage present including schistosity foliations and spaced pressure solution cleavage (Fig. 4- 16a). The schistosity cleavage reflects the greenschist metamorphic facies (Le Metour et al. 1990), and stretching lineations defined by elongate clasts along the foliation planes plunge gently towards NE. Spaced pressure solution cleavage takes the form of two sets, one verging NE and the other towards massif. The NE-

verging cleavage strikes NW and dips moderately of 45° SW, while stretching lineations on cleavage surfaces plunge NE. This cleavage set is theaxial planar cleavage present across the NE-verging folds, while along some detachments the cleavage is sigmoidal in shape. However, the massif-verging cleavage strikes NE and dips more steeply at 55° SE acting as axial planar cleavage across the massif-verging folds. Stylolites are well established along the micritic limestone of the Sahtan and Salil Fm and are bedding-parallel and bedding-orthogonal. The bedding-parallel stylolites are folded by the NE-verging folds and are hence older than the NE-directed deformation. The bedding- orthogonal stylolites imply a SE-NW shortening perpendicular to bedding (Fig. 4- 20d).

Boudinaged structures have developed within the more competent limestone and sandstone beds interbedded within shaly limestone sediments (Fig. 4- 20a). These stiff beds were stretched, thinned and separated by the progressive extensional deformation. Some limestone beds have been subjected to intensive thinning making them 1-5 times thinner than the initial thickness (Fig. 4- 20b). In some places the stiff beds have been separated for up to a metre. The boudin axes plunge SE, perpendicular to NE-stretching lineations. However, the sense of shearing can not be determined with confidence as the boudinage was subjected to severe forward and backward rotation by synthetic and antithetic slip surfaces. The mechanism of boudin development is explained as follows (Fig. 4- 20c). Partitioning began with the more competent units by the formation of orthogonal extensional fractures, oriented perpendicular to the stretching direction, which reflected the coaxial components of the extensional deformation. The extensional fractures were filled due to calcite mineralization and formed veins. Continued sinistral shearing resulted in a clockwise reorientation of the initially orthogonal veins, turning them into synthetic slip faults by which the adjacent boudins are separated. Subsequently, the boudins are rotated backward. The reoriented boudin structures also develop flanking folds in the adjacent wall rocks (Swanson 1999).

The pre-Permian Mistal sediments comprise metamorphosed siltstones and greywacke. They are dominated by penetrative structures forming extensive foliations and slaty cleavage, marked with stretching lineations plunging NW and SW. In places foliations are folded at asymmetrical SSW plunging folds. Determining the exact mechanism behind such deformation is uncertain, as the pre-Permian sediments have experienced a multitude of deformational events (Mann et al. 1990).

Interpretation and summary

The transect is predominated by km-long NW-SE and E-W faults penetrating the entire stratigraphic profile (Fig. 4- 17a). These faults form a series of horsts and graben structures and record the highest fault displacements seen across the whole study area, which indicates that the amount of fault displacement increases towards the NE. Fault kinematic data indicates poly movements that started before or during the early stage of the folding onset, then reactivated again during or after the latest stage of the folding event again as dip slip and strike slip movements.

The structural deformation is classified into two main systems with respect to the shearing direction; the NE-directed extensional deformation and the massif-verging deformation. Each system is interpreted in detail below.

The NE-directed extensional deformation is manifested as a linked system of layer extension shear and steep NW-oriented faults. The transect records the highest grade of the NE-directed deformation across the study area, which is marked by a very significant increase in both the metamorphic facies and the intensity of tectonic deformation. The metamorphism reached the greenschist facies at the northeast extremity of the section (Le Metour et al. 1990; Breton 2004), while the increase in the intensity of tectonic deformation is reflected by the development of recumbent folds. The recumbent folds have evolved from NE-verging folds to bedding-parallel recumbent folds under progressive NE-directed shearing (Fig. 4-18d). Layer extensional flow is manifested by intensive thinning, boudinaging, cleaving and folding deformation.

The massif-verging deformation is marked by the massif-verging cleavage and folds together with the orthogonal stylolites. These structures reflect NW-SE shortening with a top to the massif sense of shearing. Such shearing is also accommodated through bedding-parallel slipping, as evidenced from the NW-SE oriented fibre lineations. The question arises; what is the relative age between the NE-extensional deformation and the NW-SE contractional deformation? A growing body of evidence indicates that the NE extensional deformation mapped in the Jurassic-Cretaceous succession predates the massif-verging structures. The evidence for this is seen firstly by the stretched and boudinaged stiff beds that have been folded by massif-verging folds, and secondly due to the folding of the NE extensional fabric within the Jurassic-Cretaceous sequences caused by the Nakhal folding.

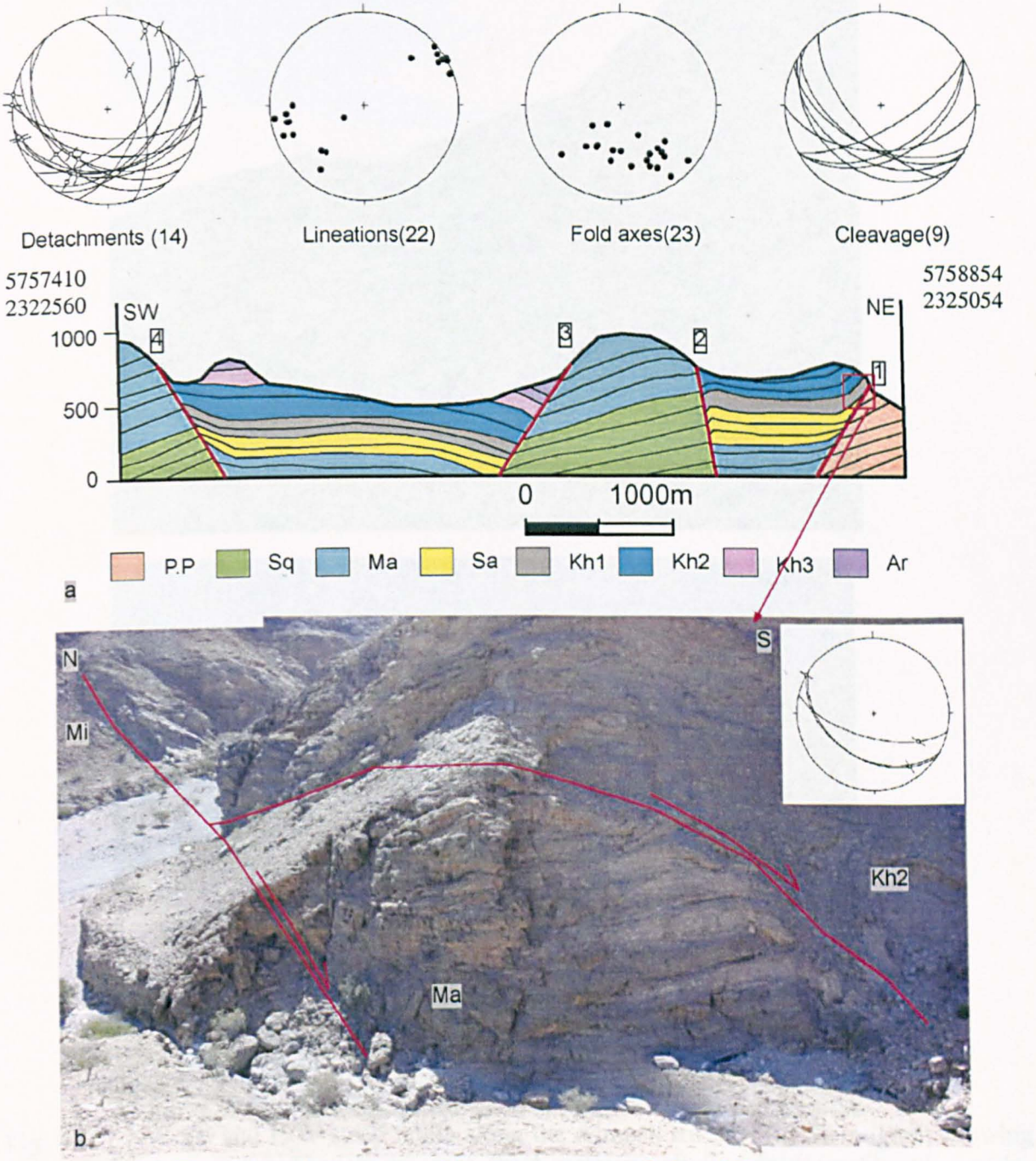

Fig. 4- 16 (a) The Almeeh transect with stereograms of the different structural elements collected along the transect. (b)The major NW- fault [1] between the Pre-Permian Mistal sediments and the Cretaceous succession, inset is a stereogram for the fault lineations expressing the strike slip component along the fault (field of view approximately 100 m).

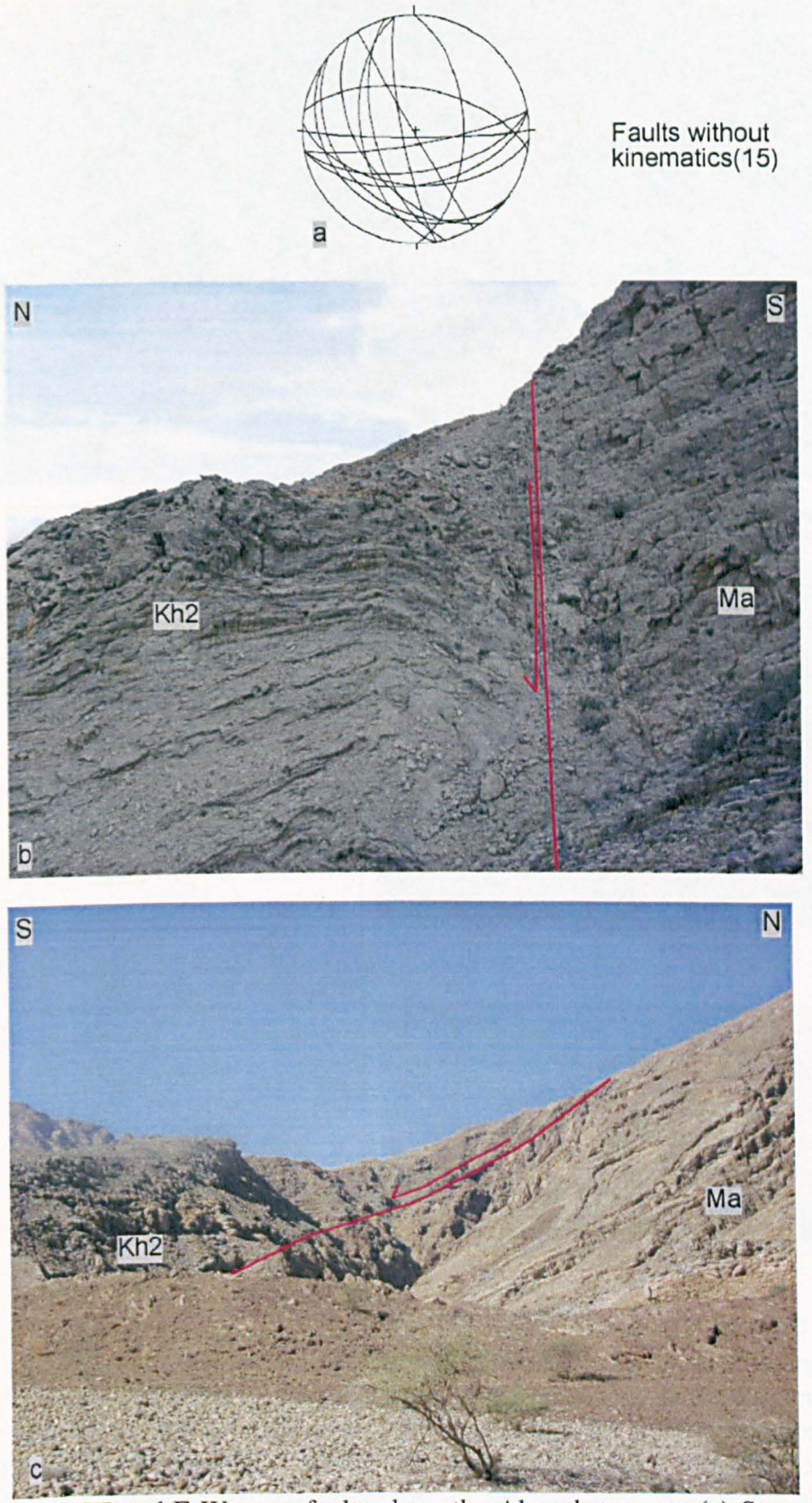

Fig. 4- 17 NW-SE and E-W steep faults along the Almeeh transect (a) Stereogram showing the major faults mapped along the transect. (b) A rollover anticline developed beside a major NW-fault [2] (field of view approximately 50 m). (c) The major NW-fault [3] between the Triassic Ma dolomite and the Cretaceous succession (field of view approximately 300 m).

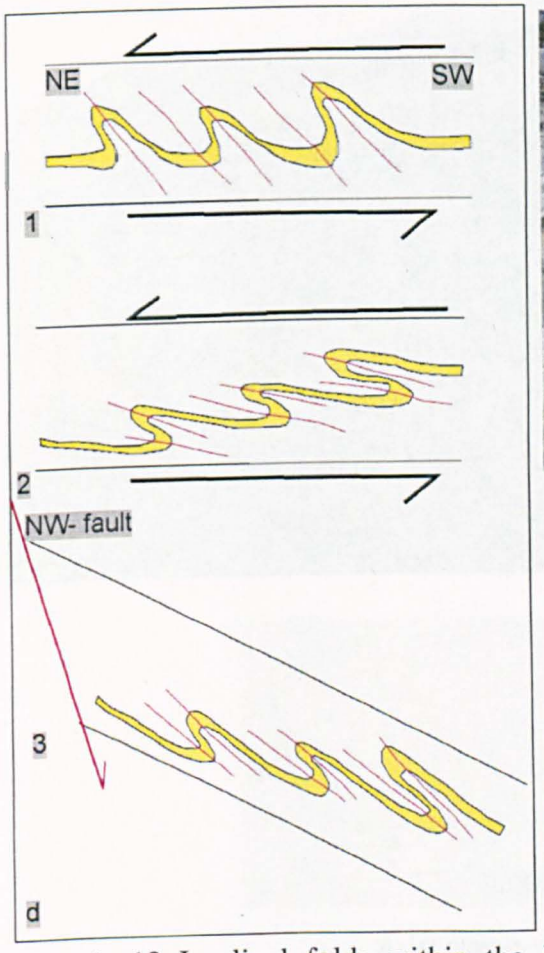

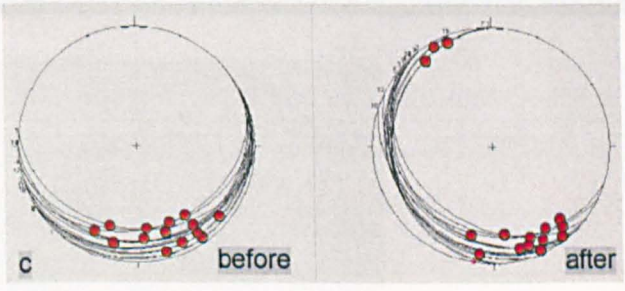

Sahtan axial planes rotated around 190\20

Fig. 4- 18 Isoclinal folds within the Jurassic-Cretaceous succession along the Almeeh transect (5758860, 2324920) (a) Isoclinal folds in the upper part of the Sa Fm (field of view approximately 20 m). (b) An axial planar cleavage across the Sahtan recumbent folds (field of view approximately 5 m). (c) Stereogram for the axial planes of the Sa folds before and after the tilting restoration, the red circles are for the fold axes. Notice that after restoration folds verge to NE (Axial planes were rotated 40° around a horizontal axis trending 340). (d) Cartoons illustrating the development of the Sa folds 1) Folds were initially formed as inclined folds verging NE. 2) under the progressive shear deformations folds rotated inward to become parallel to the bedding plane. 3) The present day structures, in which the area is tilted southward due to NW-faulting.

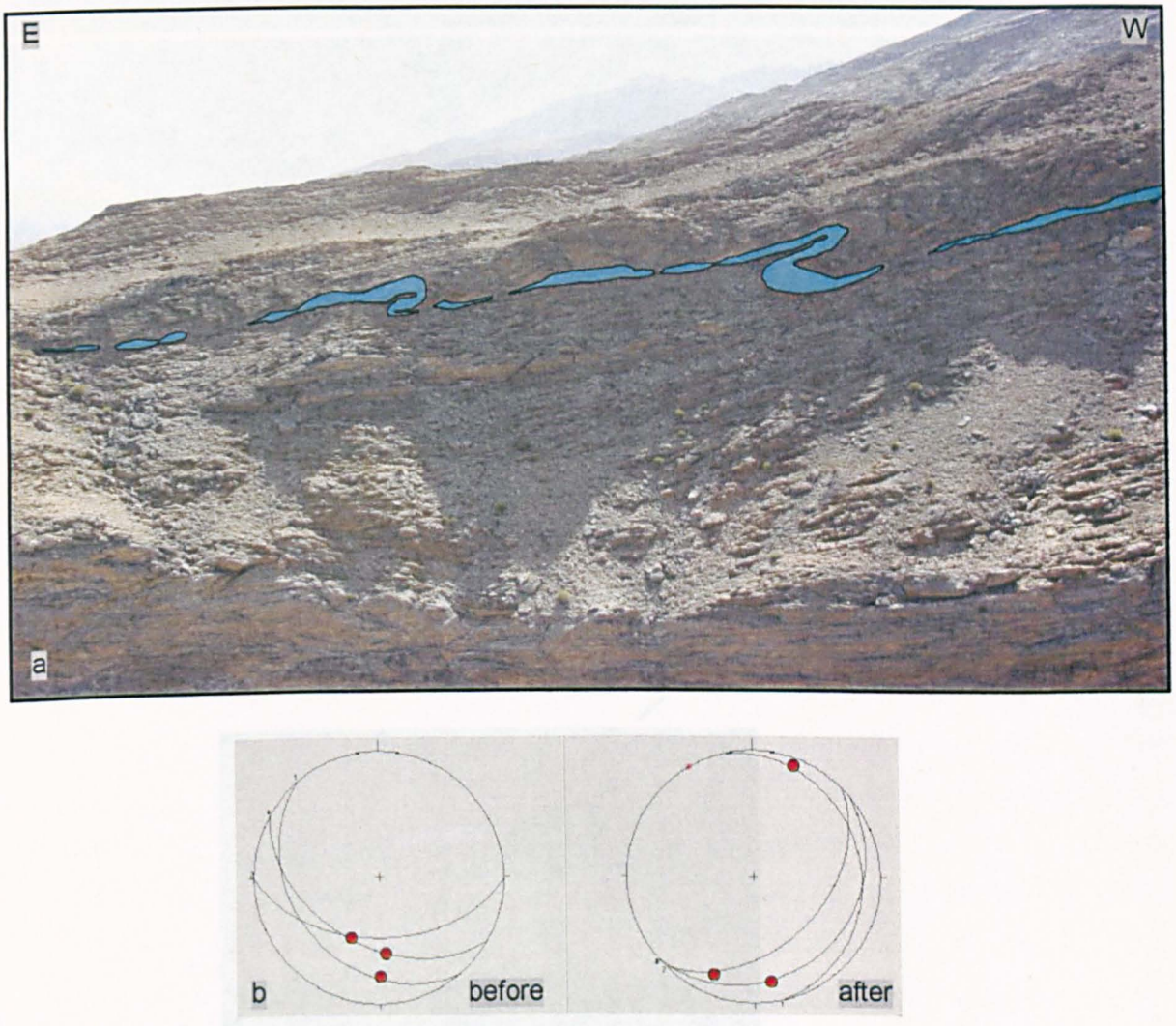

Fig. 4- 19 Isoclinal folds in a highly stretched and boudinaged limestone bed in the upper part of the Kh2 Fm (field of view approximately 200 m). (b) Stereograms for the axial planes of the Kh2 recumbent folds before and after the tilting restoration, the red circles are for the fold axes. Notice that after restoration folds verge toward the massif (Axial planes were rotated 40° around a horizontal axis trending 340).

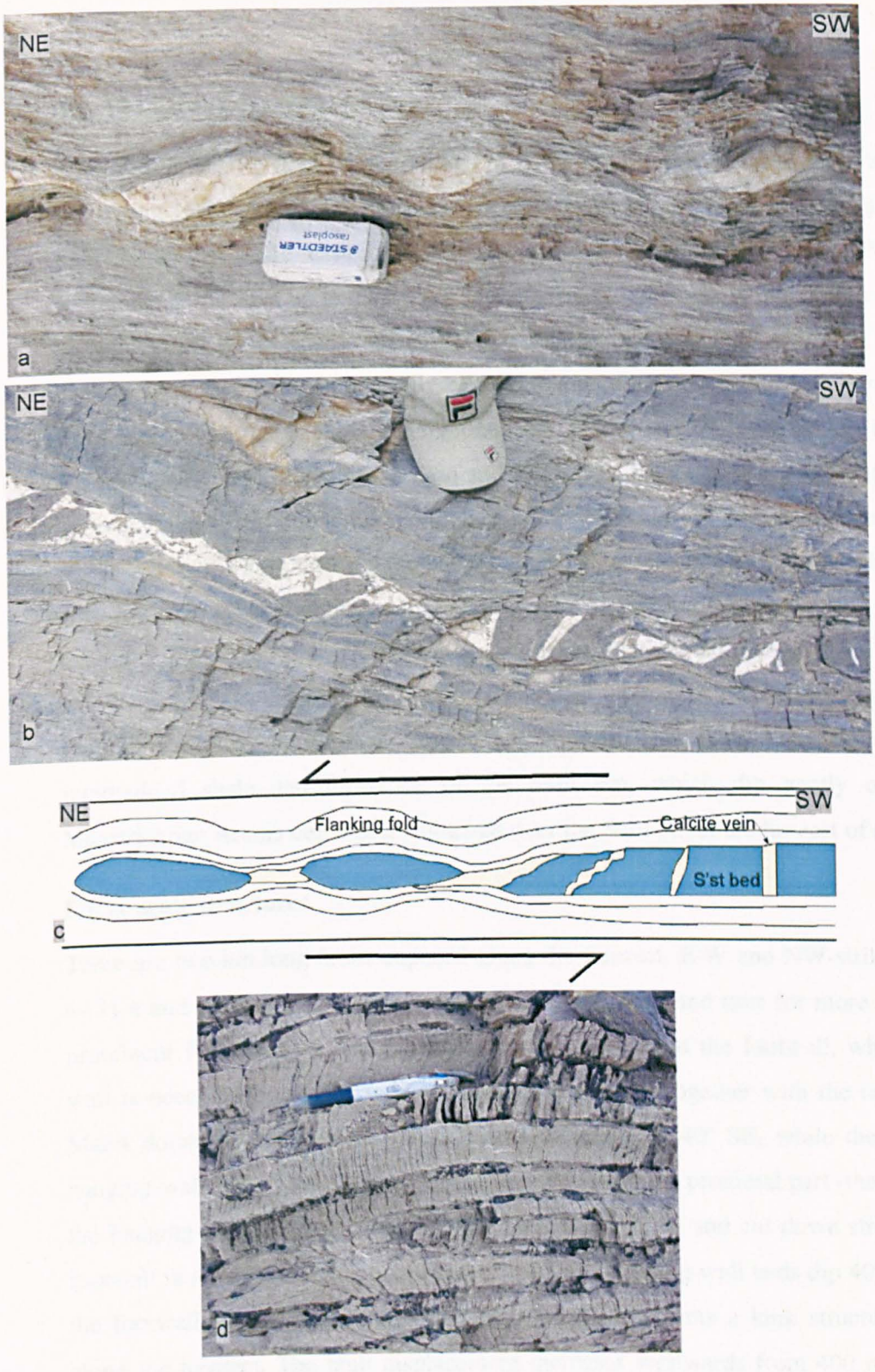

Fig. 4- 20 Deformation fabrics along the Almeeh transect (a) Breakup of calcite veins into strings of individual clasts upon rotation and elongation during top-to-the-NE shearing. (b) Boudinage of a sandstone bed floating in a micritic limestone matrix, the parting zone is filled with calcite. (c) Cartoons showing the style of boudinage, the processes started from right to left. Boudinage started initially by initiation of orthogonal fractures later filled with calcite. Further shearing led to stretching and rotation of both veins and boudinage backward along synthetic slipping surfaces. (d) Bedding-orthogonal stylolites in thinly bedded limestone of the Kh2 Fm.

4.9 AL-Tayah transect

This wadi is located between the village of Albir and the pre-Permian Albir window further north (Fig. 4-1). An 18 km transect oriented E-W, has been constructed along the wadi penetrating the entire eastern flank. The transect started with the pre-Permian Mistal sediments in the west up to the Maastrichtian Aruma sediments at the eastern wadi entrance, throughout the whole preserved Mesozoic carbonate platform sequences (Fig. 4- 21). On the eastern flank, bed strike is generally parallel to the massif (NNE) but with variable dip, apart from where faulting disrupts the regional dip. In the western part, which is occupied by Permo-Triassic carbonates of the Saiq and Mahil Fm, beds dip of approximately 30° E. The Jurassic Sahtan Fm and the Lower Cretaceous Rayda and Salil Fm are exposed at the middle of the transect, where they dip an average of 20° S, as the area is highly faulted and folded. Two km-long folds plunging roughly south were mapped at this part of the transect within the upper Triassic to Lower Cretaceous succession. Bedding attitude changed abruptly to dip 50° E for a distance, before becoming gentler and dipping at 20° N as it approached a km-long, E-W striking normal fault mapped further north. The eastern section is dominated with interbedded shale and limestone of the Salil Fm, which dip gently of 20° N. The Maastrichtian Aruma deposits are thrusted over the Salil Fm at the far east of the transect.

Large scale structures

There are two km-long faults exposed along the transect, E-W and NW-striking faults (Fig. 4- 21 a and b). The E-W fault [1] dips of 60° southward and runs for more than 4 km. The prominent Permian and Triassic dolomites are exposed at the footwall, while the hanging wall is occupied by the Jurassic-Cretaceous succession together with the upper part of the Mahil dolomite. The footwall strata dip consistently at 40° SE, while the attitude of the hanging-wall strata is variable along the fault strike. In the proximal part (the eastern side) of the hanging-wall, strata dip towards the fault at 20° NNE and cut down stratigraphy of the footwall in a westward direction. Further west, the hanging-wall beds dip 40° E in parallel to the footwall strata. This change in hanging-wall dip forms a kink structure, clearly seen along the transect. The fault displacement increases westwards from 400 m at the extreme east to 600 m at the hanging-wall kink, after which fault displacement is constant at some 600 m. The variable dipping of the hanging-wall strata is attributed to the lateral gradient in the fault displacement along the fault strike. Such phenomena will be explained in great detail aided by illustrative diagrams in the Qet transect.

The Second km-long fault is a NW-striking fault [2] that dips shallowly at 20° -30° NE. The fault separates between the Mahil dolomite of the footwall from the Jurassic-Cretaceous succession of the hanging-wall, but the amount of the fault throw could not be determined.

The hanging-wall strata lie parallel to the fault plane and are frequently truncated by a series of small NW-oriented faults merging onto the underlying low angle fault (Fig. 4- 22a). The low angle fault is truncated by the major E-W fault and a small NE-striking fault, which displaced it down by some 10 m towards the NW (Fig. 4- 22b). Fault lineations along the NE-striking fault reveal a dip- and strike-slip displacement. It is frequently seen that the NE-oriented faults cross-cut the earlier structures, while nothing like that has been seen for the E-W faults.

Two large fold structures of the Triassic-Cretaceous sequences were mapped at the middle of the transect. At the first fold [3] the upper part of the Mahil, Sahtan, Rayda Fm and the lower part of the Salil Fm are folded by a massif-verging fold plunging 40° SSE (Fig. 4- 21b). The upper part of the Salil Fm is unfolded as the fold is dies upward through this formation. The western limb of the fold is overturned and rest over an upright stratigraphic succession, without any recognizable separating faults in between. This is also supported by the lack of any fault penetrating across the unfolded overlying succession. However, the fold is truncated at the northern side by the major E-W fault, but this truncation may have taken place after the fold development. On the other hand it may have taken occurred during the fold development, in which the fault acted as a lateral wall constraining the lateral growth of the fold

The second fold [4] was mapped at the middle of the transect, folding the upper part of Mahil, Sahtan, Rayda and the lower part of the Salil Fm (Fig. 4- 21a). It plunges gently towards the SSE, verges towards the massif and it extends for a km along the eastern flank of the Nakhal anticline. Second order M folds were developed at the fold hinge, particularly within the thinly bedded limestone of the Sahtan Fm. The plunges of the second order folds are scattered between N and S directions (Fig. 4- 21a). Axial planar cleavage appears across the fold hinge, while bed-parallel stylolites are folded throughout the fold. The folding mechanism is still ambiguous due to the fact that there are no detectable faults beside or underneath the fold structure.

A NE-verging fold of metric scale has been recognized within the upper limestone of the SALIL Fm (Fig. 4- 22c). The fold axis is oriented SE-NW, while the axial plane dips gently SW, suggesting this fold was developed under NE-directed shearing with a top to NE sense of shearing.

A thrust structure [5] has been mapped at the mouth of the wadi, thrusting the Maastrichtian Aruma sediments onto the horizontal Mid-Cretaceous Salil sediments (Fig. 4- 23a). A footwall syncline with a gently inclined axial plane towards the SE was formed within the

Salil sediments. The thrust strikes NNE- and verges towards the massif, but the amount of the fault throw cannot be determined, as the stratigraphy is not well enough constrained due to intensive erosion associated with the Aruma-Wasia break. However, the gentle inclination of the footwall syncline axial plane suggests intensive thrust shearing. Axial planar cleavage is associated with the fold structure, with massif-verging cleavage at the horizontal limb and sub horizontal cleavage within the hinge area. Bedding-parallel cleavage, stylolites and veins are folded around the fold (Fig. 4- 23a).

Deformation fabrics

Deformation fabrics are expressed in term of shear zones, cleavage and folds. A shear zone of intensive localized shear deformation bounded by less deformed rocks is called detachment. The classic detachments with branching normal faults are poorly developed along this wadi, yet experienced intensive ductile deformation is present manifested by stretching lineations and folds structures. Detachments are common within the Rayda and Salil Fm's trending N-S and possessing NNE-plunging lineations (Fig. 4- 21a). Elongate carbonate aggregates oriented NNE-SSW appear along the detachment zones (Fig. 4- 21a and Fig. 4- 23b). Folds, particularly kink bands are well developed within the thinly bedded limestone units of both Rayda and Salil Fm (Fig. 4- 23c), with fold axes oriented SE-NW, orthogonal to the NNE stretching direction (Fig. 4- 21a). The most developed deformation fabrics is the spaced pressure solution cleavage, especially within the Salil Fm. Cleavage is variably oriented depending upon the cleaved rocks, but in general it is parallel to the massif with an average vergence towards the massif (Fig. 4- 23d), despite the SW vergence at some differently tilted beds (Fig. 4- 21a).

Small faults are commonly seen across the entire stratigraphic profile. They are of metric throw, and are classified into three different sets, NE-SW, NW-SE and E-W (Fig. 4- 21a). The majority of these faults are associated with the large scale faults.

Interpretation and summary

The area represents a major graben structure bounded by two km-long faults trending NW- and E-W respectively. The NW-oriented fault will be described and analyzed during the next transect analysis, where it is clearly exposed. The graben acted as a keystone and tilted differently due to the differential fault throw of the main bounding faults. This differential fault throw tilted the hanging-wall strata differently, giving them the present attitude. The truncation of the low angle NW-oriented fault by the steep E-W and NE-oriented faults reveals that the low angle faulting is older.

The mechanism of the SSE-plunging fold structures is still ambiguous. They verge to the massif reflecting approximate E-W shortening. The major thrust mapped at the mouth of the wadi exhibits the same trend and vergence as the fold structures. In this instance, both fold and thrust structures must be associated with the folding of the massif, under NW-SE shorting. The question now is what controls the special and stratigraphic locations of these folds? There are no clear faults along or below these folds, which may have induced them. However along the Qet transect, major massif-parallel folds have been recognized to be associated with inverted steep normal faults. Such correlation and interpretation will be investigated thoroughly at the end of this chapter.

Small scale ductile structures are classified under two main deformations with respect to the vergence direction. The NE-directed deformation is manifested by bedding-parallel detachments of NNE-SSW lineations, along with NE-verging folds and intensively developed kink bands. The massif-directed deformation is expressed by massif-verging cleavage, which acts as an axial planar cleavage for the massif-verging folds. Bedding-parallel stylolites, indicative of vertical flattening, are thrusted and folded by the massif-verging structures. Both main deformations are heterogeneously distributed as evidenced from their variable distribution and intensity. Zooming out the same classification can be used on the large scale structures. The km-long E-W and NW-striking faults along with the resulting graben structures reflect a NE-directed extensional deformation, while the major massif-verging folds and thrusts represent massif-verging contractional deformation.

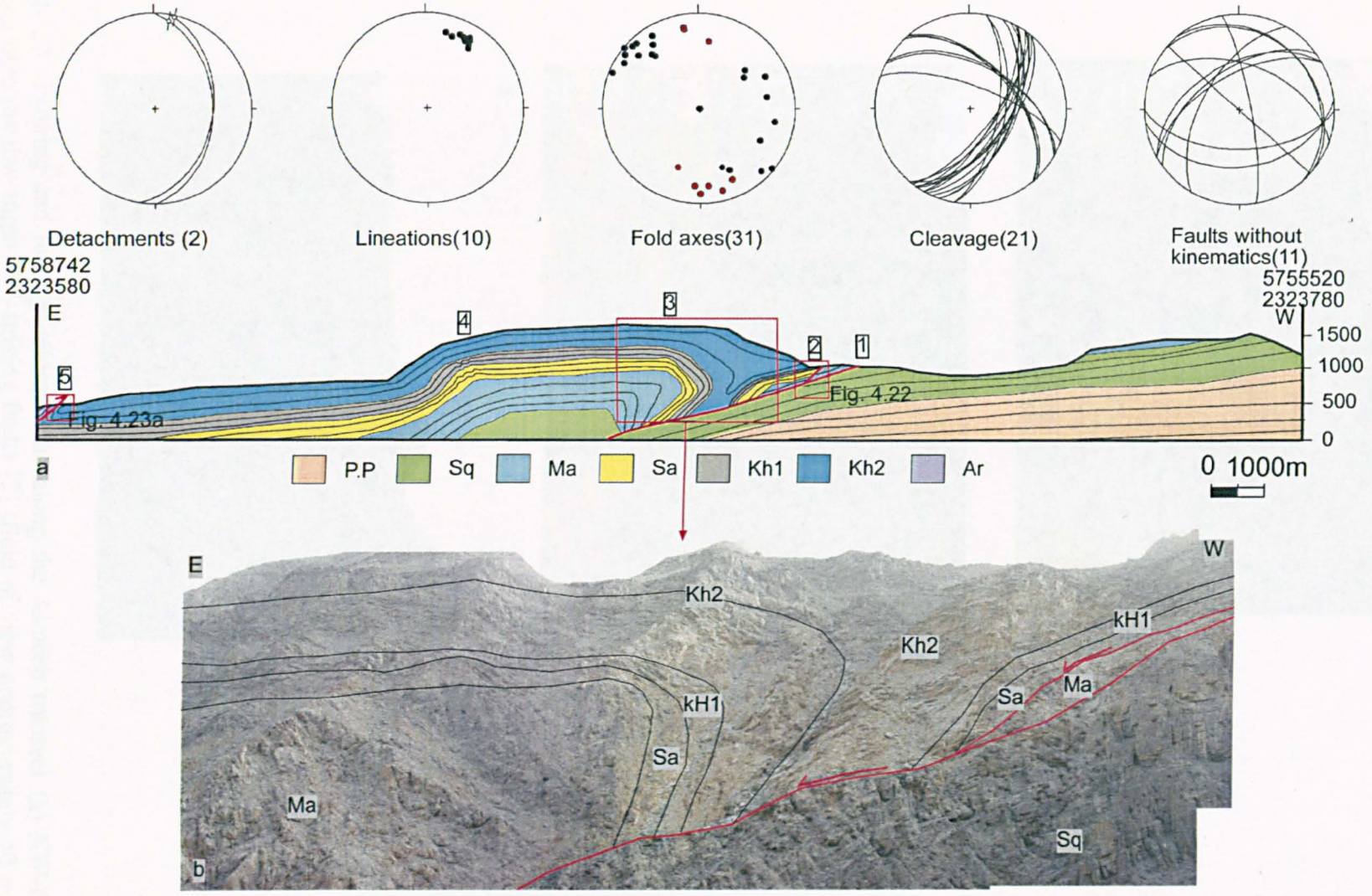

Fig. 4- 21 (a) Tayah transect with stereograms of the different structural elements collected along the transect. The red circles on the folds stereogram are for the hinge line [4]. (b) Massif-verging anticline with an inverted limb [3] (field of view approximately 1km).

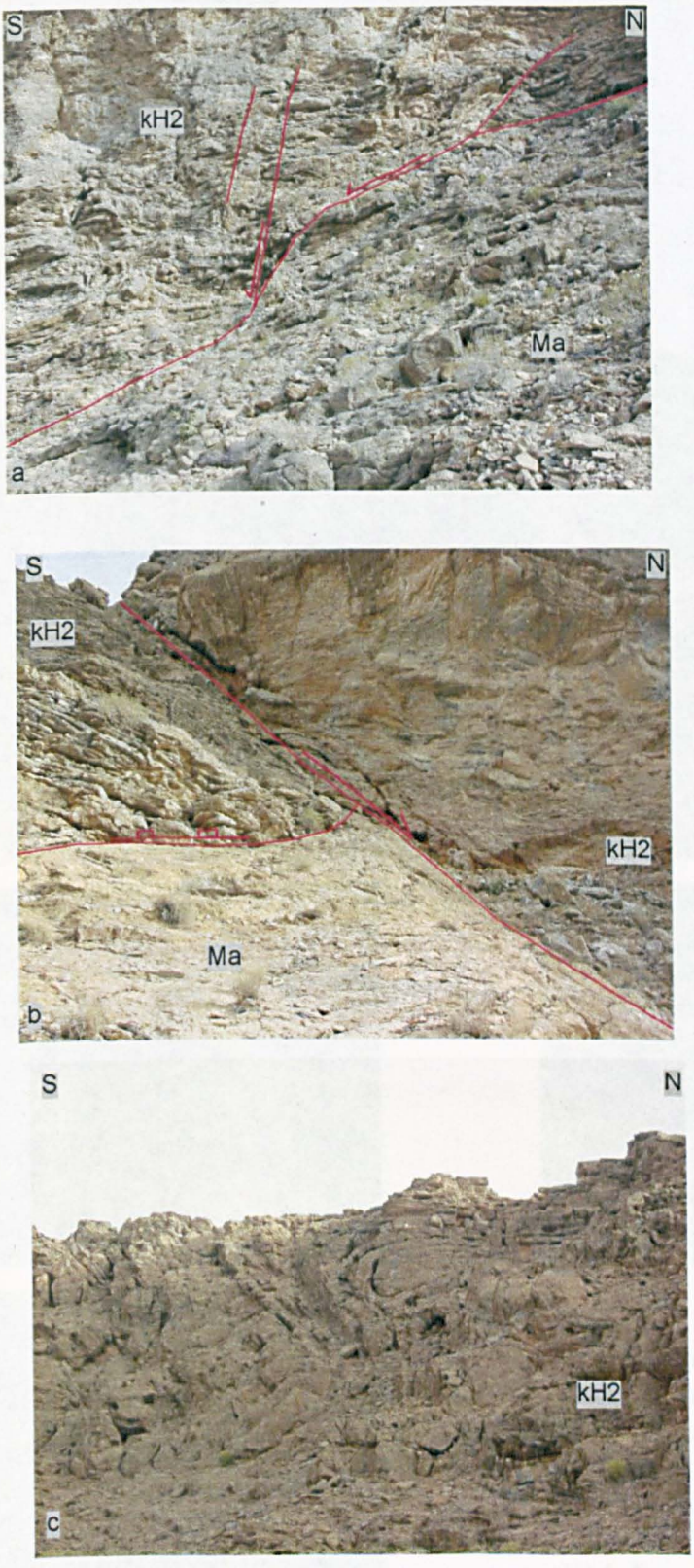

Fig. 4- 22 Faulting and folding deformations along the Almeeh transect (a) NW-Faults merging onto the low-angle NW-striking faults [2] (field of view approximately 40 m). (b) The major NW-fault [2] shown here is transect by a NE-striking fault (field of view approximately 10 m). (c) NE-verging folds within the Kh2 sediments (field of view approximately 100m).

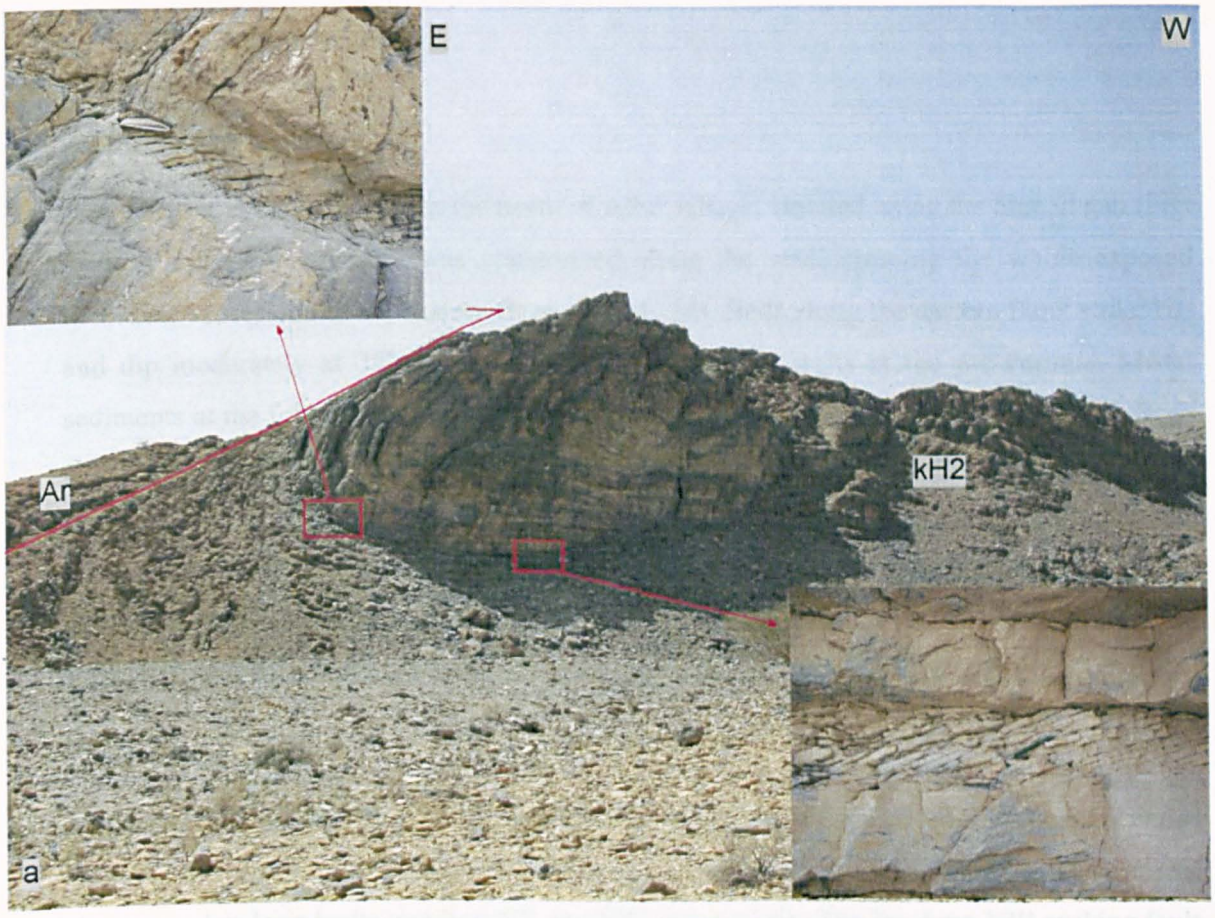

Fig. 4- 23 Deformation fabrics along the Tayah transect (a) A massif-verging thrust [5], the inset shows axial planar cleavage along the limb and hinge area as shown above, (field of view approximately 300 m). (b) NE-SW trending lineations at Kh1 Fm. (c) NW-SE trending kink bands within the Kh2 Fm (field of view approximately 1m). (d) Massif-verging cleavage within the Kh2 Fm.

4.10 AL-bir transect

Wadi AL-bir is the first wadi to the north of Albir village, situated along the Semail gap (Fig. 4-1). A 5-km-long transect was constructed along the wadi crossing the whole exposed Mesozoic succession of the eastern flank (Fig. 4- 24). Beds along the eastern flank strike NE and dip moderately at 35° SE. The ESE-WNW transect starts at the pre-Permian Mistal sediments at the fold crest and runs until the Late-Cretaceous Aruma rocks in the ESE. Beds are sub-horizontal at the fold crest where after dip increases rapidly to 35° SE across the fold limb. A local angular unconformity was identified between the Triassic dolomite and the Sahtan Fm. This unconformity is underlain by steep beds of the Mahil dolomites dipping westward, while the overlying Sahtan beds dip eastward parallel to the regional dip. The Jurassic-Cretaceous strata are locally deflected by adjacent km-long NW-SE striking faults.

Large sale structures

The transect is marked by NW-SE and NE-SW steeply dipping fault sets cutting the entire stratigraphic profile (Fig. 4- 24). Fault throw varies from a few metres to 400 m. The transect shows two km-long faults trending NE and NW respectively. The km-long NW-striking fault [1] with a steep dip of 60° NE has been mapped running for several km across the eastern flank (Fig. 4- 24and Fig. 4- 25a). The prominent Mahil dolomites occupy the footwall, while the less competent Jurassic- Cretaceous succession has been displaced down for 400 m within the hanging-wall. The hanging-wall strata are disrupted by synthetic and antithetic subsidiary faults and form full and half graben structures. Part of the fault displacement has been taken up laterally through the Jurassic-Cretaceous units and therefore the amount of shear deformation increases towards the fault plane. Kinematicaly, the steeply dipping NW-striking faults show both dip slip and massif-pitching lineations (Fig. 4- 24). When untilted by the local flank dip of the culmination, the massif-pitching lineations turned into dip slip, which means the corresponding faults took place before or during the early stage of the folding deformation. The dip slip lineations must post date the folding deformation as they are not subjected to any fold-related rotation.

A local angular unconformity has been recognized along the contact between the Mahil dolomites and the overlaying Sahtan clastics (Fig. 4- 25b). In the unconformity, the Mahil beds dip steeply westward, while the overlaying Jurassic- Cretaceous units dip gently eastward in parallel with the dip of the regional flank. This means tilting of the Mahil dolomites must have occurred before the deposition of the Jurassic- Cretaceous sequences. After this everything were tilted eastward due to the massif folding. The westward-dipping Mahil beds are truncated from below by a normal fault that detaches them from the rest of

the massive Mahil dolomite, which dip consistently eastward. Consequently, this local tilting of the Mahil dolomite must be related to a pre-Jurassic faulting deformation.

The second largest fault shown on the transect as a steeply dipping NE fault [2], with a vertical fault displacements of 400 m. It forms a half graben structure occupied by the Sahtan and Rayda sediments (Fig. 4- 26 a) and b), and has been interpreted as a thrust-related klippe structure by BRGM (Rabu et al. 1986). The Jurassic-Cretaceous rocks in the half graben structures are also affected by a series of NW-trending faults, which in turn are truncated by the main NE-striking fault. The fault throws along the NW-oriented faults range from a few metres to tens of metres. The hanging-wall strata also exhibit sub-horizontal to gently dipping faults, with metric displacements and a normal sense of shearing (Fig. 4- 26 a). The hanging-wall cut off angles along the sub-horizontal faults are around 60°- 70°, indicating that faults were once steeply dipping rather than sub-horizontal as currently seen. Restoring the tilting deformation turned the sub-horizontal faults into steeply dipping, NW-striking faults, hence such faulting must pre-date the regional tilting deformation. Furthermore, there are also numerous small scaled faults distributed along the transect with NW-and-NE-orientation (Fig. 4- 24), with vertical displacements ranging from a few cm to tens of metres.

Deformation fabrics

Deformation fabrics are developed within the Jurassic-Cretaceous succession, particularly within finer-grained sediments. Intensive layer parallel cleavage with layer parallel veins is concentrated along highly strained narrow shear zones, surrounded by less deformed wall rocks on both side. They can be described as detachments zones. Bedding-parallel detachments appear in micritic units of the Jurassic and Cretaceous succession, striking NW-SE and NE-SW depending on the bedding attitude (Fig. 4- 24). Associated calcite fibre lineations pitch NE and SW, while fibre stepping reveals top to NE shearing. NW-striking faults with sub-metric throw merge and branch onto the detachments. Folds, with close interlimb angles and detachment-sub-perpendicular axial surfaces are common within the incompetent units of the Jurassic- Cretaceous strata. Fold hinges are variably oriented but define a cluster plunging SSE with minor folds lying parallel to the stretching direction (Fig. 4- 24). Where the SE-plunging folds are asymmetrical they verge towards the NE. Different forms of cleavage have been seen along the transect. Foliations are developed along the bedding-parallel detachments. Spaced pressure solution cleavage strikes NW-SE with NE and SW vergence (Fig. 4- 24). Anastomosing layer-parallel stylolitic cleavage is common along the carbonate units of the Salil and Shams Fm's.

Interpretation and summary

The transect is marked by two fault sets oriented NW- and NE. The relative timing of the faulting and folding deformation is addressed below. The local angular unconformity between the Mahil and Sahtan Fm took place before Jurassic time, along a N-S fault. The NE-oriented fault set is consistently cross-cut by the different forms of the NW-oriented faults indicating they are the youngest. The sub-horizontal NW-striking faults have been interpreted as pre-folding faults, while the steeply dipping NW-striking faults were initiated before or during the early stage of the folding onset, then were reactivated as dip slip faults after the folding process. This shows there were several events of NW-oriented faulting, which took place before, during and after the folding deformation. Such fracturing events could be continuous or intermittent with respect to the onset of the folding on the other hand the NE-oriented faults show dip slip striations, indicative of post-folding faults (Fig. 4- 24). In general the NW-striking faulting has been attributed to the NE-directed deformation, while the mechanism of the NE-striking faults will be analyzed with respect to other transects at the end of this chapter.

The deformation fabrics is strongly developed along the fine-grained sediments of the of the Jurassic- Cretaceous rocks, while the more competent units were deformed in a brittle manner forming NW-striking normal faults. Various indicators for the sense of shearing, such as fibre stepping, verging folds and cleavage indicate a top to NE simple shear. The intensity of the shear deformation increases towards the km-long faults, suggesting that part of the fault displacement was accommodated laterally through ductile shear deformation within the hanging-wall units. Massif-verging deformation is shown only by the SW-verging cleavage.

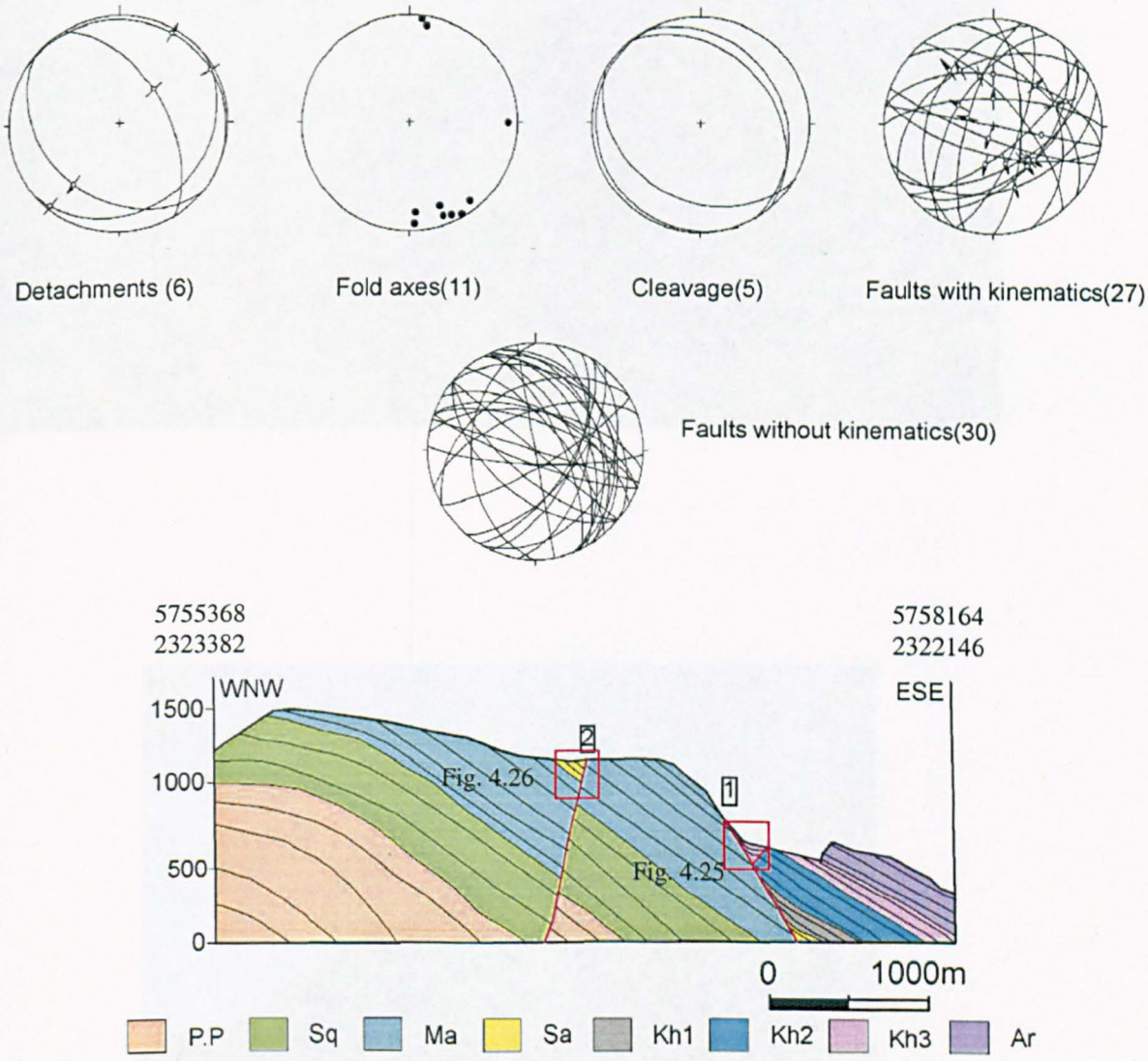

Fig. 4- 24 The Albir transect with stereograms of the different structural elements collected along the transect. The red circles on the faults stereogram are for the massif-pitching lineations along the NW-striking faults.

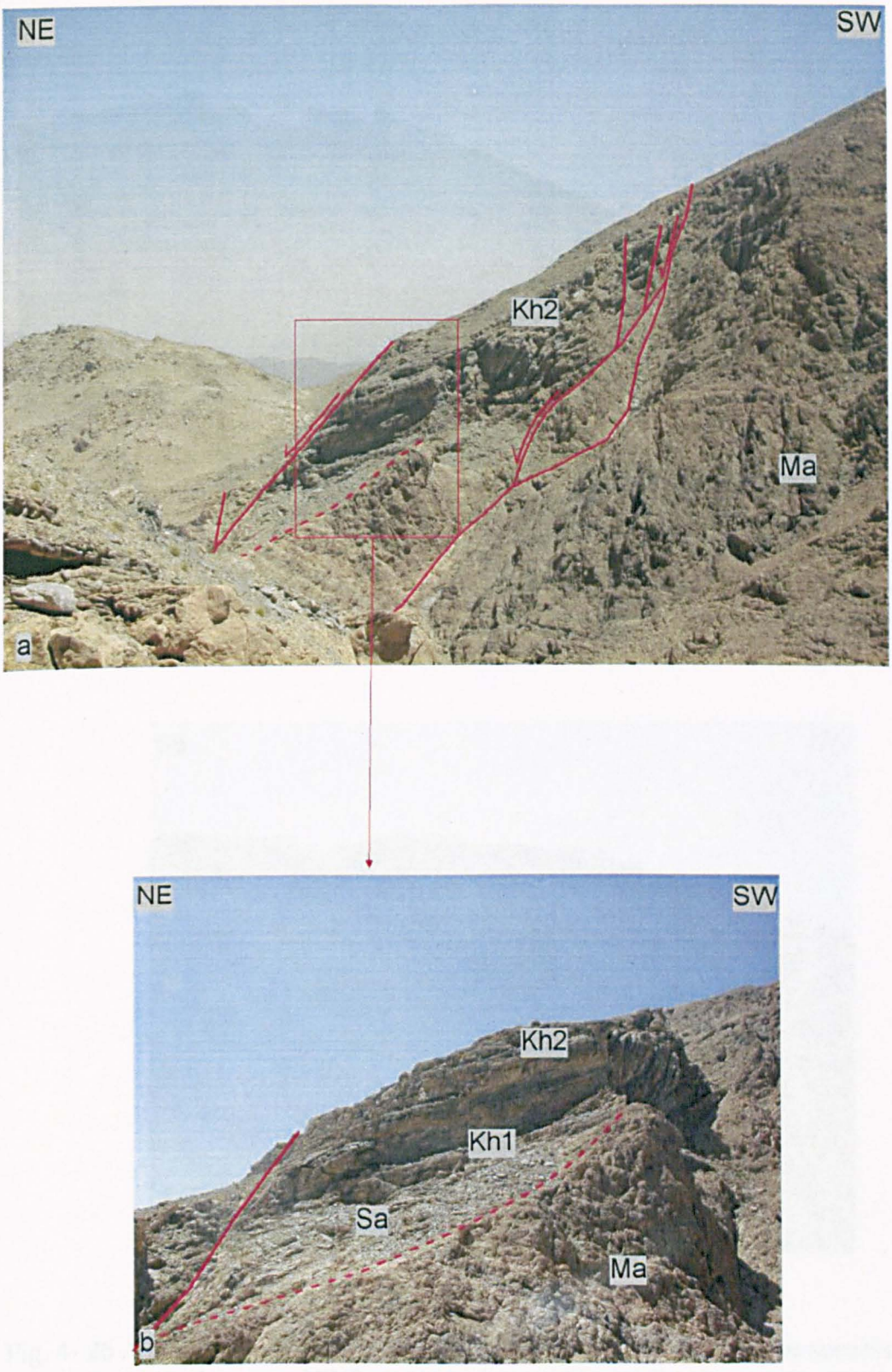

Fig. 4- 25 Faulting deformation along the Albir transect (a) The major NW-trending fault [1] on the Albir transect (field of view approximately 1 km). (b) A close up view of the Jurassic fault-related unconformity, in which tilted Ma beds are overlain by a gently dipping Jurassic-Cretaceous succession (field of view approximately 200 m). In both images the red dashed line is for the Jurassic faults-related unconformity

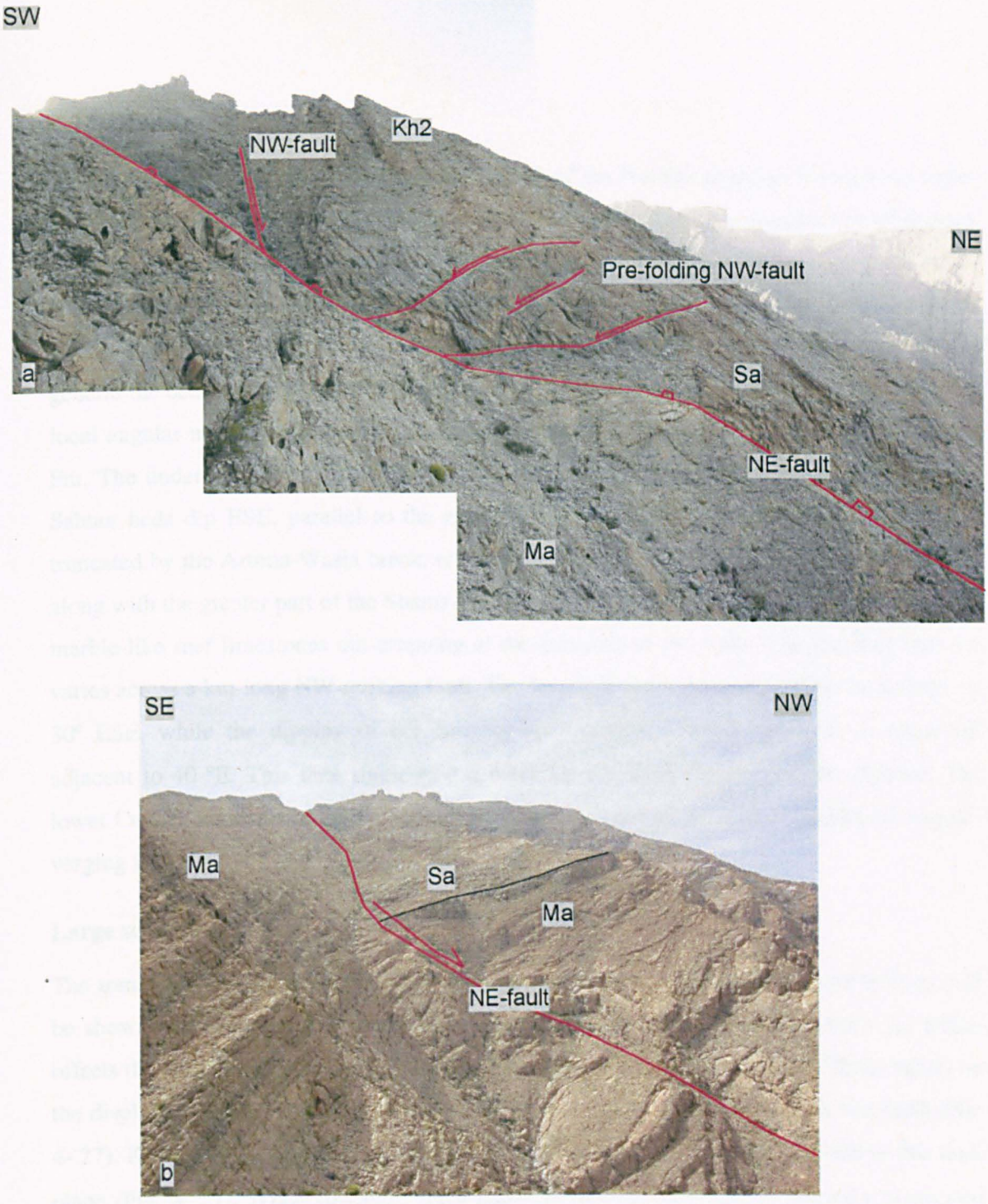

Fig. 4- 26 A half graben structure occupied with the Jurassic-Cretaceous succession and its association with the major NE-fault [2] is shown at (a), notice the gently dipping pre-folding faults and the steeply dipping NW-faults across the half graben (field of view approximately 500 m). (b) A northern view of the structure illustrating the NE-half graben structure (field of view approximately 1km).

4.11 Dhabiah Transect

Wadi Dhabiah is situated across the Eastern flank of the Nakhal anticline, between the cities of Semail and Bidbid (Fig. 4-1). A 400 m detailed transect has been constructed along wadi Dhabiah which represents a type locality of structural deformation in the eastern flank of the Nakhal anticline. The WNW-ESE transect extends from the Triassic Mahil dolomite in the west to the Maastrichtian Aruma deposits, at the eastern entrance of the wadi (Fig. 4- 27). In general the beds on the eastern flank strike NE-SW and dip variably between 20°-40° ESE. A local angular unconformity can be identified between the Triassic dolomite and the Sahtan Fm. The underlying beds of the Mahil dolomite dip steeply westward, while the overlying Sahtan beds dip ESE, parallel to the regional dip. The carbonate platform sequences are truncated by the Aruma-Wasia break, resulting in the erosion of the whole of the Wasia Gp along with the greater part of the Shams Fm. The Late-Cretaceous Aruma Gp is composed of marble-like reef limestones out-cropping at the entrance to the wadi. The regional bed dip varies across a km-long NW-striking fault. The footwall strata dip consistently on average of 30° ESE, while the dipping of the hanging-wall Jurassic-Cretaceous strata is steepened adjacent to 40 °E. This then shallows out reaching 20° E by the start of the transect. The lower Cretaceous strata of the Rayda and Salil Fm's are folded by a 10-m-amplitude, massif-verging fold.

Large scale structures

The transect is dominated with different sets of faults striking NW-, NE- and E-W as will be shown subsequently. The transect is marked by a km-long NW-striking fault [1] which offsets the entire stratigraphic section (Triassic- Lower Cretaceous) for about 20 m, based on the displaced angular unconformity between the Mahil and Sahtan Fm across the fault (Fig. 4- 27). Kinematicaly, dip slip and NW-pitching striations have been recorded along this fault plane (Fig. 4- 27). When structures were restored, by rotating them 30° around a horizontal axis trending 040 chosen to be parallel to the fold axis, the massif-pitching lineations turned into dip slip, suggesting that the fault must have been initiated before or during the early stage of the folding onset. The purely dip slip lineations correspond to a post-folding movement as they are not affected y the folding deformation.

Across the NW-striking fault, the contact between the Mahil dolomites and the overlaying Sahtan clastics is marked by an angular unconformity [2] (Fig. 4- 27), while elsewhere the contact is normal. At the angular unconformity the Mahil beds dip steeply westward, while the overlaying Jurassic- Cretaceous units dip gently eastward similar to the regional dip of the eastern flank. For this reason tilting of the Mahil dolomite must have occurred before the

deposition of the Jurassic- Cretaceous sequences. Subsequently everything was tilted eastward during the folding deformation. The westward-dipping Mahil block is truncated from below by a normal fault separating them from the rest of the Mahil dolomites, which dip eastward. Accordingly, the local westward tilting of the Mahil dolomite must be related to a pre-Jurassic faulting deformation.

An E-W-trending fault [3] was recorded within the Jurassic-Cretaceous succession (Fig. 4-27), with a throw of approximately 50 m, a dips of 70° S, and a series of synthetic faults along either side. Faults striations indicate dip slip and strike slip displacements (Fig. 4- 27) most likely having taken place after or during the late stage of the folding process, as they are not rotated under the folding deformation. Furthermore the identified lineations indicate pure dip slip and strike slip displacements (Fig. 4- 27).

Another km-long structure was mapped at the entrance to the wadi, where Aruma sediments juxtapose with the massive Shams limestone. This occurs along a steep, NNE-striking fault with down-throw of at least 50 m, away from the massif (Fig. 4- 28a). The Aruma reef limestone in the hanging-wall is truncated by a series of steeply dipping synthetic faults. This fault bounds the eastern flank of the Nakhal anticline, and can be traced south for several km's. Kinematicaly, the fault shows dip- and strike-slip striations.

A massif-verging fold [4] has been mapped within the Rayda& Salil beds, with an amplitude of 10 m (Fig. 4- 27). The fold axial plane strikes N-S and dips 80° E, while its hinge plunges 12° S.

The competent limestone succession of the Salil Fm are faulted by a series of subsidiary faults (horses) forming extensional duplex structures [5] and are bounded on either side by bedding-parallel detachments (Fig. 4- 27 and Fig. 4- 29). These detachments run along the less competent micritic limestone units, which are inter-bedded with the massive limestone units. These subsidiary faults strike NNE with steep dip of 60° ESE, while the bounding detachments strike approximately NNE with gentle dip of 25° ESE, in parallel with the regional dip. The horse throws range from 1-5 m. A hanging wall ramp is developed along the basal detachment as seen in Fig. 4- 29c. In places, there are larger faults branching off the basal detachment and breaching through the entire overlaying sections, along with the roof detachment itself. Mineral lineations on the detachment surfaces plunge gently NE and SE (Fig. 4- 29a). The SE-plunging lineations cross-cut the NE-plunging ones, indicative of a younger shearing towards SE. Regarding the horse faults, fibre lineations cluster into two plunging populations (Fig. 4- 29a) a SE plunge reflecting a dip slip displacement and an oblique NE plunge. When structures were restored by rotating them 30° around a horizontal

axis trending 040 chosen to be parallel to the fold axis, the oblique lineations turned into nearly dip slip with down-throw towards NE (Fig. 4- 29b). Subsequently the azimuth of the corresponding horse faults was transposed from NNE-NE into NNW-NNE. Therefore the horse faults were initiated as bedding-confined dip slip faults during a NE-directed extension, which most probably took place before or during the early stage of the folding onset. Subsequently, some faults were reactivated as dip slip towards SE, which explains why occasional larger faults breach through the roof detachments as they are not part of the bedding-confined duplex structures. The detachment kinematic data is in agreement with such an interpretation of multi-movements. Timing of such a reactivation is not certain yet, but more likely to be after or during the later stage of the folding process, since they are not rotated by the folding deformation.

Sub-horizontal faults were mapped truncating and displacing the steeply dipping strata of the Sahtan Fm at high angles of 60° (Fig. 4- 28b). Such faults have been only recognized within the Sahtan Fm suggesting that they are detached along the same stratigraphic unit. The apparent fault horizontal displacements range between 1-15 m with a top to the south sense of movement. The truncated beds are deflected adjacent to the fault planes, forming drag folds revealing a top to south shear. The faults truncate calcite-filled bedding-parallel detachments, possessing fibre lineations plunging NE. When the steeply-dipping beds were untilted, around a horizontal axis trending 160, the sub-horizontal faults were transposed into NW-striking normal faults dipping steeply to the south (Fig. 4- 28b). This matches with the top-to-the-south sense of shearing deduced from the drag folds and the displaced bedding. Consequently, the sub-horizontal faults took place within flat strata, presumably before or during the early stage of the folding event. At once point they formed half graben structures, implying a NE-directed extension. This can be suggested from the fault orientations (NW-SE) and the relative timing of the faulting event, as it took place after the formation of some bedding-parallel detachments, but before the folding process.

This section interprets, summarize and interrelate the large scale structures with the folding deformation. The area experienced several faulting events spanning across the geological time scale. The oldest recognizable deformation event took place during the Late Triassic, when N-S faults formed half graben structures. Such faults and associated tilting resulted in a local angular unconformity between the Triassic dolomite and the Jurassic Sahtan Fm. After that, faulting was resumed again, before or during the early stage of the folding onset, through bedding confined faults within the Jurassic-Cretaceous strata. This is manifested by a linked system of steep faults and detachments reflecting a NE-directed extension. The NE-extensional duplexes bounded by bedding-parallel detachments and marked with NE-

plunging lineations exemplify this deformation. Furthermore, the NW-trending sub-horizontal faults mapped within the Sahtan Fm represent the same deformation. These extensional structures within the Jurassic-Cretaceous succession were folded and rotated by the folding deformation. Evidence for this comes from the rotation of the fault striations and the fault planes as previously discussed.

Furthermore, the transect is characterized with steep NW-SE and E-W striking faults penetrating the whole exposed stratigraphic succession, and are hence detached within the pre-Permian sequences. The fault orientations and associated kinematic data indicate a NE-directed extensional shearing, while kinematic data along the NW-striking faults indicate mulitiple movements. The massif-pitching lineations correspond to dip slip fault movements that took place before or during the early stage of the folding process (Fig. 4- 27), while the associated dip slip lineations reflect fault reactivation during or after the latest stage of the folding deformation. The E-W faults show dip-and-strike-slip striations indicative of post folding fault movements; however this does not exclude the possibility of pre-folding fault activity as seen with the NW-striking faults. So initiations of these faults as dip slip faults by the NE-directed extension occurred before or during the early stage of the folding process, and then were reactivated after or during late stage of the folding deformation.

In contrast, the NNE-striking faults with down-throw to the SE express an extension directed away from the massif. This extension reactivated bedding-parallel detachments and extensional duplexes structures [5] first initiated by the NE-directed extension. The breaching of the extensional duplex structures [5] observed within the Salil Fm occurred due to this young extensional deformation and the major NNE-striking fault bounding the eastern flank of the Nakhal anticline is also part of the same deformation.

Deformation fabrics

Deformation fabrics such as cleavage and folds are well expressed along the Jurassic-Cretaceous succession, especially within finer-grained units. Intensive layer parallel cleavage with layer parallel veins is concentrated along narrow shear zones. Such highly strained narrow zones are surrounded by less deformed wall rocks along either side and therefore behave as detachments zones. Detachments range in strike around the N-S axis depending on the bedding attitude, and dip gently eastward parallel to the regional dip of the eastern flank (Fig. 4- 27). Calcite fibre lineations on the detachments pitch NE alongside minor lineations oriented NNW-SSE. Other stretching lineations, such as elongate carbonate aggregates plunge gently towards the NE quadrant (Fig. 4- 27). Bed-confined NW-striking faults with sub-metric throw merge and branch onto the detachments. The detachments contain

centimeter-scale buckles of foliation with generally gentle-close interlimb angles and axial surfaces sub-perpendicular to the detachment surfaces. The hinges of these folds are variably oriented, ranging from 010° to 220°, but the majority plunge SSE. Geometrically, folds can be classified into two groups. In the first group, folds plunge moderately SE with open to tight interlimb angles (Fig. 4- 27) and steeply dipping axial planes which verge NE. These folds are associated with detachments showing top-NE directed shearing. Kink bands of the same trend (NW-SE) concentrate within thinly competent limestone beds of Jurassic-Cretaceous strata. In the second group, fold axes are oriented sub-parallel to the massif (NE-SW) and pitch gently NE and SW (Fig. 4- 27). However, where beds strike NNW-SSE, folds pitch gently SSE. Folds show open-close interlimb angles and are either upright or steeply tilted towards the massif. They possess axial plane cleavage verging towards the massif and are associated with detachments containing NW-SE lineations. In places they fold the NE-directed detachments.

Deformation fabrics are expressed by different forms and orientations of cleavage, which record the progressive deformations of the study area. These vary from spaced pressure solution to foliations, which are common in the bedding-sub parallel detachments (Fig. 4-27). Foliations are also commonly associated with stretching lineations plunging NE, and in places are folded by NE-verging folds. Spaced pressure-solution cleavage strikes around the N-S axis, with moderate to steep dip away from the massif, but with vergence towards the massif. Most cleavage intersects the bedding at high angles of 60° to 90°, while some cleavage has shallow intersection angles of 10° to 20°. When cleavage structure was rotated around the 040\30 axis chosen to be parallel to the fold axis, cleavage with shallow bedding-cleavage intersection angles changed into NE-verging cleavage. As the same time, cleavage of high bedding-cleavage intersection angles continues to verge towards the massif. Such NE-verging cleavage arises in an area bounded by bedding-parallel detachments, to which cleavage dip and merges. The NE-verging cleavage is sporadically seen, while the whole area is dominated with the massif-verging cleavage, which is characterized by high bedding-cleavage intersection angles, reaching 90° in places. This means that the massif-verging cleavage was once perpendicular to bedding, and then gradually rotated towards the massif by the progressive deformation.

Penetrative deformation type locality

Most of these penetrative structures can be seen clearly at one outcrop within the shaly limestone of the Salil Fm. Such structures comprise of folded layer-parallel detachments, bedding-orthogonal stylolites and several phases of cleavage including extensional crenulation cleavage. This locality therefore represents a type locality for penetrative

deformation. Each of these structures are described in detail. Layer-parallel detachments of NE-directed extension are well established, with several sheets of calcite mineralization reflecting successive shearing events. The detachments are oriented around the N-S axis (Fig. 4- 30), and are folded and deflected by steeply dipping extensional crenulation cleavage, discussed shortly (Fig. 4- 30 and Fig. 4- 31a). The fold axes plunge gently SSE, while axial planes are vertical to steeply dipping, and verge towards the massif (Fig. 4- 30). Folding of these detachments implies a NW-SE shortening.

Three phases of cleavage have been mapped at this locality. Bedding-orthogonal stylolites appear within micritic limestone beds, and are attributed to NW-SE shortening. In places, these stylolites have been deflected and displaced towards the massif, adjacent to bedding-parallel detachments. This displacement can be used to suggest that some NE-directed bedding-parallel detachments have been reactivated during the folding process, with a top to the massif sense of shear. The second phase of cleavage trends parallel to the massif hinges, and dips moderately with a vergence towards the massif (Fig. 4- 30). The third phase of cleavage also strikes parallel to the massif hinges, however dips more steeply than the previous phase, making high intersection angles with the bedding (Fig. 4- 30). The latter phase of cleavage intersects the former cleavage phase (the orthogonal stylolites and the moderately dipping, massif-verging cleavage). Bedding-parallel detachments have been deflected in a normal sense adjacent to this steeply dipping cleavage, and hence can be described as extensional crenulation cleavage (Fig. 4- 31b) (Gray and Durney 1979). The extensional crenulation cleavage represents the latest phase of cleaving by truncating the penetrative structures.

The variety and complexity of the penetrative deformation marks a continuous accommodation of the progressive NW-SE shortening. Such strain was initially accommodated through the development of bedding-orthogonal stylolites, whose orthogonality suggests that the applied stress was layer parallel rather than layer-inclined. As a result, the stylolitic structures must have been formed during the early stage of the folding process, while beds were still sub-horizontal. As the shortening proceeded, strain was accommodated through layer-parallel shearing along what was once the NE-directed detachment. Such shearing can be suggested due to the deflection of the bedding-perpendicular stylolites towards the massif along these detachments. The NNW-SSE fibre lineations along the detachments reflect bedding-parallel shearing with a top-massif sense of shearing. Meanwhile, buckling of NE-directed detachments and the formation of moderately dipping, massif-verging cleavage was occurring. The NE-directed detachments were folded uprightly, and subsequently tilted towards the massif as the shortening proceeded.

Eventually, extensional crenulation cleavage was developed to accommodate further, progressive shortening. In all cases the extensional crenulation cleavage is inclined to bedding because it was formed due to layer-inclined stress. Such conditions are more likely to occur when beds are tilted under the folding process (Davis et al. 1996).

The different deformation fabrics can be classified under two main deformational systems. The first system is marked with NE-directed extension, manifested by NE-verging folds and cleavage, bedding-parallel detachments and the associated foliations. The top to NE sense of shearing for this deformation is reflected by the NE-verging folds and cleavage structures. Such deformation marks the oldest non penetrative deformation exposed along the transect. The NE-directed, non penetrative deformation is well expressed along the shaley units of the Jurassic-Cretaceous succession.

The second system is marked by a variety of massif-verging structures, comprising bedding-parallel slipping surfaces, folds and different phases of cleavage structures. Kinematic sense indicators such as asymmetrical folds and verging cleavage indicate top-massif shearing, resulting from the NW-SE shortening. Such progressive shortening was accommodated through the development of various phases of cleavage. The orthogonal stylolites were formed firstly by layer parallel shortening. Further shortening gave rise to tilting and folding of the Nakhal massif, making the strain inclined to bedding. Subsequently, the massif-verging cleavage and fold structures were created by bedding-inclined shortening. This created folds that trend parallel to the massif with open interlimb angles, entirely different to the NE-verging tight folds, which were formed by the NE-directed extensional regime. As the compression proceeded, the area was subjected to further intensive pressure, solution forming extensional crenulation cleavage which truncates all the earlier structural fabrics.

Interpretation and summary

Based on the presented data and the provided analysis, deformation along the Dhabiah transect is analyzed and summarized below. There are two distinct systems of deformation along the wadi, the NE-directed extension and the NW-SE compression. The NE-directed extension is manifested by a linked system of steep faults and detachments. Steep faults are arranged into two sets trending NW-SE and E-W and each fault merges into sub-horizontal detachments situated within the less competent units of the Jurassic-Cretaceous succession and pre-Permian sequences. Which detachment for which fault is dependent on the fault throw, since major faults are detached along deeper detachments positioned within the pre-Permian rocks, while smaller bedding-confined faults are detached within the same stratigraphic unit.

The NE-extensional deformation seen within the Jurassic-Cretaceous succession predates the NW-SE shortening, because the former was superimposed by the shortening deformation. Evidence for that is listed in several points as follows: folding of the NE-directed detachments; switching of the bedding-parallel shearing along some detachments from top-NE into top- massif; tilting of the bedding-confined NW-striking faults by the folding of the massif; and overprinting of the NE-extensional fabrics by massif-verging structures. These observations give an explanation for the minor local distribution of the NE-verging cleavage, when it should be strongly present in response to the significant NE- extension, as seen every where along the Akhdar anticline. Subsequently the NE-verging cleavage was overprinted and replaced by the dominant massif-verging fabrics.

The interrelation between the NE-extensional deformation within the pre-Permian sequences and the NW-SE shortening is assessed below. The major NW-SE and E-W faults were initiated as dip slip normal faults before or during the early stage of the folding event as evidenced from the massif-pitching fault striations. They were subsequently reactivated as dip slip normal faults after or during the latest stage of the folding deformation. The identified strike slip component along the E-W faults is more likely to be due to the NW-SE shortening. These multi fault displacements span throughout the folding process, which may suggest that both folding and faulting deformations were contemporaneous.

The NW-SE shortening has the major role of deforming and building the whole massif. Its effect is expressed by the massif-verging folds and cleavage structures, together with the massif itself. The major massif-verging fold [4] within the Rayda& Salil beds is interpreted to be due to this shortening deformation. Furthermore, the folding of the extensional detachments within the Jurassic-Cretaceous succession can be seen as a small scale analogue for the folding of the Nakhal massif. The strike slip component along the major E-W faults is considered to be related to the same shortening strain.

The latest deformational event is a NW-SE extension, directed away from the massif, manifested chiefly by a major NNE- oriented fault bounding the eastern flank of the Nakhal anticline. Localization of such faults along the culmination margin may suggest that it took place after the folding process, due to NW-SE shortening. However, the coexistence of dip and strike slip striations along the fault complicate the kinematics, as they suggest simple away from the massif extensional shearing.

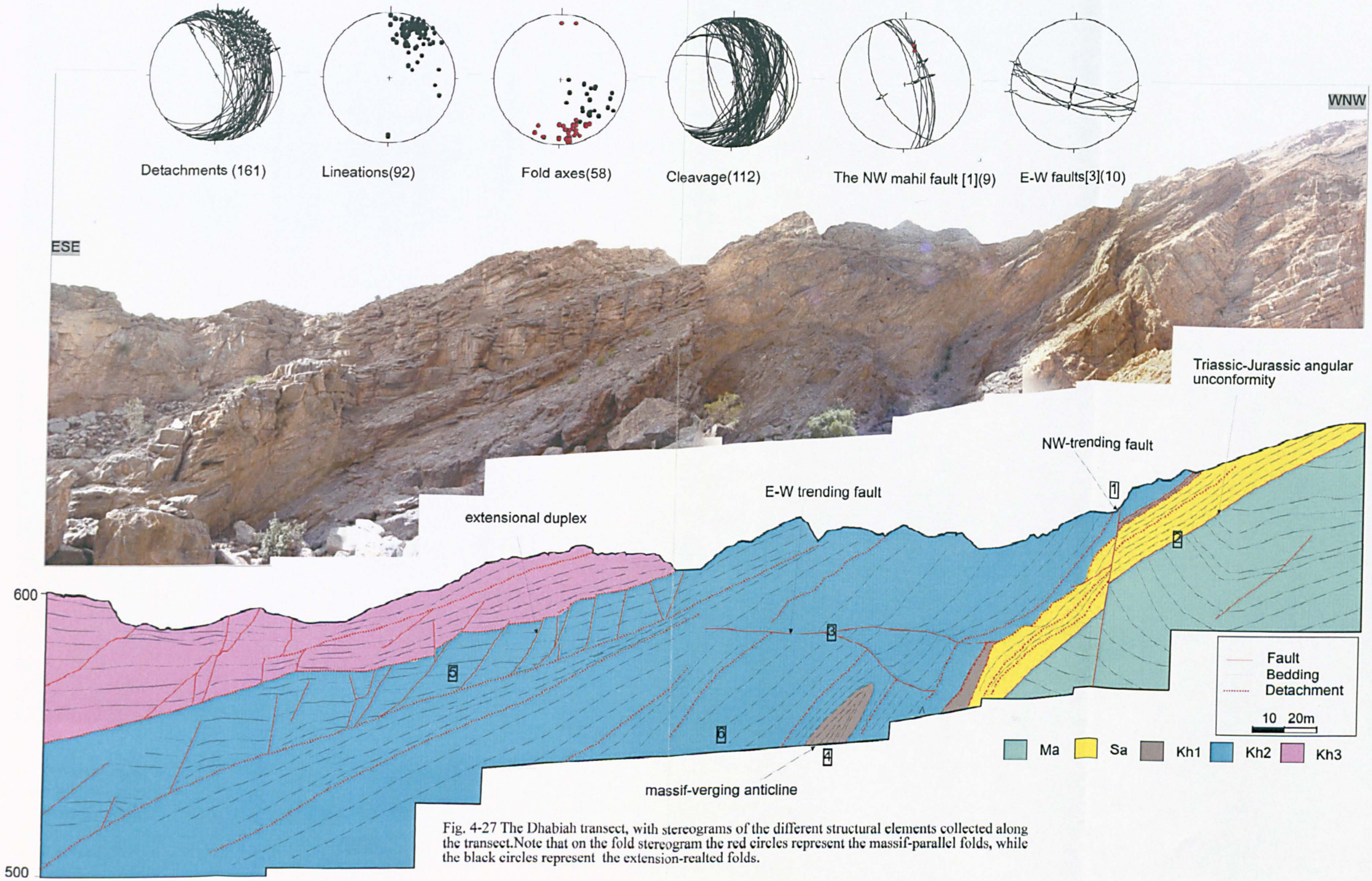

Fig. 4-27 The Dhabiah transect, with stereograms of the different structural elements collected along the transect.Note that on the fold stereogram the red circles represent the massif-parallel folds, while the black circles represent the extension-realted folds.

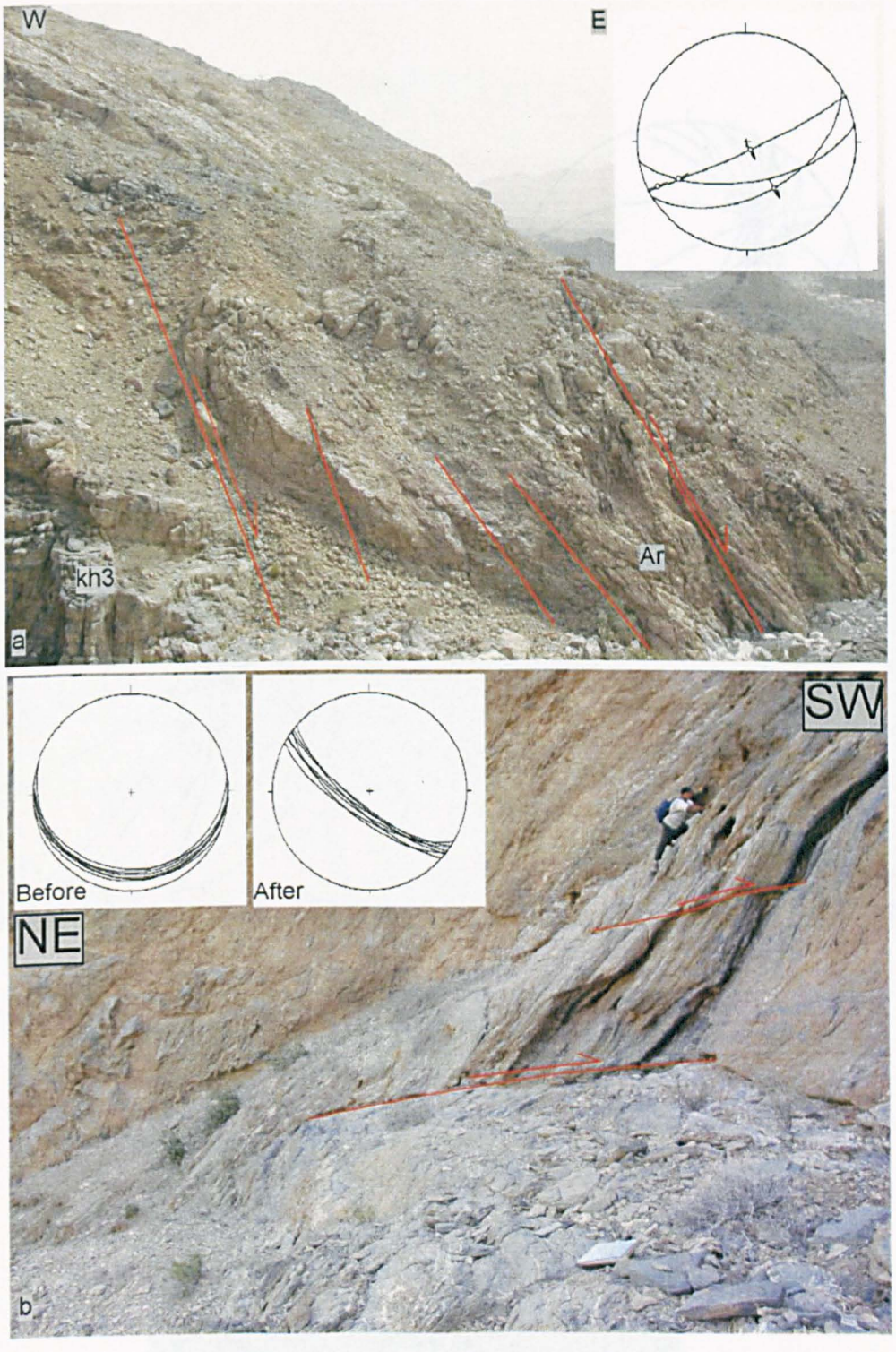

Fig. 4- 28 Different phases of faulting along the Dhabiah transect (a) The NE-faults separating the Kh3 Fm and the Ar reef limestone (field of view approximately 100 m), The stereogram shows the fault lineations, dip and strike slip displacements. (b) The pre-folding faults in the Sa Fm (field of view approximately 20 m). The stereograms show the faults before and after restoration of the folding deformation, notice that after restoration faults become NW- oriented (faults were rotated 70° around a horizontal axis trending 160).

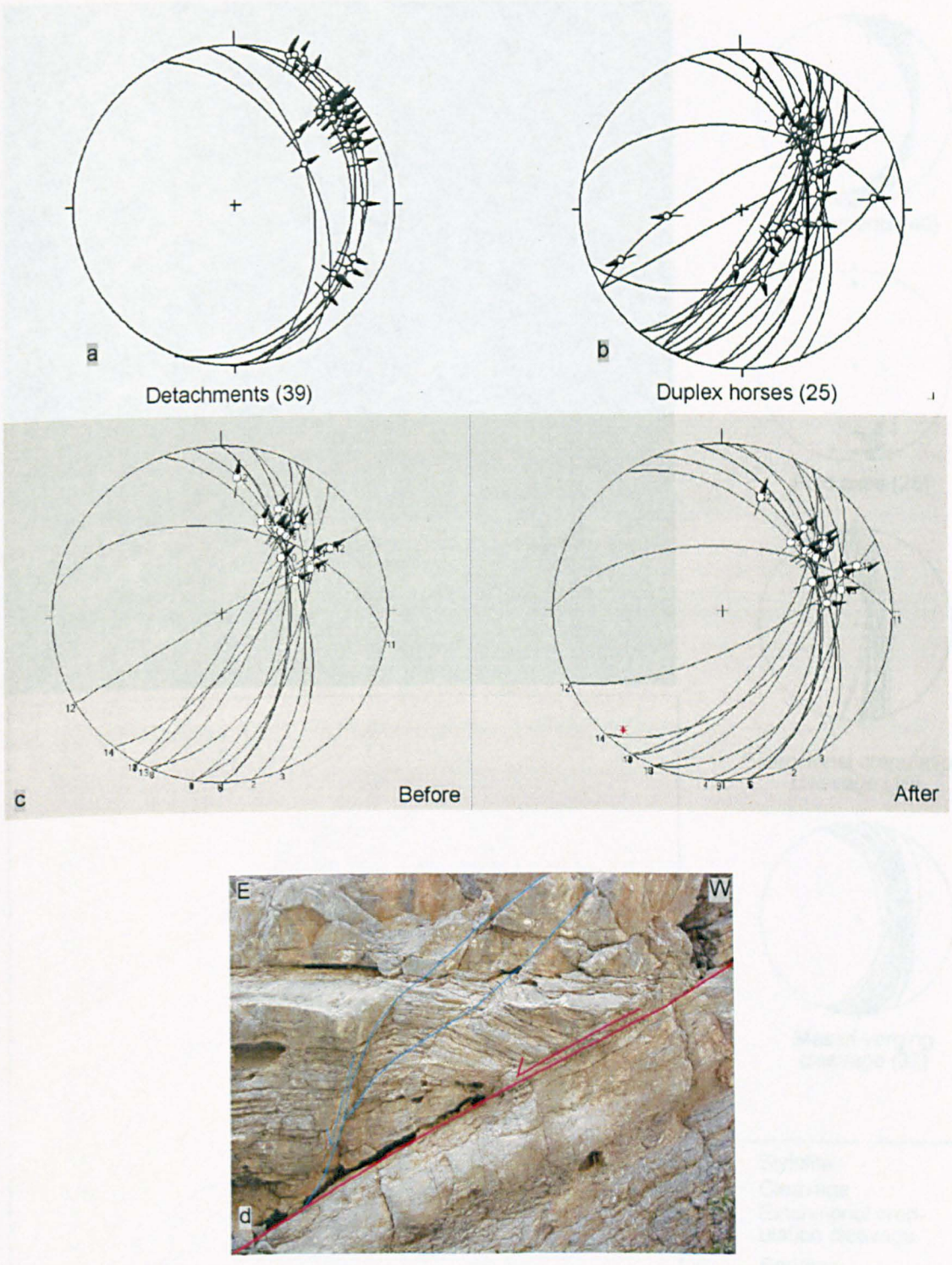

Fig. 4- 29 Structural elements of the extensional duplex structures mapped within the Kh2 Fm [5]. (a and b) Stereograms show the bedding-parallel detachments and the associated horse faults. In both stretching lineations plunge towards NE and SE. (c) Stereograms for the oblique horse faults with NE-plunging lineations. After untilting, these faults turned into dip slip faults (Horse faults were rotated 30° around a horizontal axis trending 040). (d) Hanging-wall cut off transected by steeply dipping faults merging onto the basal detachments (field of view approximately 5 m).

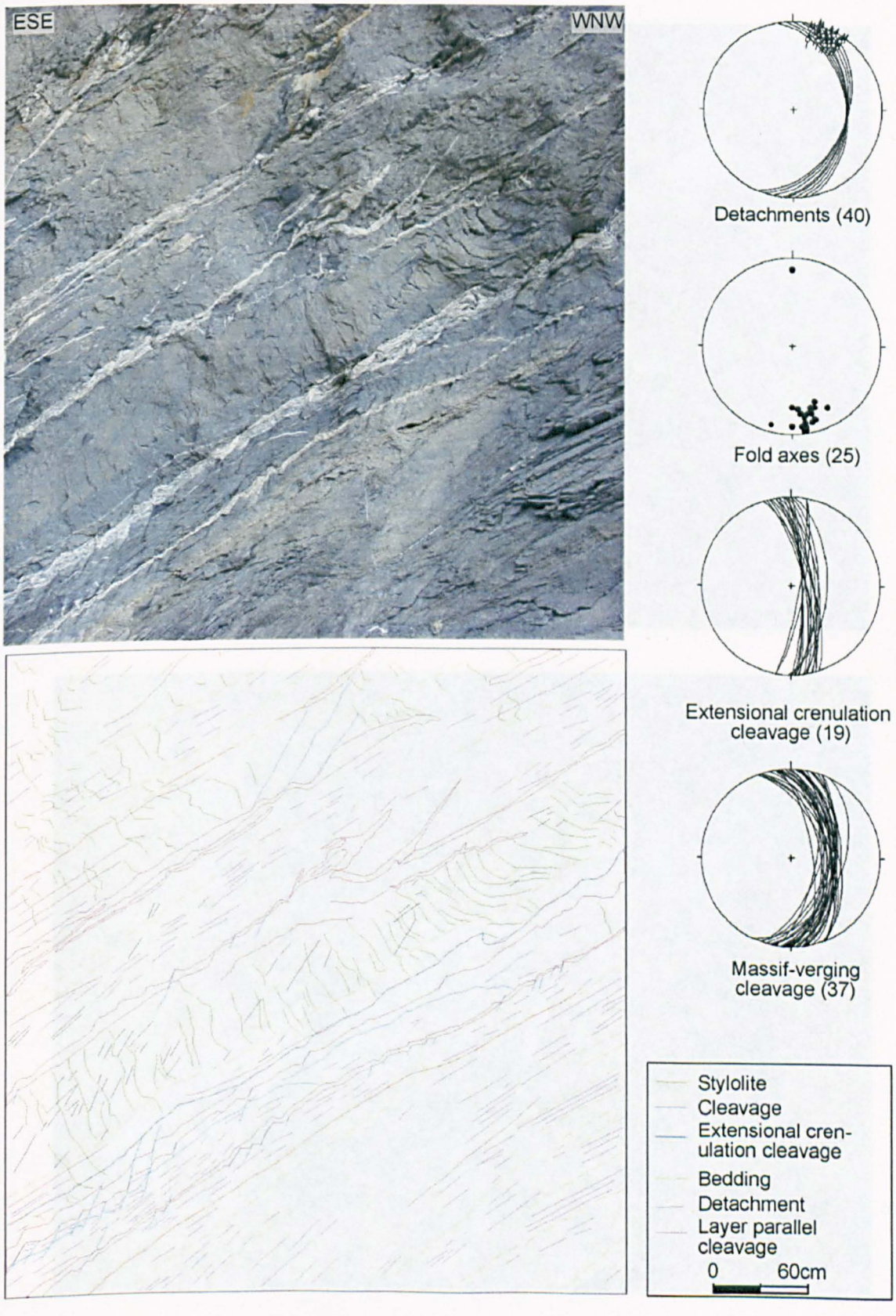

Fig. 4- 30 Line drawing for the various penetrative structures, with their stereographic projections, as mapped in the type locality [5], (Field of view approximately 6m).

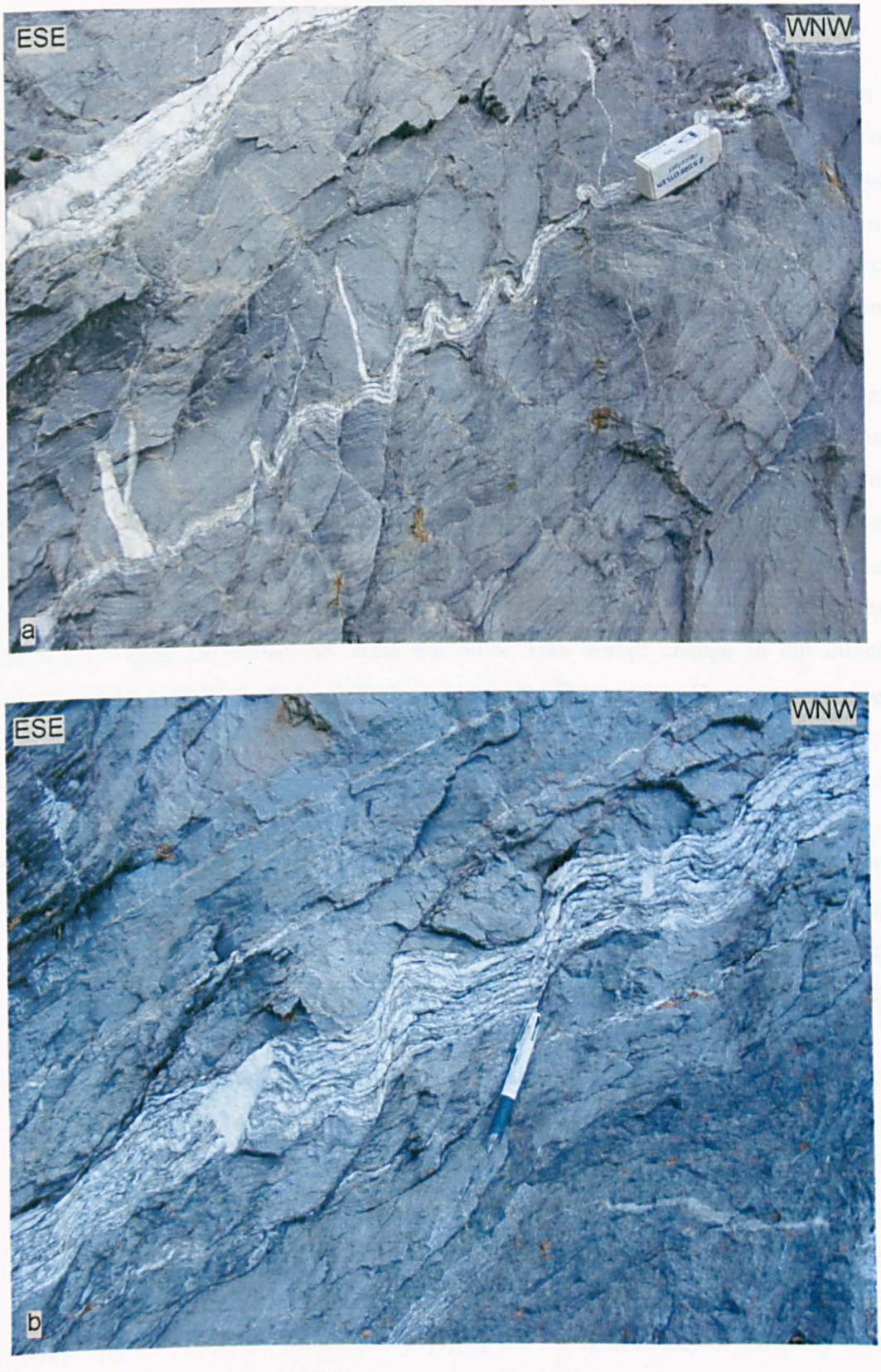

Fig. 4- 31 Close up view of the penetrative structures type locality. (a) Folding of calcite-filled bedding-parallel detachments by massif-parallel folding. (b) Extensional crenulation cleavage affecting calcite-filled detachments.

4.12 AL-Qet Transect

A detailed transect has been constructed along wadi AL-Qet, which is located 3 km to the south of AL-Bir village (Fig. 4-1). The transect is oriented E-W and runs 4 km across the eastern limb of the Nakhal anticline. The whole of the Permian-Cretaceous succession is exposed along the transect, starting from the Permian Saiq carbonate in the west until the Late-Cretaceous Aruma GP at the eastern end, while the entire Wasia Gp is missing from the whole area (Fig. 4- 32). The thickness of the Jurassic Sahtan Fm is locally variable since the lower part exhibits local thickening of metric scale across hanging-walls of steep faults, while the upper part of the Sahtan limestones is locally eroded, forming isolated angular unconformities associated with steeply dipping faults. In some places the whole limestone member has been eroded. Dip change connected to these isolated local unconformities is negligible. The upper Shams carbonate is unconformably overlain by the massive brownish reef limestone of the Aruma Gp, exposed at the mouth of the wadi. Stratigraphic units along this section dip consistently at an average of 35°- 40° SE, except in the vicinity of the wadi entrance, where the cretaceous units dip 30°S. This abrupt change in dip direction is attributed to an E-W fault running along the wadi. The Jurassic-Cretaceous succession is internally folded by intraformational folds trending parallel to the massif.

Large scale structures

The transect is penetrated by different sets of faults which are visible across a range of stratigraphic levels. These faults are presented below according to their stratigraphic locations. The Permian-Jurassic succession exhibits steeply dipping normal faults, marked with syn-thickening of the lowermost part of the Sahtan Fm in the hanging-wall of the fault [1] (Fig. 4- 32). Such syn-thickening reveals that the faulting activity took place during Early-Jurassic time and hence is called Lower Jurassic faulting [1]. Faults strike N-S and NE-SW (Fig. 4- 33), while displacements are less than 10 m, as measured by correlating the Sahtan thickness across the faults. There is no noticeable erosion along the Mahil\ Sahtan contact, and some faults die out within the lower part of the Sahtan Fm, while other have been reactivated later. The fault reactivation took place during the upper Jurassic, resulting in the development of a local angular unconformity located at the contact between Sahtan and Rayda Fm. The faults are truncated sharply by the lower boundary of the Early Cretaceous Rayda Fm and as a result, this phase of faulting is dated and named as the Upper Jurassic faults [2]. The Sahtan upper limestones were eroded and truncated by the unconformity, particularly in the uplifted footwall, which was more vulnerable to erosion (Fig. 4- 33). The minimum fault displacement is approximately 15 m based on stratigraphic offsets across the faults. In addition, some faults have been weakly reactivated with a dip slip movement as

shown from the displacement of the Rayda strata. This weak fault reactivation could have take place at any time after the deposition of the Early Cretaceous Rayda sediments.

Kinematically, the NW faults are marked with massif-pitching lineations, which turn into dip slip once the folding deformation is unfolded by rotating them 30° around a horizontal axis trending 040 chosen to be parallel to the fold axis (Fig. 4- 33). Such kinematic data supports the stratigraphic dating for these faults as pre-folding faults. However, the N-S faults show dip slip lineations owing to their parallelism with the massif strike. Generally, these faults have been initiated before the folding onset and have experienced poly-movements since the Early Jurassic and onwards. During the folding deformation, faults have been rotated clockwise making some steep faults appear like reverse faults.

There are two, km-long steeply dipping NNE-striking faults visible within the Cretaceous sediments at mouth of the wadi, both are not shown on the transect. The fault displacements across each fault are more than 200 m. The first fault is located within the Cretaceous units nearby the wadi entrance, strikes NE and dips steeply at 70° SW. The massive carbonate of the Shams Fm was displaced down to juxtapose with the Salil rocks of the footwall. The hanging-wall is truncated by numerous synthetic normal faults. Kinematicaly, the fault shows dip- and strike-slip lineations, with the strike slip component having a sinistral sense of movements as deduced from tension gashes running parallel to the fault.

The second fault was mapped at the mouth of the wadi separating the Aruma reef carbonate of the hanging-wall from the Shams rocks of the footwall. This fault runs for several kilometers and bounds the eastern flank of the Nakhal anticline. Ridges and grooves lineations seen along the fault plane suggest a dip slip displacement.

Kinematic data along the NNE fault set reflects two components of displacement; dip-and-strike-slip (Fig. 4- 32). So far it cannot be resolved whether these movements took place during or after the folding event. Both major faults were displaced across the wadi in a sinistral manner for some 100 m, predictive of another left lateral fault running along the wadi. The strike slip fault can be traced upstream for about 100 m, but after this no evidence for it can be seen. The existence of a strike slip fault may also be supported by the unexplained southward dipping of the Cretaceous strata at the southern side of the wadi nearby the wadi entrance. Now the unjustified dipping can be attributed to this fault.

A sub-horizontal NW-trending fault has been mapped as truncating the steeply dipping beds of the Permian-Triassic succession. The Triassic Mahil dolomite in the hanging-wall has been juxtaposed adjacent the Permian Saiq carbonates of the footwall. The fault

displacement is in the order of tens of metres with top-NE sense of shearing, and cutting-off angles are 80°. Because of this the fault must have taken place either before or after the folding deformation. However, when the steeply-dipping beds were untilted, the sub-horizontal faults changed into NW-striking normal faults dipping steeply NE. As a result, the fault must have occurred before or during the early stage of the folding onset, since it is kinematically unpractical for a sub-horizontal fault to arise across steeply dipping massive competent units after the folding deformation, especially when these faults are not marked with down-slope throws, like the gravity-driven faults for instance.

A steeply dipping reverse fault situated in the middle of the transect penetrates through the Mahil and Sahtan Fm's (Fig. 4- 34a). The fault strikes NNE- and dips steeply at 84° ESE. There is no obvious syn-thickening or erosion within the Sahtan succession, which commonly characterizes the Lower and Upper Jurassic faulting. The reverse fault displacement is up to 20 m towards the massif, forming a hanging wall anticline with an inverted frontal limb. This anticline hinge axis plunges 50° towards the SSE, while the vergence of the reverse fault and the hanging-wall anticline indicate a top to WNW sense of shearing. The fault shallows upwards across the incompetent rocks of the Sahtan Fm. Such a contractional structure is more likely to have arisen by the inversion of a pre-existing normal fault, rather than the creation of a new sub-vertical reverse fault, which is kinematically difficult, especially when the area is disrupted by numerous normal faults. The inverted normal fault is likely to be part of the Lower and Upper Jurassic faulting systems, since it is sharply truncated by the Lower Cretaceous sequences, seemingly regardless of the undetected syn-thickening or erosion within the Sahtan succession.

The competent limestones units of the Salil Fm are highly deformed through a series of bedding-confined, subsidiary faults (horses), forming extensional duplex structures [4] bounded on either side by bedding-parallel detachments. These detachments run along the less competent micritic limestone units inter-bedded with the massive limestone units. The subsidiary faults strike NE with steep dips of 60° SE, while the bounding detachments strike approximately ENE-WNW with gentle dips of 30° SSE. The area is locally tilted southward by a major E-W trending fault that runs along the wadi. The horse displacements are small within sub-metric scale and the stacking direction of the horses indicates top-SE shearing. Fibre lineations in the detachments plunge gently to the ESE, while within the subsidiary faults, mineral lineations pitch moderately away from the massif (Fig. 4- 32). When the tilting deformation was restored, the oblique lineations on the subsidiary fault turned into approximately dip slip, with down-throw towards SE as suggested from the stacking of horses. At the same time, the detachment lineations have not been changed significantly,

because they were parallel to the tilting axis. Therefore, this extensional duplex structure might have occurred before the southward tilting of the area by the E-W trending fault.

The uppermost part of the transect forms a major graben structure bounded by NW-striking faults [5] (Fig. 4- 32 and Fig. 4- 35). This graben transects the whole eastern flank of the Nakhal anticline and exposes the Jurassic-Cretaceous succession in the shared hanging-wall, while the Permian-Triassic dolomites occupy both footwalls. The km-long bounding faults will be referred to in the text as the northern and the southern faults. The WNW-striking northern fault is sub-vertical, whereas the southern fault is changeable in trend around the E-W axis and dips 40° northward (Fig. 4- 35d). The fault displacements change gradually along the fault strike, from tens of metres in the extreme east, where the fault is dying within the Cretaceous units, to some 500 m in the far west. The E-W lateral gradient in the fault displacement results in a corresponding gradual change in the attitude of the hanging-wall strata, while the footwall strata dip consistently of 40° SE. In the vicinity of the eastern fault tip, the hanging-wall strata dip at approximately 30° N (Fig. 4- 35c) while further west, where the fault displacement is at maximum, both hanging-wall and footwall beds dip consistently at 40° SE (Fig. 4- 35c). The geometry and morphology of the hanging-wall units resemble clinoformal geometry (Fig. 4- 35e), but displacement profile along the fault strike is more likely to be elliptical in shape (Stewart 2001). Only one half of the elliptical shape is exposed along the transect and hence the hanging-wall resembles a clinoform in shape. In the elliptical fault profile, both sides of the hanging-wall dip towards the fault centre (Stewart 2001), which itself should be flat. However, it is not the case in this fault. Such a disagreement can be solved if the fault structure is assumed to be a pre-folding structure. In this case, the eastern part of the fault would dip westward since it is close to the eastern fault tip, while the western part would be flat as it corresponds to the maximum fault displacement. Unfolding of the folding deformation gave matching results and showed (Fig. 4- 35b) the dip of the bounding faults supported the arguments for a pre-folding origin. The northern sub-vertical fault is very steep for a normal fault, while the southern fault is very shallow for a normal fault. When the folding deformation was unfolded around the 040/30 axis; however both faults attained a realistic fault dip of 60°. In conclusion, the graben structure acts like a rotated keystone, a fault-bounded block, rotated by the differential fault throw.

The area exhibits folding structures of different scales, particularly along the Sahtan and Rayda Fm. Folds range in amplitude from a few centimeters to a few metres, with fold axes plunging moderately across a wide range of distribution from SSW to SE (Fig. 4- 32). Folds

are classified into two groups with respect to the vergence direction and attitude, the NE-verging folds and massif-parallel folds.

NE-verging folds plunge SE, orthogonal to the NE-stretching direction. Most of the recognized folds are mainly centimetric in scale and they are accompanied with NE-verging cleavage and bed-parallel detachments marked, with NNE-SSW stretching lineations. In places the NE-verging cleavage is deformed by these folds. The fold asymmetry indicates a top to NE sense of shearing.

Massif-parallel folds are metric in scale and well pronounced along the Sahtan\Rayda contact (Fig. 4- 34b). Such folds are also detected within the thinly-bedded units of the lowermost and the uppermost parts of the Triassic Mahil dolomite. These gentle folds trend around the N-S axis, and the majority are upright with bedding-orthogonal axial planes. Folds are detached from below along bedding-parallel slipping surfaces situated within micritic limestones units. Significant slipping surfaces, underlying the folds within the Rayda Fm, runs along the Sahtan\Rayda contact. The spatial distributions of most of these folds are not influenced by structural anisotropy such as pre-existing Jurassic faults; nevertheless some massif-parallel folds resulted from an inversion along steeply dipping Jurassic normal faults. The fold orientations and being associated with the massif-verging thrusts may suggest that these folds were resulted from an E-W shortening.

The transect is predominated by numerous small faults of metric to sub-metric throw that are recognized throughout the entire stratigraphic section, including the massive Permo-Triassic units. They can be grouped into two main sets, NE-SW and NW-SE. The NE-SW set concentrates around an extensional duplex structure within the Salil Fm, which has previously been described. The NW-striking fault set displays, both dip slip and massif-pitching lineations (Fig. 4- 32). The dip slip lineations suggest post folding fault activities since they are not rotated by the folding deformation. The massif-pitching lineations which turned into dip slip when the folding structure was restored, by rotation around the 040/30 axis, mark pre-folding faults. In short, the NW-oriented fault set was initiated as dip slip before or during the early stage of the folding onset, and then was reactivated as dip slip once again after or during the latest stage of the folding deformation.

Small scale deformations

Deformation fabrics comprises of bedding-parallel detachments, folds and cleavage. The transect displays highly deformed bedding-parallel zones with an intensive ductile shear deformation bounded by less deformed rocks. Such structures are named detachments. Bedding-parallel detachments strike around the E-W axis and dip 35° S on average (Fig. 4-

32). Fibre lineations (Fig. 4- 32) and elongate fragments (Fig. 4- 32) on the detachments surfaces cluster into two main groups trending NNE-SSW and SE-NW, with the NNE-SSW being the dominant group. Bedding-parallel detachments are extensively developed within the shaly limestone units, however the most significant detachments have been mapped below the more competent massive succession such as those underneath the Sahtan and Shams Fm. Such stiff units are deformed in a brittle manner forming extensional duplex structures and normal faulting, which merge onto the underlying detachments. The detachments zones marked with NNE-SSW lineations are accompanied with bedding-parallel fabrics, NE-verging folds and cleavage, while in contrast the detachments zones marked with NW-SE lineations are associated with massif-verging cleavage alongside massif-parallel folds. In these instances, detachments were reused frequently by variously directed deformations. The NNE-SSW oriented lineations with the NE-verging cleavage indicate a top-NE sense of shearing, while the NW-SE lineations and the massif-verging cleavage reflect shearing with a top to the massif sense of shearing. However, the sense of the horses stacking along extensional duplex structures, which are bounded by detachments marked with NW-SE lineations, reveal a top-SE sense of shearing.

Different forms of cleavage have been recorded along the transect, including spaced pressure solution cleavage and bedding-parallel stylolites. Two sets of spaced pressure solution cleavage have been identified, one verging towards the NE and the other towards massif. The NE-verging cleavage strikes ESE-WNW and dips moderately at 30° SW (Fig. 4- 32 and Fig. 4- 34b). Stretching lineations recorded on the cleavage surfaces plunge SSW, and is well developed along bedding-parallel detachments characterized with NNE-SSW stretching lineations. Massif-verging cleavage strikes ENE-WSW and dips steeply of 55° SE (Fig. 4-32). This is commonly associated with bedding-parallel detachments characterized with NW-SE stretching lineations. Bedding-parallel stylolites are folded by both NE- and massif-verging folds.

Thinly competent limestones beds within the Sahtan and Salil Fm are fractured by NW-trending tensile calcite veins. They are orthogonal to bedding, indicative of bedding-parallel extension. Veins are terminated against bedding-parallel detachments marked with NNE-SSW lineations. *Belemnites* fossils within the Lower Cretaceous Rayda sediments are undeformed, indicating heterogeneously distributed strain.

Interpretation and summary

The available structural data along the transect expresses prolonged fault activity at this part of the massif. The oldest faulting event was dated to the Late Triassic-Early Jurassic, when

NE-and NW-trending faults took place. During the Late Jurassic, the pre-existing faults were rejuvenated again, resulting in a local angular unconformity along which the Sahtan Fm is partially eroded. During the folding of the Nakhal massif, some of these pre-existing faults were inverted. Jurassic faulting has not been mapped anywhere apart from the eastern flank of the Akhdar, and therefore must be governed by a structural feature limited to this limb only. Such a structural element might be the Semail lineament. Throughout early and Middle Cretaceous the area was tectonically stable, as there is no record for any faulting over that time. However, tectonic activities were resumed again before or during the early stage of the folding onset. This is evidenced from the deformation of the NW-striking faults by the folding deformation manifested by the massif-pitching fault striations and the highly rotated fault plane. Furthermore, the rotation of the major graben structure [5] with its classical elliptical hanging-wall is crucial evidence for such timing. After or during the latest stage of the folding process, some of the NW-striking faults were reactivated as dip slip and strike slip faults.

The relative timing of NE- dip slip faults with respect to the folding deformation is still ambiguous, since these faults strike parallel to the massif hinge, and extend over the entire flank, bounding the eastern limit of the Nakhal anticline. The major NE-oriented faults mapped at the wadi entrance were displaced along a sinistral strike slip fault running along the wadi. This strike slip fault can be interpreted as a transfer fault that relayed the displacements between the segmented NE-striking faults, or alternatively it could be a later event of strike slip faulting.

Inversion deformations took place mainly along the NE-striking faults, which make up half graben structures. The vergence of the inversion structures is top-massif indicating NW-SE shortening. The immediate question is why the inversion deformation is just localized along the eastern flank? The eastern flank is disrupted with NE-trending pre-existing faults. Therefore these faults are more vulnerable to an inversion by a NW-SE contractional deformation. However, the other pre-existing fault sets such as the NW-oriented faults are not favorites for inversion by a NW-SE contraction. In this manner the major NE-striking faults mapped at the wadi entrance cannot be pre-folding faults since they are not inverted, so must be syn or post folding faults.

The presented data reveals at least four different phases of deformation. Firstly, a vertical flattening strain expressed by the bedding-parallel stylolites. Secondly, a NE-directed extensional deformation is suggested by the NW-SE fractures, together with the NE-verging folds and cleavage. Thirdly, massif-verging deformation is manifested by massif-verging cleavage and massif-parallel folds. Fourthly, away from the massif directed extensional

deformation is expressed by the NNE-striking faults and extensional duplex structures. The bedding-parallel detachments are involved separately in most of these deformations as recorded by the various detachment lineations. The bed-parallel stylolites are folded by the NE extensional deformation, the massif-verging deformation, and for this reason the vertical flattening deformation could be the oldest deformational event. The relative timing of the other phases cannot be estimated based on the deformation fabrics alone.

So how are the major faults and deformation fabrics linked to one another? By correlating the large and small scale deformations, three systems of deformations have been recognized. The major NW-striking faults, along with the NE-verging deformation fabrics represent NE-directed extensional deformation. The massif-verging folds and the inversion structures, together with the massif-verging deformation fabrics reflect a NW-SE contractional system. The third system, which is local and weakly developed, is an extensional deformation directed away from the massif and manifested by major NE-striking faults and the away from the massif-verging deformation fabrics. The localization of these faults along the massif margin may infer that such deformation took place after the formation of the massif itself.

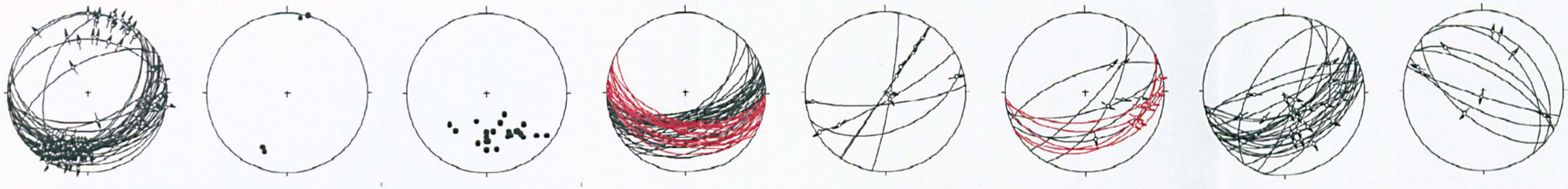

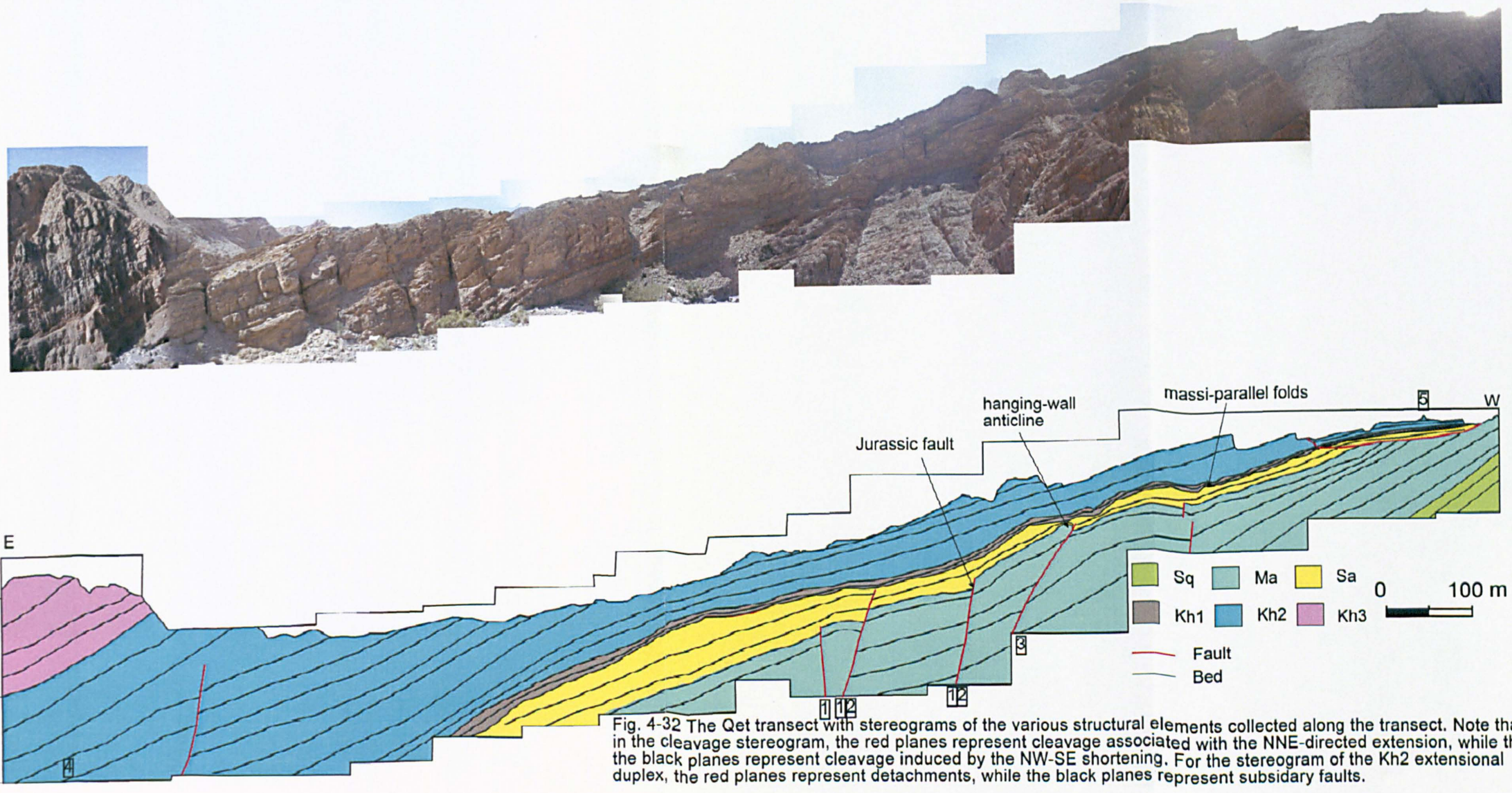

Fig. 4-32 The Qet transect with stereograms of the various structural elements collected along the transect. Note that in the cleavage stereogram, the red planes represent cleavage associated with the NNE-directed extension, while the the black planes represent cleavage induced by the NW-SE shortening. For the stereogram of the Kh2 extensional duplex, the red planes represent detachments, while the black planes represent subsidary faults.

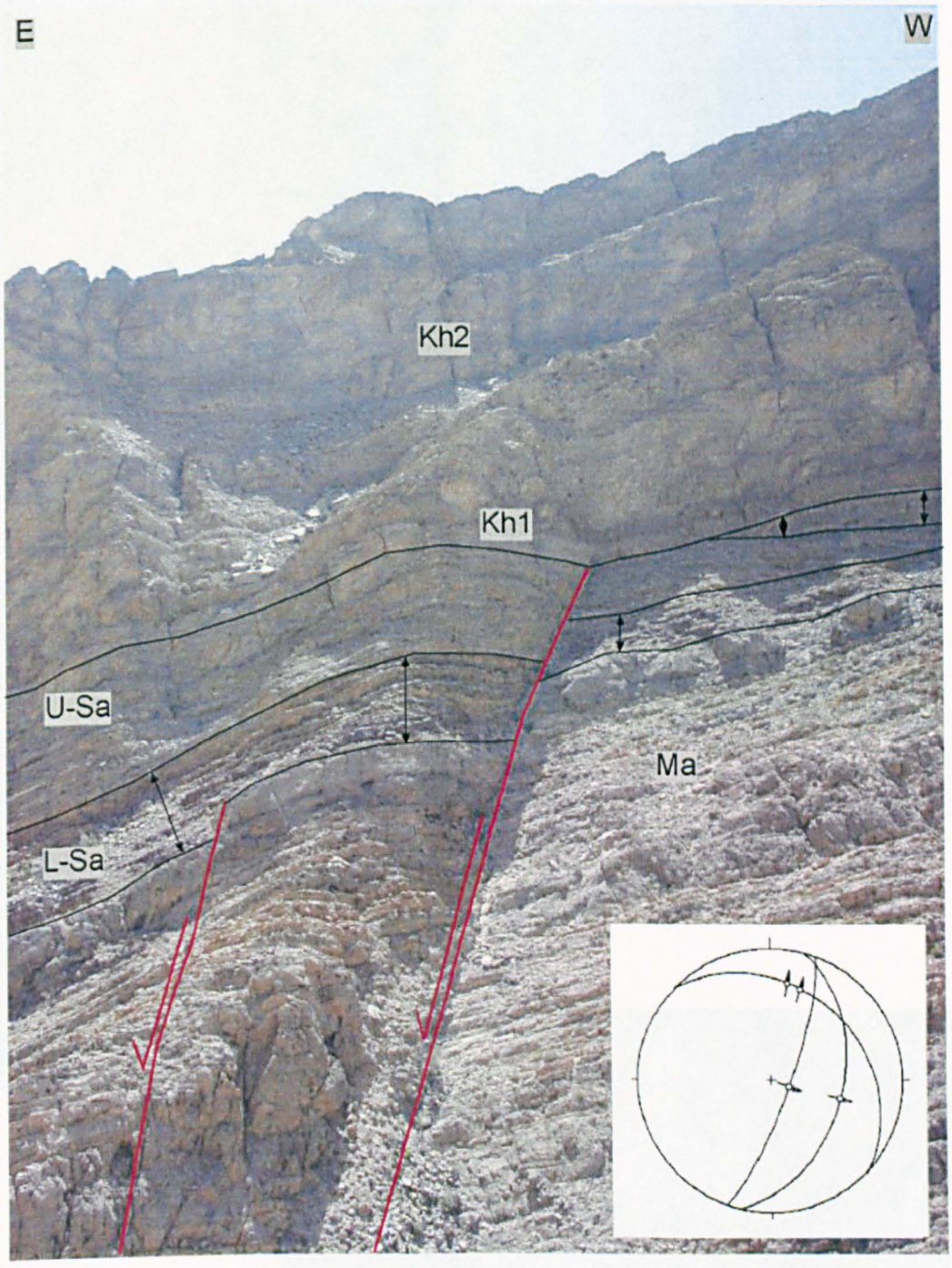

Fig. 4- 33 Lower Jurassic faulting marked by thickening of the lower Sa succession across the fault. The upper Jurassic faulting is marked an angular unconformity along which the upper part of the Sa Fm is locally eroded. The stereogram inset shows the Jurassic (Lower and Upper) faults with their corresponding faults lineations. Note the massif-pitching lineations along the NW-striking fault (Field of view is approximately 200 m).

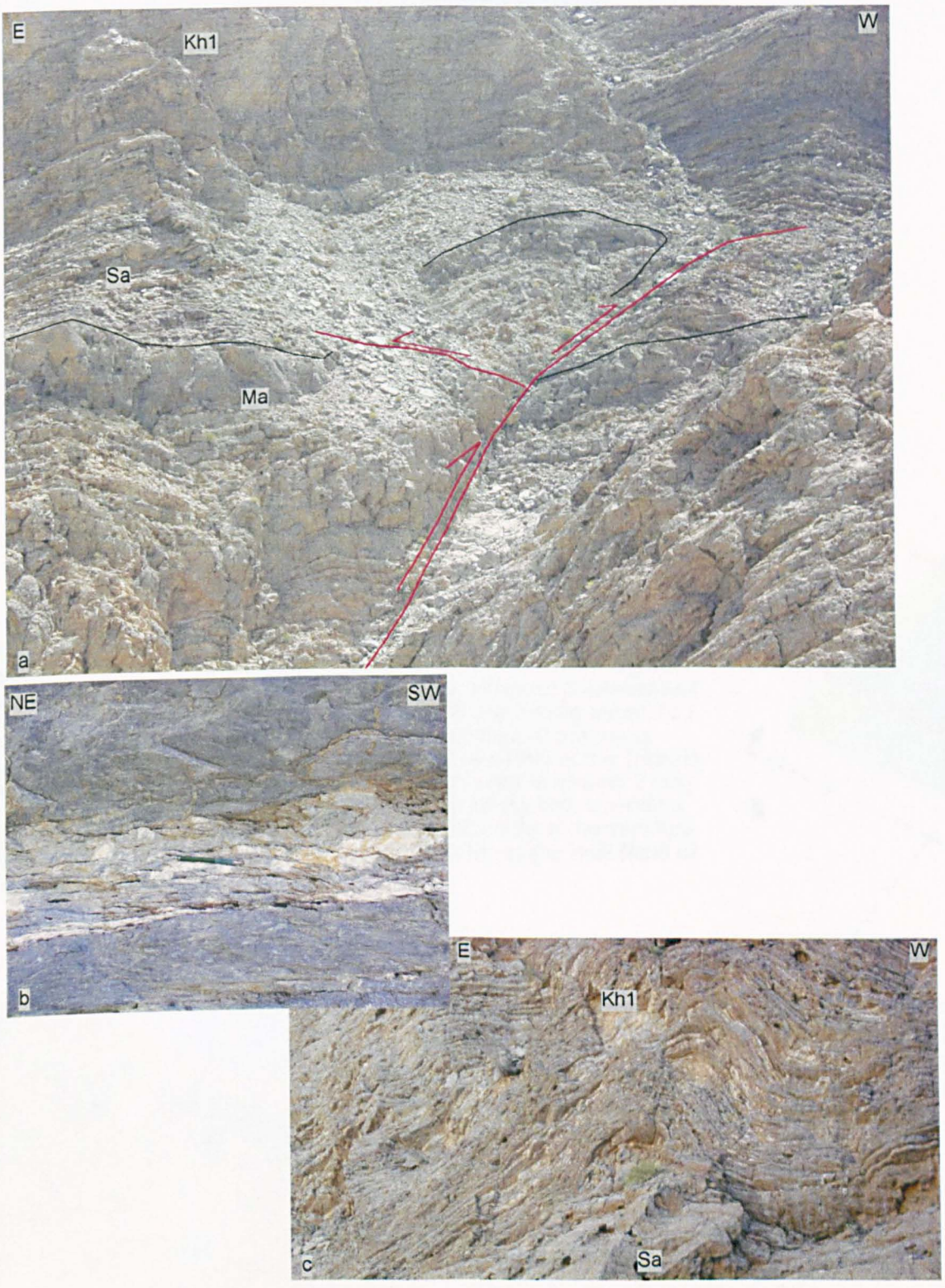

Fig. 4- 34 Deformation fabrics along the Qet transect (a) Inversion structure along steeply dipping NNE-striking fault resulted in forming a hanging-wall anticline within the Triassic and Jurassic succession (Field of view is approximately 150 m). (b) NE-verging cleavage at the Sa Fm. (c) Massif-parallel fold within the Kh1 Fm, notice that the fold is detached along the Sa-Kh1 contact (Field of view is approximately 50 m).

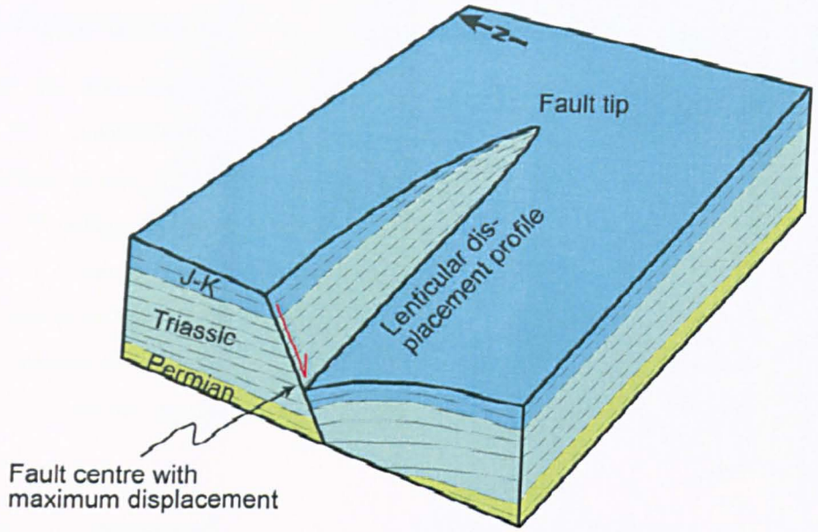

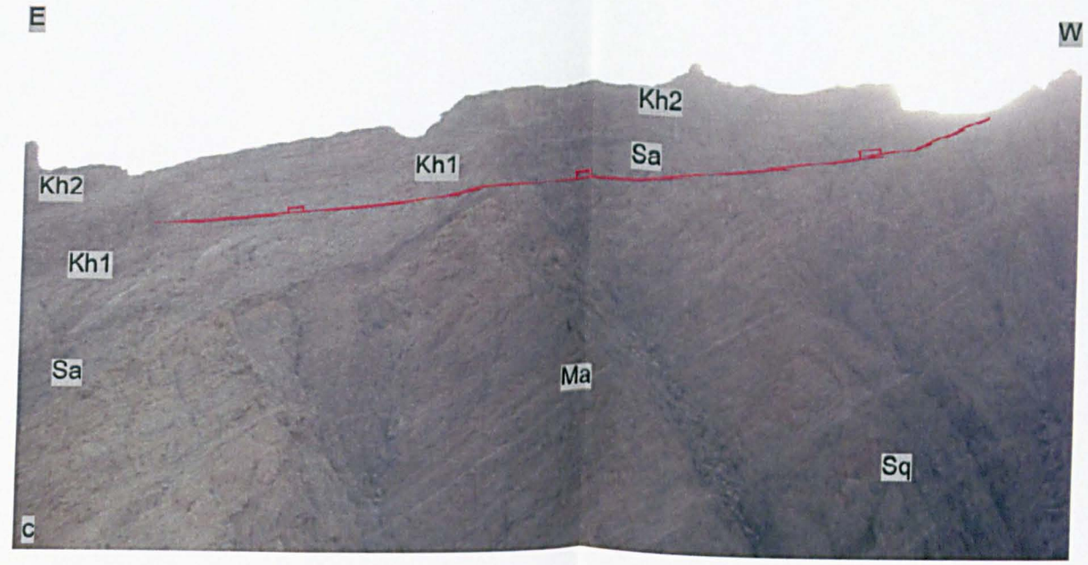

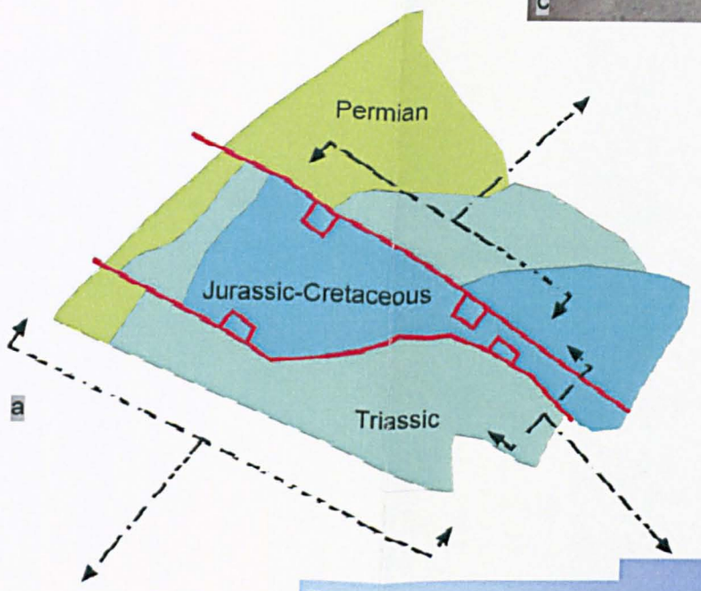

Fig. 4-35 Structural analysis of NW-trending graben structures mapped along the Qet transect (a) A geological map for the NW-oriented graben structures . (b) Cartoon diagram illustrating an elleptical displacement profile created along the northern fault before the folding event. (c) Northern view of the structure showing the Jurassic-Cretaceous succession of the hanging-wall cutting down the profile of the Triassic and Permian carbonate in the footwall (field of view is around 2 km). (d) Eastern view of the graben structures illustrating both bounding faults (field of view is around 500 m). (e) Southern view of the structure. The clinoformal geometry can be clealy seen along the fault (field of view is around 3 km)

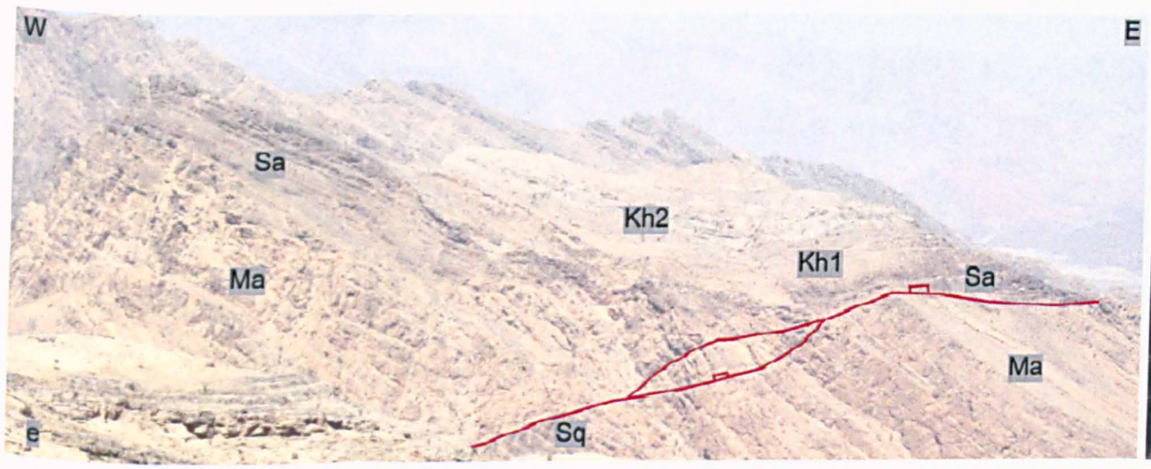

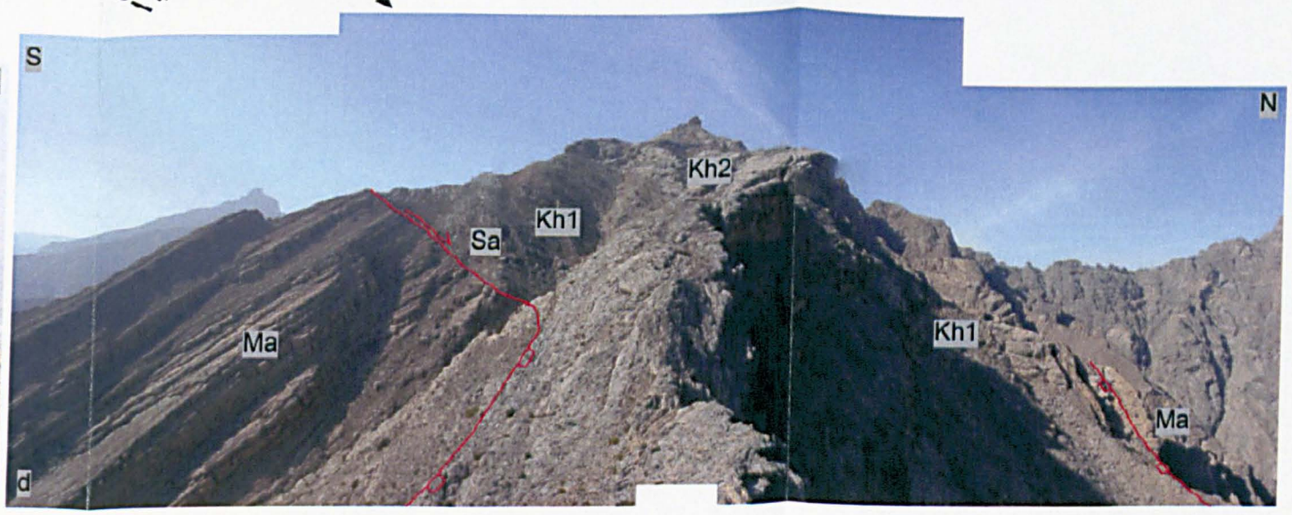

4.13 Toyan transect

Toyan transect is situated 2 km to the west of the Al-hobe village and town of Semail (Fig. 4-1). The transect runs E-W for 6.5 km across the Eastern flank of the Nakhal culmination. The whole preserved Mesozoic stratigraphic units are seen across the transect, together with the pre-Permian Mistal sediments mapped at the core of the culmination (Fig. 4- 36). Generally, beds are sub-horizontal at the fold crest and regionally tilted SE of approximately 40° along the eastern flank. In all the visible stratigraphic units, bedding planes are parallel to the formation boundaries. However, the transect is penetrated by km-long normal faults, which disrupts the dip of the local beds to 10°E within the Natih carbonate at the wadi entrance.

Large scale structures

There are three km-long, NNE-striking normal faults penetrating the whole stratigraphic section and stretch the section along the SE-NW axis (Fig. 4- 36). These faults are described and analyzed in turn below.

The first fault [1] strikes NNE and is exposed at the mouth of the wadi between the Natih Fm in the footwall and the Aruma Gp in the hanging-wall together with allochthons units. The fault plane is covered by scree, preventing in depth observation and analysis.

The second km-long fault [2] strikes NE- and dips steeply of 50° SE. The Wasia Gp in the hanging-wall is displaced downwards for 150 m and is juxtaposed against the Shams Fm in the footwall (Fig. 4- 37a). The fault striations express dip slip displacements. Part of the fault displacement has been taken up laterally through the Natih Fm at the hanging-wall by a series of bedding-confined synthetic faults, detached along bedding-parallel detachments.

The third km-long fault strikes NE-SW [3] separating the Triassic Mahil dolomite in the footwall from the Jurassic-Cretaceous succession at the hanging-wall. The fault dips of 50° SE, with a vertical displacement of approximately half a km. The fault extends for more than 15 km along the Nakhal anticline, while kinematic data reveals a dip slip displacement.

The western end of the transect is marked by two major, steep faults striking NNE-SSW and forming a graben structure [4] situated at the fold crest (Fig. 4- 38a). This structure has been interpreted by Rabu et al. (1986) as klippe structures underlain by a southward-verging thrust. Synthetic dip slip normal faults of metric displacement are common in the hanging-wall strata. Hanging-wall beds are deflected and folded adjacent to the both faults forming drag folds that suggest a normal dip slip movement. Fault striations back this up by indicating dip slip fault movement. The estimated vertical displacement for each fault is

more than 200 m, and cuts down the whole stratigraphic profile until the pre-Permian Mistal sediments. The graben-bounding NNE-striking faults transect a major NW-striking fault.

Deformation fabrics

Intensive deformation fabrics are localized within thin zones composed of shaley limestone strata. Such deformation involves intensive foliations along with calcite-filled veins. These highly strained narrow zones are surrounded by less deformed wall rocks along either side, and consequently can be described as detachments zones. Detachment zones strike approximately N-S and dip of 30 °E (Fig. 4- 36). Detachment stretching lineations cluster into two groups, plunging to NNE-SSE and ESE. Dip slip NNE-striking normal faults branch and merge onto the detachments as mapped in the Natih Fm. Elongated sedimentary clasts, particularly within the Aruma detrital sediments, plunge NNE (Fig. 4- 36).

Intraformational fold structures are well established within the thinly-bedded units of the Salil and Sahtan Fm, but are rarely seen in the massive competent units of the Natih and Shams Fm's. The fold axes are widely scattered ranging from NE to SSW (Fig. 4- 36) and consequently, folds vergence varies between the NE and E directions. Sporadically, the NE-verging folds are recumbent showing bedding-parallel axial planes, while the axial planes of the E-verging folds are steeply dipping to the E.

Two phases of cleavage were identified within the clay limestone units (Fig. 4- 36). The first phase is NNW-striking cleavage, intersecting bedding at low angles. Such cleavage is refracted at variable angles across lithologically contrasting units (Fig. 4- 37b). The second phase is manifested by NE-striking cleavage, steeply dipping of 45° SE. and verges towards the massif. unlike the NNW-striking cleavage, this phase is not widely distributed.

Deformation fabrics within the graben are described separately, owing to its location at the fold crest. Beds are sub-horizontal along the graben. The most evident ductile structure, particularly in the Salil Fm, is the NE-verging cleavage with small bedding-cleavage intersection angles (Fig. 4- 37b and c). Calcite-filled, bedding-parallel detachments are also developed. No deformation fabrics could be seen similar to those verging to the massif documented along the flank side. Bedding-confined faults oriented E-W and NW-SE have been recorded with dip slip and strike slip lineations (Fig. 4- 37d).

Interpretation and summary

The transect is stretched by NNE-striking dip slip normal faults, corresponding to an E-W extension. Ductile non-penetrative structures such as E-verging folds are associated with E-W extension along bedding-sub-parallel detachments. The relative timing of such faults with

respect to the folding event cannot be determined based on the fault striations, since both faults and the massif hinge are parallel. The previously risen question was whether there is any relation between the graben faulting mechanism and its location at the hinge area of the Nakhal anticline. Such as occurrence is not of key significance with respect to the faulting mechanism, since NNE-oriented faulting also developed on the eastern flank. For this reason faulting deformation is not related to outer arc extension, especially faulting which penetrates the entire stratigraphic column.

The deformation fabrics are classified into two groups based on its sense of shearing. Firstly, the NE-verging structures include the NE-verging folds, cleavage and detachments with NE lineations. Secondly the massif-verging structures, which reveal NW-SE shortening, are manifested by massif-verging cleavage and detachments with E-W lineations. Fig. 4- 37 presents two clusters of detachment lineations plunging NE and E. The NE-plunging lineations are associated with the NE-directed deformation, while the E-plunging lineations are either related to bedding-parallel flexural slipping, accommodating the folding deformation, or the E-W extensional deformation. Deformation fabrics at the fold crest (graben structures) correspond to the NE-directed deformation, but there is no evidence for the massif-directed deformation, which is robust on the flanks. This indicates that the massif-verging structures are enhanced through flexural slipping, which concentrate at the fold flank but is absent from the fold crust (Ramsay, 1967).

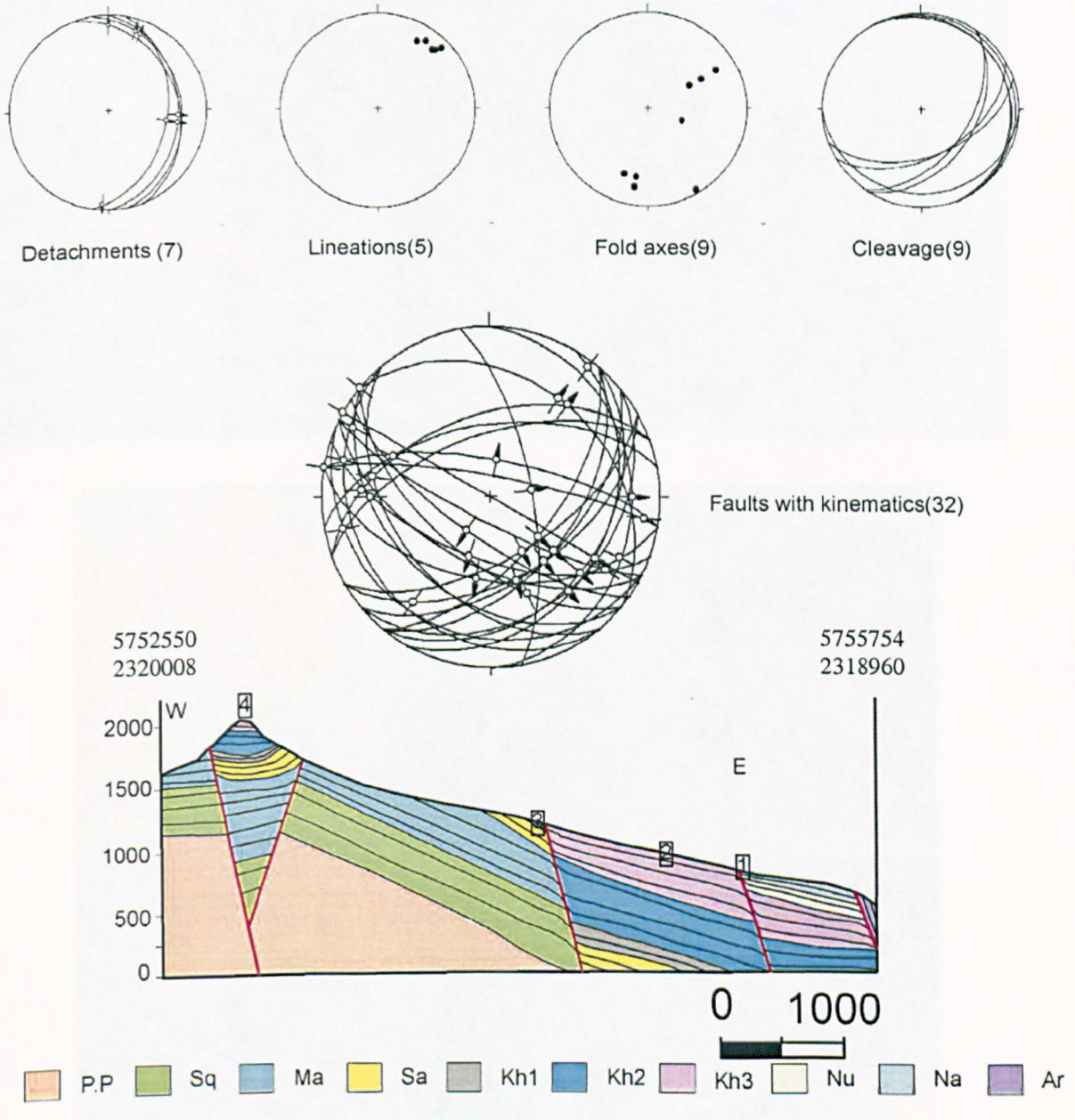

Fig. 4- 36 The Toyan transect with stereograms of the different structural elements collected along the transect.

Fig. 4- 37 The major NE-fault across the Toyan transect [2] separating the Kh3 and Na Fm's (Field of view is approximately 50 m), is shown at (a) . (b) Refracted NE-verging cleavage at the Kh3 Fm

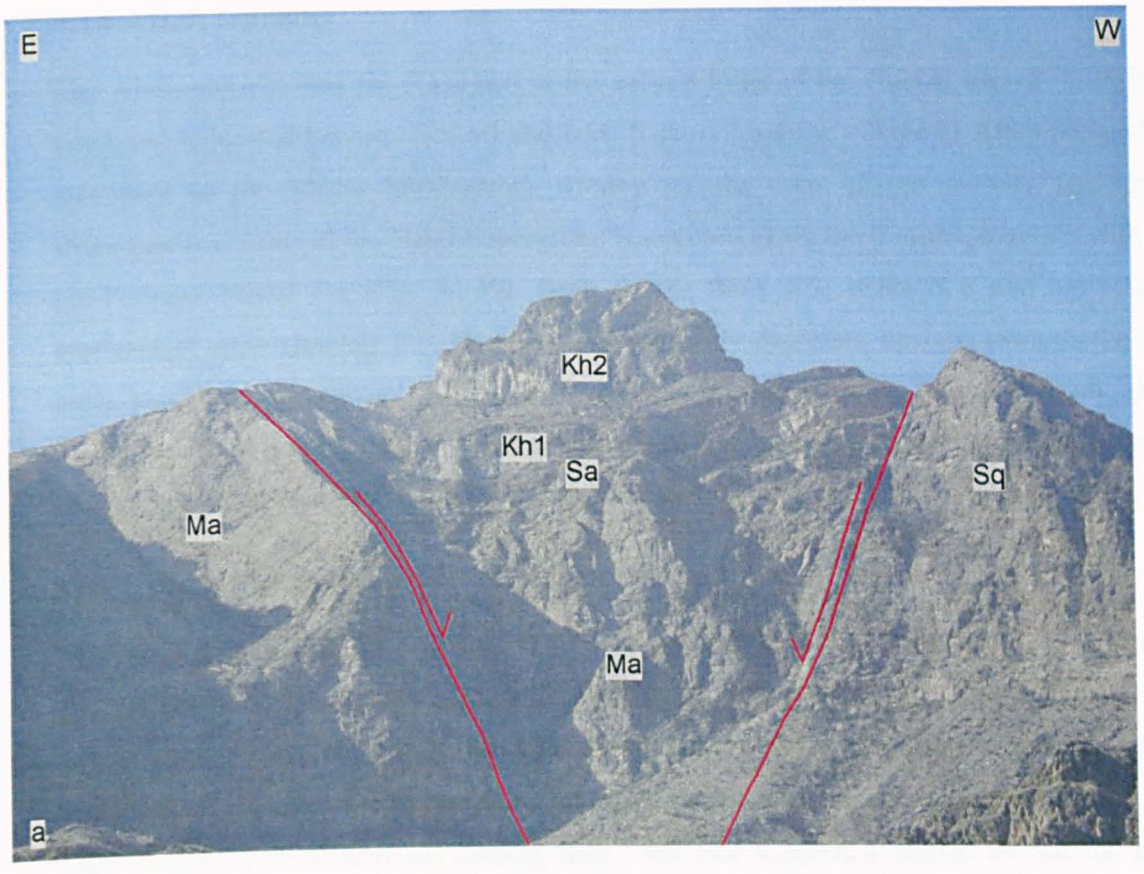

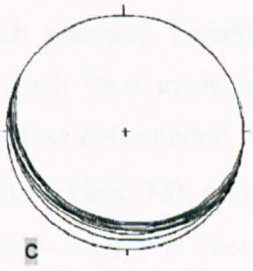

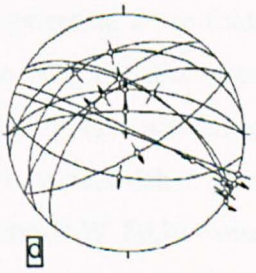

Fig. 4- 38 Structural deformations in the fold crest. (a) The major graben structures [4] at the crest of the Nakhal anticline (Field of view is approximately 1 km). (b) The NE-verging cleavage mapped at the fold crest. (c &d) Stereograms of the cleavage and faults mapped at the fold crest. Notice that faults are either dip or strike slip in kinematics.

4.14 Afiah transect

The Afiah transect runs for 6 km across the eastern flank of the Nakhal massif in an E-W trend and is located between Semail and Izki. It starts from the village of Afiah proceeding westward to the Mistal pre-Permian window at the core of the massif. The entire stratigraphic column of the Hajar Supergroup is exposed along the transect, together with the pre-Permian Mistal Fm (Fig. 4- 39). Beds on the flank side strike N-S and dip steeply eastward of approximately 50°. However, dip gradually decreases upslope towards the fold crest, reaching approximately 20°E. The transect is crossed by a km-long E-W fault, along which locally adjacent hanging-wall strata are deflected. In all the visible stratigraphic units, bedding planes are parallel to the formation boundaries.

Large scale structures

The transect is marked by two km-long faults penetrating through the whole stratigraphic profile, along with numerous associated small faults (Fig. 4- 39c). The first major fault [1] swings in trend from E-W to WNW-ESE, dips steeply of 70° S (Fig. 4- 40a) and has a fault throw of approximately 350 m. Hanging-wall strata are disrupted by synthetic faults and folded adjacent the fault plane forming drag folds that suggests a normal movement. Fault striations show four distinct plunging populations (Fig. 4- 39c) dip slip, strike slip, massif-pitching and away from the massif-pitching lineations. Such plunging variably reveals multiple movements. Understanding the relative timing of each fault movements, with respect to the folding process requires the unfolding of the folding deformation. When this was completed, by rotating faults 30° around a horizontal axis trending 040, each lineation group rotated differently depending on its original attitude (Fig. 4- 39c). The massif-verging lineations turned into dip slip indicating a pre-folding dip slip fault movement, while the away from the massif-pitching lineations became strike slip reflecting a pre-folding strike slip fault displacement. However, the existing dip- and strike- slip lineation groups, were randomly scattered in a meaningless manner. As a result the applied unfolding was not applicable and hence the dip-and-strike- slip lineations must have been taken place after or during the late stage of the folding process. In conclusion the E-W faults were initiated before or during the folding onset experiencing dip slip and strike slip displacements. Subsequently they were rejuvenated as dip slip and strike slip faults after or during the latest phase of the folding process.

The second km-long fault strikes NW- and dips steeply of 80° SW, penetrating the exposed Cretaceous succession. The fault is not shown on the transect since the fault is parallel to the transect. The fault throw is approximately 100 m. The fault plane is marked with thick

calcite mineralization and breccia reaching 2 m thick in some places (Fig. 4- 40b). Fault striations show three plunging populations (Fig. 4- 39c) strike slip, massif-pitching and away from the massif-pitching lineations. Like the previous fault [1], identifying the timing of each fault movement relative to the folding process involves restoration of the folding deformation. Conducting this restoration indicates that the E-W faults were initiated before or during the folding onset, experiencing dip slip and strike slip displacements. Subsequently the faults were rejuvenated as strike slip after or during the latest phase of the folding process (Fig. 4- 39c).

Deformation fabrics

Deformation fabrics are poorly developed compared with previous transects. Bedding parallel calcite veins were developed locally between stratigraphic units, and are oriented N-S with calcite fibre lineations plunging to the NE and the E (Fig. 4- 39a). These calcite-filled bedding-parallel planes have not been called detachments because they lack any evidence of great horizontal displacement or brittle faulting.. Alternatively, they can be called flexural slipping surfaces

Cleavage is developed across the whole Jurassic-Cretaceous succession. The majority of cleavage strikes NE-SW and dips steeply to moderately towards the SE (40° -80°) (Fig. 4-39a). It verges mainly to the massif, without any NE-verging cleavage. Bedding-parallel, teeth-like stylolites are common across the whole Jurassic-Cretaceous succession, however, bedding-orthogonal stylolites are locally seen reflecting an E-W shortening (Fig. 4- 40c). Tensions gashes appear in the shale-bearing units of the Salil Fm. Conjugate tension gashes recorded in Nahr Umr Fm express bedding-perpendicular shortening and when tilting was restored, the maximum shortening axis become vertical.

Interpretation and summary

Two km-long fault sets have been identified striking E-W and NW-SE; each set experienced poly-movements and took place at different stages with respect to the folding process. Both sets suffered from dip slip and strike slip displacements before or during the early stage of the folding onset. Subsequently they were reactivated after or during the latest stage of the folding process, either as dip slip or strike slip or both. The similarity in the fault displacements suggests that both sets are part of the same deformational regime. This is also supported by the unfolding, which results E-W striking faults changing into WNW-trending faults. Both set therefore could be related to the NE-directed extensional system.

The deformation fabrics is poorly developed, particularly the NE layer extensional shearing, which is only reflected by NE-plunging lineations along some calcite-filled slipping surfaces. The massif-verging structures are more developed as manifested by spaced pressure solution cleavage, but with a frequency and intensity still much lower than of previous transects. For example, the massif-verging folds and thrusts are missing from this area. The massif-verging structures together with the bedding-orthogonal stylolites imply WNW-ESE shortening. The development of the NE-directed deformation and a WNW-ESE shortening decreases southward. Other structures like the bedding-parallel stylolites and conjugate tension gashes express a flattening deformation oriented orthogonal to bedding. Consequently the flattening deformations may have taken place, while beds were untilted, which is more likely before the folding deformation. The flattening deformations may be associated with the NE extensional deformation, when the flattening strain was vertical.

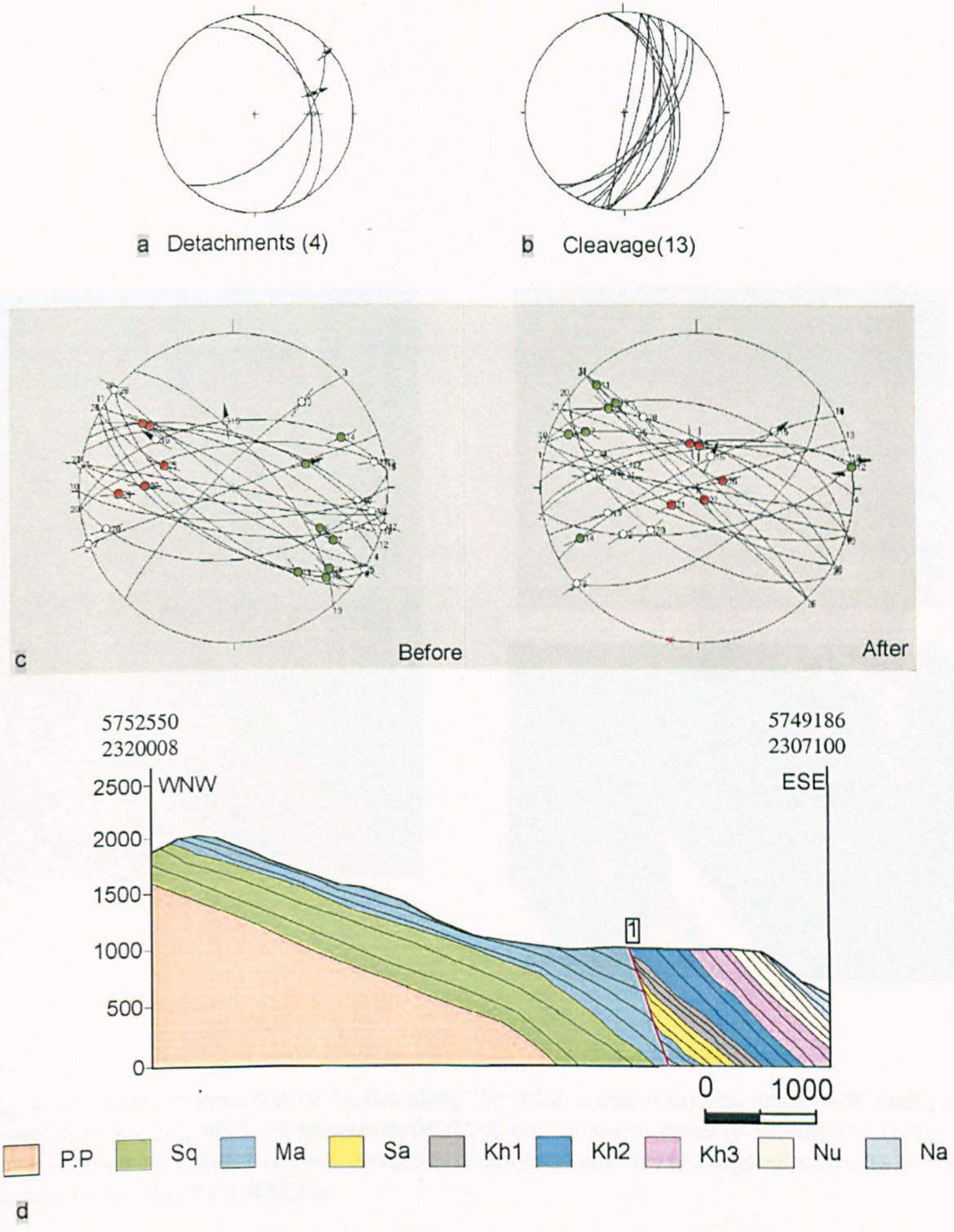

Fig. 4- 39 The Afiah transect with stereograms of the various structural elements collected along the transect (a & d). (c) Stereograms showing faults mapped along the transect before and after conducting the folding restoration, the red circles are for the massif-pitching lineations, while the green circles represent the away from the massif-pitching lineations (faults were rotated 30° around a horizontal axis trending 040).

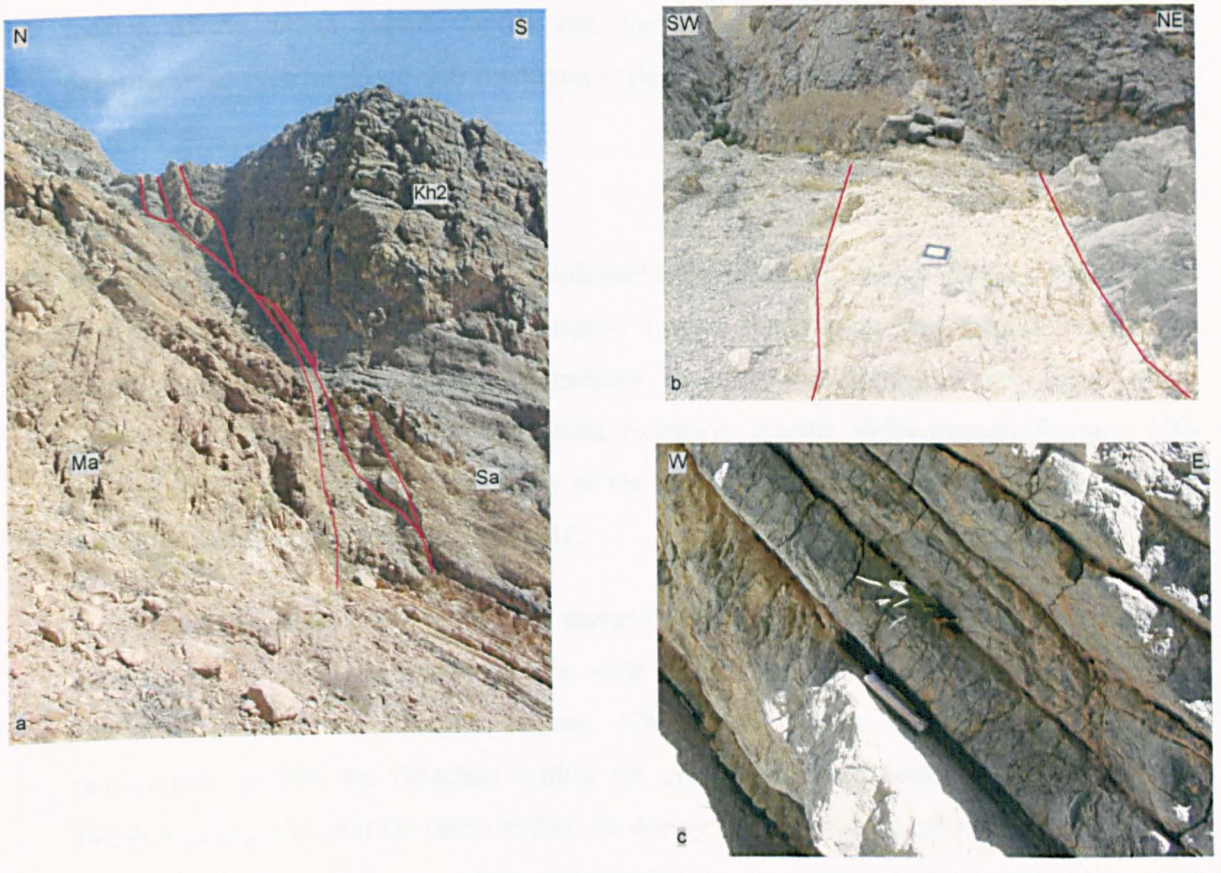

Fig. 4- 40 Fault and deformation fabrics along the Afiah transect (a) The major E-W fault [1] across the Mesozoic platform sequences (Field of view is approximately 300 m). (b) Thick calcite mineralization of 2 m thick along a NW-striking fault. (c) Orthogonal stylolites within micritic limestone of the Kh2 Fm.

4.15 Discussion and Summary

The Nakhal anticline is deformed by several different deformation regimes. In general, the various structural elements can be classified under two distinctive systems. Firstly, the NE-directed extensional shear deformation manifested by a series of faults and detachment system, and secondly, the NW-SE oriented contractional deformation, which resulted in the folding of the whole massif. Brittle and ductile deformations are associate with both deformational systems. Each deformational system is analyzed and summarized from finding throughout.

The NE-extensional system

The NE-extensional deformation is manifested by a series of steeply dipping NW-striking faults detached along various stratigraphic levels, comprising the Jurassic-Cretaceous succession and the pre-Permian sedimentary basement. Stratigraphic unit along which detachment zones are situated underwent extensive ductile deformations forming NE-verging folds and cleavage. A summary of the different structural elements associated with this deformation is presented in Fig. 4- 41.

Steeply dipping brittle faults branch and merge onto the detachments, omitting and extending the stratigraphy in a NE direction. The style of faulting varies from one detachment to another. The km-long steeply dipping NW-striking faults, cross-cutting the entire stratigraphic profile, are detached within the pre-Permian sequences. These faults were initiated as dip slip normal faults before or during the early stage of the folding onset as evidenced from the corresponding massif-pitching lineations. Subsequently they were reactivated as dip- and strike-slip faults after or during the latest stage of the folding event. Because of this, the extensional deformation along a detachment situated within the pre-Permian rocks is likely to be coeval with the folding process.

NE-extensional deformation within the Jurassic-Cretaceous succession is manifested by bedding-confined steep normal faults within the competent units, and layer-extension shear along the incompetent units. The kinematic of the NE-extensional deformation within the Jurassic-Cretaceous succession is consistent over the whole Nakhal anticline giving a top-NE sense of shearing. However, the deformation intensity and frequency is variable across the massif and shows an increase in a northeastward direction. The NE-extensional deformation within the Jurassic-Cretaceous succession took place before the folding onset, as the whole NE-extension fabrics had been folded by the folding process. NE-extensional fabrics such as NE-verging cleavage and folds, stretching lineations and boudinage structures are explored next.

The attitude and geometry of intraformational folds associated with the NE-extensional shearing systematically change in a NE trend across the massif. These changing parameters are described individually. Firstly, fold orientations are variable, ranging from orthogonal to sub-parallel to the NE stretching direction. Secondly, the inclination angle of the fold axial planes decrease in a northeastward direction, from steeply dipping at the far south to gently dipping at the extreme north in the vicinity of the Almeeh transect. This results in a varying fold geometry, from tilted in the south to recumbent in the N, as recognized at the Almeeh transect. Thirdly, the fold amplitude increases northeastwards across either flank, especially within the Sahtan Fm, as mapped along the Qarah and Almeeh transects where fold amplitude is in the order of several metres. Such significant boosting of the fold amplitude corresponds to an increase in the shear strain, capable of folding thicker stratigraphic packages.

The area experienced different phases of cleavage under the NE-extension deformation. These are expressed by spaced pressure solution cleavage, foliation, and schistosity. Spaced pressure solution cleavage developed over the entire Jurassic-Cretaceous succession, while other cleavage is only localized along highly deformed detachment zones. Therefore the intensity of cleaving corresponds to a gradual increase in the shear strain towards the northeast. This explains the appearance of the schistosity cleavage in the extreme NE of the Nakhal culminations. The inclination of the NE-verging spaced pressure solution cleavage reflects the strain gradient of the shear deformation, as cleavage was originally initiated at acute angles to the shear plane, then subsequently rotated by the progressive shear deformation to eventually align parallel to the bedding-parallel detachments.

Further deformational structures developed by the NE-extension deformation are the boudinage structures. The boudins axes are oriented orthogonal to the stretching direction across the whole area and the amount of boudinage increases gradually from the SW to the NE. At the extreme NE of the Nakhal culmination boudinage is well established, recording stretching rate of some 80%.

The geometry, orientation and frequency of the NE-extensional fabrics express a steady increase in the intensity of the NE-directed shear deformation, in a northeastward trend. However, such deformation is greatly variable across the massif and these variations are pronounced from both steep faulting and layer-extension flow. The steep NW-striking faults collectively experience total fault throws of more than 3 km, while fault throws do not exceed 500 m in the western flank. The layer-extension flow is more amplified on the eastern flank, as evidenced from extensively developed recumbent folds and greenschist foliations, while the western flank exhibits NE-verging folds and non-penetrative cleavage.

The NW-SE contractional deformation

The NW-SE shortening deformation resulted in the development of massif-verging contractional structures on both flanks of the culminations. These structures are manifested by massif-verging thrusts, folds and cleavage. The shortening deformation is partitioned into plane and out of plane strain. The out of plane strain resulted in strike slip displacements along the NW-SE and E-W striking faults, while the plane strain is reflected by massif-verging thrusts, folds and cleavage. Deformation fabrics are common within the fine-grained Jurassic-Cretaceous units. A summary of all these structural elements is presented in Fig. 4-42 and synthesized below.

The NW-SE shortening deformation developed massif-verging thrusts and inverted pre-existing normal faults oriented at high angles to the shortening direction; such as the NNE-striking normal faults. Large scale hanging-wall anticlines and footwall synclines lying parallel to the massif were developed and marked by fold lengths of hundreds of metres, as seen in the wadi Tayah transect. On the contrary, such large scale folds and thrusts are missing from the western flank. This contrast is attributed to two factors: stronger contractional strain across the eastern flank compared with the western side and the existence of NNE-trending structural anisotropy along the eastern flank manifested by Triassic and Jurassic faulting. The occurrence of pre-existing NNE-oriented normal faults along the eastern flank but not the western side is attributed to basement structures of the Semail lineament situated along the eastern flank. Therefore, the identified Triassic and Jurassic faulting on the eastern flank were influenced by the underlying basement structures of the Semail lineament. Consequently, most of the large scale folds on the eastern flank are initiated by thrusting and inversion structures.

Contractional deformation fabrics were developed across the whole culmination, expressed by massif-verging folds and cleavage. These fabrics are common within thinly bedded units especially Jurassic-Cretaceous strata. The fold amplitude of the massif-parallel folds is variable across the massif; from centimetric scale on the western flank to metric scale on the eastern flank. This is attributed to high shear strain recorded along the eastern flank unlike the western side and this point is explored shortly. These folds are upright or steeply dipping to the massif and associated with massif-verging cleavage.

Pressure-solution cleavage accommodated part of the NW-SE shortening strain. The massif-verging spaced pressure solution cleavage appears robustly across the whole massif. In most cases it strikes generally sub-parallel to the massif. This pressure solution cleavage underwent multiple phases to accommodate the progressive shortening deformation. Initially

orthogonal stylolites were formed, then massif-verging pressure solution cleavage, and eventually an extensional crenulation cleavage that truncated the earlier fabrics with a normal sense of shear, as identified along the Hedk and Dhabiah transects. Folding deformation was also accommodated through flexural slipping between the adjacent structural units, as evidenced from bedding-parallel slipping surfaces marked with calcite fibre lineations of a top-massif sense of shearing. In many cases the NE-extensional detachments within the Jurassic-Cretaceous succession were reused as slipping surfaces throughout the folding process.

The intensity of the contractional deformation is greatly variable across the massif. The eastern flank is dominated with massif-verging thrusts, folds and cleavage, while such deformation is much less developed along the western flank, with large scale thrusts and folds completely absent. Therefore towards the eastern flank there is an abrupt increase in the contractional deformation.

Linking between the extensional and contractional deformational systems

The interrelation between the extensional and contractional deformation is the focus of this section. It has been stated that the extensional deformation within the Jurassic-Cretaceous succession predates the folding deformation, while the extensional activity within the pre-Permian sequences outlasting the latest stage of the folding process as indicated by pure dip slip and strike slip fault striations.

The intensity of the extensional deformation increases towards the northeast, but this is not the case for the shortening deformation. This can be seen from the stronger extensional deformation at the Fanja zone of the Nakhal anticline, as reflected from the schistosity fabrics and high rate of stretching strain, while the NW-SE shortening deformation is missing. However, the eastern flank is characterized by intensively developed extensional and shortening deformation together. This means there is an interrelation between the gradient of shortening and extensional deformation. The highest gradient of shortening strain corresponds to a stronger extensional deformation, but the vise versa is not true, as seen at the Fanja zone. For this reason both extensional and contractional deformations therefore are interrelated to each other, and such relationship is clearly seen across the Nakhal anticline. The eastern flank is typified with intensively developed extension and contraction, while the western flank is marked with weakly developed extension and contraction.

Far south at the Afiah transects, deformation fabrics of both deformation systems are poorly developed. This is attributed to the decreases of extensional deformation in a SW trend, which subsequently resulted in weaker contractional fabrics.

The extensional structures appear everywhere throughout the whole anticline, whilst the shortening-related deformation fabrics appears robustly on flanks only. That is because the contractional fabrics have not developed on the fold crest, as documented at the Toyan transect. That is because the shortening-related structures are enhanced by bedding-parallel shearing, which accommodates the folding process. The bedding-parallel shearing is dominant over the fold limbs, but it is absent from the fold hinge area.

Furthermore, the massif is marked with two other styles of faulting. The first style is steeply dipping normal faults rounding the entire massif with down-throw away from the massif. In this system the allochthons and the Maastrichtian Aruma sediments are displaced down slope away from the massif. In the Fanja zone, these faults are marked with Listwaenite thermal deposits. Kinematically, these faults are purely dip slip with a small component of strike slip. Localization of these faults around the massifs may suggest that they took place after or during the latest stage of the folding process. The second style of faulting is only localized on the eastern side of the massif, through a series of steeply dipping normal faults. These faults truncate and hence postdate the km-long NW-oriented faults. The NNE-striking faults are localized on the eastern flank along with the fold crest, dipping towards and away from the massif and penetrating the whole stratigraphic profile. For this reason they cannot be related to an outer arc extension. Kinematically the faults are dominated with dip- and strike-slip lineations, but oblique lineations to both sides are also common. Mechanisms behind both faulting styles will be explored in the next chapter.

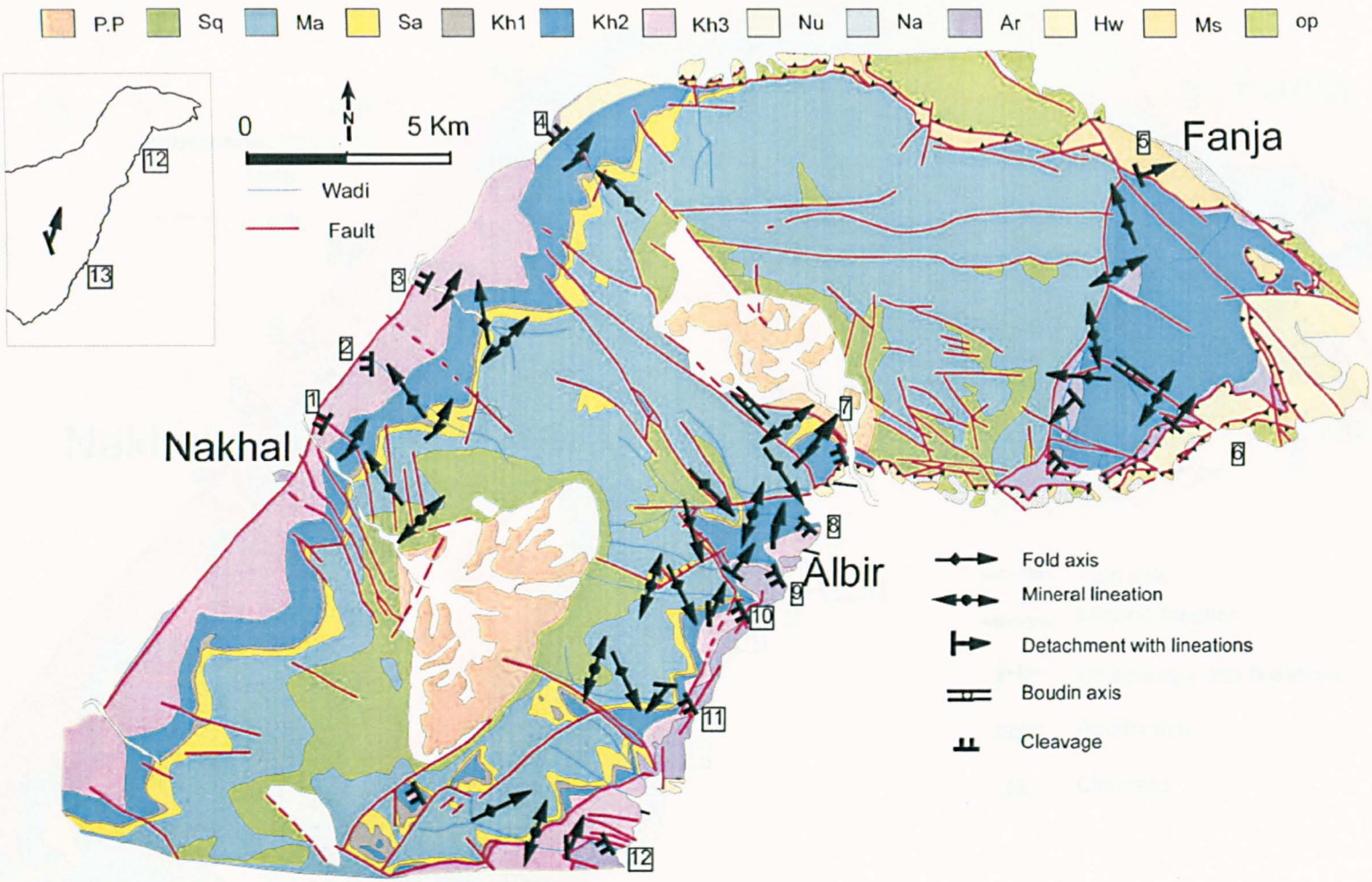
P.P
Sq
Ma
Sa
Kh1
Kh2
Kh3
Nu
Na
Ar
Hw
Ms
op
0
N
5 Km
Wadi
Fault
Nakhal
Fanja
Albir
Fold axis
Mineral lineation
Detachment with lineations
Boudin axis
Cleavage

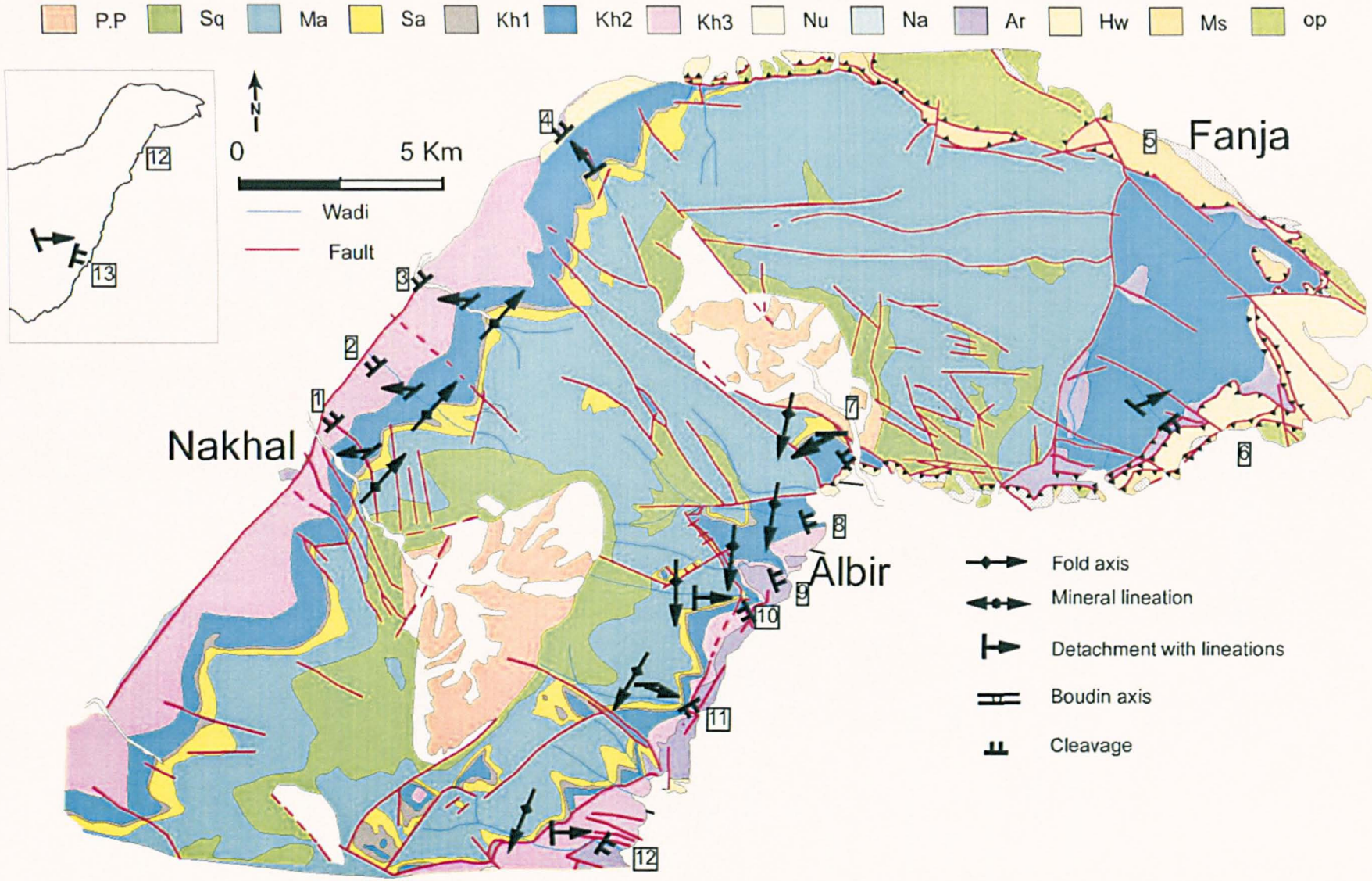

Fig. 4- 42 Summary of the NW-SE directed shortening deformation along each transect of the Nakhal anticline

Chapter 5: Saih Hatat

5.1 Introduction

The Saih Hatat culmination situated, due south of Muscat is the easternmost window of the northern Oman mountains (Fig. 1.1). Saih Hatat is well known by its HP rocks of eclogite and blueschists facies, which were formed and exhumed during the Late Cretaceous in a convergence setting (Miller et al. 2002 and Searle et al. 2004). Although the HP rocks of the Saih Hatat culmination are well studied, the mechanisms of formation and exhumation of such rocks are still controversial among various authors, including Jolivet et al. (1998); Miller et al. (2002) and Searle et al. (2004). The present study aims to give an insight into the exhumation and folding of the northern Oman Mountains, by correlation of the structural deformation of the shallowly buried rocks in the Akhdar-Nakhal culminations with the deeply buried rocks of Saih Hatat. Because Saih Hatat has been thoroughly studied previously, only short reconnaissance field work has been conducted in Saih Hatat. This study centers on the exploration of the NNE-directed extension, which was pointed out by Jolivet et al. (1998) and Breton et al. (2004), along with the investigation of the N-S trending upright folds.

5.2 Structural setting of Saih Hatat

The Saih Hatat window is rimmed by the Mesozoic carbonates and exposes some of the deepest level rocks in the Oman Mountains. Large tracts of over turned rocks on the eastern limb of the Saih Hatat dome were identified initially by Glennie et al. (1974) and subsequently interpreted as part of a common limb between a regional, NE-facing anticline and a large synformal isocline exposed in wadi Meeh (Fig. 5- 1)(Miller et al. 2002). The core of the culmination is occupied by strongly deformed pre-Permian rocks, which exhibit well developed NNE stretching lineations. Any pre-Permian deformation has been intensively overprinted by the Late-Cretaceous deformation. The HP rocks which typify Saih Hatat are exposed at the extreme NE of the culminations. Eclogites occur within the mafic boudins exposed in the Sifah area (El-Shazly, Coleman et al. 1990).

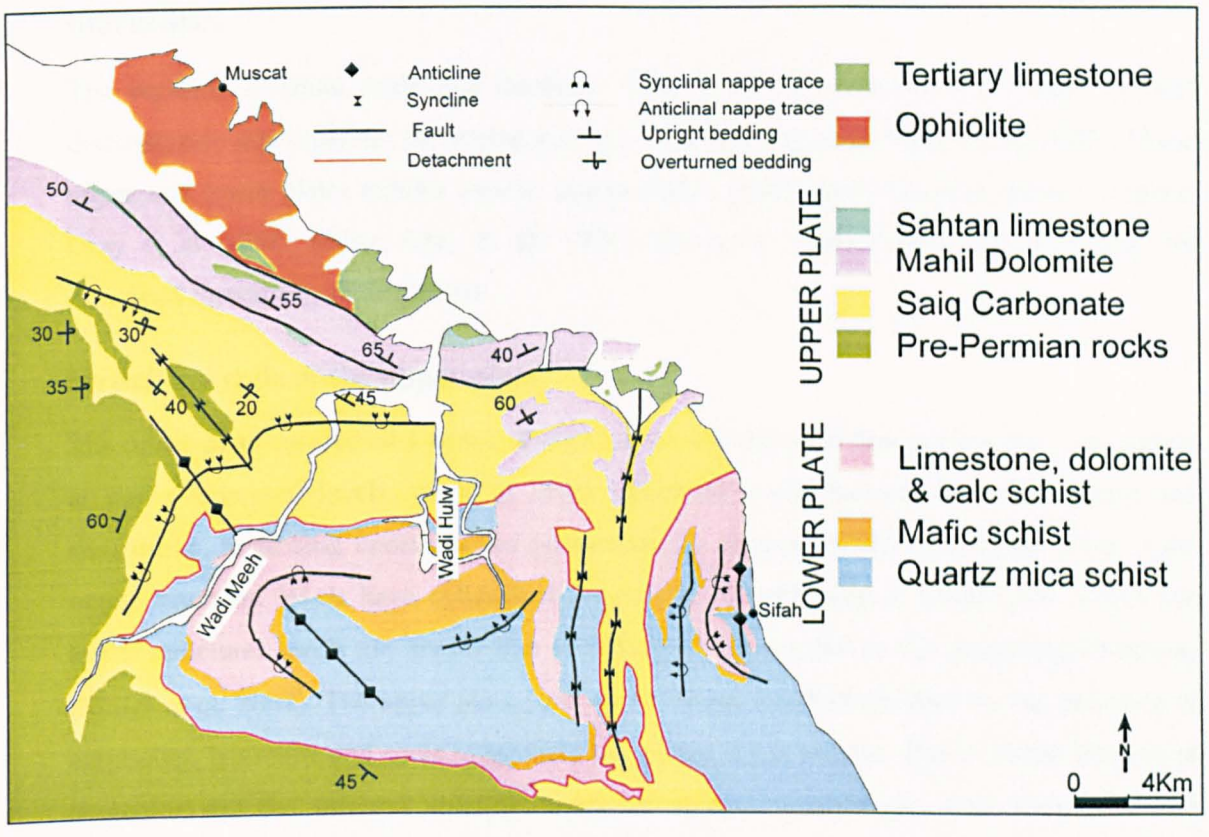

Fig. 5- 1 Geological map of northeastern Saih Hatat (modified after Gray et al. 2004). The upper and lower plates are separated by a major detachment. Notice the N-S trending upright folds in the eastern side of the massif.

5.3 The structural geology of HP rocks in Saih Hatat (according to the literature)

The regional isoclinal folds that dominate Saih Hatat are truncated by a major crustal discontinuity that separates the region into upper and lower plates (Miller et al. 2002). These upper and lower plates exhibit various metamorphic grades and structural styles (Gregory, Gray et al. 1998; Miller, Gray et al. 1998). Structural characteristics of each plate are described thoroughly in turn below.

Structural style of the upper plate

The upper plate consists of a series of regional recumbent folds that thicken the stratigraphy at upper structural levels, while at lower structural levels become more attenuated and sheath-like. Stretching lineations are predominantly oriented NNE. Recumbent folds at the upper structural levels have cylindrical forms and NW-SE hinges, while folds within the lower structural levels are sheath-like with hinges sub-parallel to the stretching lineations (Miller et al. 2002). The upper plate peak assemblages are distinguished by the presence of carpholite, lawsonite and sodic amphibole but garnet is not present. Based on the absence of aragonite and the inferred stability fields of magnesio–carpholite, ferro–carpholite and chloritoid, El-Shazly (1994.1995) pointed out that these upper plate units were metamorphosed between 6.8 and 9 kbar and 315 and 435°C. This plate contains extensive crenulation cleavages that are axial planar to the upper plate nappes. Asymmetric shear sense indicators are rare, but minor asymmetric pressure shadows suggest a top-NE sense of shear (Miller et al. 2002).

Structural style of the lower plate

The lower plate displays pervasive NE-directed non-coaxial shear with associated schistose L–S tectonite fabrics and sheath-folds at all scales. Folding in the lower plate reflects fold interference between regional-scale, sheath-like, recumbent isoclines and more open, upright northwest-, north- and northeast-trending fold sets. Different shear sense indicators reveal top-NNE shearing, including: C- and C′- shear bands, asymmetrically sheared clasts and pressure shadows around porphyroblasts. Deformed conglomerates and calc schists within the lower plate indicate a component of flattening, accompanied by stretching along a NNE trend, the maximum principal elongation direction. This produces flattened 'cigar-like' forms and extensive shear bands. The lower plate is folded by a series of sheath-like regional recumbent folds that trend parallel to the stretching lineations (Miller et al. 2002). The

eclogite facies exposed in the easternmost exposure of the lower plate at As Sifah, record minimum pressures of approximately 10–12 kbar (El-Shazly et al. 1990), with temperatures estimated at 500–580°C (El-Shazly, Coleman et al. 1990).

N-S trending folds

The N-S folds across the Saih Hatat culmination are observed by Miller et al. (2002), Gray et al. (2004) and Searle et al. (2004). Such folds were described as later, upright, N-S trending folds affecting both the lower and upper plate structures. However, the folding mechanism of such folds is still ambiguous and unexplained.

Timing of the eclogite metamorphism

The timing of peak high-pressure metamorphism within the eclogites of Saih Hatat is controversial. Rb-Sr (El-Shazly et al. 2001) and $^{40}Ar/^{39}Ar$ cooling ages (Miller et al. 1999) are given as 82-78 Ma. These ages are broadly consistent with the stratigraphic ages on the timing of orogenesis in the northern Oman Mountains. However, Gray et al. (2004) reported Sm-Nd ages on high-pressure garnets from As Sifah of c. 110 Ma, data which they interpreted as reflecting the timing of subduction of this part of continental crust. It is difficult to attribute these ages to the age of the oceanic lithosphere, which is generally considered to have formed the hanging-wall of this subduction zone (Searle and Cox 1999). The oceanic lithosphere, preserved as the Semail Ophiolite, gives ages for the formation of this crust that are much younger (c. 80 Ma, El-Shazly, Coleman et al. 1990). For this reasons, the nature of the subduction zone that generated the high-pressure metamorphism in Saih Hatat is a matter of continuing debate (see Gray & Gregory 2004).

5.4 Results of the current work

Structural style of the upper plate

The collected structural elements throughout the Saih Hatat culmination are attached with a N-S transect constructed by Jolivet et al. (1998), collectively are presented at Fig. 5- 2.The lower part of the Permian Saiq carbonates, which mark the base of the upper plate, is exposed at the southern part of wadi Meeh (Fig. 5- 1). The upper plate is folded by a regional synformal isocline exposed in wadi Meeh and as a result, structures within the upper plate consist of a series of regional recumbent folds (Fig. 5- 3). These folds appear at all scales, from regional to outcrop. The trends of the fold axes are variable, but tend to cluster along

two trends: NW-SE and NNE-SSW (Fig. 5- 2). Extensive axial planer fabrics are associated with the recumbent folding. The carbonate layers are disrupted into large boudins by shallowly dipping faults. These disrupting faults merge onto boudinage-bounding detachments characterized by NE-SW trending lineations (Fig. 5- 2). The NE-SW stretching lineations are pervasively developed over the whole upper plate. It seems to be that, boudins axes are aligned highly oblique to the stretching direction. Extensively developed bedding-parallel stylolites are folded by the isoclinal folds.

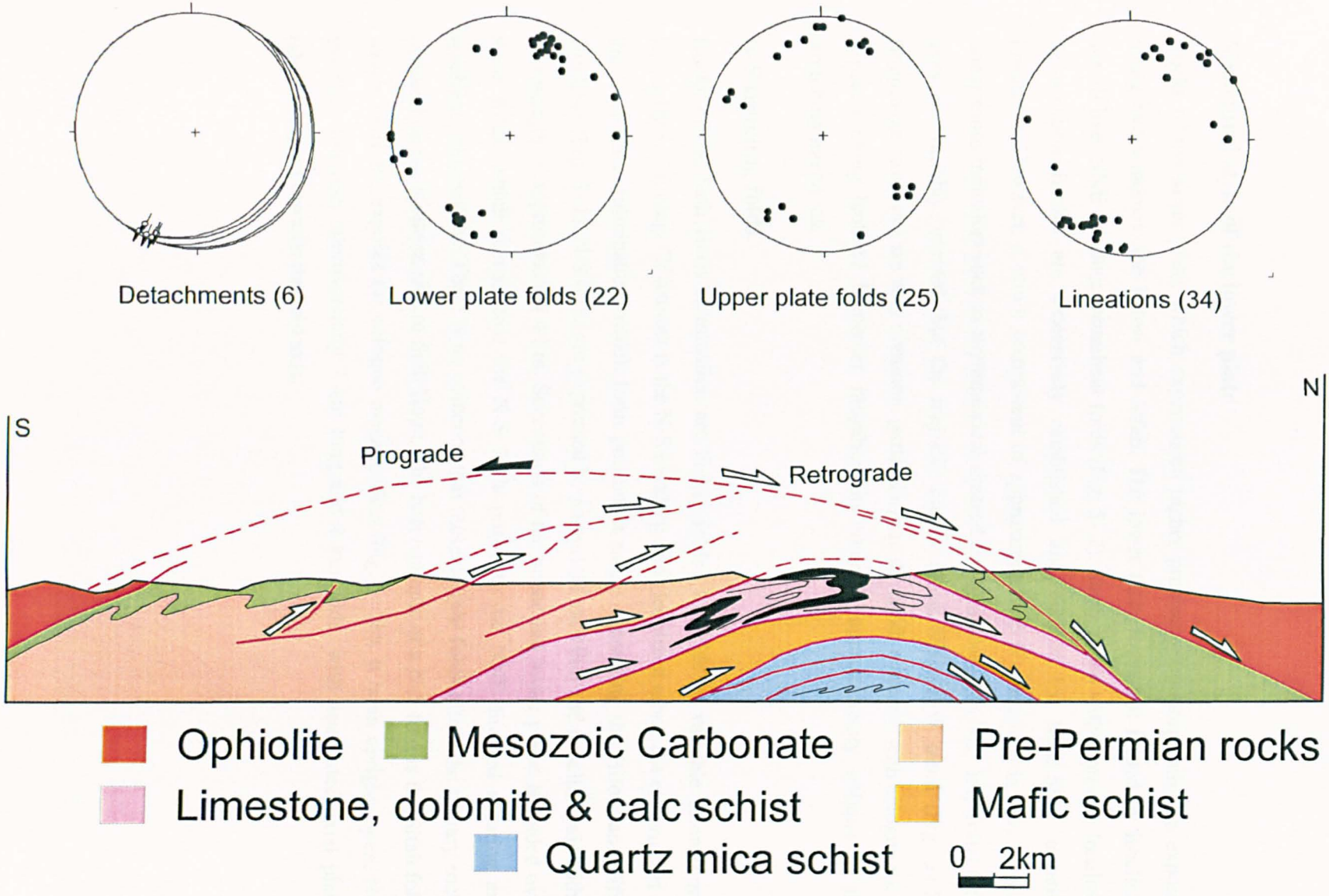

Fig. 5- 2 Structural transect across the Saih Hatat culmination with stereograms of the various structural elements collected along the transect (the transect is adapted from Jolivet et al. 1998)

Structural style of the lower plate

Rocks of the lower plate, which experienced higher pressure metamorphism, are exposed along two windows: the Hilow and Sifah. The lower plate rocks are folded by isoclinal, sheath like, NNE-trending recumbent folds (Fig. 5- 2). Shear zones with intensive localized deformation fabrics are extensively established and marked by NNE-SSW trending lineations. However, a minor component of approximately E-W lineations is also present. Shear sense indicators such as asymmetrical sheared clasts indicate top-NE. Intrafolial folds axes are variably oriented, but the majority cluster along NNE-SSW trend (Fig. 5- 2). Boudinage structures are very common, particularly in the Sifah window, with eclogite rocks exposed along isolated lenticular megaboudins trending approximately oblique to the stretching lineations.

N-S trending folds

Rocks of the Saih Hatat culmination are highly folded by folds of variable orientations, geometry and timing. Of interest is the N-S trending folds localized along the eastern part of the Saih Hatat culmination, which form prominent ridges separating the Hilow and Sifah windows (Fig. 5- 1). N-S folds are expressed by an upright anticline and syncline pair with a wavelength of approximately 4 km. Succession of the upper and lower plates is folded over these folds, which reveals that the N-S folds post-date the NNE-directed shearing and resultant culminations. There is no evidence that these upright folds affect the tertiary rocks exposed on the northern side of Saih Hatat. The best example of a N-S fold is the Sifah fold, which folds and exposes the eclogite megaboudins (Fig. 5- 3b). It is an upright, open, N-S trending anticline, approximately 7 km long and 1 km wide, with associated axial plane fabrics verging towards the fold axis.

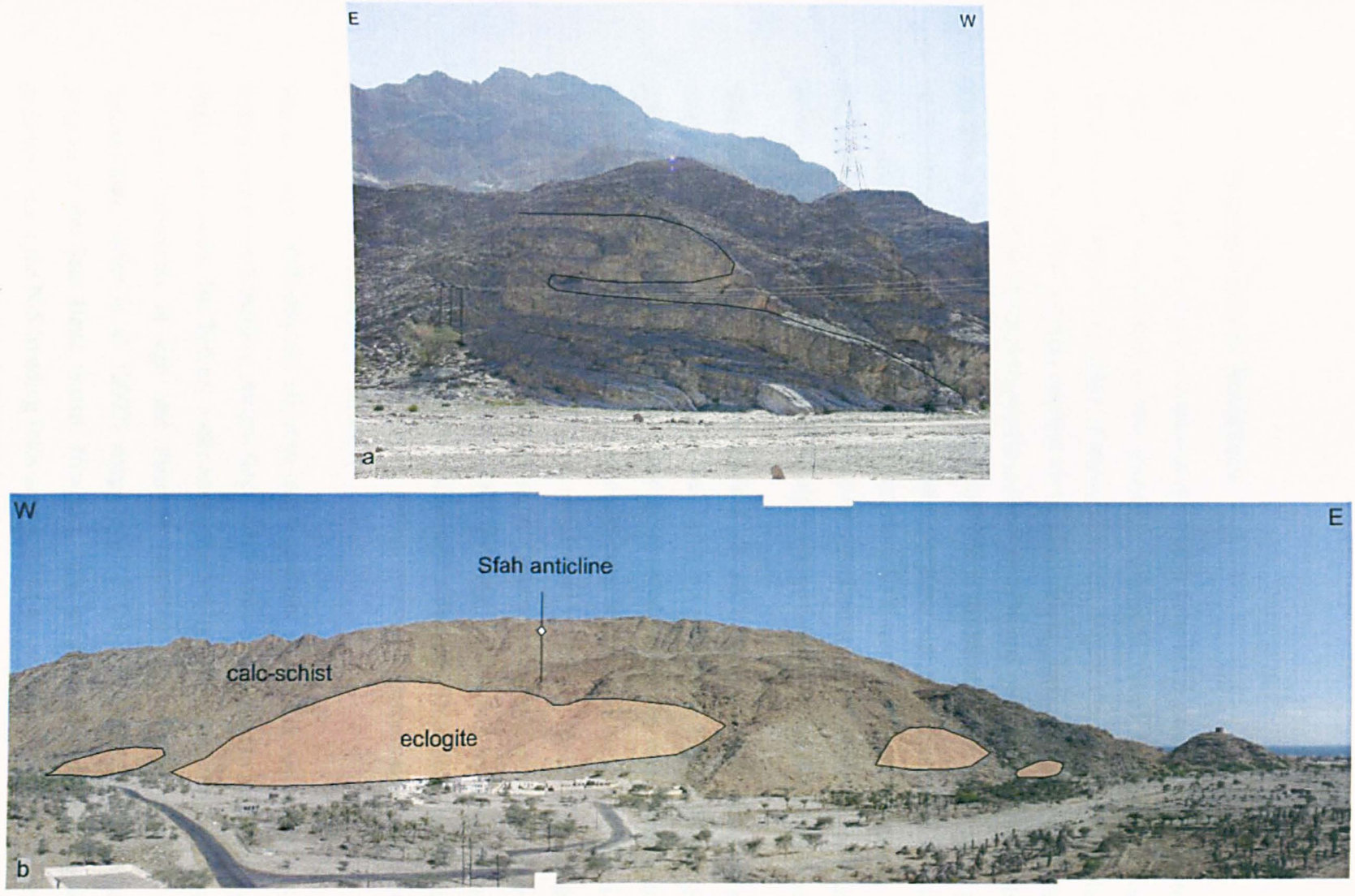

Fig. 5- 3 Different folding styles within the Saih Hatat culmination. (a) a NW-oriented isoclinal rechumbent fold within the Saiq carbonates of the upper plate (field of view is approximately200 m). (b) N-S trending Sifah anticline, where the eclogite is exposed in an isolated boudins folded by Sifah anticline (field of view is approximately2 km)

5.5 Interpretation and Summary

The Saih Hatat massif is a culmination of variably oriented regional folds. Structurally, Saih Hatat can be classified into two distinctly deformed plates that experienced different deformation intensity and grade of metamorphism, despite the fact that both plates exhibit persistent top-NNE shearing marked by NNE-stretching lineations. The upper pate displays isoclinal recumbent folds that are aligned both parallel and orthogonal to the NNE stretching lineations. The NNE-trending folds are common in the basal section of the upper plate, close to the discontinuity surface which separates the upper and lower plates. On the contrary, the lower plate is marked by isoclinal, sheath-like, NNE-trending folds. Eclogite is exposed in this plate within megaboudins separated by detachment zones. However carbonate boudins in the upper plate are separated by low-angle normal faults merging onto detachment.

The associated metamorphic assemblage of each plate reflects greatly variable PT conditions. If the lower Sifah eclogite unit reached a pressure as high as 25kbar (Searle et al. 2004), a maximum of 12-15 kbar only is recorded within the upper plate (Jolivet et al. 1998).Thus a pressure gap of 10 kbar would exist between the two plates. Such a pressure gap may indicate a tectonic denudation, which could suggest an extensional deformation. If this was the case then the discontinuity surface between the upper and lower plates would be an extensional detachment with top-NNE shearing, as inferred from the persistent NNE stretching lineations and the associated kinematic indicators. These ideas will be investigated thoroughly in the Discussion chapter, where structural deformations from the various culminations are linked and correlated.

The pervasive NNE-directed shearing and resultant recumbent nappes of both plates are folded over the N-S trending upright folds, which are concentrated in the NE part of the Saih Hatat culmination. The Tertiary rocks are unaffected by these folds, revealing that they must be Late-Cretaceous in age and therefore possibly part of the ongoing NNE-shear deformation. Miller et al. (2002) suggested that the upright folding occurred prior the doming of the Saih Hatat massif. However, field evidence for such a suggestion is not definitive, since the N-S trending folds are localized across the gently dipping northern flank of the culmination. These folds will be explored in great detail and correlated with the Nakhal anticline in the Discussion chapter.

Chapter 6: Data synthesis

6.1 Introduction

The Oman orogen is dominated by NNE-extensional deformation, which is locally partitioned into orthogonal extension and contraction. Both styles of deformations are analyzed thoroughly across the northern Oman Mountains. The NNE-extensional deformation is manifested by a linked system of steep faults and layer-parallel extensional shearing. The contraction deformation is oriented NW-SE and expressed by lineation-parallel folds.

6.2 Top-to-the-NNE layer-extensional shearing

Layer-extensional shearing is manifested by low angle faults associated with extensively developed deformation fabrics. They are localized within the fine-grained units, commonly in Jurassic-Cretaceous strata. The low angle faults shallow downwards and become bedding-parallel. These low angle faults are characterized by intensive localized shear deformation and are marked with NNE-trending lineations. Variously deformed strata are separated by these low angle faults and therefore behave as detachments. As a result, these faults are called bedding-parallel or subparallel detachments throughout the thesis. The intensity and geometry of the associated structures vary with a NE trend, extending from the southern flank of the Akhdar anticline to the extreme northeast of Saih Hatat (Fig. 6- 1). Such variations are described below.

Across the southern flank of Jebel Akhdar, layer-extensional shearing is manifested by NNE-verging spaced pressure-solution cleavage and bedding-parallel detachments with NNE-trending mineral lineations. Bedding-confined faults and intraformational folds are rarely developed. However, the northern flank shows extensive evidence for low-angle, northward directed extension. This is chiefly expressed in the Cretaceous interbedded shale and limestone of Cretaceous age and is shown by a linked system of shear and detachments. Bedding-confined, NW-oriented steep faults observed at a high angle to bedding branch onto bedding-parallel detachments (Fig. 6- 1). Listric low angle dipping faults inducing hanging-wall anticlines are prominent, before becoming bedding-subparallel detachments. The estimated displacements of these low angle faults are otherwise of hundreds of meters, as detected from the hanging-wall and footwall ramps. The detachments show top-to-the-NNE shear senses. Steep faults concentrate within competent units and form extensional duplex

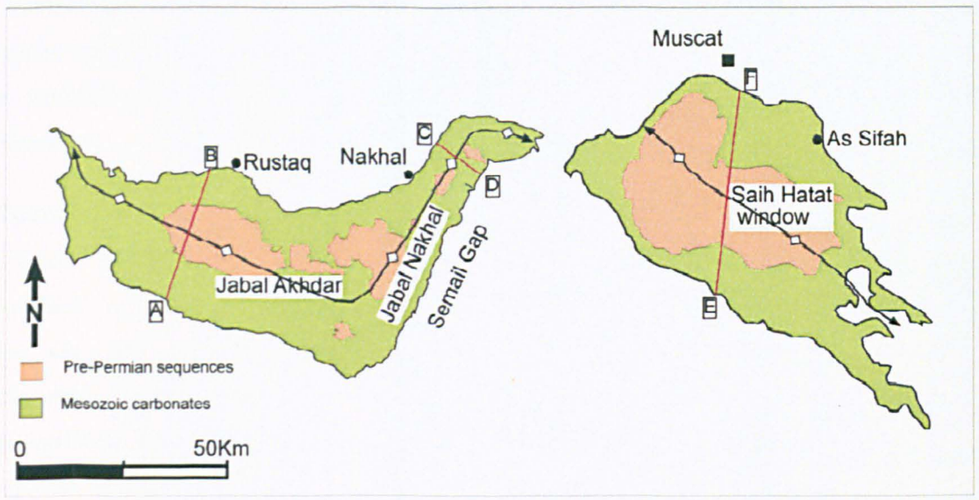

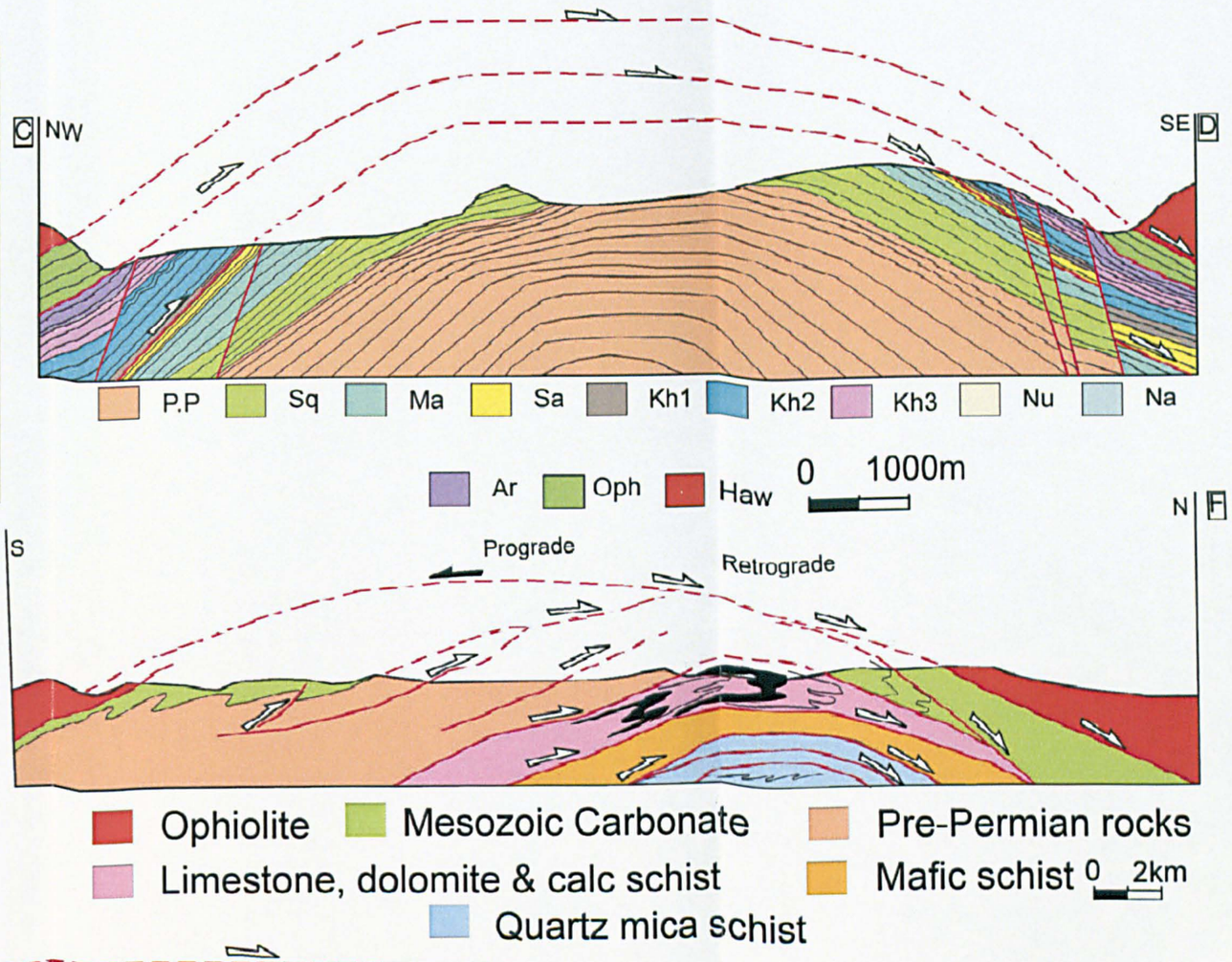

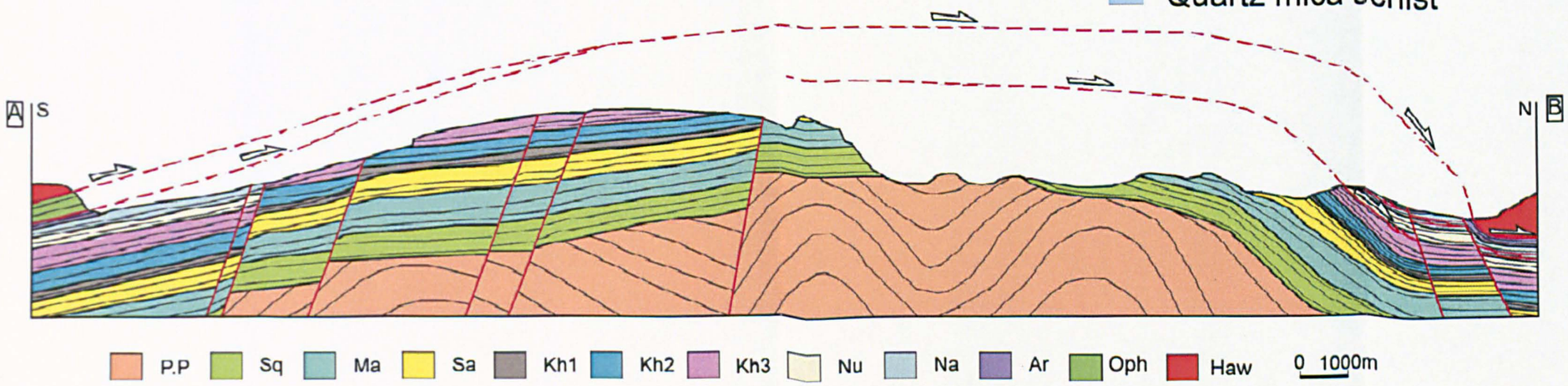

Fig. 6.1 Structural transects across the Akhdar-Nakhal-Hatat culminations of the Oman orogen, the Hatat transect is modified after Jolivet et al. (1998)

structures bounded by bedding-parallel detachments. However, where detachments are situated, incompetent units are deformed in a ductile manner to form NE-verging folds and cleavage. Intraformational folds exhibit open to close interlimb angles and are marked with hinges oriented orthogonal to highly oblique to the NNE stretching direction (Fig. 6- 2). Boudinage structures with NW-oriented boudin axes are common within the interbedded shale and limestone succession, but reflect only a small amount of stretching.

In Jebel Nakhal the NNE-extensional shearing is extensively developed, however it is slightly different to what is observed in Jebel Akhdar (Fig. 6- 1). Low angle faulting and bedding-confined faults are less common, while bedding-parallel detachments and ductile deformation are more pronounced compared with Jebel Akhdar. Bedding-parallel detachments appear approximately along every incompetent unit within the Jurassic-Cretaceous succession and are marked by NNE lineations. The detachments are marked with numerous sheets of calcite mineralization reflecting several consecutive shear movements, while bedding-confined faults are oriented NW-SE and NNW-SSW. Intraformational folds are extensively developed at varying scales and orientations. The attitude and geometry of folds vary consistently along the Nakhal anticline (Fig. 6- 2). In the southwest folds have centimetric amplitude, open to close interlimb angles, NW-SE oriented hinge lines, tilted axial plane and NE-directed vergence. Conversely, in the extreme northeast at wadi Meeh in particular, some folds have metric amplitude, tight to isoclinal interlimb angles, NNE-SSW oriented hinge lines and horizontal axial planes. Boudinage structures with NW-SE boudin axes record a maximum amount of stretching of 68% and foliations are common along the detachment zones. The metamorphic gradient increases toward the northeast, where it reaches the greenschist facies at the extreme northeast of the Nakhal culmination. Extensional deformation across the Nakhal anticline increases from the western flank towards the eastern flank, as shown by an increase in intensity and frequency of extensional fabrics. An example of this can be seen with the more frequent detachments and recumbent folds on the eastern flank.

The maximum gradient of the NNE-extensional shearing is recorded on Saih Hatat, where detachments of more than 10 kbar metamorphic gap (Jolivet et al.1998) separate variously deformed and metamorphosed units, called upper and lower units (Fig. 6- 1). Top-to-the-NNE shear deformation within the upper units induced isoclinal recumbent folds, which are oriented both parallel and orthogonal to the NNE stretching lineations (Fig. 6- 2). The lower unit however is characterized with isoclinal sheath-like recumbent folds aligned parallel to the stretching direction (Fig. 6- 2). Eclogite rocks are exposed along boudin structures within the lower plate and penetrative NNE-verging cleavage appears throughout the area.

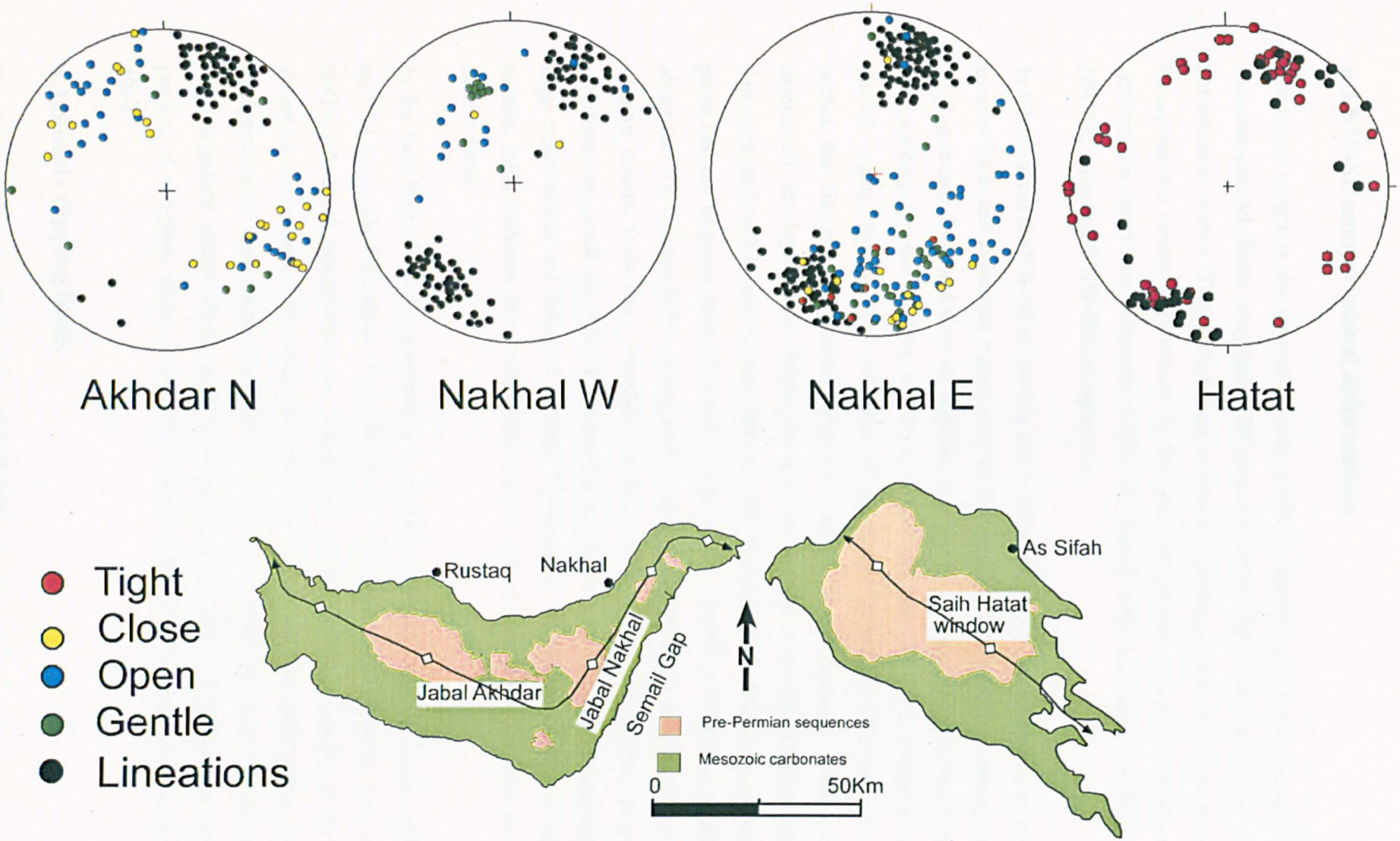

Fig. 6- 2 Lineations and fold hinge data throughout the various culminations of the Oman orogen. Note that folds are classified according to their interlimb angles

6.3 NW-SE compressional deformation

The Oman orogen is also characterized by a NW-SE shortening deformation, manifested by lineation-parallel folds, conjugate NW-oriented strike slip faults and other associated deformation fabrics. This deformation is locally developed and shows great variability throughout the various culminations. In the Jebel Akhdar there is no clear evidence of such deformation, apart from conjugate weekly developed strike slip faults trending E-W and NW-SE, reflecting WNW-ESE compression.

In Jebel Nakhal the NW-SE shortening deformation resulted in the development of lineation-parallel folds and associated massif-verging contractional structures, comprising of massif-verging thrusts, folds and cleavage together with bedding-orthogonal stylolites. In places the NNE-striking Jurassic faulting has been inverted by the NW-SE contraction and form massif-verging, hanging-wall anticlines. Contractional deformation fabrics are common within the fine-grained Jurassic-Cretaceous units. Lineation-parallel folds, which are extensively developed in the Nakhal anticline, are upright or steeply dipping to the massif and associated with massif-verging cleavage. The shortening deformation is partitioned into plane and out of plane strain. The out of plane strain resulted in strike slip displacements along the NW-SE and E-W striking faults, while the plane strain is reflected by massif-verging thrusts, folds and cleavage. On the western flank, contractional structures are manifested by small size fabrics represented by massif-verging folds and cleavage, while large scale thrusts and folds are missing. Furthermore, the fold amplitude of the massif-parallel folds increases from centimetric scale on the western flank to metric scale on the eastern flank.

In the Saih Hatat, NW-SE compression is probably expressed by two phases of lineation-parallel folds. The first phase is manifested by N-S trending upright folds, over which the NNE-extensional deformations are folded. The second phase is expressed by isoclinal sheath-like recumbent folds extensively developed throughout the culmination. In general, interpretation of such sheath-like folds is controversial, since they are normally related to high-magnitude simple shear model (Cobbold and Quiquis 1980), but may also be the product of non-plane strain, coeval NW-SE layer-parallel shortening (Jiang and Williams 1999).

6.4 Steeply dipping faults

The Oman orogen is dominated by prominent NW-striking faults, particularly in and around the culmination structures (Fig. 6- 3). The NW-striking faults penetrate the whole

stratigraphic profile including the pre-Permian sequences. They are 2-30 km long with throw ranging from 50 m to over 1000 m. Investigating the timing relations between these faults and the folding of the culminations can be established across the Nakhal anticline, where both fold and faults are highly oblique, unlike the case for the Jebel Akhdar. The structural characteristics of the faults differ slightly across each culmination, as described below.

In the southern flank of Jebel Akhdar faults are dominant, closely spaced and generally oriented WNW-ESE with dip slip and strike slip lineations (Fig. 6- 3). In the northern flank, the NW-striking faults are widely spaced and marked with dip slip and strike slip lineations (Fig. 6- 3). However, where faults and fold axes are oblique some fault striations plunge to the NE and SE directions, as mapped in the Mistal transect. When tilting structures were restored by rotation around a 060/30 axis presumed parallel to the fold axis in that area, the plunging striations turned into dip slip. Furthermore, in places the steep NW-striking faults dipping towards the massif are characterized with up-thrown blocks overlaying the fault plane, and hence appear like reverse faults. When structures were restored around 060/30 axis, these reverse-like faults transposed into normal faults with down-throw towards the NE. Consequently the plunging fault lineations and the reverse-like geometry of some faults may reveal that these faults took place before or during the early stage of the folding onset. The allochthons contact with the Mesozoic carbonates along the northern massif boundary is commonly disrupted by steep faults with down-throw away from the massif. The trends of these faults vary in correspondence with variations in the culmination boundary, as both are parallel.

The Nakhal-culmination is characterized with several sets of steep faults marked by various kinematic data (Fig. 6- 3). The NW-striking faults across the Nakhal anticline exhibit four distinct fault lineations: oblique plunging towards and away from the massif, together with dip and strike slip lineations. The dip and strike slip lineations must be associated with faulting movements that occurred after the folding event as they are not affected by the folding deformation. The oblique lineations on the other hand seem to be affected by the folding deformation and therefore must be restored in order to analyzed. Restoring the folding deformation was undertaken by unfolding the structures around an approximately 040/40 axis, chosen to be parallel to the Nakhal anticline. The massif-plunging lineations turned into dip slip while those plunging away from the massif became strike slip. Consequently, the NW-striking faults were initiated as dip slip normal faults before or during the early stage of the folding onset as evidenced from the corresponding massif-pitching lineations. Subsequently they were reactivated as dip- and strike-slip faults after or during the latest stage of the folding

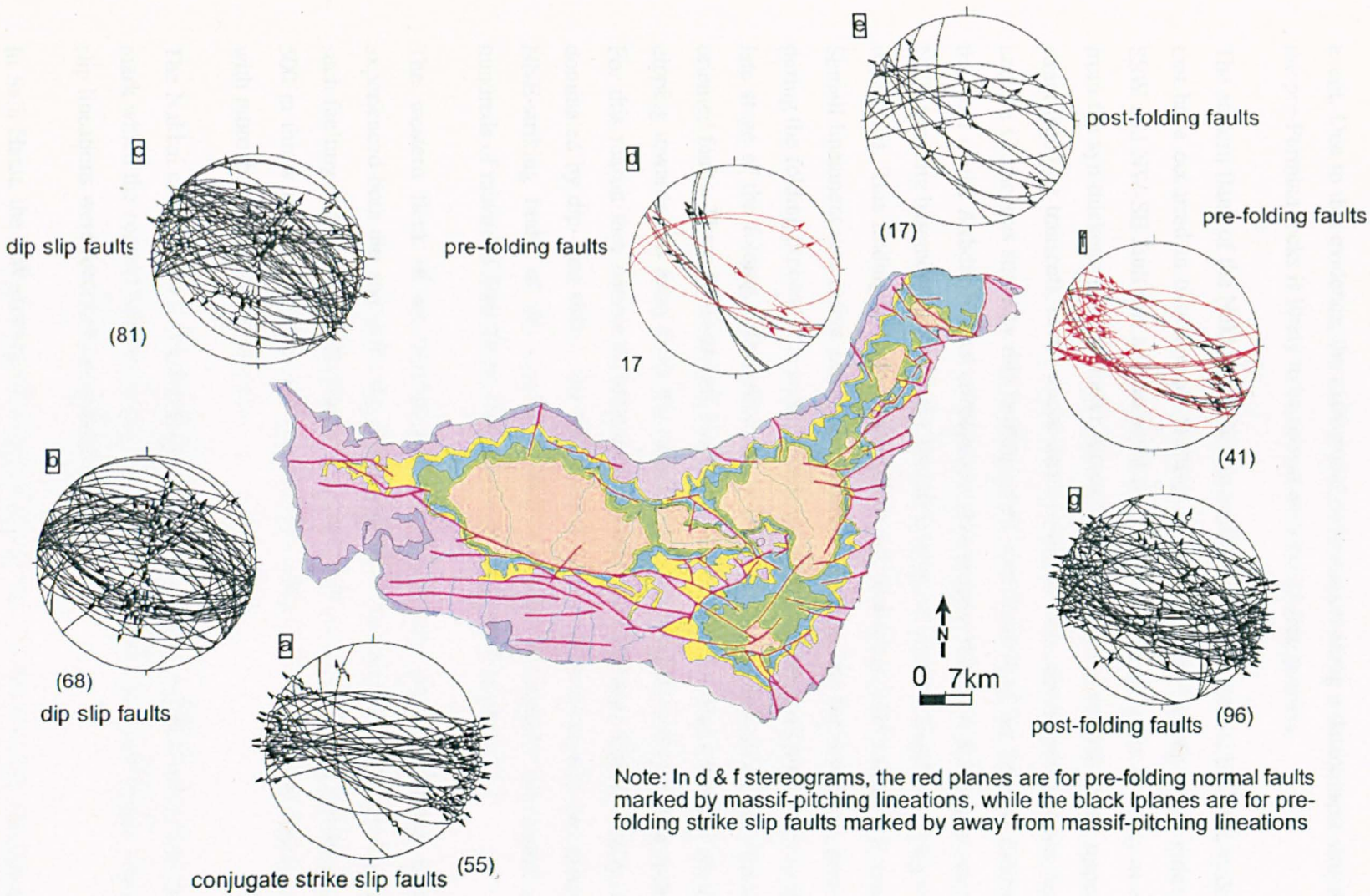

Fig. 6- 3 Attitude and kinematics of the NW-striking faults across the Akhdar-Nakhal culminations. (a and b) for the southern flank of Akhdar, (c) northern flank of Akhdar, (d &e) for the western flank of Nakhal, while (e and f) for the eastern flank of Nakhal

event. Due to this evidence, the extensional deformation along a detachment situated within the pre-Permian rocks is likely to be coeval with the folding process.

The eastern flank of the Nakhal anticline is exclusively characterized by NNE-striking faults that have occurred in two separate faulting events. The first faulting event induced NNE-SSW and NW-SE fault sets and occurred during the lower and upper Jurassic, as evidenced from the syn-thickening of the lower Jurassic units and partial erosion of the upper Jurassic strata (see Qet transect). Local minor unconformities were developed between the Jurassic and the Cretaceous strata by this faulting event. Localization of the Jurassic faulting within this part of the Akhdar-Nakhal culmination may suggest that such faulting is related to the NNE-trending basement structure, the Semail lineament, which is localized along this part of the massif. This finding is supported by Pratt and Smewing (1990) who indicated that the Semail lineament was active during the Jurassic. In places the Jurassic faults were inverted during the folding process. The second faulting event probably took place after or during the late stage of the folding deformation, since faults of this event truncate the km-long NW-oriented faults. These NNE-striking faults are localized on the eastern flank of the fold crest, dipping towards and away from the massif and penetrating the entire stratigraphic profile. For this reason they cannot be related to an outer arc extension. Kinematically, faults are dominated by dip- and strike- slip lineations, but oblique lineations are also common. The NNE-striking faults of the second faulting event are extensively developed and have hundreds of meters of fault throw compared with the Jurassic faulting.

The western flank of the Nakhal anticline shows only the NW-striking faults which experienced both dip and strike slip movements prior and after the folding event. However, such faulting is not strongly developed compared with the eastern flank, exhibiting less than 500 m throw in total, while in the eastern flank numerous NW-oriented faults are present with more than 3000 m total throws.

The Nakhal culmination is circulated by steep faults with down-throw away from the massif, mark which the contact between the allochthons and the Mesozoic carbonates. Dip and strike slip lineations were recorded along these faults.

In Saih Hatat, the NW-striking faults are common but to a lesser extent compared with the Akhdar-Nakhal culminations. Saih Hatat is also bounded by steep fault with down-throws away from the massif, marking the contact between the allochthons and the Mesozoic carbonates. The most prominent fault is the wadi Alkabir fault at the northwestern edge of the culmination. Searle et al. (2004) have reported that the Tertiary strata are displaced down towards north by 450 m across this km-throw fault.

6.5 The base of the Semail allochthon as an extensional detachment?

The allochthons that rim and structurally overlie the massifs of Arabian continental crust consist of the Semail ophiolite, metamorphic sole and thrust sheets of oceanic and continental margin rocks, known as the Hawasina units. The stacking of these sheets onto the Arabian continent has been explained in terms of simple thrust tectonic models (Searle & Cox 1999). Displacements on the base of the thrust sheet, comprising the Semail ophiolite plus its metamorphic sole, are shown transferring downwards onto the sedimentary cover of the Hawasina units. These are in turn accreted onto the allochthon that is them emplaced as a composite thrust sheet up onto the foredeep sediments of the Arabian continent. The frontal part of the allochthon comprises Hawasina rocks. In this sector of the orogen the Semail ophiolite does not abut the foreland. Consequently, a simple thrust interpretation predicts that everywhere throughout the northern Oman Mountains, Hawasina units should separate rocks of the Semail ophiolite from the rocks of the Arabian continent. The immediate footwall to the allochthon should be Aruma Group foredeep sediments. PT conditions for the metamorphic sole to the Semail ophiolite are estimated by Searle & Cox (1999) to lie between 5 and 10 kbar with temperatures of 700-900°C. For simple thrusting models to be valid, this requires the ophiolite Nappe sole to contain significant thicknesses (10+ km) of suboceanic mantle.

Fig. 6- 4 documents sites where the tectonic units have judged to have been removed from the allochthon zone. Although mantle rocks are found throughout the Semail Nappe, they are generally just a few kilometres thick. Furthermore, in places upper parts of the ophiolite stratigraphy lie directly against the Hawasina units. Elsewhere, ophiolite units lie on Arabian continental rocks, including directly on pre-Aruma sediments. In short the base of the allochthon nowhere shows the geometric relationships predicted by Searle & Cox (1999). The omission of expected units can be illustrated using a transect constructed across the Akhdar anticline (Fig. 6- 1). Here the Hawasina nappes are absent, while ophiolite units lie on the Mesozoic carbonates of the Hajar Super Group. This geometry is effectively explained by extensional faulting, dismembering the original thrust stack and reducing the thicknesses of once-continuous units. The present tectonic contacts are provisionally interpreted as forming an array of extensional shears associated with those within the underlying Hajar Supergroup.

A series of large-scale antiforms, within which the thickness of Hawasina units is preferentially preserved, are found in the allochthon around the Jebel Akhdar and Saih Hatat massifs. These folds do not continue down into the structurally underlying Arabian

continental rocks indicating that they are either detached upon, or have been truncated by, the base of the allochthons. The folds trend NNE-SSW, sub-parallel to the main Nakhal fold (Fig. 6- 4). Consequently the main allochthon in the northern Oman mountains shows evidence for extension (of the tectonic stratigraphy) and for orthogonal compression.

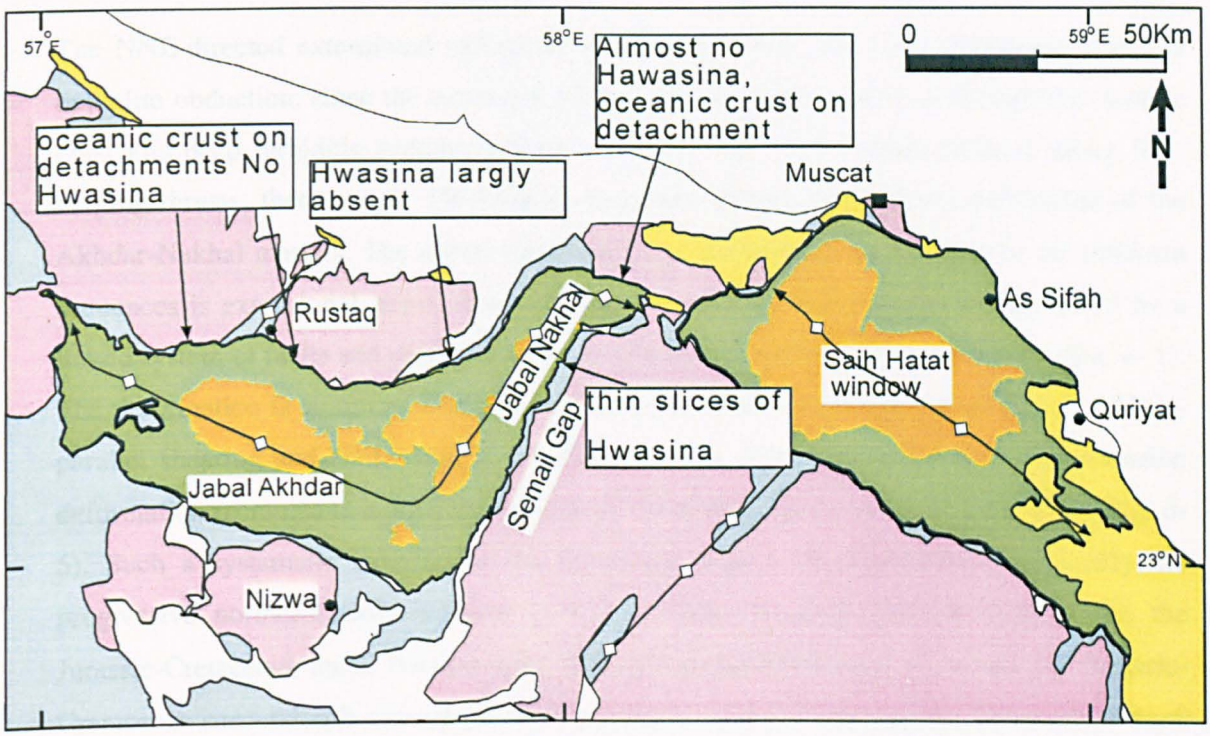

Fig. 6- 4 Collation of structural relationships at the base of the tectonic allochthon around the northern Oman Mountains

6.6 Interpretation and assessment of the relative chronology of various structural deformations

Various structural deformations have been developed within the Oman orogen comprising of top-to-the-NNE layer-extension deformation, steep NW-oriented faults, NNE-trending faulting and NW-SE contractional structures. Each phase of deformation is analyzed thoroughly and dated relatively, with respect to the other deformations. They are interpreted below in sequence, according to their relative chronology.

The Jurassic faulting

The oldest detectable deformation since Permian rifting is Jurassic faulting localized along the eastern flank of the Nakhal Anticline, probably connected with deformation along the Semail lineament. This deformation is manifested by an average of N-S oriented faults.

Since the Jurassic no clear evidence of tectonic activities can be recognized within the platform carbonates until the Late Cretaceous ophiolite obduction.

The NNE-extensional deformation

The NNE-directed extensional deformation occurred during the Late Cretaceous after the ophiolite obduction, since the extension affects the allochthons units. Although the oceanic crust and deep turbiditic sediments were obducted over the Arabian platform along SW-verging thrusts, there are no SW-verging structures within the platform carbonates of the Akhdar-Nakhal massifs. The oldest mappable Late Cretaceous deformation in the platform sequences is extensional, top-to-the-NNE kinematics. This deformation is manifested by a linked system of faults and detachments representing layer-extension deformation (Fig. 6- 1). The deformation is common within the Jurassic-Cretaceous succession marked by bedding-parallel shearing and NNE-verging ductile structures. The intensity of the layer-extension deformation increases in a NNE trend towards the deeply buried rocks of Saih Hatat (Fig. 6-5). Such a systematic increase in the depth and degree of deformation can justify the progressive northeastwards increase in the ductility of extensional shearing within the Jurassic-Cretaceous units. For example, NNE-extensional deformation within the Jurassic-Cretaceous succession is accommodated by pressure-solution cleavage on the southern flank of the Akhdar culmination, and by steep and low angle faulting across the northern flank of the Akhdar culmination. In the Nakhal culmination however, deformation tends to be more ductile, expressed by detachments and pervasive deformation fabrics such as intraformational folds and boudinage structures. In Saih Hatat, deformation is taken up mostly by extensively developed penetrative ductile deformation (Miller et al. 2002).

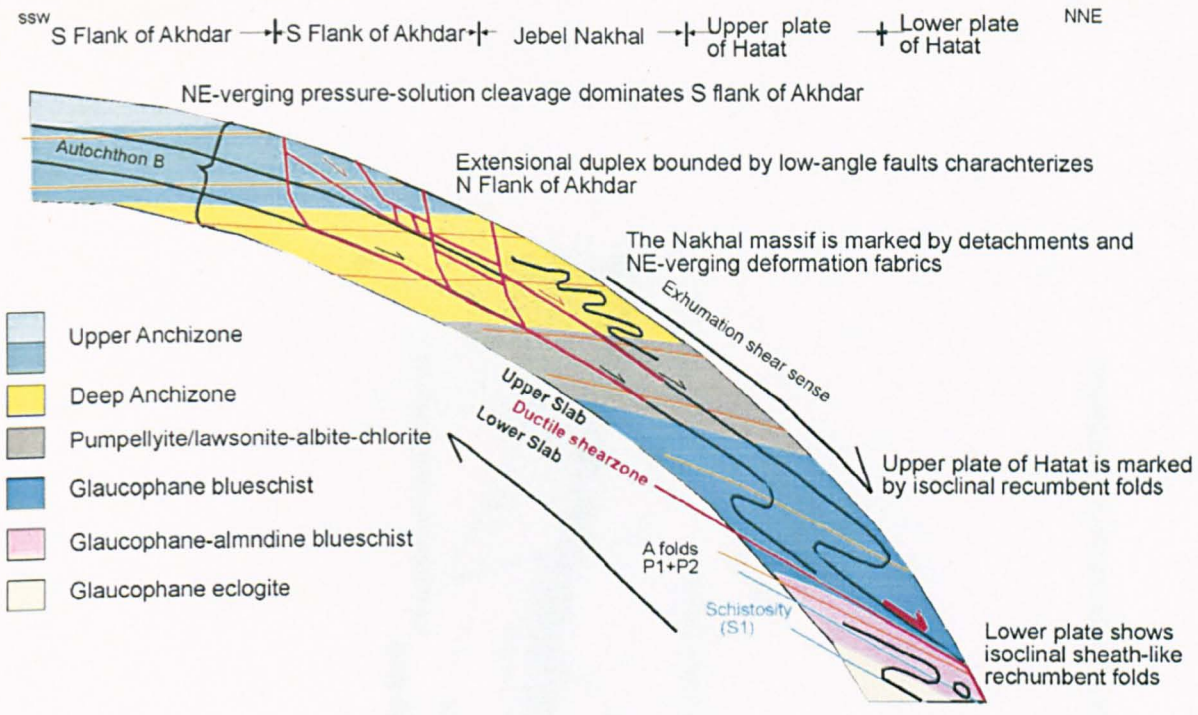

Fig. 6- 5 Schematic representation of geometry and kinematics of NNE-directed extension within the NE margin of the Arabian plate from SW of Jebel Akhdar to NE of Saih Hatat (out of scale) (adapted from Breton et al. 2004)

In the Akhdar massif, the NNE-extension deformation is mostly accommodated by NW-striking faults and layer-parallel extensional shearing developed extensively within the Jurassic-Cretaceous succession and transected by the steep NW-faults (Fig. 6- 6). These faults penetrate the entire stratigraphic profile and presumed merge onto a detachment situated within the pre-Permian units. It seems to be that extensional deformation has migrated downwards from base allochthons detachments to a detachment within the pre-Permian units through layer-parallel shearing within the Jurassic-Cretaceous units.

The NNE-extensional deformation marks its highest peak in the Saih Hatat culmination, where structural plates of more than 10 kbar pressure gap overlaying each other (Jolivet et al. 1998). These plates are separated by a major detachment of a top-to-the-NNE sense of shearing. The amount of extensional deformation increases downward towards the lower plate, which is characterized by the eclogite exposed within megaboudins. These boudins formed by the NNE-directed extension along ductile shear zones within the lower plate.

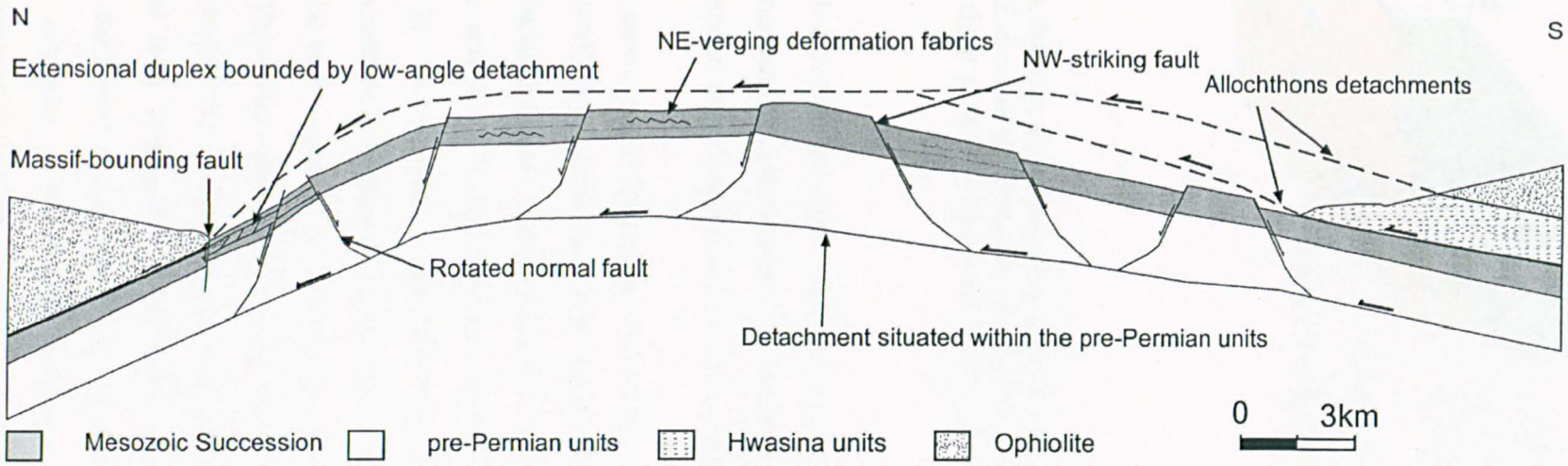

Fig. 6- 6 Schematic cross section across the Akhdar culmination illustrating the NNE-directed extensional deformation

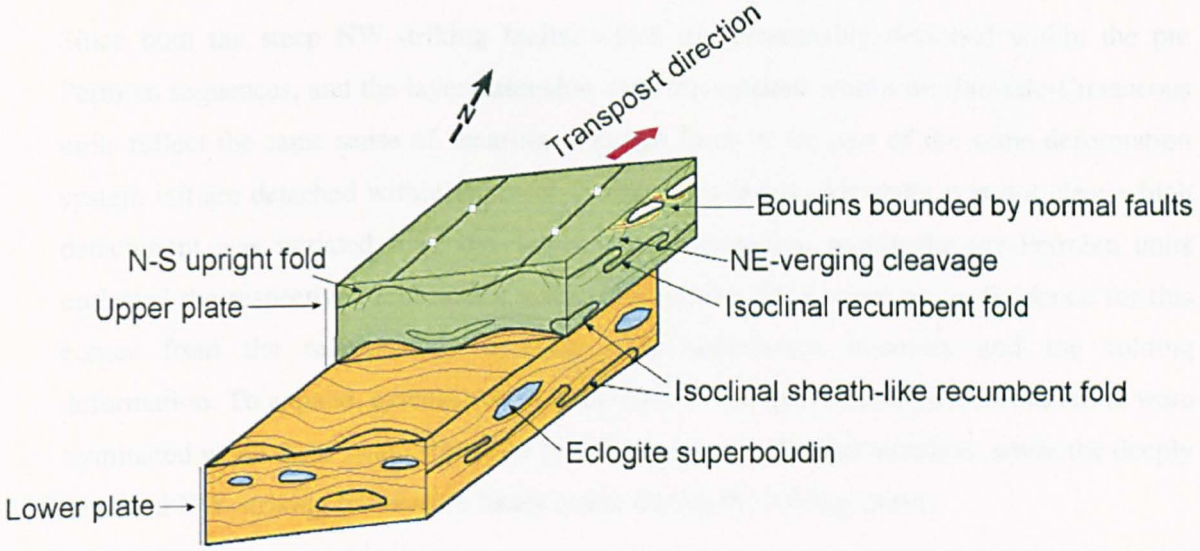

Fig. 6- 7 Schematic block diagram of the Saih Hatat massif showing the structural characteristics of the NNE-directed deformation within the upper and the lower plates, which are separated by a major shear zone of a top-to-the-NNE sense of shearing

However carbonate boudins within the upper plate are isolated by low-angle normal faults, which merge onto bedding-parallel detachments. These variations in the structural styles of the NNE-extension correspond to the depth of burial and the associated P-T conditions.

The steep NW-striking faults, which penetrate the whole exposed stratigraphic profile, crosscut the top-to-the-NNE layer-extension deformations situated within the Jurassic-Cretaceous units. The structural evolution and kinematics of the NW-striking faults can be revealed with confidence across the Nakhal anticline, where both faults and fold axes are highly oblique (Fig. 6- 3) . It has been found that these faults are marked by various lineations of different kinematics indicating that these faults were initiated as dip slip normal faults before or during the early stage of the folding event as evidenced from the massif-pitching fault striations. They were subsequently reactivated as dip slip and strike slip faults after or during the latest stage of the folding deformation. The dextral and sinistral strike slip components are arranged in a conjugate set reflecting NW-SE maximum compression direction, which matches the shortening direction inferred from the Nakhal folding. Because of this, top-to-the-NNE extension and NW-SE compression are probably coeval, and therefore NW-striking faults and the Nakhal folding are most likely synchronous.

Since both the steep NW-striking faults, which are presumably detached within the pre Permian sequences, and the layer-extension shearing situated within the Jurassic-Cretaceous units reflect the same sense of shearing, they are likely to be part of the same deformation system but are detached within different stratigraphic levels. Although it is not clear which detachment was initiated first, the detachment deformation within the pre-Permian units outlasted the respective deformation within the Jurassic-Cretaceous units. Evidence for this comes from the relationships between each detachment structure and the folding deformation. To expand, extensional detachments within the Jurassic-Cretaceous strata were terminated when these strata started to be folded over the Nakhal anticline, while the deeply detached NW-striking faults were likely active during the folding onset.

The NW-SE compression

The NW-SE compression is expressed chiefly by lineation-parallel folds together with conjugate strike slip faults, with the ideal examples being the Jebel Nakhal anticline and some N-S folds in the northeast vicinity of Saih Hatat. The amount of the NW-SE compression varies from one culmination to another. In Jebel Akhdar, the compression is mainly manifested by weakly developed conjugate strike slip faults with no lineation-parallel folds, hence deformation is apparently plane strain and solely top-to-the-NNE extension. However, in Jebel Nakhal the NW-SE compression is robust, together with the NNE-extension deformation and therefore deformation is non plane strain (Fig. 6- 8). Across Jebel Nakhal, the intensity and frequency of the NW-SE contractional structures, such as massif-verging thrusts, cleavage and the lineations-parallel minor folds, increase from west to east. Such a relationship could be attributed to the prominent Semail lineament, and kinematically this will be explored in the Discussion chapter. In Saih Hatat, which suffered the highest depth of burial, both top-to-the-NNE extension and NW-SE compression are strongly developed, revealing non plane penetrative deformation. Since the Oman orogen experienced various grades of NNE-directed simple shear deformation, how are lineation-parallel folds induced by the high grade simple shear model (as suggested by Miller et al. 2002 for Saih Hatat) distinguished from those induced by orthogonal NW-SE shortening (following a model proposed by Jiang and Williams 1999). In the simple shear model, where fold axes lie sub-parallel to the stretching lineation, it is commonly assumed that they have been rotated into such an orientation by very high simple shear strains (following the sheath fold model of Cobbold & Quinquis 1980) (Fig. 6- 9). For this to occur, these folds with axes that lie parallel to the lineation must have formed earlier and have been more greatly distorted than those with axes at a high angle to the lineation.

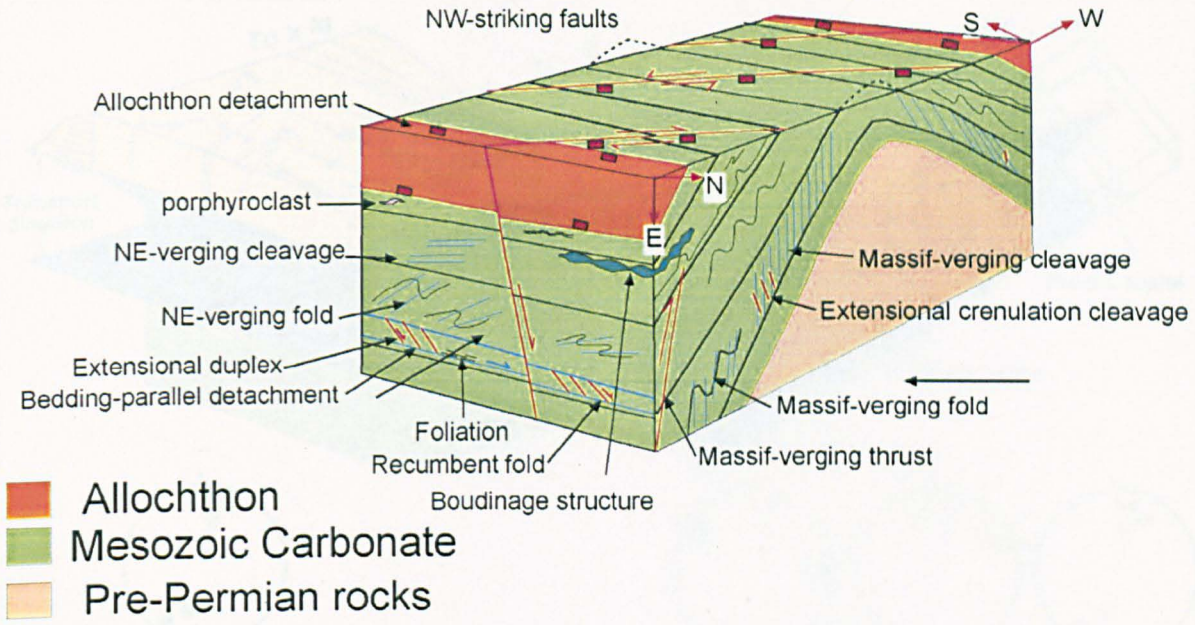

Fig. 6- 8 Schematic block diagram across the Nakhal culmination, which is marked by two orthogonal deformations: NNE-directed extension represented by NNE-verging structures, and NW-SE compression expressed by lineation-parallel folds and massif-verging fabrics.

To test this model fold interlimb angles are used as a proxy for the magnitude of the finite distortion of structures. NNE-trending fold axes should be associated with tight inter-limb angles while those trending perpendicular to the NNE-stretching direction should be gentle. However, the data for the three dip domains around the culminations do not show this pattern and there is no significant relationship between interlimb angle and orientation of the fold axis. Consequently it can be deduced that folding is not a simple result of plane strain, NNE-directed simple shear. The folds are better explained as the result of a mixture of layer sub-parallel, NNE-shear and nearly orthogonal layer-parallel shortening. Strain partitioning of these orthogonal components can explain the variations in fold geometry and orientation.

The NNE-oriented faults along the eastern flank of the Nakhal anticline

The eastern flank of the Nakhal anticline is characterized by NNE-oriented faults transecting the major NW-striking faults. The mechanism and timing of such faulting is ambiguous. Given that they penetrate the entire exposed stratigraphic profile, these faults cannot be induced by an outer arc extension, especially as they occur over the entire eastern flank including the fold crest itself. How such faulting is related to the prominent Semail lineament is also unclear.

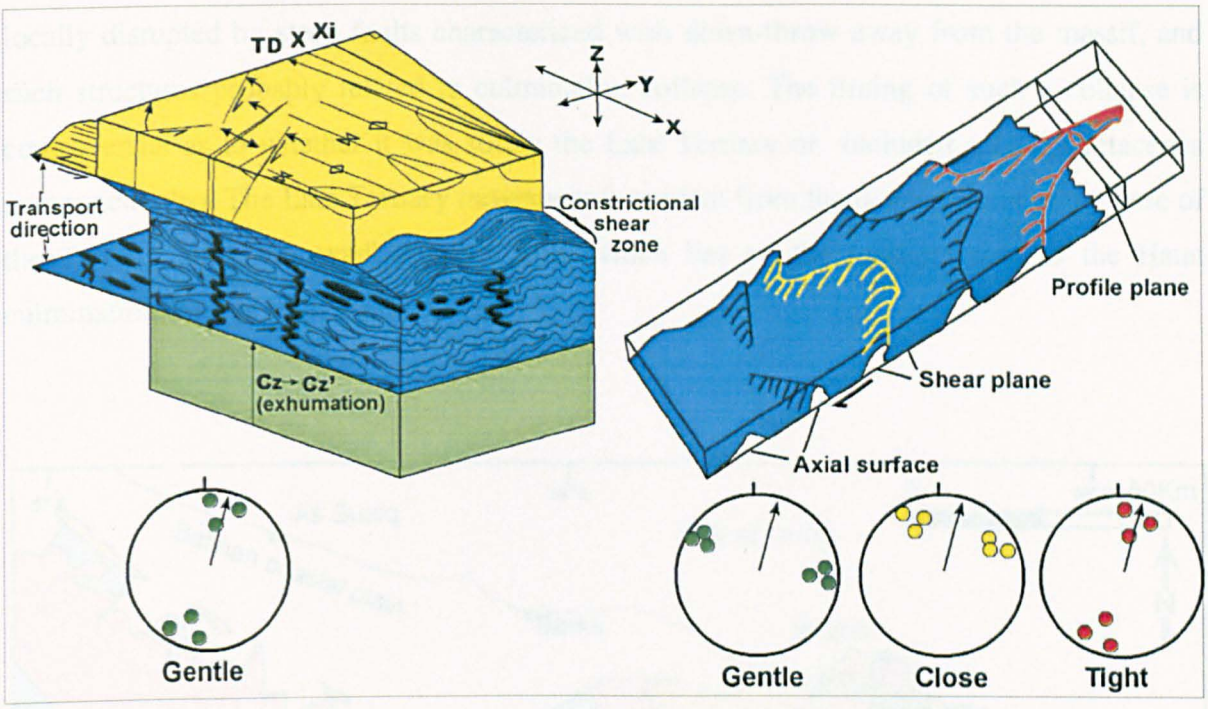

Fig. 6- 9 Structural models for the development of lineation-parallel folds. (a) Transtension model with constrictional strain (Krabbendam et al. 1998), (b) Simple shear model (Pluijm et al. 2002)

The massif-bounding faults

The northern edges of the various culminations are bounded by intermittent steep faults with down-throw away from the massif, which mark the contact between the allochthons and the Mesozoic carbonates (Fig. 6- 6 and Fig. 6- 10). Localization of such faults along the culmination edges suggest that they took place after or during the latest stage of the folding deformation. These faults are called the massif-bounding faults. Hanna et al. (1990) argued that the allochthons were slipped away from the culminations along these faults during the culmination collapse. This idea can be rejected in several aspects. Firstly, internal deformations within the allochthons and the adjacent platform carbonates indicate consistently top-to-the-NNE extensional shearing. Secondly, the allochthons are partially omitted every where along their contact with the platform carbonates exposed in the various culminations, while these faults are just sporadically developed. This can be clearly recognized on the southern flank of the Akhdar culmination, where in places the entire Hawasina sediments are omitted with no steep massif-bounding fault. Alternatively, based on the detected top-to-the-NNE shearing within the allochthons, the base of the allochthons can be interpreted as a top-to-the-NNE detachment along which allochthons have been stretched and omitted. This detachment is part of the same NNE-directed extensional

deformation as mapped within the platform carbonates. However, this detachment has been locally disrupted by steep faults characterized with down-throw away from the massif, and such structures probably related to culmination collapse. The timing of such a collapse is controversial as to whether it was solely the Late Tertiary or included a Late Cretaceous component also. The Late Tertiary movement is evident from the displacement at the base of the Tertiary along the wadi Alkabir fault, which lies on the northern side of the Hatat culmination (Searle et al. 2004).

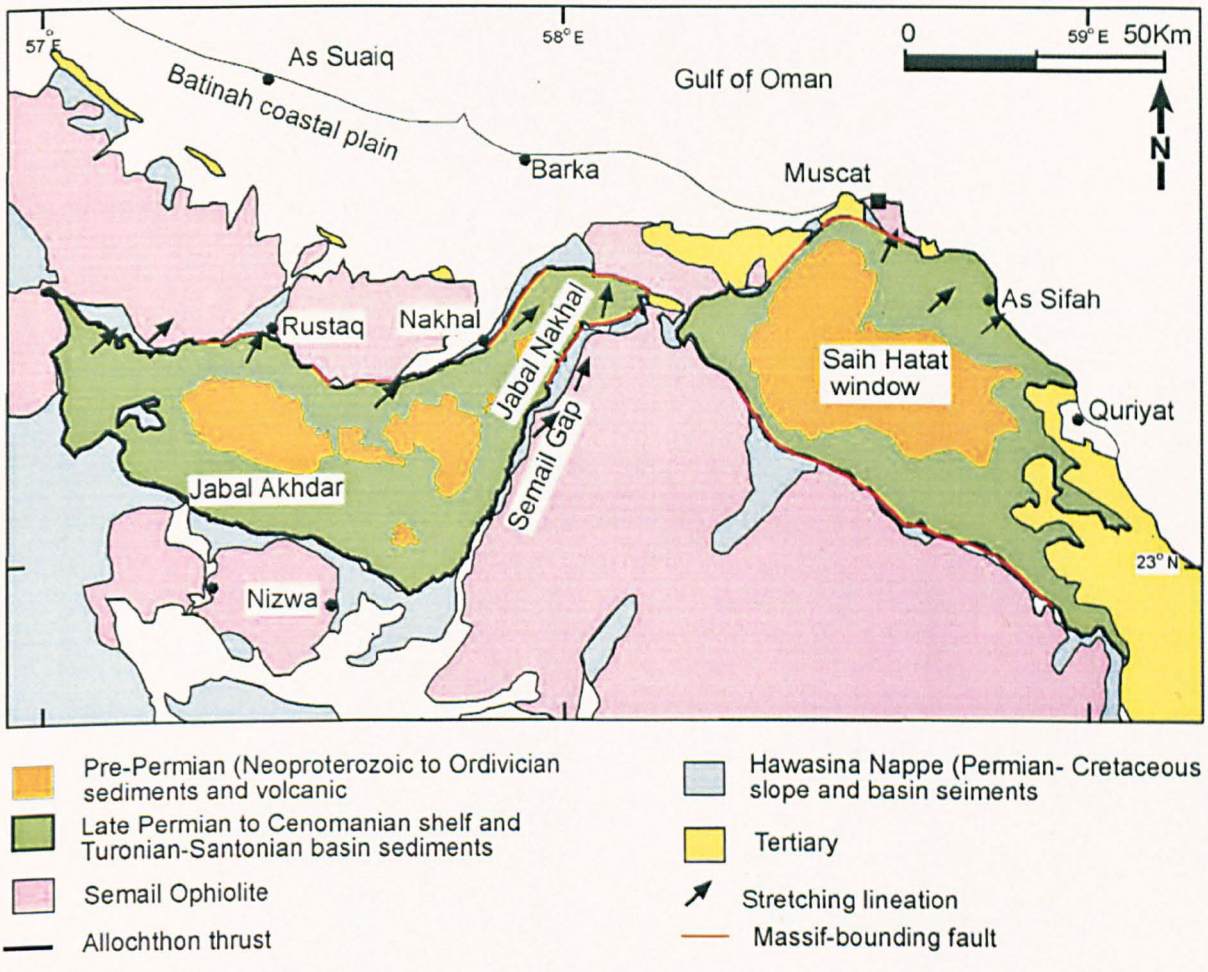

Fig. 6- 10 The distribution of the massif-bounding faults throughout the Oman orogen. Notice the difference in spatial distribution of allochthons detachment and the massif-bounding faults

Chapter 7: Discussion of a transtensional model for the structural evolution of the Akhdar Massif

7.1 Introduction

Breton et al. (2004) pointed out that the Oman orogen exhibits top-to-the-NNE extensional deformation. This deformation was investigated thoroughly through the current study across the Akhdar-Nakhal culminations. It appears that this deformation is pervasively developed and displays evidence of synchronicity with the folding deformation, which has not been addressed before. Furthermore the model of Breton et al. (2002) model does not address the cross-folding developed within the Oman orogen. As a result a new model is proposed to account for the synchronous folding and extensional deformation together with the mechanism of cross-folding. The study also focuses on linking the extension deformation of the shallowly buried rocks in the Akhdar-Nakhal massifs with the well documented deformations across the deeply buried rocks of the Saih Hatat. This linking may provide a clearer picture about the Late Cretaceous exhumation of the NE margin of the Arabian plate and how it is related to the ongoing extension deformation.

7.2 Geometry and kinematics of Late Cretaceous extensional deformation in the Oman orogen

The windows of deformed Arabian continental crust in the northern Oman Mountains represented by Jebel Akhdar, Jebel Nakhal and Saih Hatat illustrate two apparently contradictory structural styles: NNE-directed shearing and vertical thinning together with a local NW-SE contraction manifested by lineation-parallel folds. The intensity of the NNE-directed shear deformation increases NE towards Saih Hatat (see Syntheses chapter). In the Jebel Akhdar massif, the NNE-shear deformation is extensively developed forming steep faults and bedding-parallel detachments extending stratigraphy with top-to-the-NNE sense of shearing. No evidence of ongoing NW-SE contraction is seen, and hence deformation is apparently plane strain. Jebel Nakhal, in contrast, is marked with wide spread deformations of both NNE- shearing and the concomitant NW-SE contraction, indicating non-plane strain. In Saih Hatat NNE- shearing is penetrative with a component of orthogonal contraction. The top-to-the-NNE shear deformation is manifested by a linked system of steep faults and layer-parallel shearing. Steep faults are oriented NW-SE with down-throws to NNE, while layer parallel shearing is expressed by bedding-subparallel detachments together with NNE-verging ductile structures comprising of folds and cleavage. These faults and detachments extend stratigraphy and have a clear normal sense throw of top towards NNE. Therefore the

pervasive NNE-directed shearing is extensional deformation. The localized NW-SE contraction deformation, particularly across Jebel Nakhal developed NNE-lineation-parallel folds and massif-verging thrusts and cleavage. Conjugate sets of strike slip faults oriented NW-SE and E-W are also attributed to this contraction.

The trends of the northern Oman culminations exhibit a cross-folding geometry, with reference to the NNE extensional direction. The Hatat and Akhdar anticlines are longitudinal folds trending WNW-SSE, while the Nakhal anticline is a transverse fold oriented NNE-SSW, in alignment with the NNE shearing direction.

7.3 Evaluating the plane strain extension model (Breton's model)

Breton et al. (2004) have recently pointed out the existence of NNE-directed extension deformation affecting the entire autochthonous units, from the SW edge of Jebel Akhdar to the northeast edge of Saih Hatat (Fig. 7- 1). This deformation is expressed by top-to-the-NNE low-angle detachments along with NNE-verging ductile shear deformation. They linked this deformation to the exhumation of the autochthon during the Campanian based on top-to-the-NNE kinematic data and retrograde metamorphic parageneses associated with the deformation fabrics. Breton et al. (2004) went further in classifying the deformation structures into two different phases reflecting two stages of exhumation. The earlier exhumation stage is marked with pressure-solution cleavage and foliation resting parallel to the axial planes of stretching lineation-parallel recumbent folds. This stage corresponds to the exhumation of the eclogite and blueschists facies exposed at the extreme NE of Saih Hatat. The later stage of exhumation corresponds to the exhumation of the autochthon over the whole Oman orogen. Deformation associated with this stage is manifested by recumbent folds with hinge lines oriented perpendicular to oblique to the stretching lineation with axial planer pressure solution cleavage.

The study of Breton et al. (2004) forms the starting point for our discussions. Their study clearly pointed out the development of NNE-directed extension over the whole Oman orogen. However, several structural features are still unaccounted for as listed below. Firstly, the relationship between NW-striking faults, which truncate the entire stratigraphic profile, and the folding deformation is still unexplained. Secondly, doming of Saih Hatat is related to the Late Cretaceous post exhumation process, in this way there is no synchronicity between folding and the NNE-directed extension. Furthermore, folding of the Akhdar-Nakhal culminations are attributed to the Tertiary, much later than the Late Cretaceous extension. Thirdly, cross folding in the Oman orogen, parallel and perpendicular to stretching lineations, is attributed to two different deformation stages.

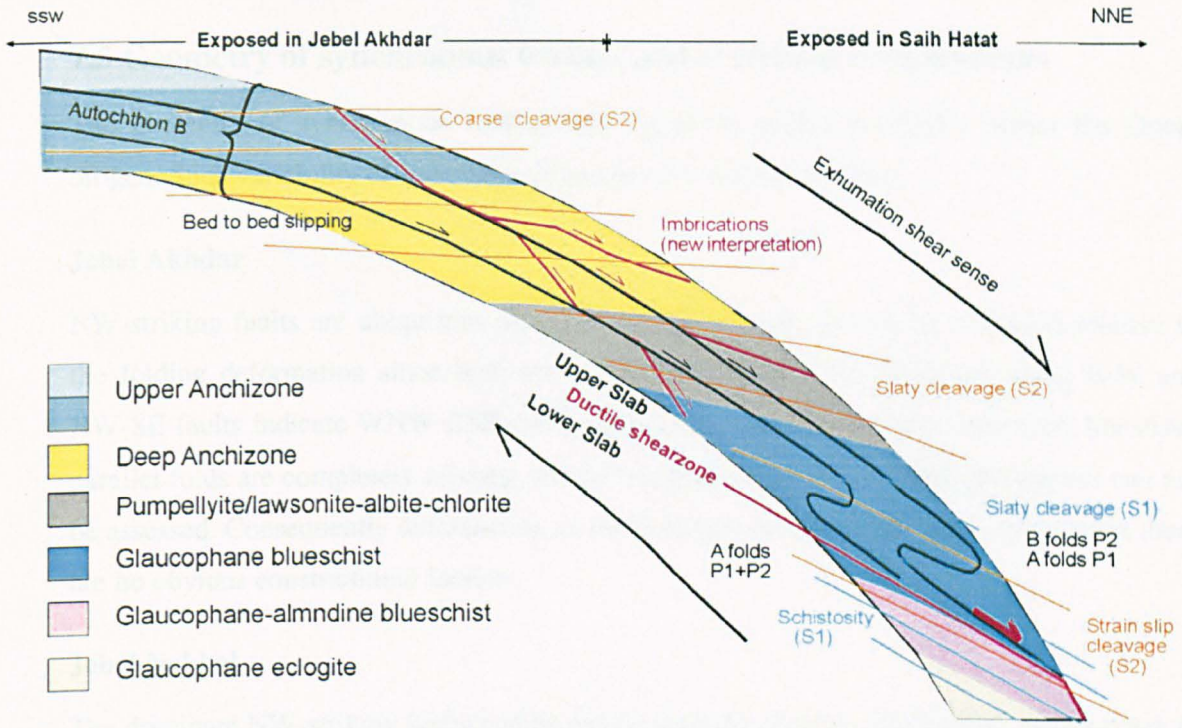

Fig. 7- 1 The Breton et al. (2004) model of the Late Cretaceous structural deformation of the NE margin of the Arabian plate

7.4 Synchronicity of folding and extension deformations

Breton et al. (2004) related did not recognize synchronicity between folding and the NNE-directed extension. However, the current study reveals a synchronicity between folding and extension supported by the following field evidence: firstly, NW-striking normal faults, which truncate the entire exposed stratigraphic profile across the Nakhal anticline, are marked with massif-pitching lineations, indicative of syn-folding faults. Secondly, the absence of distinguishable cross-cutting relationships between extension and folding structures suggests that both were synchronous. Thirdly, the development of stretching lineation-parallel open folds suggests contemporaneous folding and extension deformations, this is explained shortly. Fourthly, the intensity and frequency of the of the NW-SE contraction fabrics increase with increasing grade of the NNE-directed extension as evidenced from the eastern flank of the Nakhal anticline. Therefore based on the previously presented evidence, the NNE-directed extension and the NW-SE contraction are coeval rather than representing two different events.

7.5 Geometry of synchronous folding and extension deformations

The geometry of synchronous folding and extension varies drastically across the Oman orogen. Such variability of individual culmination is explored below.

Jebel Akhdar

NW-striking faults are ubiquitous along Jebel Akhdar, yet can not be evaluated relative to the folding deformation since both are sub-parallel. Strike slip lineations along E-W and NW-SE faults indicate WNW-ESE compression (See Akhdar chapter). However, lineation-parallel folds are completely missing and the amount of the strike slip displacements can not be assessed. Consequently deformation in Jebel Akhdar is apparently plane strain since there are no obvious constrictional fabrics.

Jebel Nakhal

The dominant NW-striking faults can be evaluated with respect to the folding deformation in Jebel Nakhal, where the faults lie sub-perpendicular to the fold axis. In the Nakhal anticline these faults were initiated as dip and strike slip faults before or during the early stage of the folding onset (Fig. 7- 2), as reflected by the massif-pitching lineations and away from the massif-pitching lineations respectively (See Nakhal chapter). After or during the late stage of the folding process, these faults were reactivated again as dip and strike slip faults. In this way NW-trending faults were probably active during the folding deformation.

The steep normal faults are generally oriented NW-SE, however their orientations differ slightly throughout the different culminations. In the Akhdar-Hatat culminations, faults are oriented between E-W and WNW-ESE, reflecting NNE stretching direction. However, in the Nakhal culmination, faults are distributed in a wide range from E-W to NNW-SSE representing a NE-SW stretching direction. Such local change in the inferred stretching direction along Jebel Nakhal will be justified later on.

Conjugate sets of strike slip faults striking NW-SE and WNW-ESE have developed across the Nakhal anticline. They enclose a NW-SE oriented shortening component. Strike slip displacements increase towards NE, reaching approximately 100 m at the extreme NE of the massif.

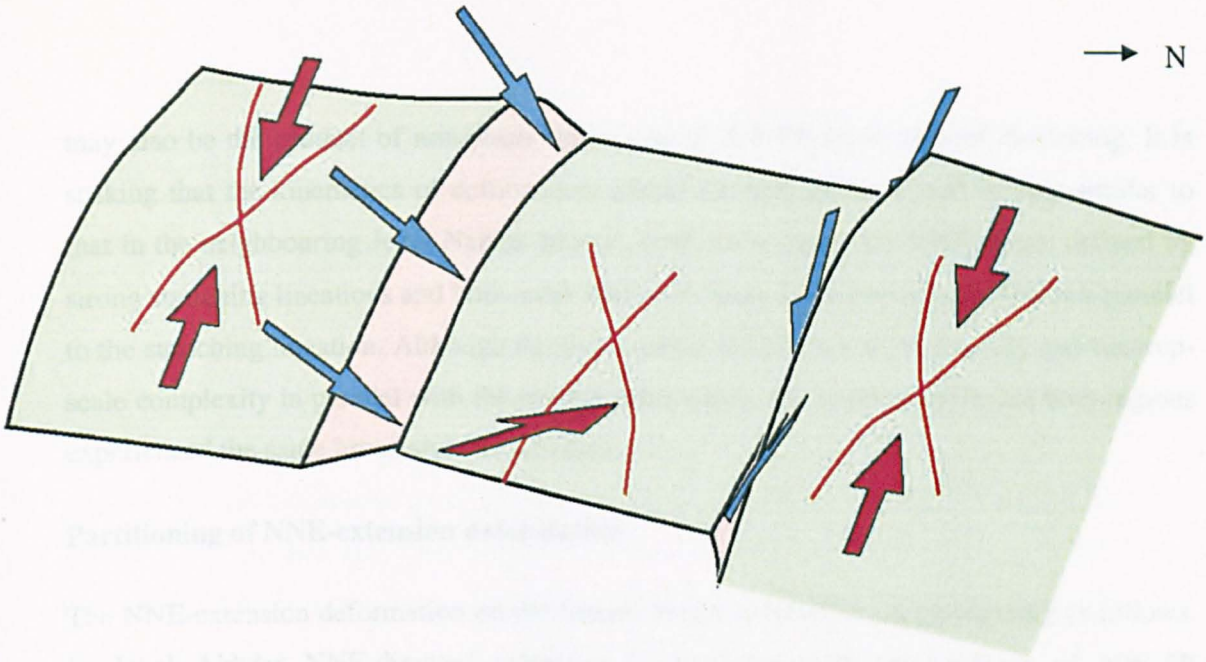

Fig. 7- 2 NW-striking faults with massif-pitching lineations across the Nakhal anticline have been interpreted as pre or syn-folding dip slip faults. The Nakhal culmination is also marked by a conjugate set of strike slip faults reflecting NW-SE compression

Lineation-sub-parallel minor folds are common along both flanks of Jebel Nakhal. These folds are open and upright, with some verge towards the massif. Such folds could be likely formed by high grade simple shear deformation or by transtension deformation with constrictional strain. A test based on correlating the interlimb angles with the orientation of the fold hinges was carried out to determine the folding mechanism of these folds (See Data synthesis chapter). Since these folds are characterized with open interlimb angles, therefore they are better explained to have been induced by transtensional deformation. Furthermore, stretching lineation-parallel fold axes on either flank of the Nakhal anticline are anticlockwise of the NNE-stretching lineations. The measured discrepancy angles, which clearly indicate a sinistral wrench component, are not less than 10° in average. In short, the coeval deformations, NNE-extension with vertical thinning and NW-SE contraction, reflect non-plane strain deformation, a manifestation of constriction strain.

Saih Hatat

The Saih Hatat culmination contains widespread small and large-scale folds with axes plunging sub-parallel to the regional stretching lineation (see Saih Hatat chapter). This pattern coincides with the high temperature parts (NE part of Jebel Nakhal) of the Jebel Akhdar culmination. Many of these folds are tight and have been convincingly explained by high-magnitude simple shear models (Miller et al. 2002; Searle et al. 2004). However they

may also be the product of non-plane strain, coeval NW-SE layer-parallel shortening. It is striking that the kinematics of deformation within the Saih Hatat Massif is very similar to that in the neighbouring Jebel Nakhal Massif. Both show top-to-the-NNE shear, defined by strong stretching lineations and both areas also have many folds that are oriented sub-parallel to the stretching lineation. Although the deformation increases both in ductility and outcrop-scale complexity in parallel with the metamorphic grade, the implication is that both regions experienced the same broad style of tectonics.

Partitioning of NNE-extension deformation

The NNE-extension deformation on the Oman orogen exhibits strain partitioning as follows. In Jebel Akhdar NNE-directed extension is pervasive with no evidence of NW-SE contraction, implying an apparent plane strain. However, Jebel Nakhal is characterized with orthogonal NNE-extension and NW-SE contraction reflecting non-plane strain, a manifestation of constriction strain. In Saih Hatat, both styles of NNE-extension and NW-SE contraction are well developed under more ductile deformation expressing, penetrative constriction strain. In Nakhal-Hatat culminations, constrictional fabrics are clearly defined by open folds aligned parallel to the stretching lineations.

Summary

The NNE-directed extension and the folding deformation, particularly of the Nakhal anticline, are coeval. Further analysis of the syn-folding extension revealed that NNN-extension is locally partitioned into NNE-directed extension and an orthogonal NW-SE contraction, a manifestation of constriction strain.

7.6 Why a transtension model ?

Before introducing the new model, the existing folding models of the Oman orogen are highlighted to investigate how synchronous folding and extension are addressed. Then the relationship between extension and exhumation of the NE margin of the Arabian plate is investigated to assess the interaction between them. The different models, which account for the synchronous development of extensional shearing and folding, are discussed together with the transtension model. Finally the new transtension model is introduced.

Folding models of the Oman orogen

Emphasis the need for a new model explaining the coexistence of folding and extension deformation, let us investigate the previous models of the Oman orogen to outline how these contrasting deformations are interpreted particularly the cross-folding of Akhdar-Nakhal

culminations. (Glennie et al. 1974) attributed this cross folding of the Oman Mountains to two separate orthogonal events; SW-directed thrusting and E-W shortening. Hanna et al. (1990) invoked a thrust model of flat ramp flat geometry associated with the Late Cretaceous Ophiolite emplacement (Fig. 2-6a). Hanna interpreted the Nakhal anticline as a lateral culmination, while the collected field data here indicates a true NW-SE shortening. Mount et al. (1998) attributed the Oman orogen to a thick-skinned fault-propagation folding model that took place during Oligocene time (Fig. 2-6b). Breton et al. (2004) attributed the Hatat doming to Late Cretaceous local crustal thickening related to lithospheric delamination. All the previous models therefore neither account for coeval orthogonal deformations nor address syn-folding extension.

Extension and exhumation of the NE margin of the Arabian plate

The pervasive NNE extension is associated with the exhumation of the NE margin of the Arabian plate during the Late Cretaceous convergence (Jolivet et al. 1998). Thus it is essential to understand this exhumation in order to evaluate and understand the NNE extension. In Saih Hatat, the eclogite and blueschists facies are separated from rocks above that have not experienced high P-T conditions, by high strain zones marked with loss of barometric section (Jolivet et al. 1998) (Fig. 2-1). The tectonic significance of top-NNE-directed shear within the metamorphic rocks of Saih Hatat is still controversial (Jolivet et al. 1998; Miller et al. 2002 and Searle et al. 2004). Miller et al. (2002) considered at least some of these structures to be back-thrusts because they repeat stratigraphy and therefore accommodated crustal shortening (Fig. 2-4). Searle et al. (2004) related the Saih Hatat structures to thin-skinned back-thrusting and extension associated with a single, evolving NNE-dipping subduction zone (Fig. 2-5).

Such controversy regarding the mechanism of exhumation can be assessed through several criteria as follows. The stratigraphic omission or pressure gap is not sufficient to diagnose crustal extension, since such an omission could be an artefact resulting from superimposed deformation and complex pre-thrusting geometry (Wheeler &Butler 1994; Jolivet et al. 1998). Therefore other criteria should be used to prove such processes. The first key method will rely upon the vertical distribution of type I and type II retrograde P-T paths. In Saih Hatat, the P-T path of rocks found today immediately below the major extensional shear zones show a fast cooling during decompression while deeper rocks show an isothermal decompression down to approximately 5 kbar before they reached the surface conditions (Jolivet et al. 1998). This systematic observation of the two retrograde paths is strong proof for the extension-driven exhumation, since the coexistence of these retrograde P-T paths indicates a tectonic denudation achieved by extension deformation. The second method is

based on the fact that true extensional structures should ultimately intersect the Earth's surface when traced out in a direction opposite to that of hanging-wall transports (Wheeler & Butler 1994). This method has been implemented over the low-angle faults throughout the Akhdar-Nakhal culminations. It has been found that all these faults intersect the earth's surface when traced out in a direction opposite to that of hanging-wall transports. For this reason, these faults are extensional in kinematics. The third method, which was the focus of this study, is based on linking deformations within the weakly buried and hence less deformed rocks of Jebel Akhdar, with the respective deeper and complicated deformation within the Saih Hatat. It has been found that the NNE shear deformation is pervasive across Akhdar-Nakhal culminations with top-to-the-NNE sense of shearing. The NNE shear deformation is manifested by a system of steep faults and detachments, which collectively accommodate evidence for stratal extension directed top-NNE. In this regard, the controversial shearing across the deeply buried rocks of Saih Hatat are extension rather than contraction in kinematic. Consequently, the exhumation of the northern Oman Mountains is achieved by NNE-directed extension.

Models of synchronous folding and extension

The synchronous development of extensional shearing and large-scale upright folds has been well documented in extended terranes throughout the world (Fletcher 1994; Mancktelow and Pavils 1994; Martinez and Soto 2002). Moreover, folding affecting both detachment faults and their respective footwalls have fold axes both parallel and perpendicular to the direction of extension. Of great interest for this study is the folding mechanism for lineation-parallel folds, the Nakhal anticline for example. Several models have been suggested for such transverse folding. Firstly, a lateral displacement gradient model, through which strong constrictional strains result from the superposition of differential shear (simple shear with a vertical shear plane) and layer extensional flow (Fig. 7- 3a) (Coward and Potts 1983; Ridley 1986). Secondly, shortening along the Y axis of the shear zones, in a constrictional strain regime, induced by switching of $\sigma 1$ from vertical to horizontal. For this process to occur the fault zone should be inclined to the principle stress axes (Fletcher 1994; Mancktelow and Pavils 1994; Martinez and Soto 2002). Thirdly, flow perturbation can result in the development of transport direction-subparallel folds (Alsop et al. 1996; Alsop et al. 2002). Flow perturbation can be tested by checking the down-plunge asymmetry of fold hinges relative to the stretching lineations, which should consistently display an opposing sense of obliquity across the culmination. Minor folds within the Nakhal anticline exhibit a consistent sense of obliquity relative to the stretching lineations on both flanks. Consequently they are not related to flow perturbation. Finally, transtension deformation results in constrictional strain developing folds, parallel to the maximum elongation direction (Fig. 7- 3b) (Janecke

et al. 1998; Krabbendam and Dewey 1998; Ramani and Tikoff 2002). Which of these models applicable to the study area will be assessed later, based on the geometry and kinematic of the NNE-directed extension deformation?

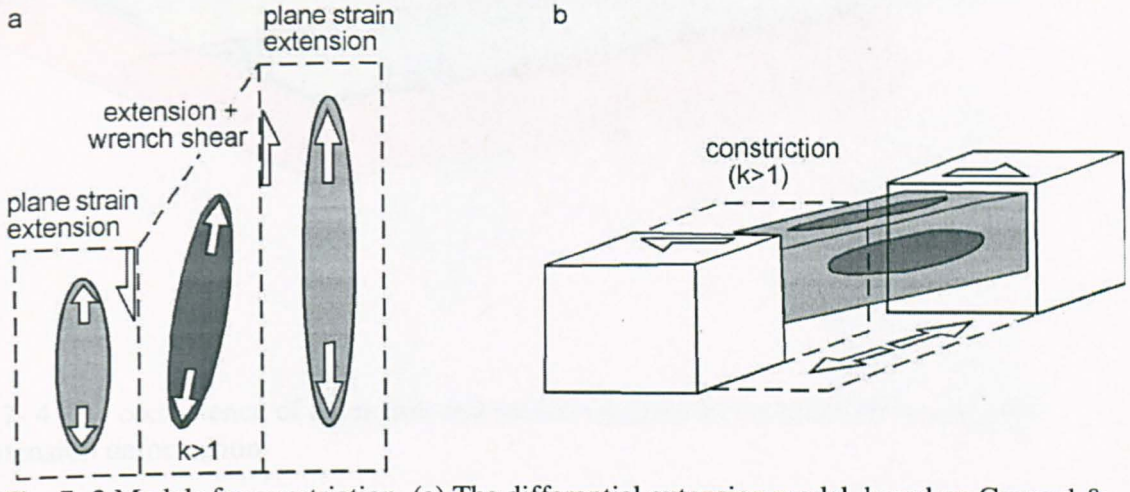

Fig. 7- 3 Models for constriction. (a) The differential extension model, based on Coward & Potts. (b) The transtension model (see Dewey et al. 1998)

Transtension model

The previous models of deformation in the Oman orogen do not account for the syn-folding extension and the coexistence of the NNE-extension and the orthogonal NW-SE shortening. From the various models of synchronous folding and extension, the best compromise for the Oman orogen is a transtensional deformation induced by lateral displacement gradient (following a model proposed by Coward and Potts (1983). The plane strain NNE-directed extension is locally partitioned into the NNE-directed extension and vertical thinning together with NW-SE contraction. This type of deformation is clearly non-plane strain and is weakly constrictional. Constant volume constriction (k>1) can readily be explained by regional transtensional strain (e.g. Dewey et al. 1998). So the NNE-directed extension is locally partitioned into transtension of NNE-extension and NW-SE contraction. In such deformation, both extension and folding are synchronous (Fig. 7- 4). A transtension model is proposed for the Oman orogen to explain the synchronous folding and extension.

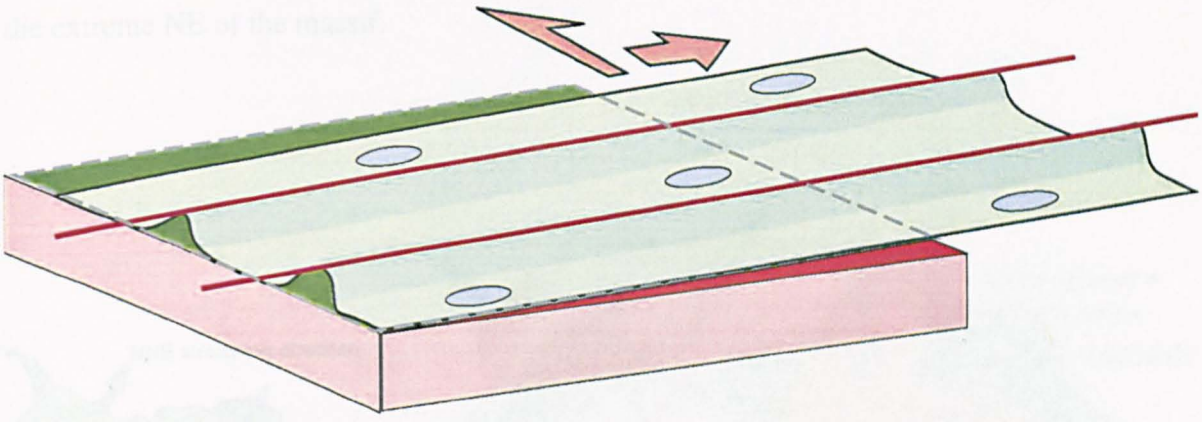

Fig. 7- 4 The coexistence of extension and stretching lineation-parallel folds suggests transtension deformation

7.7 Geometry and kinematics of transtensional deformation

Geometry and kinematics of transtensional deformation applied to Oman

The NNE extension deformation is locally portioned into NNE extension and a wrench component; collectively constituting to transtension deformation. The transtension is marked with NNE extension associated with vertical thinning and NW-SE shortening (Fig. 7- 5). Such a strain configuration reflects constriction deformation, which accounts for the synchronous extension and folding. The trends of constrictional fabrics with respect to the NNE stretching direction indicate a sinistral transtension oriented NE-SW. The structural characteristics of the transtension deformation vary in a NNE trend towards Saih Hatat, with a respective increase in the depth of burial and the intensity of the NNE extension. Deformation in Jebel Akhdar, which is occupied by the least buried rocks, is apparently plane strain since there are no constrictional fabrics (Fig. 6.5). WNW-ESE directed strike slip faults are less developed compared with the Nakhal anticline.

In the Nakhal culmination, the resultant constrictional fabrics indicate non penetrative bulk constriction, manifested by lineation-parallel folds and massif-verging structures, along with conjugate sets of strike slip faults (Fig. 6.7). Such constrictional strain can be considered as a weak strain with (L > S). The conjugate sets of strike slip faults, NW-SE and WNW-ESE, are well

established with increasing lateral displacements NE ward reaching approximately 100 m at the extreme NE of the massif.

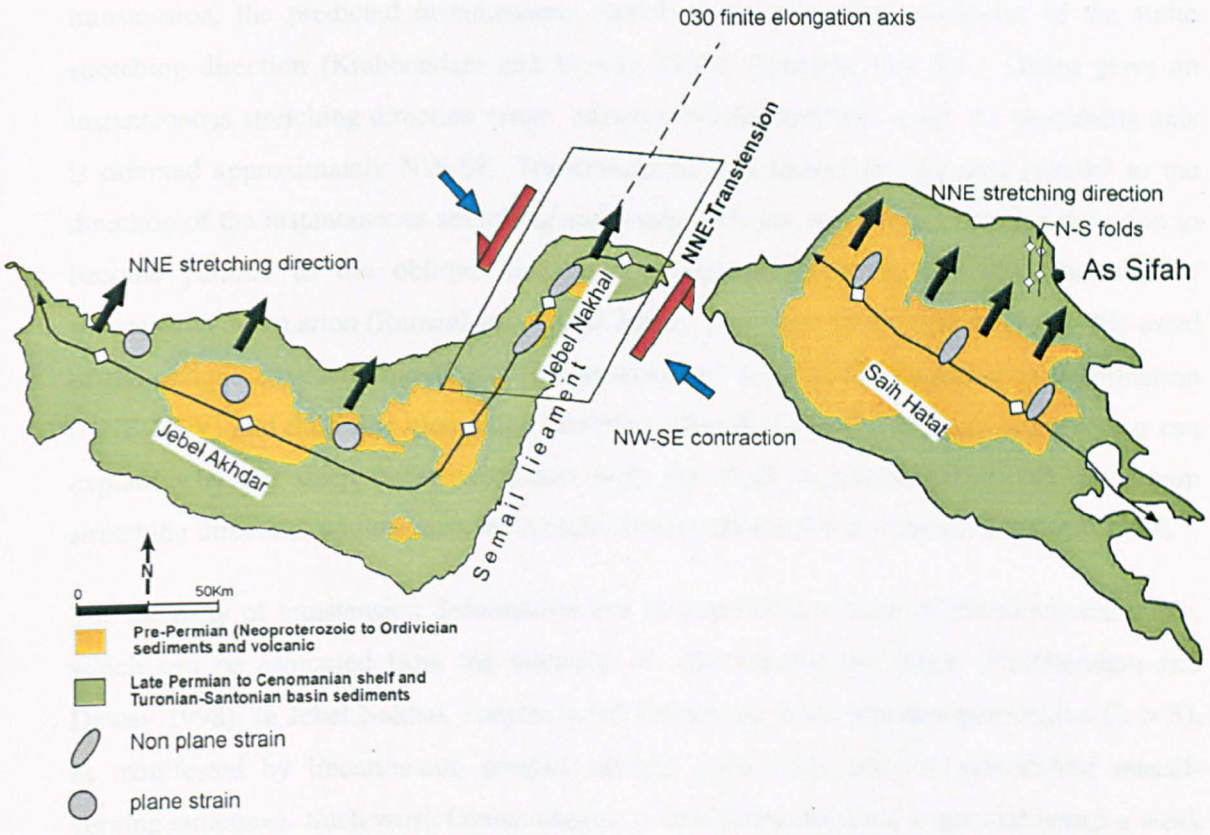

Fig. 7- 5 Partition of the NNE-directed extensional deformation in the Oman orogen induced a sinistral deformation, as can be seen along the Akhdar anticline due to lateral differential extension associated with the exhumation of the subducted plate.

In the Saih Hatat culmination, constrictional strain is penetrative forming lineation-parallel boudins, sheath and open upright folds. Miller et al. (2002) attributed these sheath folds to NNE-directed shearing, however the role of constriction can not be excluded in the development of such structures(Jiang and Williams 1999). Constrictional strain is regarded as penetrative with L >> S, especially within the eclogite and blueschists facies (Fig. 6.6).

Kinematics

Experimental modeling of transtensional deformation indicate that the transtensional folds are oriented parallel to the finite elongation direction (Ramani and Tikoff 2002). In the northern Oman orogen, the finite elongation is oriented N030E, in parallel with the Nakhal anticline (Fig. 7- 5). Dewey et al. (1998) pointed out that the obliquity between the direction of maximum elongation and the orientation of synchronous strike-slip faults is generally

about 20°. For the study area, where maximum elongation is oriented N030E, sinistral transtensional deformation is predicted to run NNE-SSW (wrench component). In sinistral transtension, the predicted instantaneous stretching direction lies clockwise of the finite stretching direction (Krabbendam and Dewey 1998). Applying that for Oman gives an instantaneous stretching direction range between N030E and NE, while the shortening axis is oriented approximately NW-SE. Transtensional fold hinges are initiated parallel to the direction of the instantaneous stretching and rotate with the maximum extension direction to become parallel to the oblique extension movement direction, not the boundary of transtension defamation (Ramani and Tikoff 2002). Therefore, in the Oman orogen, the trend of the oblique extension movement lies between the trend of the transtension deformation (NNE-SSW) and the finite elongation direction (N030E). The transtension deformation can explain why the steep faults associated with the NNE extension reflect NE maximum stretching direction, while across the Akhdar-Hatat culmination it is directed towards NNE.

The intensity of transtension deformation can be expressed in term of transtensional angle, which can be estimated from the intensity of the constriction fabric (Krabbendam and Dewey 1998). In Jebel Nakhal, constrictional fabrics are weak and non-penetrative (L > S), as manifested by lineation-sub parallel upright open folds and non-penetrative massif-verging structures. Such weak fabrics suggest a small transtensional angle and hence a weak transtensional deformation (Krabbendam and Dewey, 1998). Other evidence of a small transtensional angle and the subsequent weak transtension deformation is as follows: the absence of different phases of massif-verging cleavage, which could be formed under variable transtensional angles; the symmetrical upright geometry of the Nakhal anticline and the other associated minor folds; the small amount of shortening of 7 % across the Nakhal anticline, as measured from several transects. Consequently, Jebel Nakhal has not experienced significant anticlockwise transtensional rotation. However, the transtensional angle and the respective constriction deformations are higher on Saih Hatat as reflected from strong lineation-parallel boudins and sheath and open folds (L >> S).

7.8- Mechanisms of transtension deformation

Transtension deformation can be induced by several mechanisms such as strike slip faulting (Krabbendam and Dewey 1998) and laterally differential shearing (Coward and Potts 1983; Ridley 1986; Armetrong and Bartley 1993; Mancktelow and Pavils 1994; Schlische 1995; Janecke et al. 1998). Each of these mechanisms is applied to and assessed using the Oman orogen as follows.

Strike slip faulting

For the northern Oman mountains, where the finite elongation of sinistral transtensional deformation is oriented N030E, strike slip faults are predicted to run NE-SW. Consequently, for strike–slip to have played a role the main faults must lie outside the present study area. Such large-scale partitioning is however not uncommon (see Dewey et al. 1998 and references therein). Masirah Fault, at the eastern margin of the Arabian plate, might experience left-lateral shearing during the early drift of the Indian continent from its position within Gondwana (Dercourt et al. 1993) This structure trends NE-SW and hence a possible candidate for the hypothetical strike-slip fault predicted by the transtension model (Fig. 7- 6). However, faults in this trend should act with a right lateral sense to generate NNE-SSW finite elongation in adjacent belts of transtension. This is in disagreement with the regional sinistral sense of shear predicted for the Arabian continental margin.

Fig. 7- 6 Hypothetical sinistral transtensional deformation along the Masirah fault

Lateral differential extension

In the Oman orogen the constrictional strains appear to relate to zones of differential exhumation, along various levels. There is far more extension associated with structures in the east (As Sifah) compared with the western side of Saih Hatat. And there is correspondingly more extension associated with the exhumation of Saih Hatat compared with Jebel Akhdar. The spatial variations in the amount of extension reflect important lateral variations in the orogen. The consequences of differential movement in deformation zones are discussed by Coward & Potts (1983) and Ridley (1986) (Fig. 7- 3a). They pointed out that strong constriction strains result from the superposition of differential shear (simple shear with a vertical shear plane) and layer extensional flow. In the northern Oman Mountains, the lateral differential extension induced transtensional deformation resulting in constriction strain (Fig. 7- 7).

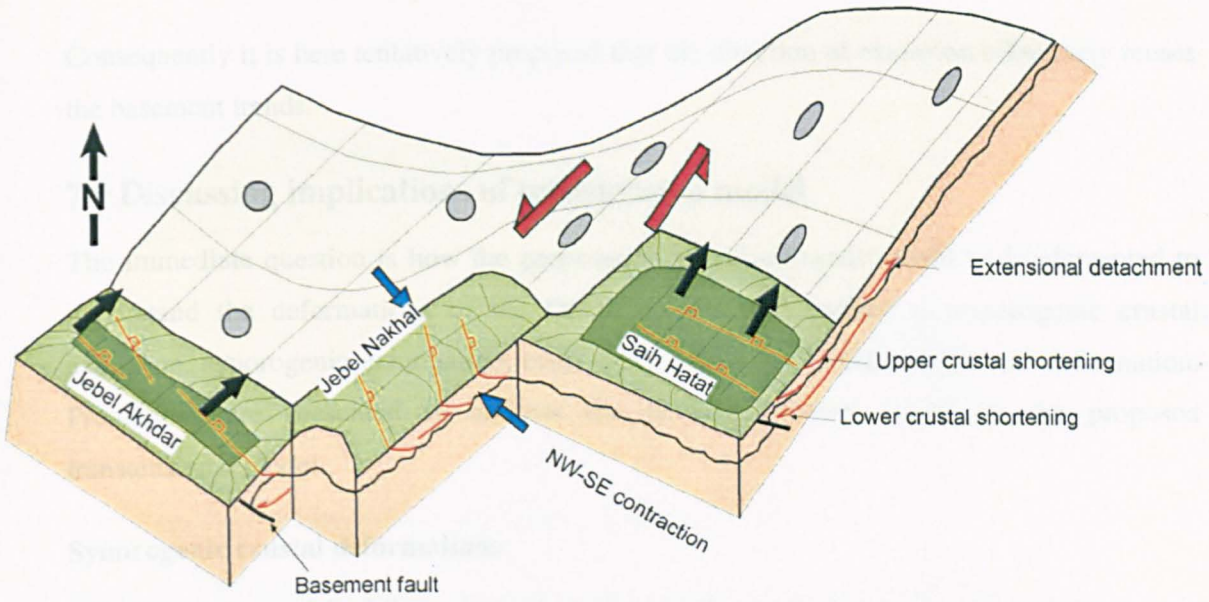

Fig. 7- 7 3-D conceptual model for the Late Cretaceous structural deformation of the Oman orogen. The upper crust is characterized by a partitioned NNE-directed extension, while the middle-lower crust is marked by SW-directed thrusting. The model also illustrate the coeval cross folding in the Oman orogen

For the Nakhal anticline, where the direction of the finite elongation axis is N030E, the orientation of sinistral transtension deformation is NNE-SSW. This is based on applying the analytical methods of Dewey et al. (1998). For Jebel Nakhal, the predicted transtension angle is small based on the weakly developed constrictional fabrics. The resultant transtension exhibits continuous strain partitioning without developing discrete strike slip faults running parallel to the shear boundary (wrench component). This explains the lack of discrete strike slip separation between the differently stretched domain; for instance between the Akhdar and Hatat massifs. The detailed geometry and kinematics of this transtensional model is discussed within the structures and kinematics of the transtension model section.

The question arises; what is the influence of the pre-existing basement faults over the transtensional deformation? The Semail lineament is a prolonged structure, which was active during Mesozoic time (Pratt et al. 1990). It has been recognized that fields of the lateral differential extension and the concomitant transtension coincide and hence are influenced by the basement fault (e.g. Semail lineament). Accordingly, the basement faults play a major role in controlling the lateral differential extension and the resultant transtension. Thus, another NNE-trending basement fault is predicted underlying the Sifah anticline of the Saih Hatat culminations, similar to the prominent Semail lineament.

Consequently it is here tentatively proposed that the direction of extension effectively reuses the basement trends.

7.9 Discussing implications of transtension model

The immediate question is how the proposed transtension model could be implemented to understand the deformations of the Oman orogen with respect to synorogenic crustal extension, synorogenic exhumation, cross folding and the Tertiary uplift and deformation. Predictions are presented to address the previous matters based on the proposed transtensional model.

Synorogenic crustal deformations

The kinematic model of the exhumation of once-deeply buried tracts of continental crust within the Oman orogen can be suggested from the NNE-directed crustal extension and the remarkable thickening of the continental crust beneath the culminations. Al-Lazki et al. (2002) pointed out that the continental crust below the culminations is 50% thicker than beneath the foreland. However, the upper crust experienced extensive thinning by the NNE-directed extension, therefore the crustal thickening detected by Al-Lazki et al. (2002) might be taken up through thickening in the middle-lower crust, probably through crustal flow (Fig. 7- 8) (based on a model suggested by (Clark and Royden 2000) for the Tibetan plateau). In Oman, Jolivet et al. (1998) attributed such thickening to the Late Cretaceous convergence during the allochthonous emplacement. However, there are no outcrops of large scale thrust around the massif, requiring these hypothetical thrusts to branch up onto the main allochthon units. Provided the lack of any major compressional event accounting for such crustal thickening after the onset of exhumation, crustal thickening might have happened during the exhumation process. Crustal deformations within the NE margin of the Arabian crust are marked with two coeval and contrasting styles of deformations; NNE-directed upper crustal extension and SSW-directed lower crustal contraction.

The commencement of crustal deformations, the upper extension and the lower shortening, associated with the rapid exhumation of the subducted slab of the Arabian platform. This rapid exhumation might have been induced by the break of the subducted lithospheric root (Fig. 7- 9), which could have triggered a rapid buoyancy-driven uplift of the subducted slab (Chemenda et al. 1996 and 2000). The ongoing convergence together with the buoyancy force, plays collectively in controlling the simultaneous upper and lower crustal deformations. Initially, the lower crustal shearing induced the upper crustal extension, similar for what has been suggested for the NW Himalaya by (Beaumont et al. 2001).

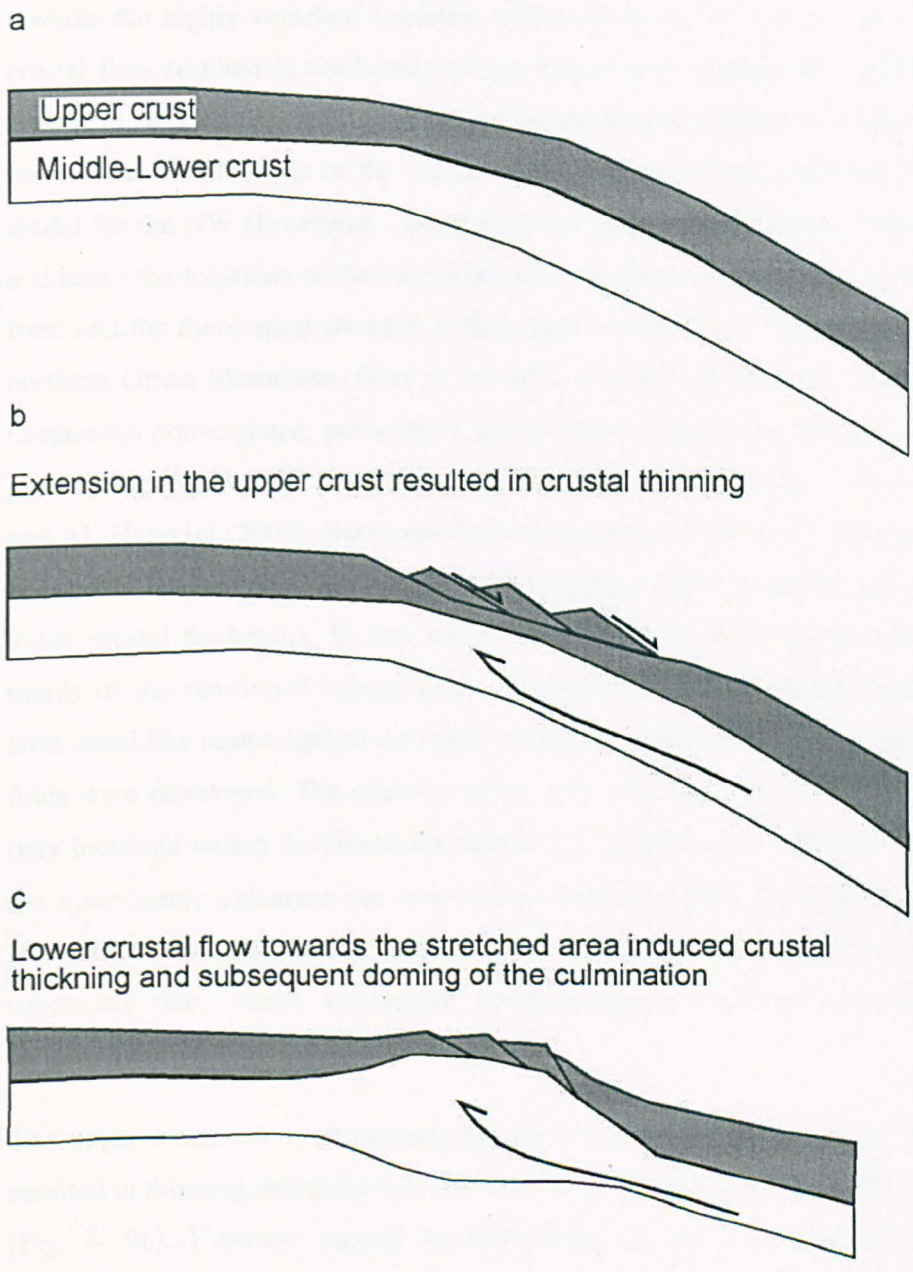

Fig. 7- 8 Schematic illustration for the crustal deformation during the exhumation of the subducted slab of the NE margin of the Arabian plate. The upper crustal extension was contemporaneously accompanied by lower crustal thrusting directed towards SW.

Mechanically, these deformations are supported by a strong buoyancy force and pre-existing weakness in the crust, expressed by basement faults to allow a normal-sense displacement in a horizontally compressive stress regime, as based on analytical methods applied over NW Himalaya by (Willett 1999).

The upper extension and the lower contraction may have being interacting with one another (Fig. 7- 9b). The upper crustal extension influenced the lower crustal material to flow

towards the highly stretched domains, where lithospheric pressure has been reduced. This crustal flow resulted in thickening of the lower crust beneath the highly attenuated upper crust (Fig. 7- 9 c & d). Subsequently, crustal thickening resulted in doming and formation of the various culminations of the Oman orogen. This prediction follows Robyr et al. (2002) model for the NW Himalayan. In general, the spatial distributions of the crustal thickening and hence the locations of the culminations are controlled by the erosion rate in the orogenic front and the rheological strength of the upper crustal rocks (Beaumont et al. 2001). In the northern Oman Mountains, there is no solid evidence of efficient erosion during the Late Cretaceous convergence, particularly across Jebel Akhdar and Nakhal. However, there are pre-existing WNW-ESE trending basement faults as pointed out by Loosveld et al. (1996) and AL-Husseini (2000). Basement faults have induced a crustal weakness which may have controlled the locations and trends of the upper crustal extension and the corresponding lower crustal thickening. In this way, basement faults have constrained the locations and trends of the developed culminations. Furthermore, the WNW-ESE basement faults may have acted like ramps against the lower crustal contractional shear, along which longitudinal folds were developed. The question arise, why such synorogenic extension and doming is only localized within the subducted slab of the Arabian plate? Willett, (1999) modeled that the synorogenic extension can only occur under restricted rheological conditions, such as low crustal viscosity. In the Arabian plate these conditions probably reached only in the subducted slab, where subsequent synconvergence extension and doming were only localized.

The upper extension is accommodated by top-to-the-NNE low-angle detachments which resulted in thinning and exhumation of the deeply metamorphosed rocks of the Arabian plate (Fig. 7- 9b). However, during the early stage of the lower crustal thickening and the concomitant doming a new phase of steeply dipping NW-trending faults were initiated in and around the growing culminations (Fig. 7- 9c). The steep faults are not developed significantly elsewhere, neither on the surface nor on the subsurface (Al-Lazki et al. 2002).They transect the entire stratigraphic succession including low-angle detachments situated at the base of the allochthons and along key horizons within the Jurassic-Cretaceous succession. The steep faults are presumably detached within the pre-Permian sequences. Kinematically, these are syn-folding faults as discussed in the previous sections (See Syntheses chapter).

Fig. 7-10 illustrates in details the late Cretaceous structural deformation across the Akhdar anticline based on the presented model. Initially, the NNE-directed extensional deformation was situated within the allochthons and the Mesozoic carbonates as sort of steep faults and

low-angle detachments. As the doming of the Akhdar anticline commenced, a series of steeply dipping NW-oriented faults, penetrating the allochthons and the underlying Mesozoic carbonates together with the initially formed extensional detachments, were developed in and around the evolving massifs. These faults are presumably detached along a detachment situated within the pre-Permian units. The progressive folding of the culmination resulted in tilting and folding of these faults along with their detachment, which is folded across the Akhdar anticline.

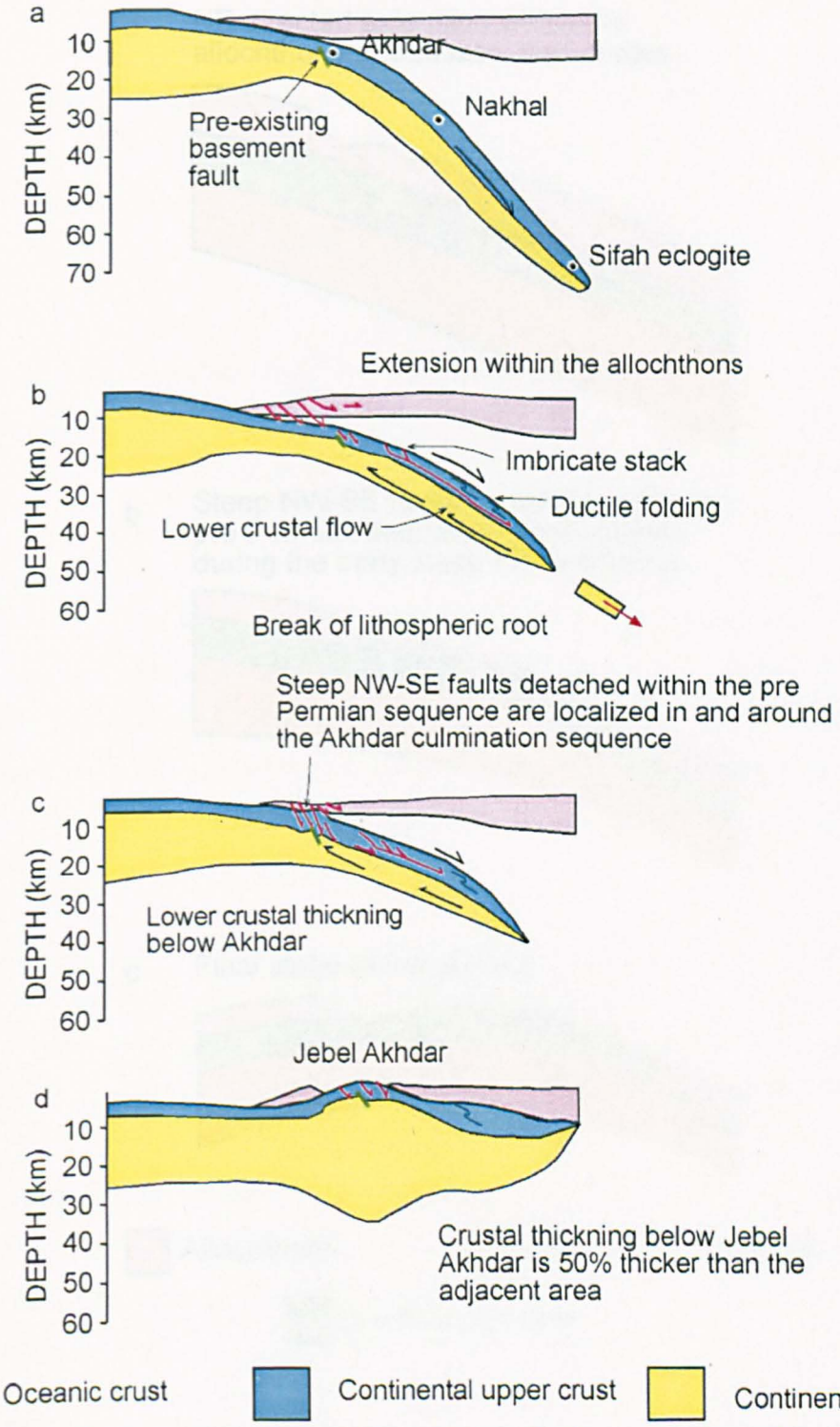

Fig. 7- 9 Qualitative structural model for the Late Cretaceous exhumation achieved by upper crustal extension and lower crustal shortening

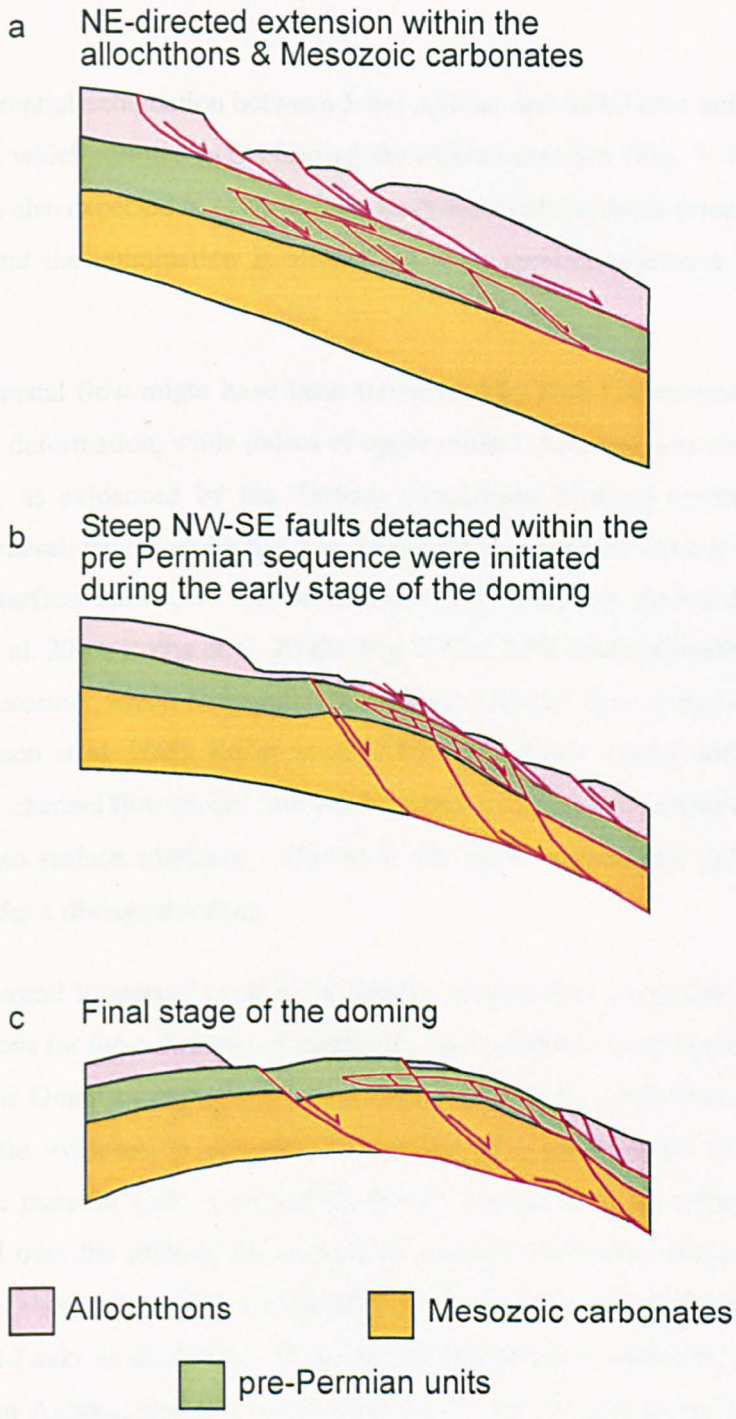

Fig. 7- 10 Qualitative structural model for the Late Cretaceous deformation across the Akhdar anticline

Lateral differential exhumation between Jebel Akhdar and Saih Hatat induced a Transtension deformation, which resulted in the folding the Nakhal anticline (Fig. 7- 7). The lower crustal thickening is also expected to occur below the Nakhal culminations since the upper crust was attenuated and the culmination is aligned by a weakening basement fault of the Semail lineament.

The lower crustal flow might have been terminated by Late Cretaceous time, at the end of convergence deformation, while pulses of upper crustal extension was continuous throughout the Tertiary, as evidenced by the Tertiary extensional faulting reported by Mann et al. (1990). In general, the lower ductile flow was weakly developed since it did not extrude onto the earth's surface unlike the typical channel flow extrusion modeled for the Himalayas (Jamieson et al. 2002; Robyr et al. 2002) (Fig. 7- 11). This could be attributed to the absence of efficient erosion, which is essential to enhance channel flow extrusion (Beaumont et al. 2001; Jamieson et al. 2002; Robyr et al. 2002). The lower crustal deformation was likely initiated as a channel flow model, but weaker erosion suppressed further development, which may lead into surface extrusion. However, the upper extensional deformation continued probably under a divergent setting.

There are several kinematic models for linking synchronous extension and contraction. Of the two options for the coherence of exhumed, once-subducted crust proposed by Wheeler et al. (2001), the Oman example here is best described as a pip rather than a sliver (Fig. 7- 12). There is little evidence to support the erosion of a large panel of intermediate grade metamorphic material such as occurs for slivers. Furthermore, a carapace of allochthonous units existed over the crest of the massifs of Arabian continental rocks. The amount of the lower crustal shortening can be estimated from the depth to the Moho and crustal thickness given by Al-Lazki et al. (2002). 50% crustal shortening is indicated by the Moho depth beneath Jebel Akhdar, across a width of about 50 km. Therefore the estimated amount of shortening is about 25 km, providing that shortening deformation is approximately plane strain and a pre-existing crustal thickness of 30 km. For the upper crustal extension in contrast, Breton et al. (2004) suggested that >100 km extension is recorded within the Arabian continent. This figure would be greatly increased by displacements along base of the allochthonous sheets proposed here. Consequently there is a substantial imbalance between the amount of the upper extension and the amount of the lower contraction. As a result it is tentatively proposed that the extensional tectonic was active towards the end of the history of the mountain belt, coeval with the final period of crustal shortening, but continued on to initiate the rifting of the orogen and the onset of renewed subsidence in the Gulf of Oman.

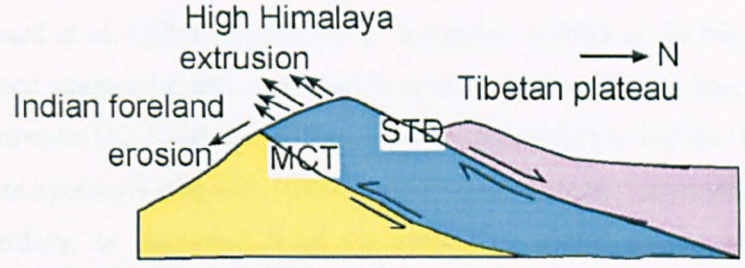

Fig. 7- 11 Channel flow model proposed for the High Himalaya (Beaumont et al. 2001)

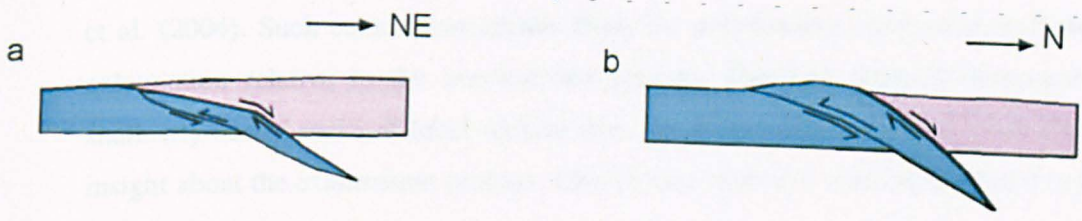

Fig. 7- 12 kinematic models for linking synchronous extension and contraction. (a) Pip model proposed for the Oman orogen. (b) Sliver model proposed by Wheeler et al. (2001) for the Alps

Synorogenic exhumation

Exhumation of the HP rocks can take place during or after the orogenic process. In the Oman orogen, the Timing of the exhumation process can be addressed relative to the other ongoing deformational events. Hacker and Mosenfelder (1996) constrained the ophiolite obduction history between the formation of the oceanic crust some 90 Ma and its final emplacement onto the continent at approximately 78 Ma. While Robertson (1987) argued that final obduction occurred at 70-80 Ma based on dating the over-ridden foredeep deposits. Subsequently, the Arabian plate was deeply subducted and metamorphosed around 80 Ma as inferred from the radiometric dating of the HP metamorphic rocks (Saddiqi et al. 1995). However, the rapid exhumation of the HP units was in progress somehow between ~80 and ~60 Ma (Saddiqi et al. 1995) spanning over 20 My. The entire complex of far-travelled nappes and deformed Arabian crust were juxtaposed and exhumed by Maastrichtian times (c. 67-68 Ma) as sediments of this age overlie all units and seal all the main tectonic contacts (Coleman 1981). In this case, cooling and final exhumation of the eclogites and blueschists was roughly synchronous with the end of the Obduction processes (Searle et al. 1994). Based on these facts there is strong chronological evidence indicating that exhumation of the HP rocks was roughly contemporaneous with the end of the ophiolite obduction. Consequently,

Jolivet et al. suggested that the early part of the exhumation path occurred during continuing convergence, while Michard et al. (1994) argued for postorogenic extension. In this study, we presented field evidence suggesting that extension was synorogenic. That is based on a synchronicity detected between the NNE-directed extensional deformation and the folding process (for more see Data syntheses chapter). The extension outlasted the convergence and continued during the Tertiary, as suggested from the substantial imbalance between the amount of extension and the amount of contraction.

Although the synorogenic extension is well documented particularly in Saih Hatat, but its mechanism is still controversial between Jolivet et al. (1998); Miller et al. (2002) and Searle et al. (2004). Such controversy results from the deformation complexity and the timing of exhumation relative to the convergence process. However, linking deformations of the shallowly buried rocks of Jebel Akhdar with the deeply buried rocks of Saih Hatat allow an insight about the exhumation process. This linking approach was implemented in this study.

The current study concludes that exhumation of the subducted slab of the Arabian plate was achieved by synconvergence crustal extension, with a local transtension deformation induced by a lateral differential extension (Fig. 7- 9). In this way exhumation does not involve upper crustal thrusting as suggested by Miller et al. (2002) and Searle et al. (2004). The rapid exhumation of the subducted slab was initiated by the break of the eclogitised root, which sunk into the mantle triggering rapid exhumation of the crustal rocks above (Chemenda et al. 1996 and 2000). Based on the published data, exhumation took place in two stages (Chemenda et al. 1996; Jolivet et al. 1998; Chemenda et al. 2000 and Miller et al. 2002). The first stage was a rapid exhumation related to a buoyancy-driven uplift, which was achieved by the NNE- extensional deformation as already discussed. The second stage of exhumation was a slow process due to erosion of the previously uplifted rocks and the isostatic readjustment (Ravaut et al. 1998). Thus, weak erosion partly aided the latest stage of the exhumation process.

The cross-folding in the Oman orogen

Cross folding in the northern Oman Mountains is expressed by two orthogonal sets of folds trending WNW-ESE represented in the Akhdar-Hatat culminations called longitudinal folds, and NNE-SSW trending manifested by the Nakhal culmination and hence named transverse folds (Fig. 7- 7). A model of synorogenic crustal extension with a local constrictional deformation is put forward to interpret this cross-folding configuration. The folding of the culminations occurred during the Late Cretaceous time before the deposition of the Maastrichtian sediments, presumed to overlay the whole region (Robertson, 1987). This

timing contradicts with Tertiary folding suggested by Mount et al. (1998) and Breton et al. (2004) for Akhdar-Nakhal culminations. Each fold set is explained in details below.

The longitudinal folds have been attributed to lower crustal thrusting, thickening and subsequent doming of the WNW-ESE orientation, whilst constrained by basement faults (Fig. 7- 7). The NW-SE trending Hawasina window, situated to the NW of the study area, can also be regarded as a longitudinal culmination. However, its NW-SE orientation may reflect a change in the extension direction (top-NE) owing to the arcuate shape of Oman orogen. The geometry of the Akhdar anticline does not resemble the typical model of a thrust-related fold, where the foreland limb is steeper than the hinterland limb. This is because the fold geometry is influenced by other factors such as the upper crustal extension. The steepness (40°) of the northern flank of the Akhdar anticline is attributed to the intensive extensional shearing along that flank, unlike the gently dipping southern flank.

The transverse folds were induced by transtensional deformation resulting from the partitioning the NNE crustal extension (Fig. 7- 5). The transtension deformation is itself partitioned into two orthogonal components, NNE extension and NW-SE shortening. The shortening component led to the development of the extension-subparallel Nakhal anticline alongside other associated fabrics such as NNE-oriented minor folds and massif-verging thrusts, folds and cleavage. Jebel Nakhal is aligned parallel to the basement structure of the Semail lineament and therefore the lateral differential extension is likely to be constrained by this basement structure. As a result the orientations of the transtensional deformation and the resultant constrictional structures are highly influenced by the Semail lineament. The trend of the Semail lineament is approximately NNE as indicated from surface pattern and gravity data. The transtensional shear boundary is expected to align NNE-SSW, in agreement with the NNE extension and the underlying basement structures.

The lateral differential extension behind the formation of the Nakhal anticline occurred along a deeper detachment situated within the pre-Permian sequences. This is reflected from the steeply dipping normal faults, which cut the whole exposed stratigraphic profile and merge onto the deeper detachment. As a result, constriction strain occurred along the detachment. The resultant NW-SE shortening buckled this detachment together with the overlaying succession to form the Nakhal culmination. The upper extensional detachments like those situated at the base of allochthons and along key horizons within the Jurassic-Cretaceous succession, are transacted by the steep NW-SE faults and are folded over the Nakhal anticline.

The Hatat culmination comprises transverse folding expressed by a series of NNE-trending upright folds such as the Sifah fold (see Data synthesis chapter). These folds exhibit the same structural characteristics of the Nakhal anticline and coincide with zones of lateral differential extension within the high-grade metamorphic rocks. Thus, a similar transtensional model has been implemented to explain these folds. The activity of extensional detachment along the base of the allochthon may have its own zones of differential movement that could generate disharmonic cross-fold structures. The resultant transverse folds such as the Rustaq and Endam folds are parallel to the Nakhal anticline.

The newly proposed model differs from the previous models of folding of the Oman orogen in several aspects. Hanna et al. (1990) invoked a thrust model of flat ramp flat geometry situated within the upper crust that took place during the Late Cretaceous Ophiolite obduction (Fig. 2.6a). They interpreted the Nakhal anticline as a lateral culmination, while the collected field data indicates a true NW-SE shortening. Significant difference between Hanna et al. (1990) model and the model presented here is in the crustal level of thrusting. Mount et al. (1998) attributed the Oman orogen to a fault-propagation folding model developed during the Oligocene (Fig. 2.6b). However, there is no major compressional event during the Tertiary and also this model fails to justify the transverse folding, presented at the Nakhal anticline for example. Breton et al. (2004) attributed doming of the Saih Hatat to local crustal thickening related to the lithospheric delamination, while the Akhdar-Nakhal culminations are Tertiary deformations. In this way Breton et al. (2004) separated the deformation of the Saih Hatat culminations from the rest of the Oman orogen, while both are stratigraphically and structurally connected.

Tertiary uplift and deformation

The post-convergence history is recorded by Maastrichtian-Tertiary sediments, which are deformed in an extensional tectonic regime (Mann et al. 1990). The Tertiary NE-SW extensional deformation has been recorded across the entire northern Oman including the Gulf of Oman (Mann et al. 1990; Al Harthy et al. 1991; Ravaut et al. 1998; Al-Lazki et al. 2002). However, in the northern Oman Mountains, the Tertiary extensional deformation is less developed compared with the Late Cretaceous extension and chiefly manifested by localized km-long extensional faults bounding the hinterland side of the various culminations. Hanna et al. (1990) attributed this faulting to culmination collapse directed away from the massifs, and hence can be called culminations-bounding faults. These faults were once active as detachments of top-to-the-NNE sense movements separating the allochthons and the carbonate platform units during the Late cretaceous synconvergence extension. Tertiary-dated listwaenite has been mapped along some of these faults reflecting

the Tertiary faulting component (Wilde et al. 2002). The northern side of Saih Hatat is marked by a km-throw normal fault, which places oceanic crust above the Triassic Mahil dolomite, and omits of the whole Hawasina sediments. However, across this fault, the base Tertiary unconformity has been downthrown to the north by about only 450 m (Searle et al. 1994; Searle et al. 2004). Therefore the great part of the fault displacement has been accommodated by an earlier displacement, probably during the Late Cretaceous synorogenic extension.

The final uplift of the northern Oman Mountains is a matter of debate centred on when and how such regional uplift took place. There are two phases of tectonic uplift; the first one took place during the Late Cretaceous under synorogenic extension. The mountains were a positive sub-aerial feature during the latest Cretaceous and early Tertiary. The second uplift was constrained around 30 My (Oligocene), by stratigraphic and apatite fission track analysis (Mount and Crawford 1998). However, the mechanism of the Tertiary vertical uplift is still ambiguous. (Mount and Crawford 1998) attributed this uplift to steeply dipping basement faults. However, the uplift is isostatic and regional over the whole NE margin of the Arabian plate (Mann et al. 1990), which can not be established by local fault structures.

Alternatively, it can be proposed that regional Tertiary uplift was induced by an isostatic rebound associated with hinterland rifting along the Gulf of Oman (Fig. 7- 13). Faulting within the hinterland basin is part of the ongoing Tertiary extension. Such unloading triggered an isostatic flexural uplift along the rift flank manifested as uplifting of the Oman orogen, based on a concept applied over the North Atlantic by (Cloetingh et al. 1990)

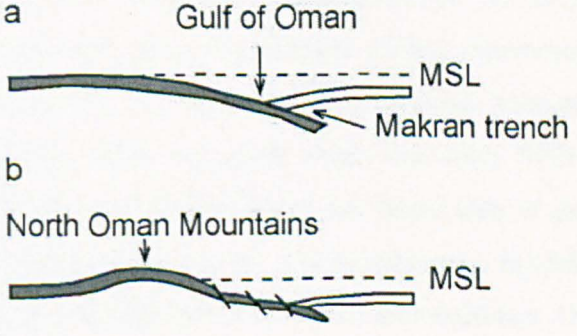

Fig. 7- 13 Tertiary uplifting of the northern Oman orogen due to rifting along the Gulf of Oman

7.10 Summary

The current study reveals that the extensional deformation that followed the obduction of the allochthons and concomitant partial subduction of the continental margin is more extensive than previously recognized by Breton et al. (2004). New discovered evidence indicates that extensional and folding deformations were synchronous. Consequently, deformation of the Arabian continental crust is characterized by coeval orthogonal layer contraction, layer-thinning and elongation. Such deformations can be described as a whole as a bulk constrictional 3D strain. While this might be indicative of regional transtension, large-scale strike-slip faults active during the extension, as predicted by general transtensional models, are not evident. However, constrictional strains appear to relate to zones of differential exhumation, for example there is more extension associated with the exhumation of Saih Hatat compared with the central Jebel Akhdar. Consequently it is inferred that the constriction was the result of laterally-varying crustal extension, where the top NNE extension was locally combined with left-lateral shearing. For the Nakhal anticline, where the direction of the finite elongation axis is N030E, the orientation of sinistral transtension deformation is NNE-SSW. The trend of the constrictional structures in the northern Oman Mountains is aligned parallel to the basement structures within the Arabian continent, represented by the Semail gap in the Oman orogen. Consequently it is tentatively proposed that the direction of extension effectively reuses the basement trends, and that these are reactivated under constriction caused by differential crustal extension.

Transtensional model could be implemented theoretically to understand the deformations of the Oman orogen with respect to synorogenic crustal extension, synorogenic exhumation, cross folding and the Tertiary uplift and deformation.

The exhumation of once-deeply buried tracts of continental crust within the Oman orogen is achieved by the synorogenic NNE-directed crustal extension. This extension occurred within the upper crust, while the middle-lower crust must experienced crustal shortening since the continental crust beneath the culminations is thicker than the adjacent Arabian foreland. These contrasting deformations involve faults and shear zones that have NNE-directed extension in the upper part and SSW-directed contraction in the lower side of the exhumed rocks. These paired kinematic systems are common on various kinematic models for the exhumation of once-deeply buried tracts of continental crust within mountain belt. Of the two options for the coherence of exhumed, once-subducted crust proposed by Wheeler et al. (2001), the Oman example here is best described as a pip rather than a sliver. There is little evidence to support the erosion of a large panel of intermediate grade metamorphic

material such as occurs for slivers. Furthermore, a carapace of allochthonous units existed over the crest of the massifs of Arabian continental rocks.

The transtensional model can explain the cross folding in the northern Oman Mountains expressed by two orthogonal sets of folds trending WNW-ESE represented in the Akhdar-Hatat culminations called longitudinal folds, and NNE-SSW trending manifested by the Nakhal culmination and hence named transverse folds. The Nakhal anticline is induced by constrictional strain resulted from lateral differential extension associated with the exhumation. The doming of the Akhdar-Hatat culminations has been attributed to lower crustal thrusting and thickening. During the early stage of lower crustal thickening and the concomitant doming, the prominent steep NW-striking faults were initiated in and around the growing culminations. These steep faults, which are presumably detached within the pre-Permian sequences, transect the entire stratigraphic succession including earlier low-angle detachments situated in the base of the allochthons and along key horizons within the Jurassic-Cretaceous units. The locations and trends of the various culminations are constrained by the pre-existing basement faults. Since basement faults induced a crustal weakness which controlled the locations and trends of the upper crustal extension and the corresponding lower crustal thickening.

Correlating between the amount of upper crustal extension and the lower crustal shortening suggests that there is a substantial imbalance between them. Consequently it is tentatively proposed that the differential extensional tectonics was active towards the end of the history of the mountain belt, coeval with the final period of crustal shortening but continued throughout the Tertiary in an intermittent manner. The lower crustal shortening was terminated by Late Cretaceous time due to halting of the convergence system and the absence of efficient erosion. The final uplift of the northern Oman Mountains took place in Late Tertiary due to isostatic rebound associated with hinterland rifting in the Gulf of Oman.

Chapter 8: Conclusions and Implications

8.1 Introduction

This study focuses on the synorogenic extensional deformation, which took place after the ophiolite emplacement at the NE margin of the Arabian plate. The first section of the conclusions summarizes new findings based on the collected field data, while the second part highlights the predicted implications of the proposed models.

8.2 Conclusions

The current study reveals that the extensional deformation within the Oman orogen is very much more extensive than previously recognized and its intensity and ductility increases progressively northeastward, towards the deeply buried rocks of Saih Hatat (See chapter 6). The extensional deformation appears to be partitioned into two apparently orthogonal structural styles: NNE-directed extensional shearing and vertical thinning, together with a local NW-SE contraction manifested by lineation-parallel folds. In the Jebel Akhdar massif the NNE-shear deformation is extensively developed, forming steep faults and bedding-parallel detachments that extend through stratigraphy with a top-NNE sense of shearing. No distinct evidence of ongoing NW-SE contraction is seen, and hence deformation is apparently plane strain. In contrast, Jebel Nakhal is marked with widespread deformation of both NNE-shearing and the concomitant NW-SE contraction, indicating non-plane strain. The NW-SE contraction induced massif-verging thrusts, folds and cleavage along with lineation-parallel folds. The contractional fabric in Jebel Nakhal increases from west to east towards the Semail gap. In Saih Hatat NNE-shearing is penetrative, with a component of orthogonal contraction. The shear zones separating the variously metamorphosed units are extensional with a top-NNE sense of shearing, while major NNE-trending upright folds express NW-SE contraction.

Field evidence indicates that both the NNE-extension and folding deformations were synchronous, as evidenced from the massif-pitching fault lineations of the NW-striking faults and stretching lineation-parallel folds. Kinematic data of the NW-striking faults across Jebel Nakhal indicates that these faults were initiated as dip and strike slip faults before or during the early stage of the folding onset, and subsequently reactivated as dip and strike slip after the folding event. The conjugate set of the strike slip faulting reflect a NW-SE compression direction.

The eastern flank of the Nakhal anticline is exclusively characterized by NNE-striking faults that occurred during two separate faulting events. The first faulting event took place during the lower and upper Jurassic, as indicated by the syn-thickening of the lower Jurassic units and partial erosion of the upper Jurassic strata (see chapter 4). Local minor unconformities were developed between the Jurassic and the Cretaceous strata during this faulting event. Localization of the Jurassic faulting within this part of the Akhdar-Nakhal culmination may suggest that such faulting is related to the NNE-trending basement Semail lineament, recognized as active during the Jurassic. The second faulting event probably occurred during or after the late stage of the folding event, since the faults truncate the km-long NW-striking faults. However, the mechanism of the second faulting event is still ambiguous.

The allochthons contacts with the platform carbonates along the hinterland side of the various culminations are commonly disrupted by steep faults with down-throw away from the massif (See chapter 6. The trends of these faults follow the variable orientations of the culmination boundaries. These sporadically developed faults cannot account for the partial omission of the allochthons along the culmination boundaries, as suggested by Hanna et al. (1990). Alternatively, based on the detected top-NNE shearing within the allochthons and the adjacent platform carbonates, the base of the allochthons can be interpreted as a top-NNE detachment along which the allochthons have been stretched and omitted during the Late Cretaceous. Practically, the process of culmination collapse occurred locally along some steep dipping massif-bounding faults. The timing of such a collapse is controversial, whether it occurred Late Tertiary time or involve a Late Cretaceous component too.

The key conclusion is that the deformation of the Arabian continental crust, which followed the obduction of the allochthons and concomitant partial subduction of the continental margin, is characterized by coeval orthogonal layer contraction, layer-thinning and elongation (See chapter 6). Such deformation can be described wholly as a bulk constrictional 3D strain. While this might be indicative of regional transtension, large-scale strike-slip faults active during the extension, as predicted by general transtensional models, are not evident. However, constrictional strains appear to relate to zones of differential exhumation, for example there is more extension associated with the exhumation of Saih Hatat compared with that of the central Jebel Akhdar. Consequently it is inferred that the constriction was a result of laterally-varying crustal extension, where the top NNE extension was locally combined with left-lateral shearing. For the Nakhal anticline where the direction of the finite elongation axis is N030E, the orientation of sinistral transtension deformation is NNE-SSW. The trend of the constrictional structures in the northern Oman Mountains is aligned parallel to the basement structures within the Arabian continent, represented by the

Semail gap in the Oman orogen. Consequently, it is tentatively proposed that the direction of extension effectively reuses the basement trends, and that these are reactivated during constriction caused by differential crustal extension.

8.3 Implications

A transtensional model could be implemented to understand the structural features of the Oman orogen with respect to synorogenic crustal extension, synorogenic exhumation, cross folding and the Tertiary uplift and deformation.

The exhumation of once-deeply buried tracts of continental crust within the Oman orogen is achieved by the synorogenic NNE-directed crustal extension. This extension occurred within the upper crust while the middle-lower crust must have experienced crustal shortening, since the continental crust beneath the culminations is thicker than the adjacent Arabian foreland. These contrasting deformations involve faults and shear zones that have NNE-directed extension in the upper part and SSW-directed contraction in the lower sections of the exhumed rocks. These paired kinematic systems are common in various kinematic models for the exhumation of once-deeply buried tracts of continental crust within mountain belt. Of the two options for the coherence of exhumed, once-subducted crust proposed by Wheeler *et al.* (2001), the Oman example here is best described as a pip rather than a sliver. There is little evidence in the studied field area to support the erosion of a large panel of intermediate grade metamorphic material such as what occurs for slivers.

The transtensional model can also explain the cross folding in the northern Oman Mountains. The Nakhal anticline was induced by constrictional strain resulting from a lateral differential extension associated with the exhumation, while the doming of the Akhdar-Hatat culminations can be attributed to lower crustal thrusting and thickening. During the early stage of lower crustal thickening and the concomitant doming, the prominent steep NW-striking faults were initiated in and around the growing culminations. The locations and trends of the various culminations are constrained by the pre-existing basement faults. This was because the basement faults induced a crustal weakness that controlled the locations and trends of the upper crustal extension and the corresponding lower crustal thickening.

Correlation between the amount of upper crustal extension and lower crustal shortening suggests that there is a substantial imbalance between them. Consequently, it is tentatively proposed that the differential extensional tectonics were active towards the end of the history of the mountain belt, coeval with the final period of crustal shortening, but continued throughout the Tertiary in an intermittent manner. The lower crustal shortening was

terminated by the Late Cretaceous due to halting of the convergence system and the absence of efficient erosion. The final uplift of the northern Oman Mountains took place in the Late Tertiary due to isostatic rebound associated with hinterland rifting in the Gulf of Oman.

References

Al Harthy, M. S., R. G. Coleman, M. W. Hughes-Clarke and S. S. Hanna (1991). Tertiary basaltic intrusions in the central Oman Mountains. Petrology and Structural Geology **5**: 675-682.

Al-Lazki, A. I., D. Seber, E. Sandvol and M. Barazangi (2002). A crustal transect across the Oman Mountains on the eastern margin of Arabia. GeoArabia (Manama) **7**(1): 47-78.

Alsop, G. I., R. E. Holdsworth and Anonymous (2002). The geometry and kinematics of sheath folds. Abstracts with Programs - Geological Society of America **34**(6): 561.

Armetrong, P. A. and J. M. Bartley (1993). Displacement and deformation associated with a lateral thrust termination, southern Golden Gate Range, southern Nevada, U.S.A. Journal of Structural Geology **15**(6): 721-735.

Beaumont, C., R. A. Jamieson, M. H. Nguyen and B. Lee (2001). Himalayan tectonics explained by extrusion of a low-viscosity crustal channel coupled to focused surface denudation. Nature **414**(6865): 738-742.

Béchennec, F., J. Le Métour, J. Platel and J. Roger (1995). Doming and down-warping of the Arabian platform in Oman in relation to Eoalpine tectonics. GeoArabia **1**: 167-178.

Breton, J.-P. B., Francois Le Metour, Joel Moen-Maurel, Laure Razin, Philippe (2004). Eoalpine (Cretaceous) evolution of the Oman Tethyan continental margin; insights from a structural field study in Jabal Akhdar (Oman Mountains). GeoArabia (Manama) **9**(2): 41-58.

Clark, M. K. and L. H. Royden (2000). Topographic ooze: Building the eastern margin of Tibet by lower crustal flow. Geology **28**(4): 703-706.

Cloetingh, S., F. M. Gradstein, H. Kooi, A. C. Grant and M. Kaminski (1990). Plate reorganization: a cause of rapid late Neogene subsidence and sedimentation around the North Atlantic. Journal of Geological Society, London **147**: 495-506.

Cobbold, P. R. and H. Quiquis (1980). Development of sheath folds in shear regimes. Journal of Structural Geology **2**: 119-126.

Coffield, D. Q., A. H. F. Robertson, M. P. Searle and A. C. Ries (1990). Structures associated with nappe emplacement and culmination collapse in the central Oman Mountains. Geological Society Special Publications, vol.49: 447-458.

Coleman, R. G. (1981). Tectonic setting for ophilote obduction in Oman. Journal of Geophysical research **86**: 2497-2508.

Coward, M. P. and G. J. Potts (1983). Complex strain patterns developed at the frontal and lateral tips to shear zones and thrust zones. Journal of Structural Geology **5**(3/4): 383-399.

Davis, B. K. and R. A. Henderson (1999). Detachment faulting in continental extension: Perspective from the southwestern U.S. Cordillera. Geological Society Special Publications **218**: 133-159.

Dercourt, J., L. Ricou and B. Vrielynck (1993). Atlas Teths Paleogeographic maps. Gauthier-Villars, Paris: 307p.,14m aps, 1pl.

Dewey, J. F., R. E. Holdsworth and R. A. Strachan (1998). Transpression and transtension zones. Geological Society Special Publications **135**: 1-14.

El-Shazly, A. K., R. G. Coleman and J. G. Liou (1990). Eclogites and blueschists from NE Oman: petrology and *P-T* evolution. Journal of Petrology **31**: 629-666.

El-Shazly, A. K., R. G. Coleman, A. H. F. Robertson, M. P. Searle and A. C. Ries (1990). Metamorphism in the Oman Mountains in relation to the Semail ophiolite emplacement. Geological Society Special Publications, vol.49: 473-493.

Fletcher, J. M., Brtley, J.M. (1994). Constrictional strain in a non-coaxial shear zone: implications for fold and rock fabric development, central Mojave metamorphic core complex, California. Journal of Structural Geology **16**(4): 555-570.

Foster, D. A. and B. E. John (1999). Quantifying tectonic exhumation in an extensional orogen with thermochronology; examples from the southern Basin and Range Province. Geological Society Special Publications **154**: 343-364.

Freeman, S. R., R. Butler, R. A. Cliff, S. Inger and A. C. Barnicoat (1998). Deformation migration in an orogen scale shear zone array; An example from the basal Brianconnais Thrust, Internal Franco-Italian Alps. Geological Magazine **135**: 349-367.

Glennie, K. W., M. W. Hughes-Clarke, M. G. Boeuf, W. F. Pilaar and B. M. Reinhardt (1974). Geology of the Oman Mountains. Verhandelingen van het Koninklijk Hederlands geologish mijnouwkundig Genootschap, Amestrdam **31**: 423.

Gray, D. R., J. M. Miller, D. A. Foster and R. T. Gregory (2004). Transition from subduction- to exhumation-related fabrics in glaucophane-bearing eclogites, Oman; evidence from relative fabric chronology and (super 40) Ar/ (super 39) Ar ages. Tectonophysics **389**(1-2): 35-64.

Gregory, R. T., D. R. Gray and J. M. Miller (1998). Tectonics of the Arabian Margin associated with the emplacement of the Oman Margin along the Ibra Transects: new evidence from NE Saih Hatat. Tectonics **17**: 657-670.

Hanna, S. S., A. H. F. Robertson, M. P. Searle and A. C. Ries (1990). The Alpine deformation of the central Oman Mountains. Geological Society Special Publications, vol.49: 341-359.

Jamieson, R. A., C. Beaumont, M. H. Nguyen and B. Lee (2002). Interaction of metamorphism, deformation and exhumation in large convergent orogens. J. metamorphic Geol **20**: 9-24.

Janecke, S. U., C. J. Vandenburg and J. J. Blankenau (1998). Geometry, mechanisms and significance of extensional folds from examples in Rocky Mountain Basin and Range province, U.S.A. Journal of Structural Geology **20**(7): 841-856.

Jiang, D. and P. Eilliams (1999). When do dragfolds not develop into sheath folds in shear zones? Journal of Structural Geology **21**: 577-583.

Krabbendam, M. and J. F. Dewey (1998). Exhumation of UHP rocks by transtension in the Western Gneiss region, Scandinavian Caledonides. Geological Society Special Publications **135**: 159-181.

Lavecchia, G. (1988). The Tyrrhenian-Apennian systems: structural setting and seismogenesis. Tectonophysics **147**: 263-293.

Le Metour, J., F. Michel, F. Bechennec, P. Platel and J. F. Roger (1995). Geology and mineral wealth of the Sultanate of Oman. Ministry of petroleum and Minerals, Directorate General of Minerals, Oman, 285p.

Le Metour, J., D. Rabu, M. Tegyey, F. Bechennec, M. Beurrier, M. Villey, A. H. F. Robertson, M. P. Searle and A. C. Ries (1990). Subduction and obduction; two stages in the Eo-Alpine tectonometamorphic evolution of the Oman Mountains. Geological Society Special Publications, vol.49: 327-339.

Lister, G. and G. A. Davis (1989). The origin of metamorphic core complexes and detachments faults formed during continental extension in the northern Colorado River region, U.S.A. Journal of Structural Geology **11**: 65-94.

Malavieille, J. (1987). Extensional shearing deformation and kilometer-scale "a"-type folds in a Cordilleran metamorphic core complex (Raft River Mountains, northwestern Utah. Tectonics **6**(4): 423-448.

Mancktelow, N. S. and T. L. Pavils (1994). Fold-fault relationships in low-angle detachment systems. Tectonics **13**(2): 668-685.

Mann, A., S. S. Hanna, S. C. Nolan, A. H. F. Robertson, M. P. Searle and A. C. Ries (1990). The post-Campanian tectonic evolution of the central Oman Mountains; Tertiary extension of the eastern Arabian margin. Geological Society Special Publications, vol.49: 549-563.

Mann, A., S. S. Hanna, A. H. F. Robertson, M. P. Searle and A. C. Ries (1990). The tectonic evolution of pre-Permian rocks, central and southeastern Oman Mountains. Geological Society Special Publications, vol.49: 307-325.

Martinez, J. M. and J. I. Soto (2002). Orthogonal folding of extensional detachments: Structure and origin of the Sierra Nevada elongated dome (Betics, SE Spain). Tectonics **21**(3).

Michard, A., B. Goffe, O. Saddiqi, R. Oberhaensli and A. S. Wendt (1994). Late Cretaceous exhumation of the Oman blueschists and eclogites; a two-stage extensional mechanism. Terra Nova **6**(4): 404-413.

Miller, J. M., D. R. Gray and R. T. Gregory (1998). Exhumation of high-pressure rocks, northeastern Oman. geology **26**: 235-238.

Mount, V. S., R. I. S. Crawford and S. C. Bergman (1998). Regional structural style of the central and southern Oman Mountains; Jebel Akhdar, Saih Hatat, and the northern Ghaba Basin. GeoArabia **3**(4): 475-490.

Nie, S., A. Yin, D. B. Rowley and Y. Jin (1994). Exhumation of the Dabie Shan ultra-high-pressure rocks and the accumulation of the Songpan-Ganzie flysch sequence, central china. GEOLOGY **22**: 999-1002.

Nolan, S. C., P. W. Skelton, B. P. Clissold, J. D. Smewing, A. H. F. Robertson, M. P. Searle and A. C. Ries (1990). Maastrichtian to early Tertiary stratigraphy and palaeogeography of the central and northern Oman Mountains. Geological Society Special Publications, vol.49: 495-519.

Platt, J. P. (1993). Exhumation of high-pressure rocks: a review of concepts and processes. Terra Nova **5**: 119-133.

Pratt, B. R., J. D. Smewing, A. H. F. Robertson, M. P. Searle and A. C. Ries (1990). Jurassic and Early Cretaceous platform margin configuration and evolution, central Oman Mountains. Geological Society Special Publications, vol.49: 69-88.

Ramani, M. V. and B. Tikoff (2002). Physical models of transtensional folding. Geological Society of America **30**(6): 523-526.

Ramsay, J. and M. Humber (1983). The techniques of modern structural geology, Academic press limited.

Ravaut, P., D. Carbon, J. F. Ritz, R. Bayer and H. Philip (1998). The Sohar Basin, western Gulf of Oman; description and mechanisms of formation from seismic and gravity data. Marine and Petroleum Geology **15**(4): 359-377.

Ridley, J. (1986). Parallel stretching lineations and fold axes oblique to a shear displacement direction- a model and observations. Journal of Structural Geology **8**(6): 647-653.

Ring, U. and M. T. Brandon (1999). Ductile deformation and mass loss in the Franciscan subduction complex; implications for exhumation processes in accretionary wedges. Geological Society Special Publications **154**: 55-86.

Ring, U., M. T. Brandon, S. D. Willett and G. S. Lister (1999). Exhumation processes. Geological Society Special Publications **154**: 1-27.

Robertson, A. H. F. (1987). The transition from a passive margin to an upper Cretaceous foreland basin related to ophilote emplacement in the Oman Mountains. Geological Society of America Bulletin **99**: 633-653.

Robyr, M., J.-C. Vannay, L. Epard and A. Steck (2002). Thrusting, extension and doming during the polyphase tectonometamorphic evolution of the High Himalayan Crystalline Zone in NW India. Journal of Asian Earth Sciences **21**: 221-239.

Roger, J. F., D. Béchennec, J. Janjou, R. Le Métour and M. Beurrier (1991). Geological map of the Ja'Alan Quadrangle, Sultanate of Oman. Geoscience map, scale 1:100,000, sheet NF 40-8E and explanatory notes. Ministry of Petroleum and Minerals, Directorate General of Minerals, Sultanate
of Oman. 90p.

Saddiqi, O., G. Poupeau, A. Michard, B. Goffe and Anonymous (2000). Fission track thermochronology of the Jabal Akhdar and Saih Hatat infra-ophiolitic windows and the denudation of the south-eastern Oman Mountains belt.

Schlische, R. W. (1995). Geometry and origin of fault-related folds in extensional settings. AAPG Bulletin **79**(11): 1661-1678.

Searle, M. P. and J. Cox (1999). Tectonic setting, origin and obduction of the Oman ophiolite. Bulletin of the Geological Society of America **111**: 104-122.

Searle, M. P. and J. Cox (2002). Subduction zone metamorphism during formation and emplacement of the Semail Ophiolite in the Oman Mountains. Geological Magazine **139**(3): 241-255.

Searle, M. P., C. J. Warren, D. J. Waters and R. R. Parrish (2004). Structural evolution, metamorphism and restoration of the Arabian continental margin, Saih Hatat region, Oman Mountains. Journal of Structural Geology **26**(3): 451-473.

Searle, M. P., D. J. Waters, H. N. Martin and D. C. Rex (1994). Structure and metamorphism of blueschist-eclogite facies rocks from the northeastern Oman Mountains. Journal of the Geological Society of London **151**(3): 555-576.

Shelton, A. W., A. H. F. Robertson, M. P. Searle and A. C. Ries (1990). The interpretation of gravity data in Oman; constraints on the ophiolite emplacement mechanism. Geological Society Special Publications, vol.49: 459-471.

Stewart, S. A. (2001). Displacement distributions on extensional faults; implications for fault stretch, linkage, and seal. AAPG Bulletin **85**(4): 587-599.

Swanson, M. T. (1999). kIinematic indicators for regional dextral shear along the Norumbega fault system in the Casco Bay area, coastal Maine. Geological Society of America **Special Paper 331**.

Tavarnelli, E. and D. Peacock (1999). From extension to contraction in syn-orogenic foredeep basins: the contessa section, Umbria-March Apennines, Italy. Terra Nova **11**: 55-60.

Thomson, S. N., B. Stoeckhert and M. R. Brix (1999). Miocene high-pressure metamorphic rocks of Crete, Greece; rapid exhumation by buoyant escape. Geological Society Special Publications **154**: 87-107.

Wheeler, J. and R. Butler (1994). Criteria for identifying structures related to true crustal extension in orogens. Journal of Structural Geology **7**: 1023-1027.

Wheeler, J., S. M. Reddy and R. A. Cliff (2001). Kinematic linkage between internal zone extension and shortening in more external units in the NW Alps. Journal of the Geological Society, London **158**: 439-443.

Wilde, A., L. Simpson and S. Hanna (2002). Preliminary study of Tertiary hydrothermal alteration and platinum deposition in the Oman ophiolite. Journal of the Virtual Explorer **6**: 9-21.

Willett, S. D. (1999). Rheological dependence of extension in wedge models of convergent orogens. Tectonophysics **305**: 419-435.

Woodcock, N. and N. Schubert (1994). Continental strike-slip tectonics. Continental deformation. P. Hancock, Pergamon press: 251-263.

Yin, A. (1991). Mechanisms for the formation of the domal and basinal detachments faults: a three dimensional analysis. Journal of Geophsical Research **96**: 14577-14594.